Dendritic Catalysts for Compartmentalized Tandem Catalysis

Dendritische Katalysatoren voor Gecompartimentaliseerde Tandemkatalyse

(met een samenvatting in het Nederlands)

PROEFSCHRIFT

ter verkrijging van de graad van doctor

aan de Universiteit Utrecht

op gezag van rector magnificus, prof. dr. G. J. van der Zwaan,

ingevolge het besluit van het college voor promoties

in het openbaar te verdedigen

op woensdag 19 oktober 2011 des middags te 14.30 uur

door

Niels Johannes Maria Pijnenburg

geboren op 26 januari 1982 te Breda

Promotoren: Prof. dr. R. J. M. Klein Gebbink

Prof. dr. G. van Koten

The work described in this Ph. D. thesis was financially supported by the Dutch National Research School Combination Catalysis (NRSCC).

Dendritic Catalysts for Compartmentalized Tandem Catalysis

Pijnenburg, Niels Johannes Maria

Title: Dendritic Catalysts for Compartmentalized Tandem Catalysis

Utrecht, Utrecht University, Faculty of Science

Ph.D. thesis Utrecht University – with ref. – with summary in Dutch

ISBN: 978-90-393-5608-1

The work described in this thesis was carried out at the group of Organic Chemistry & Catalysis, Debye Institute for Nanomaterials Science, Faculty of Science, Utrecht University, Utrecht, the Netherlands.

Cover design: Jesse Pijnenburg en Niels Pijnenburg

Table of contents

Preface

Homogeneous catalysts are the catalysts of choice for many synthetic procedures in academia and industry. The choice to use a soluble organometallic catalyst is often related to its high activity, the possibility for selective catalysis, its high tunability, the mild reaction conditions, and the well-described reaction mechanisms that characterize homogeneous catalysts.[1] An obvious disadvantage of the use of such catalysts is the difficulty in separating them from reaction mixtures, which hampers the subsequent reuse of the organometallic species and which may lead to the loss of the precious metal and the ligand.

A common approach for the removal and recycling of homogeneous catalysts is the immobilization of multiple of these catalysts on a single macromolecular support.[2-6] This can take place in a homogeneous or heterogeneous way, depending on the chosen support. Dendrimers,[7] i.e. tree-like polymers with repeating branches and multiple peripheral end groups, are widely explored for the immobilization of homogeneous catalysts because of their low polydispersity and superior solubility with respect to, e.g., linear polymers. The end groups of these dendrimers can be connected to (modified) monomeric homogeneous catalysts to create peripherally functionalized dendrimers that contain a distinct number of organometallic catalytic sites. By means of the resulting molecular weight enlargement, these dendritic catalysts can be separated from reaction mixtures via nano- or ultrafiltration, or by dialysis techniques. In this way, the dendritic catalyst can be made available for reuse in either a batch-like or a continuous manner.

Since the first example of the use and reuse of homogeneous catalytic systems by means of peripheral dendrimer immobilization in 1994 by the groups of Van Koten and Van Leeuwen,[8] the field of dendrimer catalysis has gained increased interest within the general field of immobilized catalysts. An important aspect in the successful application of these catalysts is the prevention of metal leaching. Therefore, monomeric catalytic entities in which the metal ion is connected to the ligand via a combination of covalent M–C bonds and dative M-hetero atom bonds, are considered as suitable candidates for this purpose. Metal complexes derived from tridentate ECE-pincer ligands are known for their kinetic and thermodynamic stability and are frequently used to meet these requirements.[9-11] In the past decade, the Van

Koten/Klein Gebbink group has explored the immobilization of these ECE-pincer metal complexes on dendrimers and on a series of other molecular and macromolecular supporting materials.[12-19] Especially, pincer complexes derived from the Group 10 transition metals Ni, Pd, and Pt have been studied intensively, because of the large number of chemical reactions that can be catalyzed by these complexes. In particular, ECE-pincer Pd complexes can be used as catalysts in a variety of organic transformations, including aldol condensations, Michael reactions, allylations of electrophiles, stannylations, borylations and cross-coupling reactions.[10] In ***Chapter 1*** of this thesis an overview is provided on the applications of palladium-containing dendrimers and star-shaped molecules in catalysis. Although other palladium dendrimers are also included, the scope of this overview is focused on structures in which a covalent Pd-C bond is complemented by a Pd-donor interaction to form a palladacycle. ECE-pincer Pd complexes are the most common examples of these palladacyclic compounds.

Molecularly enlarged catalysts have recently been used in compartmentalized catalysis using the immobilized catalyst inside a semi-permeable membrane compartment that can be directly placed into a reaction mixture (*figure 1, left*).[20-25] In such systems, the dendritic catalysts are unable to permeate through the membrane due to their macroscopic size and are retained inside the membrane compartment, whereas all substrates, reactants and products can pass the membrane and, accordingly, can diffuse in and out of the compartment. The semi-permeable membrane compartment containing the dendritic catalyst can easily be removed from the reaction mixture, and can be reused if desired.

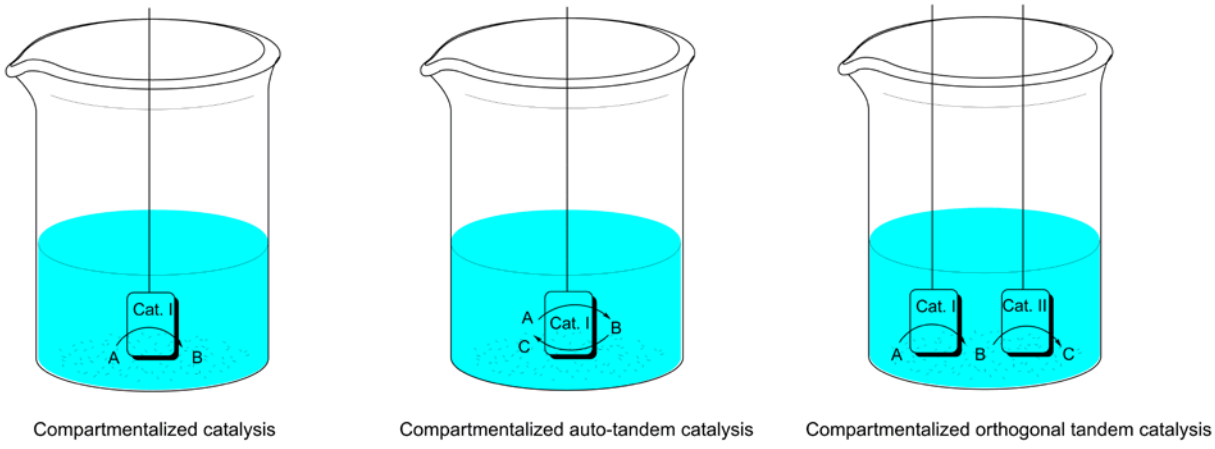

Figure 1: Schematic representation of three types of compartmentalized catalysis.

While compartmentalized catalysts have been successfully applied in single catalytic transformations, their use in multi-step catalytic reactions has only been hinted at. We became interested in extending the scope of these catalysts to tandem catalysis, a type of catalysis where various, chemically different reactions are performed in the same vessel in a consecutive manner, in view of process intensification.[26,27] Tandem catalysis can be roughly divided in three types: auto-tandem catalysis, orthogonal tandem catalysis and assisted tandem catalysis. The easiest and most commonly used type of tandem catalysis is auto-tandem catalysis, in which two or more mechanistically different reaction steps are catalyzed by *a single catalyst*. In orthogonal tandem catalysis various mechanistically different transformations are carried out by *a series of different catalysts*. In assisted tandem catalysis, on the other hand, an external trigger is used to change a catalyst in order for it to catalyze a next reaction in a series of consecutive reactions.

With regard to process intensification, the key benefit of tandem catalysis is the reduced number of workup and purification operations since the isolation of intermediate products can be prevented. Accordingly, a reduction in waste, time, energy and solvents can be achieved, which is of additional interest from a green chemistry point of view. Because workup steps are avoided in tandem catalysis, sensitive reaction products can also be handled easier than in single-step catalysis, and are readily available for the next reaction step.

As a result of carrying out multiple reaction steps consecutively in one vessel, the total number of reactants, reagents and catalysts increases considerably in tandem catalysis. This significantly enhances the chance of undesired interactions between the various reagents, of catalyst deactivation and of undesired side reactions. These issues represent a serious drawback of tandem catalysis and can hamper the successful development of synthetic routes based on tandem catalysis. Alternately, via a compartmentalization approach, a catalyst may not only be separated from a reaction mixture and eventually be recycled more easily within the setting of tandem catalysis, but its deactivation may also be avoided by preventing undesired catalyst-catalyst interactions. The introduction and removal of a semi-permeable membrane compartment filled with an enlarged catalyst, furthermore, allows for control over a particular catalytic reaction in time. In this way, side reactions are hampered and catalyst deterioration by other reagents than those engaged in the anticipated transformation is reduced.

The concept of compartmentalized auto-tandem catalysis is depicted in *figure 1, middle*. The setup for compartmentalized orthogonal tandem catalysis (*figure 1, right*) is considerably more challenging, as multiple compartments each containing a different dendritic catalyst have to be combined in a kinetically competitive manner. This thesis describes the first steps in the area of compartmentalized tandem catalysis. The experimental chapters in this thesis describe a series of studies that are aimed at developing the dendritic catalyst toolbox required for compartmentalized auto- and orthogonal tandem catalysis and detail catalytic experiments using dendritic catalysts in compartmentalized and non-compartmentalized tandem catalysis set-ups.

In ***Chapter 2*** the synthesis of novel dendritic SCS-pincer Pd complexes is described. These pallada-dendrimers were investigated in a catalytic setup where the dendrimer catalyzes two different reactions in one pot, i.e. the pallada-dendrimer catalyst acts as an auto-tandem catalyst. The auto-tandem catalytic reaction that was investigated consists of the stannylation of an allyl chloride followed by the electrophilic addition of the primary reaction product with a benzaldehyde derivative leading to a homoallylic alcohol.[15,28,29] The metallo-dendritic catalysts were furthermore tested in a compartmentalized reaction setup, using dialysis membranes to separate the dendrimers from the bulk solution.

In ***Chapter 3*** mechanistic studies are performed on the auto-tandem reaction that was described in ***Chapter 2*** in order to optimize the reaction conditions for compartmentalized dendritic catalysts. Based on these studies, an amendment of the earlier proposed reaction mechanism, which was based on the reaction mechanisms of the individual steps, is proposed. The new mechanism explains the remarkable reaction kinetics that have been observed for this tandem reaction.

The influence of the nature of the dendritic support on the reaction rate and product selectivity of a chemical reaction was investigated in ***Chapter 4***. The earlier described tandem reaction and a cross-coupling reaction between a vinyl epoxide and a boronic acid[30] have been studied through the use of dendrimer-immobilized SCS-pincer Pd complexes and monomeric analogues thereof. Various generations of apolar carbosilane and polar PAMAM-dendrimers have been used as the dendritic supports in this study.

In ***Chapter 5*** SCS-pincer Pd complexes have been coupled to PEG-based block copolymers and to random copolymers. These polymers possess an identical chemical composition but

show a different distribution of the catalytic centers along the polymer backbone. The influence of the structure of the polymeric support on the activity and selectivity of the covalently attached pincer complexes in catalysis was investigated in order to shed further light on the role of the macromolecular support on the performance of immobilized catalysts.

After the use of SCS-pincer metal complexes in ***Chapters 2-5***, ***Chapter 6*** describes the performance of another set of organometallic catalysts based on *N*-heterocyclic carbene-metal complexes that have been immobilized on carbosilane dendrimers. The NHC ligands are known to form firm metal to ligand bonds,[31] in analogy to pincer ligands, and therefore are appropriate ligands for the development of immobilized and compartmentalized catalysts. Novel dendritic Grubbs II-type ruthenium catalysts are investigated in the ring closing metathesis (RCM) of diethyl diallylmalonate and compared to monomeric analogues and to commercially available olefin metathesis catalysts. The dendritic catalysts are also investigated in a compartmentalized setup.

Finally, the ***Addendum*** of this thesis reflects on the possibilities towards compartmentalized orthogonal tandem catalysis, i.e. the use of multiple catalysts in multiple compartments in a one-pot procedure. The possibility of using the dendritic palladium and ruthenium catalysts described in ***Chapters 2 and 6*** in a novel orthogonal tandem reaction are explored.

References

1. Dijkstra, H. P.; van Klink, G. P. M.; van Koten, G. *Acc. Chem. Res.* **2002,** *35*, 798-810.
2. Chase, P. A.; Klein Gebbink, R. J. M.; van Koten, G. *J. Organomet. Chem.* **2004,** *689*, 4016-4054.
3. Janssen, M.; Müller, C.; Vogt, D. *Dalton Trans.* **2010,** *39*, 8403-8411.
4. Van Heerbeek, R.; Kamer, P. C. J.; van Leeuwen, P. W. N. M.; Reek, J. N. H. *Chem. Rev.* **2002,** *102*, 3717-3756.
5. Yazerski, V. A.; Klein Gebbink, R. J. M. *Catalysis by Metal Complexes (2010)* **2010,** *33 (Heterogenized Homogeneous Catalysts for Fine Chemicals Production)*, 171-201.
6. Vankelecom, I. F. J. *Chem. Rev.* **2002,** *102*, 3779-3810.
7. Astruc, D.; Boisselier, E.; Ornelas, C. *Chem. Rev.* **2010,** *110*, 1857-1959.
8. Knapen, J. W. J.; van der Made, A. W.; de Wilde, J. C.; van Leeuwen, P. W. N. M.; Wijkens, P.; Grove, D. M.; van Koten, G. *Nature* **1994,** *372*, 659-663.
9. Albrecht, M.; van Koten, G. *Angew. Chem. Int. Ed.* **2001,** *40*, 3750-3781.
10. Selander, N.; Szabó, K. J. *Chem. Rev.* **2011,** *111*, 2048-2076.
11. Singleton, J. T. *Tetrahedron* **2003,** *59*, 1837-1857.
12. Kleij, A. W.; Gossage, R. A.; Klein Gebbink, R. J. M.; Brinkmann, N.; Reijerse, E. J.; Kragl, U.; Lutz, M.; Spek, A. L.; van Koten, G. *J. Am. Chem. Soc.* **2000,** *122*, 12112-12124.
13. Bonnet, S.; Lutz, M.; Spek, A. L.; van Koten, G.; Klein Gebbink, R. J. M. *Organometallics* **2010,** *29*, 1157-1167.

14. Dijkstra, H. P.; Meijer, M. D.; Patel, J.; Kreiter, R.; van Klink, G. P. M.; Lutz, M.; Spek, A. L.; Canty, A. J.; van Koten, G. *Organometallics* **2001,** *20*, 3159-3168.
15. Gagliardo, M.; Selander, N.; Mehendale, N. C.; van Koten, G.; Klein Gebbink, R. J. M.; Szabo, K. J. *Chem. Eur. J.* **2008,** *14*, 4800-4809.
16. Kruithof, C. A.; Dijkstra, H. P.; Lutz, M.; Spek, A. L.; Klein Gebbink, R. J. M.; van Koten, G. *Organometallics* **2008,** *27*, 4928-4937.
17. Meijer, M. D.; Mulder, B.; van Klink, G. P. M.; van Koten, G. *Inorg. Chim. Acta* **2003,** *352*, 247-252.
18. Slagt, M. Q.; Rodriguez, G.; Grutters, M. M. P.; Klein Gebbink, R. J. M.; Klopper, W.; Jenneskens, L. W.; Lutz, M.; Spek, A. L.; van Koten, G. *Chem. Eur. J.* **2004,** *10*, 1331-1344.
19. Suijkerbuijk, B. M. J. A.; Martinez, S. D. H.; Klein Gebbink, R. J. M.; van Koten, G. *Organometallics* **2008,** *27*, 534-542.
20. Albrecht, M.; Hovestad, N. J.; Boersma, J.; van Koten, G. *Chem. Eur. J.* **2001,** *7*, 1289-1294.
21. Arink, A. M.; van de Coevering, R.; Wieczorek, B.; Firet, J.; Jastrzebski, J. T. B. H.; Klein Gebbink, R. J. M.; van Koten, G. *J. Organomet. Chem.* **2004,** *689*, 3813-3819.
22. Gaab, M.; Bellemin-Laponnaz, S.; Gade, L. H. *Chem. Eur. J.* **2009,** *15*, 5450-5462.
23. Gaikwad, A. V.; Boffa, V.; ten Elshof, J. E.; Rothenberg, G. *Angew. Chem. Int. Ed.* **2008,** *47*, 5407-5410.
24. Janssen, M.; Müller, C.; Vogt, D. *Adv. Synth. Catal.* **2009,** *351*, 313-318.
25. Janssen, M.; Wilting, J.; Müller, C.; Vogt, D. *Angew. Chem. Int. Ed.* **2010,** *49*, 7738-7741.
26. Fogg, D. E.; dos Santos, E. N. *Coord. Chem. Rev.* **2004,** *248*, 2365-2379.
27. Wasilke, J. C.; Obrey, S. J.; Baker, R. T.; Bazan, G. C. *Chem. Rev.* **2005,** *105*, 1001-1020.
28. Solin, N.; Kjellgren, J.; Szabó, K. J. *J. Am Chem. Soc.* **2004,** *126*, 7026-7033.
29. Wallner, O. A.; Szabó, K. J. *Org. Lett.* **2004,** *6*, 1829-1831.
30. Kjellgren, J.; Aydin, J.; Wallner, O. A.; Saltanova, I. V.; Szabó, K. J. *Chem. Eur. J.* **2005,** *11*, 5260-5268.
31. Fürstner, A.; Ackermann, L.; Gabor, B.; Goddard, R.; Lehmann, C. W.; Mynott, R.; Stelzer, F.; Thiel, O. R. *Chem. Eur. J.* **2001,** *7*, 3236-3253.

Chapter 1

Palladacycles on dendrimers and star-shaped molecules for applications in catalysis

Abstract

The field of dendrimer chemistry has expanded exponentially after the first dendritic structures were published in the end of the 70s. The class of metallodendrimers that often is used in catalysis comprises intriguing systems combining advantages of both homogeneous and heterogeneous catalysts.

Most publications dealing with dendritic palladium complexes report on dendrimers with palladium centers that involve either periphery, core or branching point-functionalized palladium complexes with the palladium center bound via coordinative or covalent bonds, or palladium nanoparticles encapsulated in the dendrimer manifold. A smaller part of dendrimer-based palladium complexes does contain metallocyclic moieties containing covalent palladium-carbon bonds and are envisaged as dendritic palladacyclic compounds. Although small in number, their relevance is obvious: the covalent bond increases the stability of the palladium complex, which may prevent palladium leaching. This review provides a comprehensive overview on this class of dendritic palladacyclic compounds and their application in catalysis.

Based on: Niels J. M. Pijnenburg, Ties J. Korstanje, Gerard van Koten and Robertus J. M. Klein Gebbink, *Palladacycles on Dendrimers on Star-Shaped Molecules, Chapter 15 in Palladacycles – Synthesis, Characterization and Applications by Jairton Dupont and Michel Pfeffer, Wiley-VCH Verlag GmbH & Co. KGaA,* **2008**, 361-398

1.1 Introduction

Dendrimers are highly branched, three-dimensional macromolecules with a branching point at each monomer unit. This class of macromolecules was pioneered by Vögtle *et al.* in 1978 by publishing a procedure called cascade synthesis, using repetition of similar synthetic steps leading to highly symmetrical monodisperse macromolecules.[1] Following this publication, the field of dendrimers and dendritic structures was further investigated by the groups of Tomalia,[2-4] Newkome,[5,6] and Fréchet[7-10] and has been a blossoming field of research ever since. Since major developments in NMR spectroscopy, mass spectrometry and size-exclusion chromatography made detailed characterization of dendrimers possible, these well-defined macro-molecular compounds have been used for many applications: host-guest chemistry,[11-18] drug delivery,[19-34] self-assembly,[35-46] usage as sensor,[47-52] etc. A very extensive, recent review on the applications of dendrimers was published by Astruc.[53]

Another important field of application of dendrimers is their use in catalysis.[53-77] When considering the fields of homogeneous catalysis, where the catalyst is in the same phase as the reactants and the products, and heterogeneous catalysts, where the catalyst is in another (most likely solid) phase, several clear distinctions are obvious (*table 1.1*). Quite notably, these distinctions seem to be complementary to each other. Homogeneous catalysts in general show a higher activity and a higher product selectivity compared to heterogeneous catalysts. Therefore, milder reaction conditions can generally be applied with a highly defined catalytic system. The most important disadvantage of homogeneous catalysts is their difficult separation from the reaction mixture and the resulting recycling problems.

The idea of developing catalysts that combine the advantages of both homogeneous and heterogeneous catalysts therefore seems very attractive. One objective could be to arrive at recyclable homogeneous catalysts and processes that could be operated in a continuous manner. Immobilization of homogeneous catalysts on dendrimers is an attractive strategy for this objective, because of the well-defined structure, macromolecular dimensions and excellent solubility properties of dendrimers.

Table 1.1: Properties of homogeneous catalysis compared with those of heterogeneous catalysis.[78]

	Homogeneous	*Heterogeneous*
Activity	+++	-
Selectivity	+++	-
Catalytic description	+++	-
Reaction conditions	+++	+
Catalyst recycling	-	+++
Quantity of catalyst	++	+++
Total Turnover Number	+	+++

Generally, metallodendritic catalysts combine the kinetic behavior, activity, and selectivity of the single homogeneous catalyst with the easy separation of the heterogeneous catalyst, i.e. by applying either precipitation or (continuous) membrane separation (nanofiltration) techniques of the dendritic, nanosized catalyst. Other favorable characteristics of homogeneous catalysis are also retained, like the possibility of performing mechanistic studies (due to the often excellent solubility of the metallodendrimers having defined structural features), and the possibility to fine-tune the catalytic centers by either changing the ligands or the secondary ligand sphere by changing the structural features of the dendrimer.

Metallodendrimers, or dendritic catalysts in general, can be roughly divided in five classes depending on the position of the metal centers, or active centers, in the dendrimer, as shown in *figure 1.1*. Periphery bound metal complexes, depicted in *figure 1.1(a)*, are the type of metallodendrimers that are used most frequently in catalysis. The first example of this type is Van Koten's and van Leeuwen's metallodendritic species based on a well-defined carbosilane dendrimer comprising twelve cyclometalated arylnickel functional groups acting as active homogeneous catalyst in a continuous setup (*figure 1.2*).[54] Depending on the design of the dendrimer, peripheral transition metals are in general readily accessible for substrates resulting in reaction rates per metal site that are comparable to the parent homogeneous, monomeric species. In other cases, the peripheral crowding of active-sites may lead to a decrease in catalytic activity per metal site, e.g. due to the too close proximity

of the active sites, decreased accessibility of the catalytic sites by the substrates or mass transport restrictions. Each of these factors can lead to a negative dendritic effect.[55,58] However the presence of catalytic sites in close proximity to each other may also lead to an increased catalytic activity due to cooperation (e.g. by protection of the active sites through temporarily dimerization between sites). Several examples of such positive dendritic effects in catalysis can be found in the literature.[79-88]

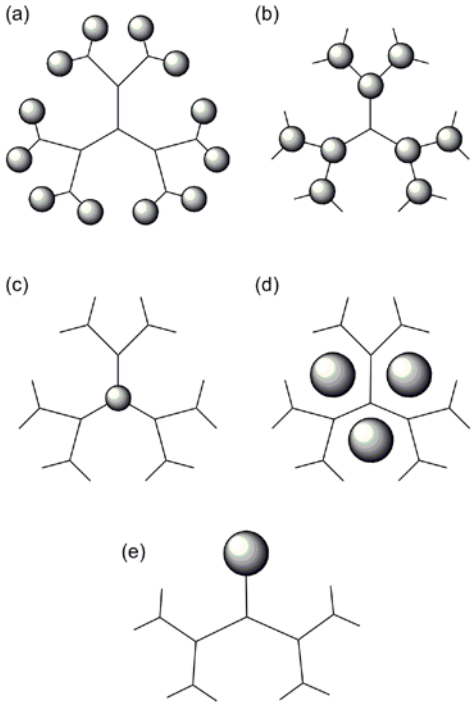

Figure 1.1: Different types of metallodendrimers. Transition metal sites can be located at the periphery (a), at or near each branching point (b), at the core (c) or as metal particles formed inside the voids of the dendrimer (d). A transition metal site acting as the focal point of a dendritic wedge is visualized in (e). The figure was adopted from Oosterom et al.[74]

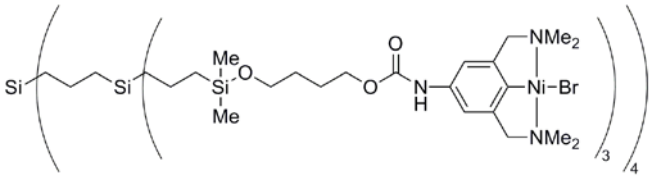

Figure 1.2: The first catalytically active metallodendrimer by van Koten and van Leeuwen.[54]

Core-functionalized dendrimers, depicted in *figure 1.1(c)*, are mostly synthesized with another goal in mind. Here, the metal centers could benefit from a site-isolation effect, caused by the dendritic environment. This dendritic shielding provides an encapsulation of the catalytic species at the core thus creating a microenvironment that affects the properties of the catalyst, and might affect its properties in either negative or positive sense.[89] An important difference between periphery- and core-functionalized dendrimers lies in their molecular weight per catalytic site. The very high molecular weight per catalytic site of core-functionalized dendrimers may hamper their activity due to restricted mass transport within the increased steric bulk of the dendritic wedges.[90]

Catalytic entities located at branching points of a dendrimer (*figure 1.1(b)*), as well as dendronized catalysts (*figure 1.1(e)*), which are single catalytic entities molecularly enlarged by one or more dendritic substituents, complete the topological picture of dendritic (metallo)catalysts. A fascinating other class of metallodendrimers involves nanoparticles that are embedded or entangled by dendritic structures (*figure 1.1(d)*).

As being an indispensable metal in homogeneous catalysis for among others carbon-carbon bond formation reactions,[91,92] a variety of palladium catalysts have been attached or immobilized to different types of dendrimers. A rather limited number of these 'palladium dendrimers' contain robust palladacyclic structures in the true sense of the metallacycle definition, i.e. structures in which a covalent Pd-C bond is complemented by a Pd-donor interaction to form a palladacycle. The covalent Pd-C bond increases the stability of the palladium complex, which may prevent palladium leaching. This is considered as a large advantage over non-palladacyclic palladium dendrimers. This review contains a concise description of these palladadendrimers in terms of structure, synthesis, and application.

A larger number of palladium dendrimers do not comprise palladium sites in the form of a palladacycle. In order to provide the reader with a conceptual overview of the field, selected examples of these dendrimers with a focus on catalysis are discussed in *paragraph 1.2* of this chapter, i.e. prior to the discussion on true 'palladadendrimers' in *paragraph 1.3*.

1.2 Palladium catalysts on dendrimers: An overview

1.2.1 Periphery-bound palladium catalysts

In many examples palladium has been introduced on the dendrimer periphery (as depicted in *figure 1.1(a)*) where the palladium centers have been bound to the dendrimer by means of coordinative bonds. Here, palladium is mostly introduced by treatment of a presynthesized dendritic poly-ligand with an appropriate palladium salt. For more insight, the recent review of De Jesús and co-workers about catalysts based on palladium dendrimers is strongly recommended.[65]

Dendritic bis-diphenylphosphino palladium complexes

Probably, the most frequently used ligand to introduce palladium onto the periphery of a dendrimer is the bis-diphenylphosphino ligand. In 1997, Reetz and co-workers developed peripheral diphosphines on DAB-based (DAB = 1,4-diaminobutane) poly(propylene)imine (PPI) dendrimers, which were coordinated to a number of different metals, including palladium (*figure 1.3*).[81] Initial catalytic studies on the palladium dendrimers in the Heck reaction of bromobenzene and styrene were successful. Due to the higher thermal stability of the dendritic compound compared to the parent monomeric one, a positive dendritic effect was observed (the turnover number (TON) of the G_2 dendrimeric compound is 50 mol product mol^{-1} catalyst, whereas the TON of the monomeric compound is 16 mol product mol^{-1} catalyst).

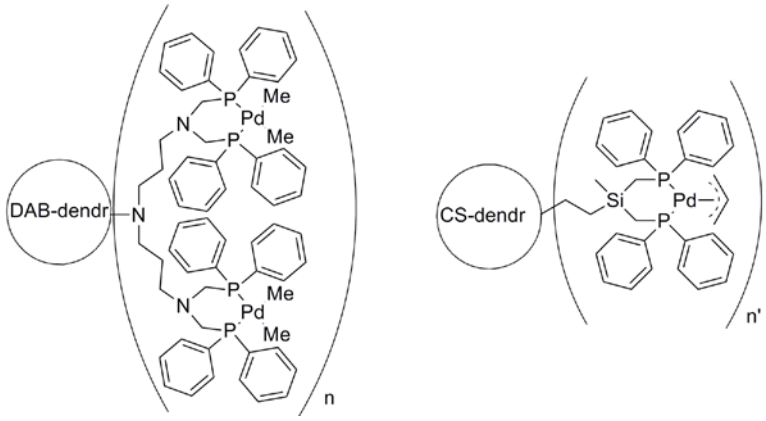

Figure 1.3: Palladium coordinated diphenylphosphine-functionalized DAB-based- and carbosilane dendrimer by Reetz[81] and De Groot,[93] respectively (n = 16; n' = 4 or 12).

De Groot *et al.*[93] reported palladium complexes of diphenylphosphine-functionalized carbosilane dendrimers. These complexes have been used as catalysts in the allylic alkylation reaction of crotyl acetate or cinnamyl acetate with sodium diethyl 2-methylmalonate.[94] As it turned out, the catalytic activity per palladium atom was almost unaffected by the size of the dendrimer in batch reactions. Unfortunately, the yields for these allylic substitution reactions dropped rapidly in a continuous flow membrane reactor, presumably due to leaching of palladium from the dendrimer.

Several other research groups have also used bis-phosphino palladium complexes on dendrimers. Heuzé *et al.* investigated a series of four different generations of bis-(di-*tert*-butylphosphine)- and bis-(dicyclohexylphosphine)-functionalized palladium(II) PPI dendrimers for carbon-carbon coupling reactions.[95] A negative dendritic effect was found for the Sonagashira coupling reaction of iodobenzene with phenylacetylene. The largest tested dendrimers appeared to be the least active ones, which is explained by the authors as being due to a decreased accessibility of the catalytic centers. Mizugaki *et al.* synthesized PPI dendrimers containing peripheral bis-diphenylphosphine palladium complexes for allylic substitution reactions of allylic acetates with amines.[96] The selectivity for the *cis*-product dramatically increased with increasing dendrimer generation in the reaction of *cis*-3-acetoxy-5-carbomethoxycyclohex-1-ene with morpholine.

Portnoy *et al.* have also used bidentate phosphine ligands, which have been prepared on polystyrene beads modified with polyether dendron spacers.[97] When complexed to Pd^0, these systems displayed a negative dendritic effect on Heck catalysis, but mostly a positive influence on carbonylation reactions.

Alper and co-workers have performed extensive research on silica-supported polyamido amine (PAMAM) palladium complexes like the one depicted in *figure 1.*4. These palladium catalysts are used in a variety of organic transformations, e.g. Heck,[98] hydrogenation,[99] carbonylation,[100-102] hydroesterification,[103] and oxidation reactions.[104] These dendritic complexes display some interesting recycling properties, whereby the activity is largely retained for up to eight cycles. Palladium loading in these materials is achieved by means of ligand complexation with $Pd_2(dba)_3$ (dba = dibenzylideneacetone), but no full loading could be obtained.

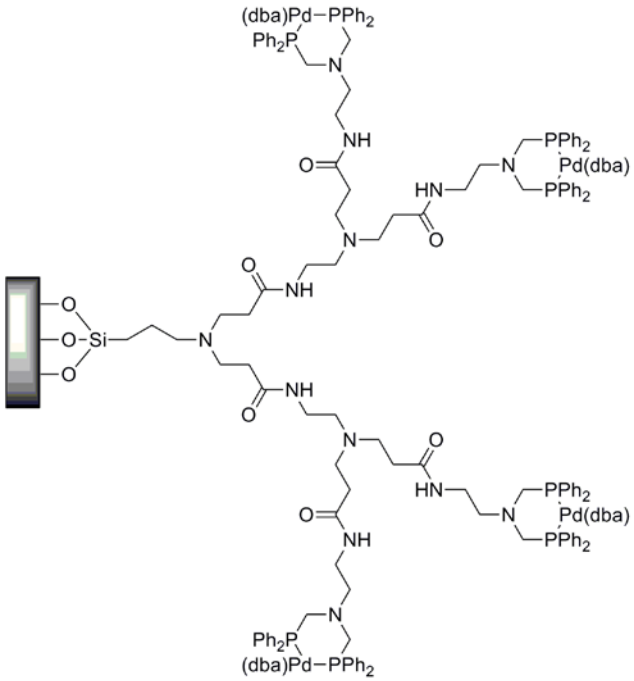

Figure 1.4: Recyclable palladium dendrimers on silica as used by Alper.[101]

Intramolecular carbonylation reactions were also performed with these palladium dendrimers on silica in the synthesis of numerous oxygen, nitrogen, and sulfur-containing medium-sized fused heterocycles by using complex substrates.[101] A remarkable array of different heterocycles showed excellent yields in these reactions. Again, the dendritic catalysts have been recovered by an easy filtration in air and were reused for up to ten cycles with only a slight loss in activity.[102]

Bis-diphenylphosphino palladium ligand systems were also applied in the group of Majoral and Caminade for in situ preparation of the corresponding Pd complexes.[105] These complexes have been used for three types of carbon-carbon cross-coupling reactions (Suzuki, Sonogashira and Heck reactions) in the presence of water. In the case of the Sonogashira reaction a small positive dendritic effect was observed with an increased conversion for higher generation dendrimers. The same group, in collaboration with the group of Moreño-Manas, recently published dendrimers up to the third generation starting from a 15-membered triolefinic azamacrocycle.[106] Iminophosphine groups were anchored on the surface of the second and third generations, and their corresponding Pd(II) complexes were prepared. To investigate the effect of shielding upon the coordinating ability of the macrocyclic core, the coordination with Pd^0 and Pt^0 atoms was studied.

Other periphery-bound palladium complexes

In this section, representative examples of bi- or tridentate nitrogen-palladium complexes are shown. G_0 and G_1 PPI pyridylimine palladium dendrimers were synthesized by Mapolie *et al.* and were used as catalyst precursors for the polymerization of ethylene[107] and for Heck reactions (*figure 1.5*).[108] For the latter reaction type, a positive dendritic effect was observed in that the conversion of the arylations of styrene and 1-octene respectively, dramatically increased compared to reactions using an analogous monomeric palladium complex or palladium dichloride, which apparently agglomerate more readily.

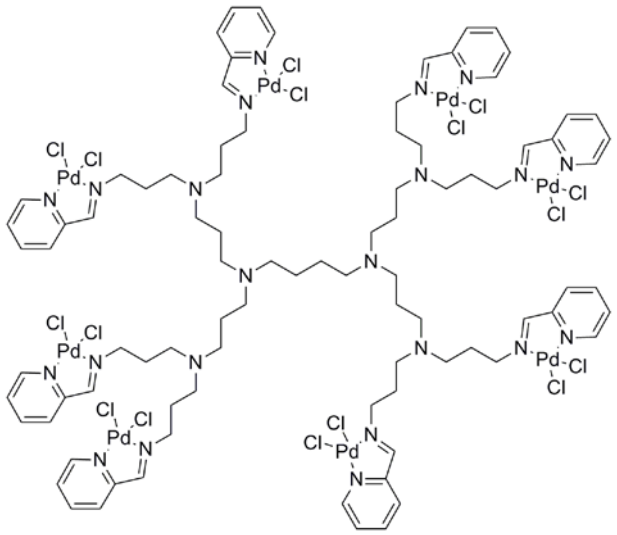

Figure 1.5: A first generation pyridylimine palladium dendrimer by Mapolie.[107]

A tridentate (*N,N,N)* palladium complex is formed by metalating (2-pyridylimino)isoindolato (BPI) ligands. Gade *et al*. connected these ligands to the periphery of a carbosilane dendrimer[109] via an alkynyl linker unit. Subsequent palladation leads to the dendritic complexes shown in *figure 1.6*. The same group also anchored polyether dendritic wedges to monomeric BPI ligands forming a dendronized ligand[110]. After palladation, the resulting dendritic complexes were investigated as hydrogenation catalysts. Styrene and 1-octene were hydrogenated without decomposition with a TOF of 5 h^{-1} (T = 295 K, $p(H_2)$ = 1 bar, 2 mol% cat.). The G_2 Fréchet-type dendron-functionalized catalyst was isolated and successfully reused several times.

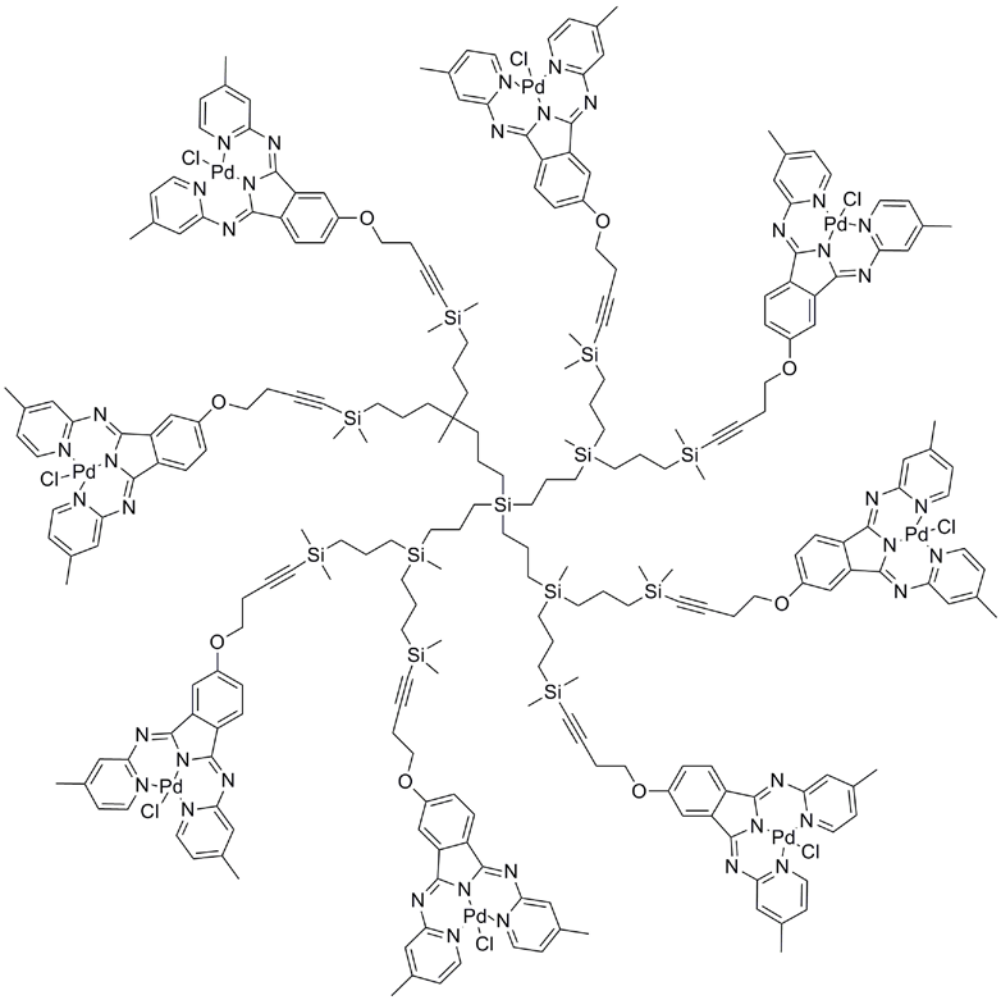

Figure 1.6: G_1 carbosilane dendrimer functionalized with eight Pd(BPI) ligands by Gade.[109]

Dendritic N-heterocyclic carbene (NHC) palladium complexes have been synthesized by Haag and co-workers.[111] These complexes were immobilized to dendritic polyglycerol supports and have been applied as catalyst for Suzuki cross-coupling reactions in water. The dendritic catalyst could be used in five consecutive reactions without loss of activity, although technically speaking a hyperbranched polyglycerol support has been used.

Vogt's group synthesized molecular-weight enlarged monodentate phosphine ligands via 'click' chemistry on tetraphenylmethane-based supports.[112] These ligands were reacted in situ to form the corresponding Pd(0) complexes and applied in the Pd-catalyzed Suzuki–Miyaura coupling of aryl halides and phenylboronic acid. The activity of these dendritic systems was found to be comparable to their monomeric analogues, and showed successful recycling for five runs by using a ceramic nanofiltration membrane.

Dendrimers and star-shaped molecules containing covalent Pd-C bonds

The above examples nicely illustrate the potential of palladium dendrimers in catalysis. Yet, due to the intrinsic properties of the palladium sites and the specific catalytic transformations, palladium leaching may be a serious limitation for the reuse or continuous use of some of these examples. One way to prevent Pd leaching is to include a covalent palladium-carbon bond. A few examples of these covalently bound palladium complexes bound to dendrimers or star-shaped molecules are described here. It is obvious that palladacycle-containing dendrimers also include covalent Pd-C bonds (*paragraph 1.3*).

Chen and co-workers synthesized a series of metal acetylide star-shaped molecules in which the metal center is covalently connected to the dendrimer (*figure 1.7*).[113] Palladium metal moieties were also added to terminal carbon atoms of the poly-yne. These compounds were tested for their fluorescent behavior. Photophysical data of these metal complexes showed that the absorption peaks shift to longer wavelengths and showed higher extinction coefficients compared to non-metalated equivalents. On the other hand, the luminescence quantum yield dramatically decreased for the palladated star-shaped molecule.

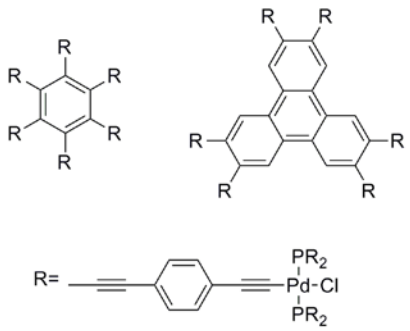

Figure 1.7: Star-shaped molecules containing a covalent carbon-palladium bond by Chen.[113]

Another example of a periphery-palladated dendrimer was synthesized in our group.[114] $Pd_2(dba)_3$ and TMEDA (*N,N,N',N'*-tetramethylethylenediamine) were reacted with a carbosilane dendrimer carrying twelve iodoarene groups and subsequent reaction with methyllithium and bipyridine (bpy) led to the air stable first generation palladadendrimer depicted in *figure 1.8*. These dendritic organopalladium(II) complexes were able to undergo oxidative addition with benzyl bromides yielding palladium(IV) compounds.[115]

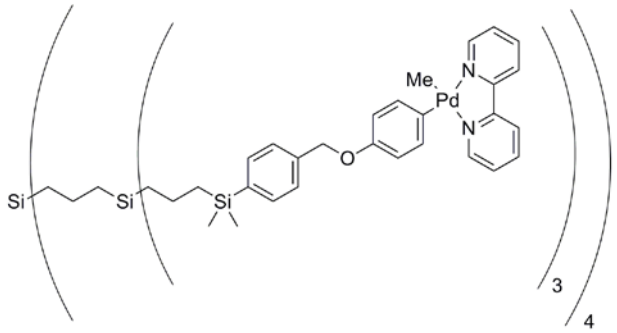

Figure 1.8: Van Koten's palladacarbosilane dendrimer containing covalent palladium bonds.[114]

1.2.2 Dendrimer-encapsulated palladium nanoparticles

A completely different type of dendrimer-based palladium catalysis has been performed with dendrimer-encapsulated nanoparticles (DENs). These metallodendrimers are examples of category d in *figure 1.1*. DENs combine the desirable physical and chemical features of metal nanoparticles with the tunable properties of dendrimers such as solubility, size, composition, structure, and surface reactivity.[116,117] Herein, the backbone of PPI or PAMAM dendrimers is used for coordinating palladium ions: it involves complexation of the palladium centers with interior tertiary amine functionalities. Once coordinated, the palladium ions can be reduced with an excess of sodium borohydride to obtain Pd(0), which aggregates into nanoparticles inside the voids of the dendrimer (*figure 1.9*). When the periphery of the dendrimer is functionalized with non-complexating entities, or in case the terminal amino groups are protonated prior to metal complexation, the metal binding can take place exclusively in the interior of the dendrimer.[117] Higher dendrimer generations (starting from G_3) stabilize metal nanoparticles by a combination of electrostatic and complexation interactions. Crooks and co-workers were able to synthesize DENs with various metals like copper, gold, platinum, iron, ruthenium and palladium.[117]

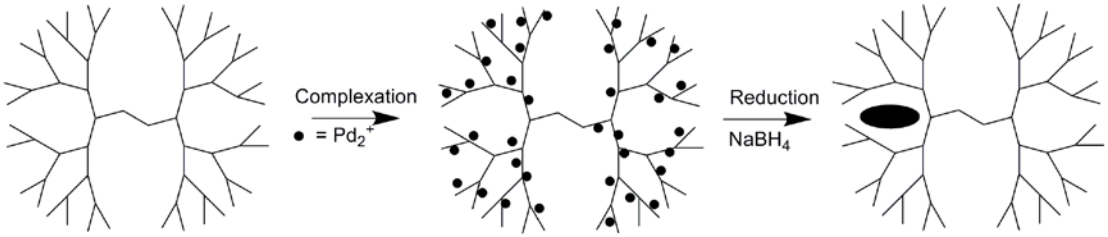

Figure 1.9: Strategy for the synthesis of nanoparticles encapsulated in PAMAM or PPI dendrimers.

Because of the ability of dendrimers to act as a molecular box by encapsulating guest molecules,[118] it is possible to filter out substrates of a certain size. This can be an interesting feature in catalysis. DENs have been used in this respect as size-selective hydrogenation catalysts in which the catalytic performance of Pd DENs is dependent on the substrate size. Larger substrates have more difficulties to reach the encapsulated nanoparticle, because of the steric bulk on the outside of the dendrimer. The same effect is observed, when the generation of the dendrimer is increased: bulkier substrates less likely reach the DEN's reactive site.

Niu *et al.*[119] reported such an effect in the hydrogenation of allylic alcohols. Comparing palladium nanoparticles in G_4-OH PAMAM dendrimers with its G_8-OH analogue, it was found that the turnover frequency for prop-2-en-1-ol dramatically decreases from 480 mol H_2 (mol Pd)$^{-1}$ h^{-1} to 120 mol H_2 (mol Pd)$^{-1}$ h^{-1}. This effect was seen for all tested substrates. Therefore, the dendrimer acts as a molecular filter. For G_4-OH(Pd_{40}) the TOF changed from 480 mol H_2 (mol Pd) $^{-1}$ h^{-1} for prop-2-en-1-ol to just 100 mol H_2 (mol Pd) $^{-1}$ h^{-1} for the more bulky enol 3-methyl-1-penten-3-ol.

Kaneda's group reported a way to hydrogenate 3-cyclohexene-1-methanol selectively out of a mixture with 3-cyclohexene.[120] Traditional Pd/C catalysts give incomplete conversions for both substrates, while PPI G_5-TEBA(Pd) (TEBA = triethoxybenzoic acid) nanoparticles give a quantitative reduction of 3-cyclohexene-1-methanol, while cyclohexene stays unaffected. Also bimetallic (palladium in combination with platinum or gold) dendrimer encapsulated nanoparticles have been successfully used in this way.[121]

Crooks recently prepared bimetallic PdAu DENs by co-complexing $PdCl_4^{2-}$ and $AuCl_4^{-}$ with a sixth generation PAMAM dendrimer and subsequent reduction by $NaBH_4$. Exposure to air resulted in selective reoxidation of the Pd atoms and subsequent re-reduction led to deposition of a Pd-rich shell on the surface of the remaining Au core. The resulting materials

are nearly monodisperse in size.[122-124] Until now, no successful use for Au or Pd-catalyzed reactions were reported for these materials. A review on bimetallic DENs has been written by Chandler and Gilbertson.[125]

Heck reactions have also been performed by using Pd DENs as catalysts. DENs based on PPI dendrimers decorated with perfluorinated tails catalyze the Heck coupling of butylacrylate with a series of aryl halides.[126] Milder conditions can be used with respect to more traditional colloidal catalysts (90 ^{o}C compared to 120 ^{o}C) and above all 100% isomer selectivity has been achieved in fluorous solvents, where colloidal catalysts usually produce selectivities of 80%. Other examples of Pd DENs acting as catalysts include Suzuki and Stille cross-coupling reactions at milder reaction conditions than necessary when using a conventional Pd(0) catalyst like $Pd(PPh_3)_4$.[127,128] On the other hand, De Jesús recently suggested that the Stille reaction catalyzed by PAMAM-dendrimer-encapsulated Pd nanoparticles occurred via Pd species that were leached from the Pd nanoparticle.[129]

Furthermore, Crooks *et al.* showed that tuning of reaction conditions including solvent, dendrimer structure, and dendrimer generation, for reactions taking place in the voids of DENs may yield isomers, which are unfavorable under 'normal' conditions. A nice example concerning this, is the use of palladium DENs in catalysis in supercritical CO_2.[130] Iodobenzene was coupled with methyl acrylate via a Heck coupling reaction to yield exclusively methyl 2-phenylacrylate (*figure 1.10*), while in hydrocarbon/fluorocarbon solvents the same DENs yielded only *trans*-cinnamate derivatives.[126] This selectivity is remarkable, since catalysis with standard palladium complexes or colloidal nanoparticles, results in *cis*- and/or *trans*-methyl cinnamate in supercritical CO_2.

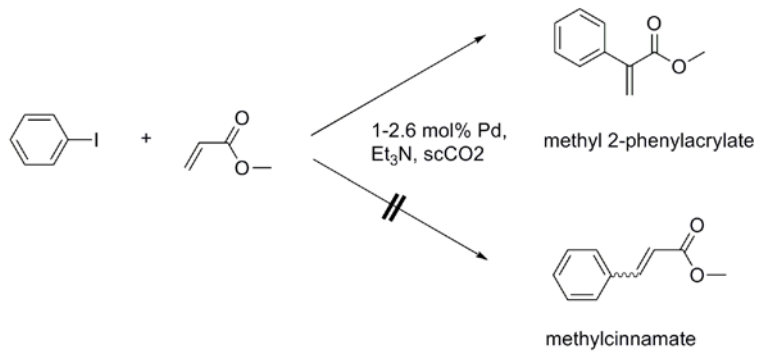

Figure 1.10: Remarkable selectivity in the Heck reaction of palladium DEN's derived from PPI dendrimers in $scCO_2$ yielding only methyl 2-phenylacrylate by Yeung et al.[130]

Astruc proved that 1,2,3-triazolyl dendrimers obtained by 'click' chemistry were ideal ligands for Pd(II).[131] These dendrimers contain ferrocenyl termini directly attached to the triazole ligand in order to monitor the number of Pd(II) that were introduced into the dendrimers by cyclic voltammetry. Reduction led to the production of various Pd DENs with a pre-organized number of Pd-atoms that was confirmed by TEM data for first and second generation dendrimers (G_1 and G_2). These DENs were efficient and size-selective hydrogenation catalysts that showed high TOFs in the hydrogenation of various olefin substrates. Analogous 'click'-dendrimer-stabilized Pd nanoparticles with other termini (including sulfonate-groups providing solubility in water) were also active in aqueous medium for hydrogenation and Suzuki–Miyaura coupling reaction with high TOF and TON numbers.[132,133]

1.2.3 Miscellaneous

A bimetallic platinum-palladium dendritic catalyst (a representative of class b in *figure 1.1*) was published by Liu and Puddephatt (*figure 1.11*).[134] A divergent route to organo-platinum or -palladium dendrimers was described. Here, mono- and tris-(2,2'-bipyridine)-containing molecules underwent metalation after treatment with a platinum precursor, subsequent oxidative addition of the platinum complexes with a focal benzylic bromide dendron decorated with two 2,2'-bipyridine end groups led to a dendrimer with platinum(IV) branching points. After dendrimer growth, the free bipyridine ligands in the periphery were platinated or palladated (see *figure 1.11* for a bimetallic complex). The latter step was performed with the precursor $[Pd_2Me_4(\mu\text{-pyridazine})_2]$. Higher dendrimer generations could not be synthesized due to solubility problems.

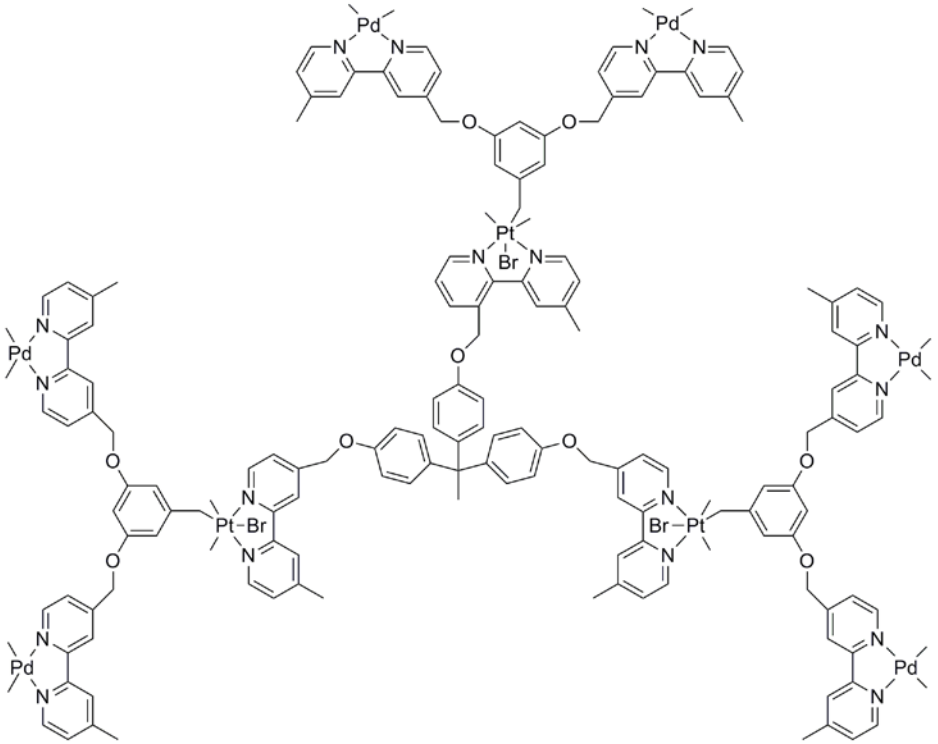

Figure 1.11: Puddephatt's double-metalated platinum-palladium dendrimer.[134]

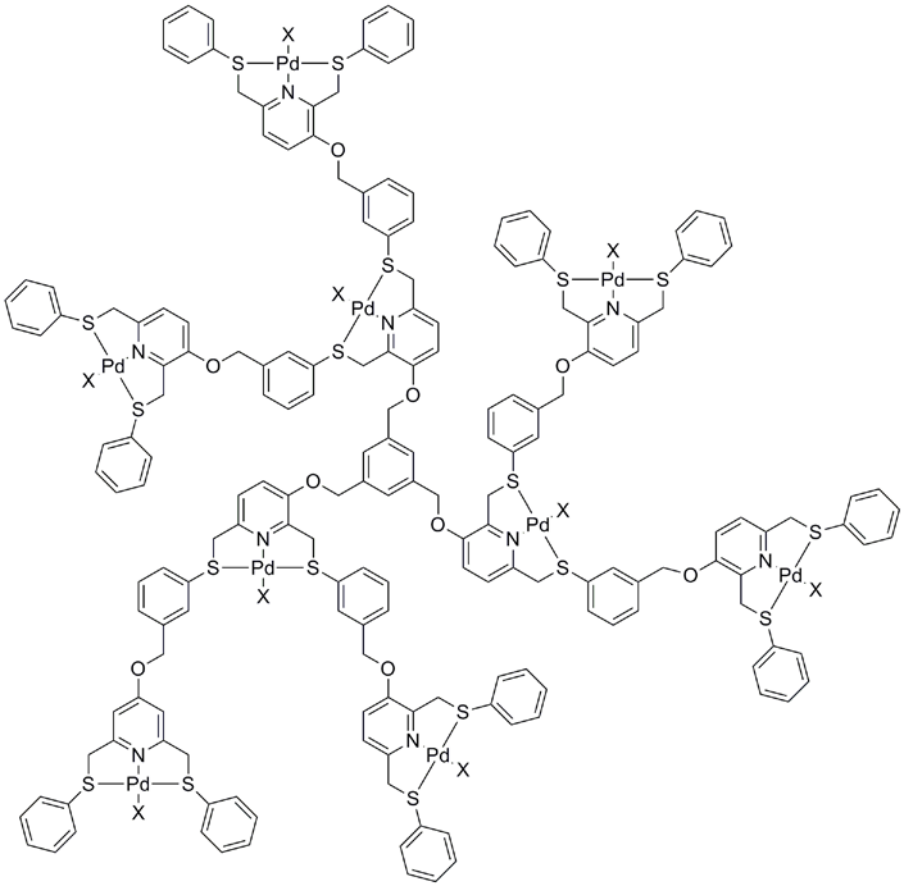

Figure 1.12: Dendritic structures synthesized by Chessa[135] *with X= NC-CH=CH-CN (idealized structure).*

Dendrimers with repeating SNS-pincer (*vide infra*) units have been synthesized by Chessa *et al*.[135] A Mitsunobu reaction was used to couple unsymmetrical pyridylthioether monomers to dendritic structures by a convergent route. In the last step, complexation of each binding site with $Pd_2(dba)_3{\cdot}CHCl_3$ led to palladadendrimers as depicted in *figure 1.12.*

Another strategy for the synthesis of bimetallic dendrimers was developed by Angurell.[136] Ru(*p*-cymene)Cl_2 was attached to the branches of a diphenylphosphino-terminated dendrimer. The key step in this synthesis involves the selective binding of the bifunctional 4-(diphenylphosphine)pyridinyl ligand via the *N*-donor atom to the ruthenium atoms (*figure 1.13*). Metalating the resulting species with $[PdCl(\eta^3\text{-}2\text{-}MeC_3H_4)]_2$ renders Ru/Pd dendrimers. Besides palladium, also gold and rhodium were incorporated in this way.

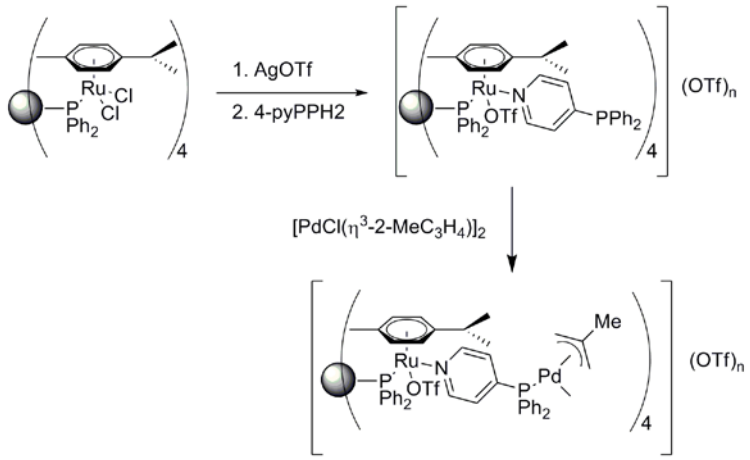

Figure 1.13: Synthesis of Ru/Pd containing dendrimers by Angurell.[136]

Palladium complexes have been used as core functionality in a few cases (see *figure 1.1(c)*). Vinogradov synthesized a series of dendritic polyglutamic palladium porphyrins via a divergent growth approach.[137,138] A widespread application of palladium(II)-porphyrin complexes is as phosphorescent indicators for oxygen measurements in various systems, including medical devices. These indicator molecules generally consist of the actual phosphor (here the metalloporphyrin) and a protective layer designed to provide biological compatibility of the molecule. Several properties of dendrimers (e.g. the globular shape and narrow molecular weight distribution) make this class of molecules interesting candidates to act as protective layer. Variation of the dendrimer size allows for the fine-tuning of the oxygen quenching properties of the phosphorescent indicator. The performance of the

probes was demonstrated in applications, including in vivo microscopy of vascular pO_2 in the rat brain.

PdTCPP (Pd-*meso*-tetra-*para*-carboxyphenylporphyrin) has been used as the core element in the dendrimer synthesis. Via an amide bond formation reaction with protected glutamic acid and subsequent basic deprotection, new carboxylic acid peripheral groups are formed. In this way the dendrimer is grown in a stepwise manner (*figure 1.14*).

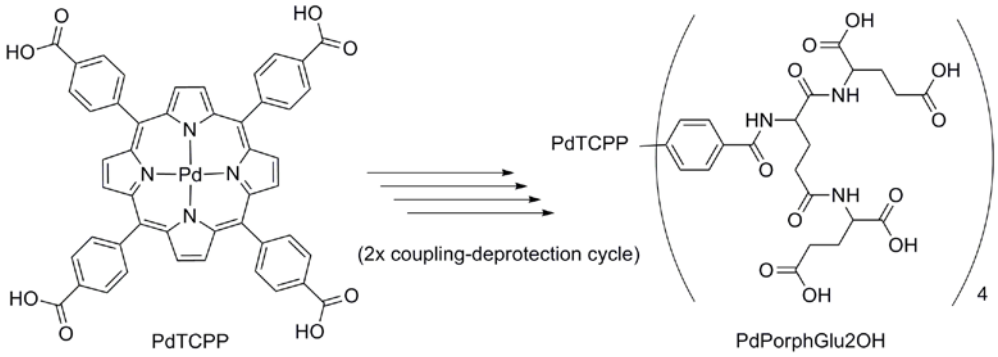

Figure 1.14: Dendrimer growth out of PdTCPP in a multistep synthesis

All these compounds phosphoresce strongly with λ_{max} = 690 nm and this phosphorescence can be quenched by addition of O_2. The quenching constants in DMF are almost unaffected by the dendrimer generation, while in water the K_q values significantly decrease with increasing dendrimer generation. Possibly, in water the conformation of the branches has changed, leading to either open or compact systems. Hereby, the oxygen diffusion barrier will be affected, and thus the kinetics for oxygen diffusion towards the phosphor.

In 2002 the same group reported a comparative study involving variation of the peripheral dendrimers.[139] Fréchet-type, and Newkome-type dendrimers were synthesized and compared to the earlier mentioned polyglutamate dendrimers. This investigation shows that the composition of the dendritic matrix has a major influence on the encapsulation properties of dendrimers.

1.3 Palladacyclic pincers on dendrimers and star-shaped molecules

1.3.1 The ECE-pincer complex: An introduction

All palladacycles attached to dendrimers and star-shaped molecules reported in literature so far, are so-called ECE-pincer palladium complexes, or highly related EC-half-pincer palladium compounds. The monoanionic pincer ligand, with general formula $[2,6\text{-}(CH_2E)_2C_6H_3]^-$ (ECE, where E is a group like NMe_2, PPh_2 or SPh, containing a neutral two-electron donor atom), and its metal complexes with the common structure as shown in *figure 1.15* have been subject of much research ever since their discovery in the late 1970s.[140-143] Probably the most interesting feature of pincer complexes is the presence of a stable σ carbon-metal bond combined with a high tunability of the coordination sphere around the metal. By varying the two-electron donor atoms E, the coordination sphere as well as the electronic properties of the metal site can be changed, while variation of the substituents of E and the *para*-substituent R modifies the steric and electronic properties of the metal site. Besides this, R is often used as anchoring site for many types of (macro)molecules including dendrimers. Furthermore, chirality can be introduced into the system by adapting the benzylic position of the pincer arms and by the use of stereogenic E groups.[144]

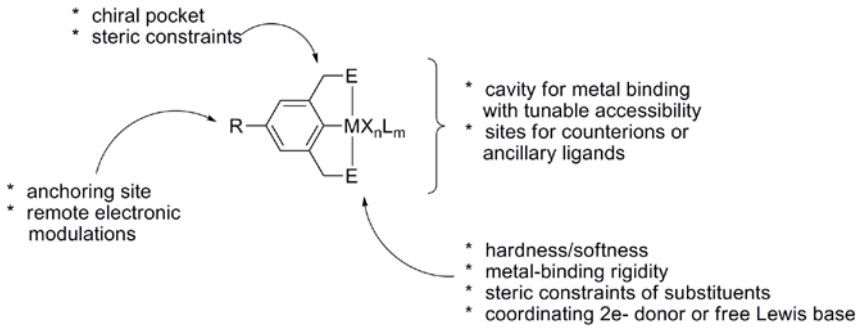

Figure 1.15: Common structure of ECE-pincer metal complexes, with potential modification sites.[144] X: halogen, L: ligand, E: neutral two-electron donor atom containing moiety, like NMe_2, PPh_2, SPh, R: substituents, usually an aliphatic, aromatic, or dendritic structure.

For the immobilization of pincer complexes on dendrimers and star-shaped molecules the substituent R is used. For such dendritic pincer constructs, NCN-,[145] PCP-,[146] and SCS-pincer[147] metal moieties have exclusively been used so far. In most of these constructs the palladium centers are introduced after connecting the ECE-pincer ligand to the dendrimer, because the resulting palladium metal complexes often do not withstand the reaction conditions used in previous steps. A disadvantage of this method is that a full dendrimer loading cannot always be achieved. Depending on the donor atom, different palladation routes have been developed.

In many cases, ECE-pincer arene ligand palladation can be achieved via an oxidative addition reaction on the pre-ligand, using either an activated C-halogen bond or otherwise a direct C-H bond activation step. In using these palladation procedures, selectivity may be an issue. Direct palladation with $[Pd(MeCN)_4](BF_4)_2$ at elevated temperatures in acetonitrile is the most often used route for synthesizing SCS-[147,148] and PCP-pincer[149,150] complexes from the corresponding arene ligands. Subsequent addition of a salt like LiCl or NaBr leads to formation of the halogenated complexes. In addition, $Pd(TFA)_2$ (TFA = tetrafluoroacetic acid) is widely used to synthesize PCP-pincer palladium complexes.[151] For NCN-pincer arene ligands, direct palladation cannot be performed selectively, so oxidative addition on NC(X)N (X = halogen) arene ligands with a $Pd(dba)_2$ or $Pd_2(dba)_3{\cdot}CHCl_3$ precursor complex in benzene is favored.[152,153] Starting from a non-halogenated NC(H)N-pincer arene ligand, the selective lithiation with *n*BuLi at C_{ipso}, followed by a transmetalation of the corresponding NCN-lithium intermediate with a palladium complex like $PdCl_2(cod)$ (cod = 1,5-cyclooctadiene) also leads to the NCN-palladium complexes.[154]

1.3.2 Pincer-palladium complexes on star-shaped molecules

The group of Van Koten reported on star-shaped molecules containing multiple NCN-palladium pincers for which the name cartwheel complexes was adopted. These structures consist of a central benzene ring, with either three or six pincer moieties attached (*figure 1.16*). The aromatic backbone of these compounds ensures a high rigidity, which is expected to be important for the use of the complexes as catalysts in a membrane reactor, since in general a high rigidity enhances the retention of compounds.[152]

These compounds have been tested as Lewis acidic catalysts in the double Michael reaction between ethyl α-cyanoacetate and methyl vinyl ketone[1] and were compared with a series of monomeric pincer complexes. In this monomeric series, the influence of the donor substituent E on the catalytic activity was investigated. It was found that for this particular reaction NCN-pincer complexes were superior to PCP- and SCS-pincer complexes. Within the NCN-pincer complexes, further research has been performed by using dimethylamine, pyrazol-1-yl, and 3,5-dimethylpyrazol-1-yl donor substituents. All three complexes showed good catalytic performance.

The pyrazole, SPh, and PPh_2 donor substituent-containing cartwheel palladium complexes have been synthesized successfully in a seven-step synthesis starting from 3,5-dimethylaniline.[148,152] Unfortunately, direct palladation of the hexakis pincer-ligand with dimethylamine donor groups did not lead to the completely metalated product. Some of these star-shaped complexes have been used for catalysis.

Although the hexakis(aqua-pincer) complex with E = pyrazole (pz), L = H_2O and X = BF_4, (*figure 1.16*) does not dissolve in dichloromethane, it does show catalytic activity in this solvent (70% conversion after 22h). To improve its solubility and thus the catalytic performance, also the tris-(pincer) complexes have been synthesized. The tris-(aqua-pincer) complex is soluble under the reaction conditions used, and shows a catalytic activity per palladium atom that is almost equal to the corresponding mono-pincer analogue (k_{obs} = 232 · 10^{-6} s^{-1} as compared to 279 · 10^{-6} s^{-1}).[152]

These shape-persistent, multimetallic materials were also used in olefin metathesis (RCM) for the template-directed synthesis of macrocycles.[155] Diolefin-substituted pyridines were coordinated to each of the six metal sites in both Pd(II) and Pt(II) cartwheel compounds and were subsequently subjected to standard olefin metathesis conditions with use of Grubbs-type Ru-catalysts aiming for a large macrocycle that would be formed after six olefin metathesis reactions of the twelve olefin arms. It was found that in particular disubstituted pyridines bound to a NCN-Pt(II) center gave fast metathesis reactions yielding the desired large macrocycles. The same reaction with the palladium analogue was less fast and less selective, since preliminary tests did not result in the formation of large macrocycles.

[1]Reaction conditions: 0.5 mol% [Pd], 10 mol% D*i*PEA, CH_2Cl_2, rt

Instead, isomerized products and a minor amount of intrapyridyl metathesis products were observed.

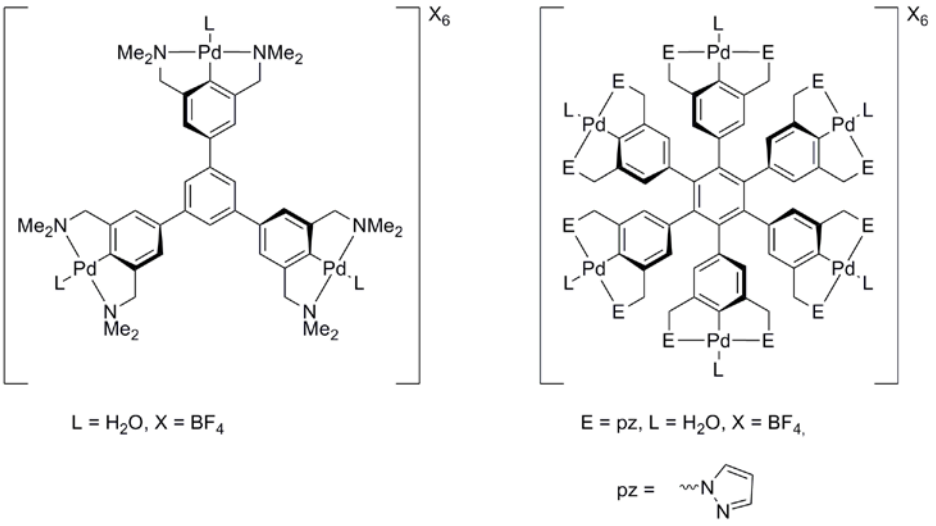

Figure 1.16: Star-shaped 'cartwheel' hexakis(NCN-Pd) dendrimer synthesized by Dijkstra et al.[152]

Further research on these type of compounds has provided a dodecakis-(pincer) compound. This compound comprises an aromatic core to connect twelve (dimethylamine) NCN-pincer palladium complexes via ether bonds (*figure 1.17*). Metalated monomers bearing a TBDMS protecting group on the *para*-position were deprotected and in situ coupled to a star-shaped dodecakis-bromide core molecule. Via this convergent approach, a complete palladium loading is ensured. This twelvefold coupling reaction was performed under mild conditions using $(NBu_4)F$, K_2CO_3 and 18-crown-6 as reagents, which do not damage the palladium centers at all.[156] A dendrimer, consisting of a tetraarylsilane core and eight NCN-pincer palladium complexes attached via ether bonds in the same way as in the dodecakis-(pincer) was synthesized in the same way.[85,145,156]

These compounds were also tested in the double Michael reaction. The tetraarylsilane dendrimer shows a comparable activity per palladium center with the earlier mentioned monomeric and trimeric compounds (k_{obs} = 2.1 · 10^{-4} s^{-1} vs. 2.3 · 10^{-4} s^{-1}). The dodecakis-(pincer) compound, however, shows an almost threefold increase in catalytic activity per palladium(II) center (k_{obs} = 8.1 · 10^{-4} s^{-1}): clearly a positive dendritic effect is observed. Probably, the closer proximity of the palladium sites and thus possible involvement of cooperative effects between different palladium(II) centers is the reason for this increase.

Another possible explanation is that aggregate formation could create highly polar micro-environments, which enhance the catalytic performance.[85]

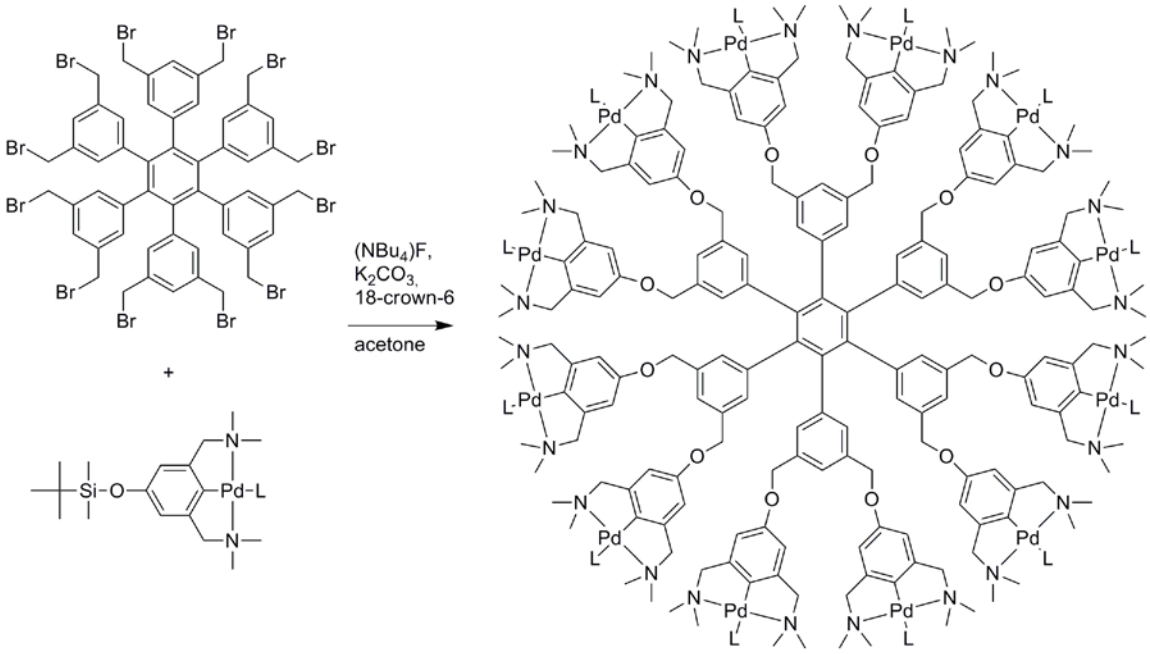

Figure 1.17: Synthetic route to a star-shaped dodecakis-(NCN-Pd) cartwheel complex as synthesized by Dijkstra et al.[145]

The high rigidity of these star-shaped molecules makes them excellent candidates for performing nanofiltration experiments. The retention of these compounds was tested by using the deep orange color of the corresponding neutral NCN-pincer Pt(II)-SO_2 complexes by monitoring them with UV/Vis spectroscopy.[144] These five-coordinate adducts were obtained by reversible binding of SO_2 to NCN-platinum complexes and were used as an extremely sensitive gas sensor which is not disturbed by the presence of other gases.[144] By using the commercially available MPF-60 membrane with a molecular weight cut-off (MWCO) of 400 Da, a carbosilane G_1-dendrimer bearing twelve Pt(NCN)(SO_2) pincer moieties shows a retention of 0.995. The dodecakis-(pincer) cartwheel compound, however, shows a retention larger than 0.999 when using the MPF-60 membrane and a retention of 0.999 is determined when an MPF-50 membrane (MWCO = 700 Da) is used.[156]

Then, the dodecakis-(pincer) palladium complex was tested for the double Michael addition in a continuous flow membrane reactor using an MPF-50 membrane.[2] The catalyst was found to be stable under the continuous reaction conditions as a constant activity was obtained over prolonged reaction times (26 h, 65 exchanged reactor volumes). The total turnover number of the catalyst increased by almost a factor 40 compared to the batch experiment (80 mol/mol Pd versus over 3000 mol/mol Pd for the continuous process). Finally the retention was determined at 0.995, thereby making these compounds suitable for the use in a continuous flow membrane reactor.[145]

The group of Van Koten in collaboration with Beletskaya's group also synthesized rigid star-shaped molecules functionalized with PCP-pincer palladium complexes. These are very similar to the earlier mentioned hexakis(NCN-pincer Pd) compounds, yet in these compounds an acetylene bridge is used to connect the core and the peripheral arene groups, which further improved the rigidity of the compounds. Metalation of the tris-ligand proceeded quantitatively to yield the corresponding trinuclear palladium complexes, whereas metalation of the hexa-ligand did not fully proceed. The tris-(pincer) complex was tested as pre-catalyst in the Heck reaction of iodobenzene and ethyl acrylate and compared to the monomeric species. In this reaction the tris-(pincer) compound showed a lower activity and TON than the monomeric species, which is presumably due to steric factors.[146,150]

The group of Vogt has recently published similar molecular-weight enlarged triple PCP-pincer ligands which were in situ palladated with $[(allyl)PdCl]_2$ and used as catalyst in continuous allylic alkylation and amination reactions.[157] In the allylic alkylation of cinnamyl acetate with dimethyl malonate and the allylic amination of cinnamyl acetate with morpholine, respectively, 30 and 80% conversion of the starting materials was observed. In these continuous experiments no Pd black formation was found.

SCS-pincer-porphyrin hybrids (*figure 1.18*) represent another type of star-shaped molecules.[158] These multi-ligand site compounds contain a porphyrin core and four pincer arms, in which each of the two different sites can be selectively metalated without metalating the other site.

[2]Reaction conditions: 4,2 µmol [Pd], 2M methyl vinyl ketone, 0.064M D*i*PEA, 0.64M ethyl α-cyanoacetate, 0.4M *n*-decane, CH_2Cl_2, flow rate = 30 mL h^{-1}, residence time τ = 0.4 h, 23 °C, 20 bar

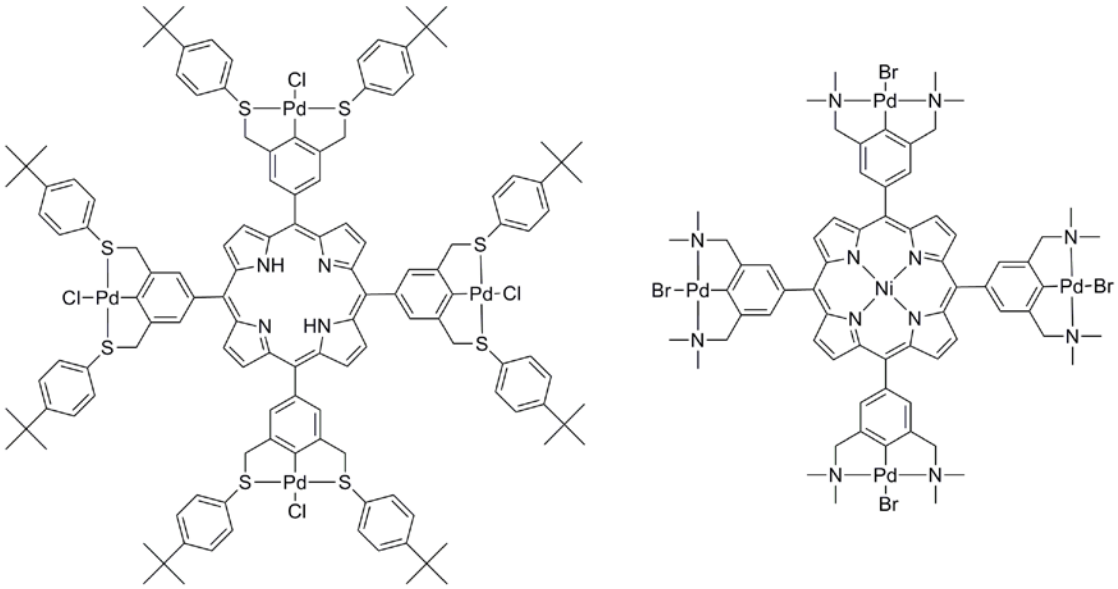

Figure 1.18: SCS-pincer palladium porphyrin hybrids synthesized by Suijkerbuijk et al.[158,159]

A series of various *meso*-tetrakis-(SCS-pincer PdCl)-(metallo)-porphyrin hybrids (with as central metal M = 2H, Mg(II), Mn(III)Cl, Ni(II)) were used as pre-catalyst for the Heck reaction of styrene with iodobenzene in DMF. Although none of these complexes reached the initial catalytic activity of the monomeric SCS-pincer palladium chloride complex, the catalytic performance of the reaction mixtures was strongly dependent on the metal present in the porphyrin center. The magnesium chelate turned out to have the highest initial activity of the bimetallic complexes, followed by the nickel-, the free base, and the manganese complexes. The order of activity follows the order of the electron-donating ability of the (metallo)porphyrin, that is, the more electron-donating the (metallo)porphyrin, the greater the initial catalytic activity. This study demonstrated that catalytic rate can be influenced by remote tuning of the catalyst by changing a distant modulating substituent in one step (in this case metalation of another 'remote' metal complex).[160] In a following paper this was manifested in changes in the optical and ligand-binding properties of the metalloporphyrin part upon reactions at the peripheral pincer sites.[159] In particular, the fact that only one reaction step performed under mild conditions can lead to remote control, makes this discovery even more intriguing.

1.3.3 Non-covalently bound dendrimer-pincer palladium complexes: Dendritic catalysts

Non-covalent metallodendritic assemblies containing NCN-pincer palladium complexes have been reported by Van de Coevering *et al*.[161] In this study, ionic core-shell dendrimers, were used as a dendritic host molecule. This core-shell molecule consists of a tetraarylsilane core, eight quaternary ammonium groups and accordingly eight bromide counterions, and a dendritic shell of different generations Fréchet-type dendrons. Three generations dendritic hosts have been used. Incorporation of (functional) guest molecules in these dendrimers can be achieved by means of anion exchange. Exchange of the bromide anions with eight anionic, sulfate-terminated pincer complexes yields the octakis-NCN-pincer Pd dendrimer, shown in *figure 1.19* (as an typical example of class a in *figure 1.1*). This exchange reaction can be performed via simply adding eight equivalents of the tetrabutylammonium salt of the pincer anionic monomer to the octacationic dendrimer with bromide counterions in dichloromethane. Subsequently, the metallodendritic assembly was isolated by aqueous washing steps to remove tetrabutylammonium bromide, followed by passive dialysis.

The formation and stoichiometry of this assembly and the strength of the ionic bonds were investigated by various analytical techniques. NOESY NMR measurements showed that the sulfato groups of the catalysts are located in close proximity of the octacationic core, and nano-ESI mass spectroscopy proved the stoichiometry of the non-covalent metallodendritic assemblies. Pulse gradient spin-echo (PGSE) NMR diffusion measurements were also performed on these dendritic assemblies to determine the diffusion coefficients for the octa-cation and the anions. Octacationic dendrimers of generation 1-3 were compared to gain insight in the freedom of movement of the anion in the dendritic shell of the assembly. For the first and second generation dendritic assemblies, a small, but reproducible, difference (1.5% for G_1, 3.2% for G_2) in the diffusion coefficients between anion and cation was found with the anion diffusing slightly faster than the cation. This might be due to an equilibrium in which small quantities of the separated cations and anions contribute. For G_3 this difference in diffusion coefficients is not observed. Apparently, the anion is more tightly trapped into the dendrimer when the dendritic shell is larger.

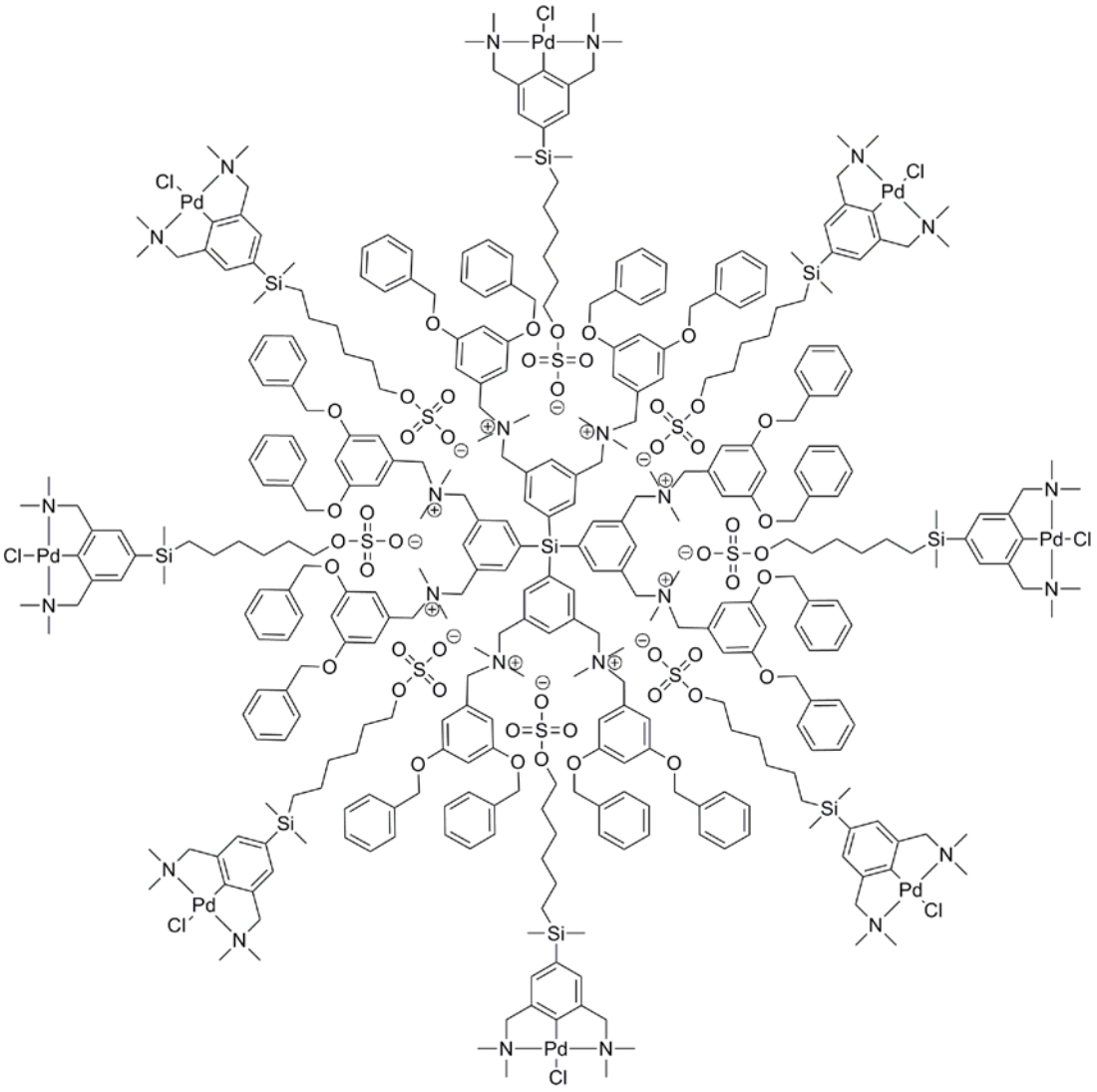

Figure 1.19: G_1 non-covalent metallodendritic assembly by Van de Coevering et al[161]

The catalytic performance of the dendrimer-supported and unsupported NCN-pincer Pd complexes was investigated by performing the aldol condensation reaction between methyl isocyanoacetate and benzaldehyde.[154,162] It was found that the metallodendritic NCN-pincer palladium chloride assemblies show comparable turnover frequencies (TOFs), conversion, and product distributions per Pd center compared to their monomeric anionic analogue with tetrabutylammonium ions as countercations.

In this study, two strategies were used to vary the structure of the dendrimer from exposed catalytic sites at the periphery towards encapsulated catalytic sites at the inside of the dendrimer. The first strategy was to alter the thickness of the dendritic shell, which was achieved by changing the generation of the dendrimer or by the attachment of dodecyl groups at the periphery. The latter method also heavily influences the polarity of the

dendrimers. The other strategy was to vary the length of the tether between the pincer and the sulfato group. Using these strategies, only small differences in catalytic performance were found. Apparently, the structure of the dendritic shell in the assemblies is relatively open, which keeps the catalytic Pd(II)-sites reasonably well accessible for the reactants. The dendrimer decorated with dodecyl groups at the periphery, however, displays a significantly lower activity, pointing to a more dense structure, in which the palladium center is less accessible for reactants.

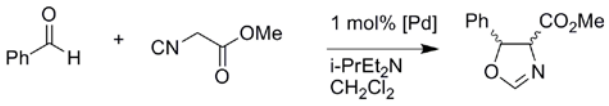

Figure 1.20: Aldol condensation reaction between benzaldehyde and methyl isocyanoacetate

These non-covalent, metallodendritic assemblies offer an interesting addition to the palette of dendritic catalysts. Remarkably, they do not show a decrease of the catalytic activity upon incorporation of the homogeneous catalyst on the dendritic hosts, which is possibly due to the flexibility of the resulting metallodendritic assemblies. The modularity in the synthesis of those assemblies, furthermore, opens the way for the incorporation of many other homogeneous catalysts. The non-covalent nature of the assemblies also allows the recycling of either or both the dendritic support and the anion-tethered catalyst as well.[163] Reviews on non-covalent catalyst anchoring to functionalized dendrimers and other polymeric supports has been reported by Ribaudo *et al.*[164] and Van de Coevering *et al.*[165]

1.3.4 Non-covalently bound dendrimer-pincer palladium complexes:

Self-assembled dendrimers

The group of Reinhoudt has performed extensive research on the incorporation of SCS-pincer palladium complexes in dendrimers and has published a range of articles starting from 1995. Unlike the non-covalently bound dendrimers shown in the previous section, these dendrimers have metal sites at every branching point (class b in *figure 1.1*). Numerous

self-assembled dendritic structures have been synthesized, all of which are based on coordinative interactions and hydrogen bonding between different building blocks.

The first report by Huck *et al*.[147] used a G_0 tweezers dendron (*figure 1.21* with R = CN and X = MeCN), which upon evaporation of the acetonitrile solvent formed self-assembled spheres by coordination of the cyano group of one building block to the palladium center of another. In this manner non-covalent, hyperbranched polymers were obtained. Different size measurement techniques such as Quasi-Elastic Light Scattering (QELS), Atomic Force Microscopy (AFM) and Grazing-Angle FT-IR spectroscopy have been performed on these spheres. All techniques showed objects with a diameter of about 200 nm with a relative narrow distribution: 95% of the diameters were found within $2\sigma_d$ of the mean value.

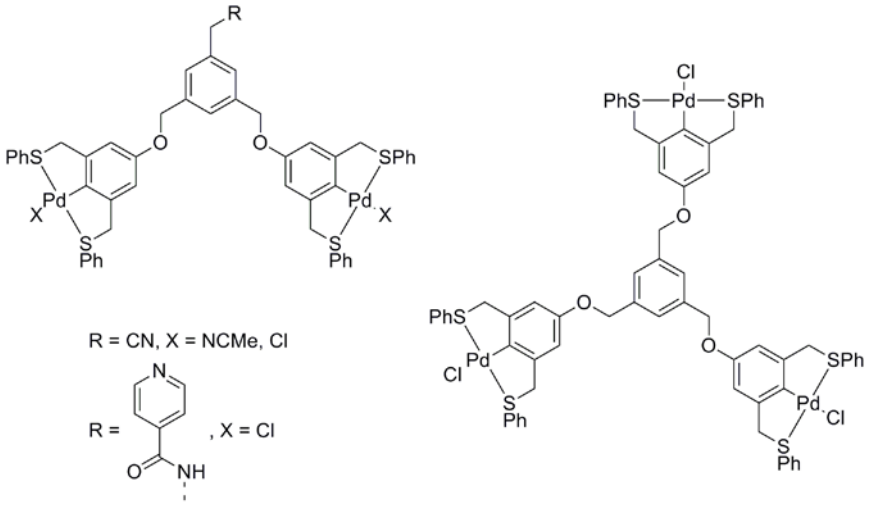

Figure 1.21: A tweezers SCS-pincer palladium dendron[166] (left) and an tris-SCS-pincer palladium complex dendrimer core moiety (right)[167]

This protocol was adapted by using the dendron depicted in *figure 1.21* with R = CN and X = Cl in combination with a tris-(pincer) core (*figure 1.21*).[167] In this way, G_0 dendrimers can be formed in a controlled manner: the chloride ions of the core molecule are replaced by non-coordinating BF_4^- ions by reaction with silver tetrafluoroborate. Addition of three equivalents of the dendron shown in *figure 1.21* yields the G_0 dendrimer. Halogen removal and subsequent coupling enables further growth of the self-assembled organometallic dendrimer. This process can be repeated several times to obtain non-covalent dendrimers up to the fifth generation and proceeds in a very controlled manner due to the strongly

bound chloride ion, which temporarily protects the palladium center. The G_1 resulting dendrimer is shown in *figure 1.22*.

To give insight in the diameter of these nanoscale molecules, Tapping Mode Atom Force Microscopy (TM-AFM) measurements have been performed. These measurements illustrated that the G_5 dendrimers have diameters of approximately 15 nm. Similar structures containing star-shaped dendrimer consisting of a benzyl ether core and three PCP-pincer palladium complexes were later published by Huck as well.[149]

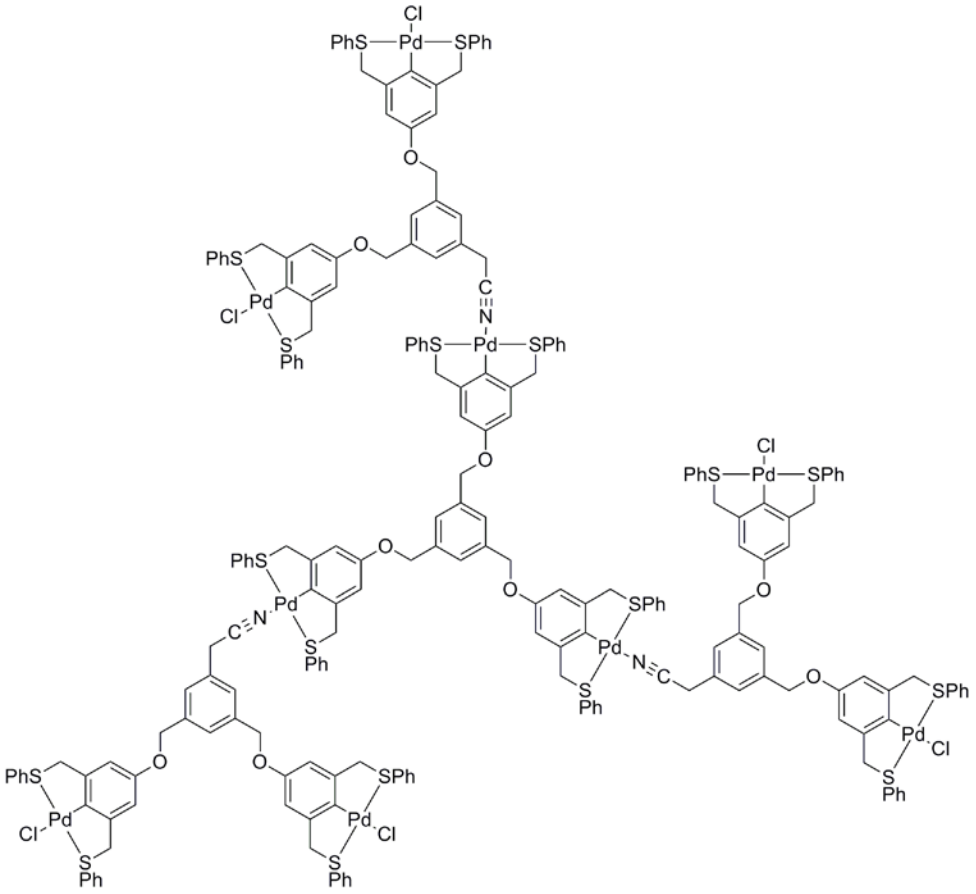

Figure 1.22: Non-covalently bound G_1-pincer dendrimer by Huck et al.[167]

For the controlled assembly of metallodendrimers in either a convergent or a divergent way, besides a cyano-based building block, also a pyridine-based building block was synthesized (*figure 1.21*, R = isonicotinamide (= NHC(O)-C_5H_4N)).[168] With a combination of pyridine- and cyano-based building blocks, dendrons and metallodendrimer assemblies up to the third generation were obtained. Stable dendrons are formed in a divergent way by using the relatively strongly coordinating pyridine-based ligands, however for convergent assemblies

to the trivalent core molecule (*figure 1.21 right*) dendrons bearing a cyano-based ligand has to be used. By doing this (in a convergent strategy), the coordinative strength of the ligands bound to the palladium(II) pincers from the periphery to the core decreases. In this way, scrambling of various building blocks is avoided.

Due to the presence of SCS-pincer palladium complexes at the periphery of these polycationic metallodendrimers, their solubility in organic solvents is moderate. With the introduction of a hydrophobic dendritic layer this solubility increases.[166,169] Again, ligands that are stronger than the interior ligands are required for a convergent synthetic route. Dendritic phosphine ligands (Fréchet-type dendrons were used) met these requirements and were successfully coordinated to the peripheral SCS-pincer palladium(II) complexes. In this case, in every new generation, another class of functional group (i.e. cyano-, pyridine- and phosphine ligands), has been used as the coordinating assembly motif. For these assemblies, indeed, the solubility in apolar solvents increases accordingly.

This self-assembly strategy also allowed the introduction of redox- or photoactive fragments in both the core and periphery, provided that those moieties can be functionalized with palladium pincer complexes or suitable ligands.[170] For example, Huck used porphyrins in the non-covalent assembly of dendrimers, functioning both as core molecules and as peripheral groups.[170] Starting from a porphyrin core moiety that contains four SCS-pincer palladium complexes at its meso-positions, dendrimers of generation 0 and 1 were grown by BF_4^- anion exchange and subsequent addition of the dendritic SCS-pincer palladium-based building blocks of *figure 1.21 (left)*. Then porphyrin end groups that coordinate via a pyridine nitrogen to the palladium in the pincer (as the peripheral porphyrin groups in *figure 1.23*) were introduced. This process has yielded dendrimers with a porphyrin core and either four (G_0Por_4, *figure 1.23*) or eight (G_1Por_8,) porphyrin end groups. These dendrimers may be interesting for the construction of donor-acceptor systems in which energy transfer from the core porphyrin to the periphery porphyrins and vice versa can take place.

In a similar way, the tris-(pincer) core as shown in *figure 1.21* is used as core molecule and was grown to G_1 and G_2 dendrimers with the building blocks that are also depicted in *figure 1.21*. These dendrimers were then functionalized with porphyrins in the same manner as described above and have yielded G_0Por_3, G_1Por_6 and G_2Por_{12}.

For visualization and, ultimately, manipulation of individual nanosized dendritic molecules on a surface, G_0, G_1 and G_2 pyridine-coordinated dendrimers have been attached to either a

sulfide monolayer coated gold surface[171,172] or gold nanocluster.[173] Due to their regular structure, these self-assembled monolayers (SAMs) are useful starting materials for the development of nanometer-scale devices, which require controllable positioning of functional nanosized molecules.

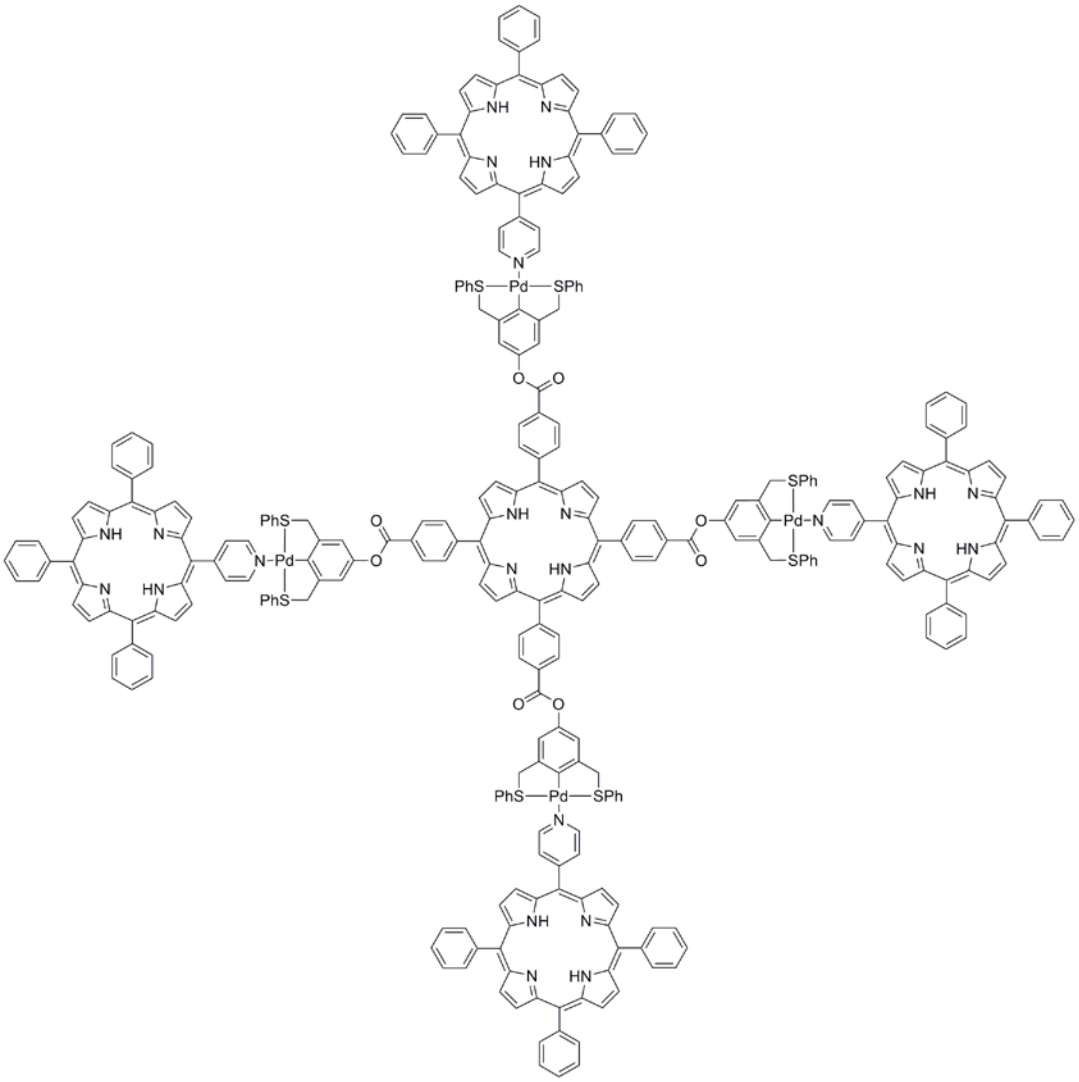

Figure 1.23: The multiporphyrin dendrimer G_0Por_4 by Huck et al.[170]

In a first attempt,[171] it has been shown that metallodendrimers functionalized with long sulfide side chains can be inserted as individual particles in an alkanethiol monolayer. Moreover, the number of isolated dendrimers could be controlled, since the amount of desorption of the alkanethiol chains from the SAM, and subsequent adsorption of the derived metallodendrimers at these deficiencies in the surface are time-dependent processes.

Van Manen *et al.* synthesized the same sort of nanometer-scale dendritic structures.[172] A dendritic wedge containing peripheral pyridines and a focal dialkylsulfide chain was synthesized. The peripheral pyridines were coordinated to a second generation Fréchet-type dendron functionalized with a focal SCS-pincer moiety. The focal dialkylsulfide tail has been used to anchor these nanomolecules to the gold surface. Highly complex assemblies have been made in this way (*figure 1.24*). TM-AFM height images clearly showed an increase in size when the second dendritic moiety with the focal SCS-pincer complex (grey cone in *figure 1.24*) was coordinated to the dendron-containing SAM.

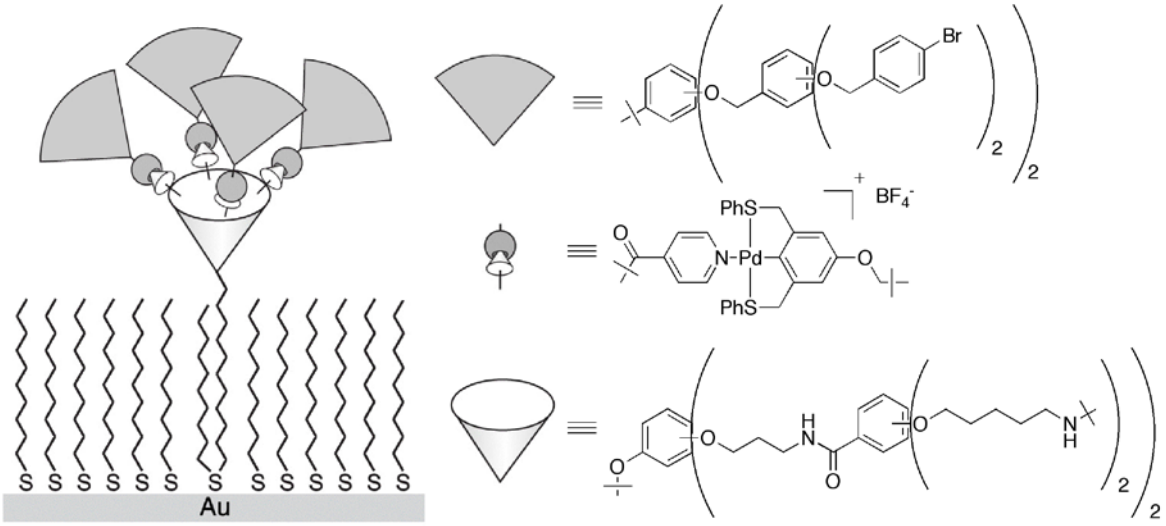

Figure 1.24: Schematic representation of the non-covalent surface-confined dendrimers synthesized by Huck et al.[172]

Later, Friggeri monitored the growth of surface-confined, nanometer-sized, coordinative SCS-pincer dendrimers on gold nanoparticles.[173] The embedding of the isolated dendritic pincer palladium complexes bearing a long sulfide chain adsorbed onto the decanethiol SAMs on gold was carried out in dichloromethane. Dendrimer growth was performed in a similar way as in the examples shown above. TM-AFM measurements showed that individual molecules were obtained with a height and diameter of 4.3 $\pm$ 0.2 nm and 15.3 $\pm$ 4 nm, respectively.

A very interesting combination of coordination chemistry and hydrogen bonding was reported by Huck *et al.*, using a barbituric acid residue (*figure 1.25*, left molecule) as a core moiety.[174] The tweezers-like dendrons of *figure 1.21* were used to build up the dendritic

wedges via repetitive deprotection-coupling steps (*vide supra*). Upon acquiring the desired dendrimer generation, the melamine derivative is added at low temperature (-30 °C). Three wedges self-assemble by numerous, selective hydrogen bonds around three melamine derivatives. The core moiety of the obtained rosette assembly is shown in *figure 1.25* (right); its structure was confirmed by the use of low-temperature ^{1}H NMR (-30 °C – -60 °C) in combination with 2D NOESY and TOCSY NMR.

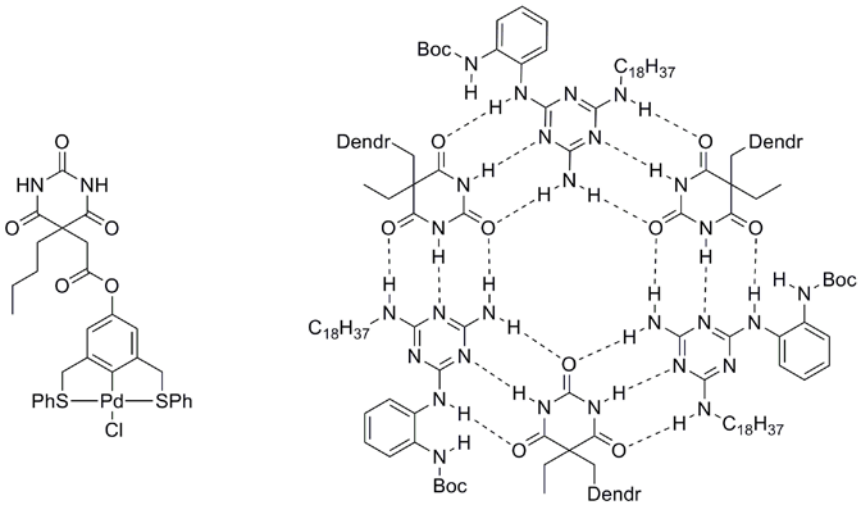

Figure 1.25: Barbituric acid functionalized SCS-pincer palladium complex used for hydrogen bonding-assisted self-assembly (left) and the hydrogen bonding based self-assembled dendrimers by Huck et al. (right).[174]

Furthermore, the group of Reinhoudt has published the synthesis of a non-covalent water-soluble dendrimer containing ligands based on either linear sugars or tetraethylene glycol (*figure 1.26*).[175] These ligands were coordinated via the pyridine or phosphine group to either a tris- or hexakis(pincer) palladium compounds with a benzyl ether as core molecule. In *figure 1.27* a peripheral fragment of a water-soluble dendrimer based on tetraethylene glycol is depicted. Three molecules, as shown in this figure, have been coordinated via the focal pyridine moiety to a tris-(SCS-pincer palladium complex) (*figure 1.21 right*) leading to a large, nanoscale-sized metallodendrimer having 18 peripheral tetraethylene glycol groups.

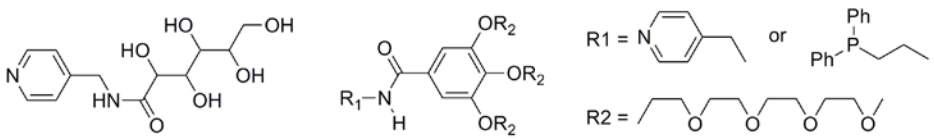

Figure 1.26: Water-soluble ligands based on a linear sugar (left) or tetraethyleneglycol (right)[175]

The compounds based on the linear sugar, unexpectedly, turned out to be poorly soluble in water, resulting in an aqueous gel. The solubility of the pyridine-coordinated compounds that were decorated with tetraethyleneglycol chains in water was also moderate. However, the compounds containing phosphine-bound tetraethyleneglycol moieties were highly water-soluble. Therefore, this ligand was used to synthesize water-soluble G_1 metallodendrimers bearing a hydrophilic periphery. A general, comprehensive review on non-covalent metallodendrimers was published by Van Manen *et al.* in 2001.[176]

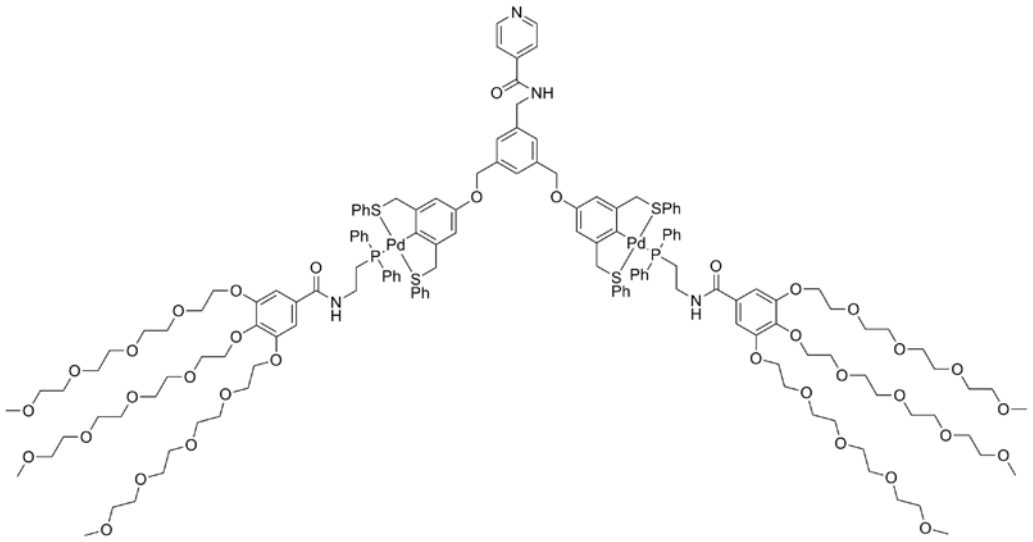

Figure 1.27: A peripheral fragment of a water-soluble wedge based on tetraethylene glycol by Van Manen.[175]

1.3.5 EC-half-pincer palladium complexes on dendrimers

One of the most simple ways of obtaining a palladacyclic compound is the reaction of benzylamines with $Pd(OAc)_2$ to yield so-called 'half-pincer' complexes. These complexes have e.g. been used in catalysis[177] and as resolving agents.[178] In a report by Kleij *et al.* NC-half-pincer palladium compounds were coupled to a second generation carbosilane dendrimer, resulting in a dendritic structure as shown in *figure 1.28*. An interesting characteristic of the half-pincer compounds is the possibility to dimerize. In the absence of a suitable Lewis base (like e.g. pyridine), the Pd-Cl group bridges with another Pd-Cl group,

forming either *cis*- or *trans* chloride bridged dimers. Upon addition of an excess of pyridine these dimers can be broken down to monomeric NC-half-pincer palladium units.

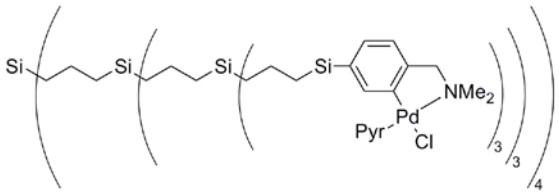

Figure 1.28: NC-half-pincer palladium-functionalized G_2-dendrimers by Kleij et al.[177]

Three generations of these metallodendrimers functionalized with the corresponding cationic aqua complexes (as depicted in *figure 1.28*, but with the chloride ion replaced by a water ligand), as well as the G_0 and G_1 dendrimers containing a shorter two carbon-atom linker per branching unit, were tested for their catalytic performance in the earlier mentioned aldol condensation reaction[3] and compared with their monomeric equivalents. It was found that all conversions were very high (96 - 99%) after 24h, except for the G_1-two carbon linker, which showed a significantly lower conversion of 55%. A slight decrease in total turnover numbers per palladium(II) atom was determined with increasing dendrimer generation. Therefore, it was concluded that the increased bulk around the palladium centers decreases the catalytic activity due to decreased accessibility. The less crowded, lower generation dendrimers are as active per palladium center as the monomeric species and thus might be interesting for application in catalysis in a continuous flow membrane reactor, provided that their retention is high enough.[177]

1.3.6 Dendrimers containing functional groups in the vicinity of palladacycles

Via the introduction of functional entities in the vicinity of the ECE-pincer metal center on a dendrimer, attempts have been made to influence the catalytic properties of the metal center. To the best of our knowledge, two reports on this subject have been published. These reports represent encapsulated pincer complexes or pincer complexes in the vicinity of functional groups were expected to promote regio- and stereocontrol.

[3]Reaction conditions: 0.94 - 1.19 mol% [Pd], 10 mol% D*i*PEA, CH_2Cl_2, rt

Rodríguez synthesized macrocyclic carbodiazasilane molecules containing NCN-pincer ligands.[153] In these complexes, the NCN-pincer palladium(II) sites are encapsulated by strategic placement of diphenylsilane moieties. By means of a *para*-hydroxy functional group on the pincer moiety of these encapsulated complexes, the pincers were connected to tricarboxy core molecules to yield new metallodendrimers. The pincer ligands could be palladated by addition of $Pd(dba)_2$, thereby forming *meso*-diastereoisomers in a selective way (*figure 1.29*, left compound). With these compounds, possible changes in catalytic properties by secondary interactions were studied. In aldol condensation reactions,[4] the catalytic activity per palladium site of these dendrimers was higher than for the mononuclear system (conversion >99% vs. 89%): a small, yet significant positive dendritic effect. Other catalytic properties, like the diastereoselectivity, did not show a significant change.

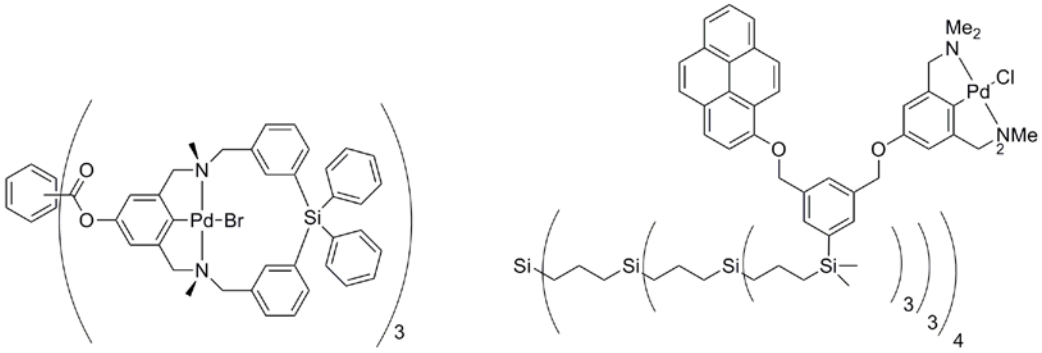

Figure 1.29: Multimetallic dendritic system with encapsulated catalytic sites synthesized in the group of Van Koten by Rodríguez (left) and Slagt (right)

Slagt prepared pyrenoxy-based NCN-pincer palladium molecular tweezers which were coupled to inert carbosilane dendrimers.[179] This tweezers consists of three parts: (1) a NCN-pincer palladium complex, (2) a pyrenoxy unit and, in between, (3) a xylyl spacer. Crystal structures show a completely flattened conformation of the tweezers in the solid state, due to favorable intramolecular π-stacking interactions. The close proximity of the pyrenoxy unit and the NCN-pincer palladium unit, which is caused by cation-π interactions leads to a small, but significant, rate enhancement of the aldol condensation reaction of aromatic aldehydes with methyl isocyanoacetate.

[4] Reaction conditions: used substrates are methylisocyanate and benzaldehyde, 1 mol% [Pd], 10 mol% D*i*PEA, CH_2Cl_2, rt

The tweezers was coupled to a carbosilane dendrimer by lithiation of the tweezers bromide with *t*BuLi, and subsequent quench with a G_2 dendrimer, containing 36 peripheral chlorodimethylsilyl groups. After palladation, the molecule in *figure 1.29* (right) was obtained. The monomeric tweezers and the dendrimer-decorated tweezers were both tested in the aldol condensation reaction of methyl isocyanoacetate and benzaldehyde[5]. Compared to the monomeric species, the dendritic compound showed a lower conversion, while at the same time, the *cis*/*trans*-ratio was not affected. This negative dendritic effect regarding to conversion was attributed to the increase in steric crowding, making various catalytic sites inaccessible for substrate molecules.

1.3.7 ECE-pincer palladium complexes on polymers

Not only dendrimers have been used as support for palladacycles. The groups of Bergbreiter and Weck have performed extensive research on pincer palladium complexes attached to polymers to be used in carbon-carbon bond-formation reactions. Bergbreiter connected SCS-pincer palladium catalysts to poly(ethylene glycol) (PEG), poly(*N*-isopropylacrylamide) (PNIPAM), and poly(*N*-octadecyl-acrylamide) (PNODAM) polymers. These polymeric materials were selected because of their high thermal stability with respect to Pd(0) catalysts.[180-182] Heck and Suzuki reactions with aryl iodides and various acceptor substrates were successfully performed in a *N*,*N*-dimethylacetamide/heptane mixture with triethylamine as the base in air at elevated temperatures.

In 2002, Weck and co-workers published side-chain functionalized polymers containing palladated SCS-pincer complexes at each repeating unit.[183,184] A palladated monomeric unit containing a bicyclic alkene was polymerized via ring-opening metathesis polymerization (ROMP) with a Grubbs I catalyst to form these poly(norbornene) chains. These metallopolymers were used as catalysts in Heck coupling reactions and subsequently as coordinative centers for pyridine- or nitrile-containing substrates (*figure 1.30*). In another publication, cross-linked functionalized polymers were obtained by coordination via

[5] Reaction conditions: 1.0 mmol methyl isocyanoacetate, 1.2 mmol benzaldehyde, 1 mol% catalyst, 10 mol% D*i*PEA, CH_2Cl_2, rt

molecules like 1,2-(dipyridin-4-yl)-ethane, bearing two pyridine ligands in the same molecule, provide the possibility for cross-linking.[185]

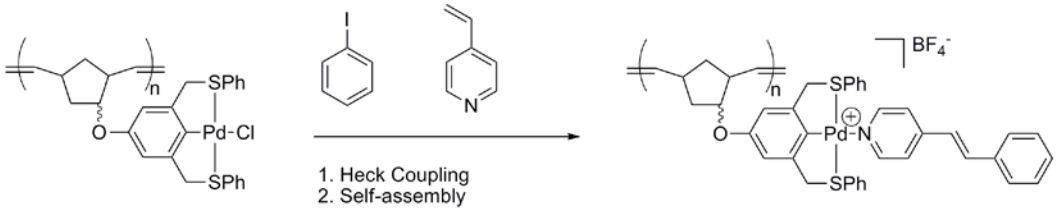

Figure 1.30: Side-chain functionalized polymers possessing SCS-pincer Pd complexes used for Heck catalysis and subsequent self-assembly of the formed species.

The groups of Bergbreiter and Weck independently found that both the homogeneous species and the tethered SCS-pincer palladium(II) complexes were not stable during the conditions used for Heck catalysis, while the conversion remained very high.[186-188] Furthermore, studies have shown that electronically different palladacycles showed a remarkable consistency in reactivity. After establishing mercury poisoning and kinetic studies, it was suggested that all pincer palladium(II) complexes act as pre-catalysts during Heck coupling reactions, and that the real catalytic species are poorly-defined, yet highly active palladium(0) nanoparticles.

Bergbreiter and co-workers obtained a further confirmation for this hypothesis by performing an unambiguous experiment that showed decomposition of palladacycles.[186] Here, in a thermomorphic system (i.e., a combination of liquids that in one temperature range is a homogeneous single phase, but in another temperature range forms two immiscible layers) containing heptane and aqueous DMA, Heck chemistry was performed with PNODAM polymer-bound palladacycles. After the substrate was completely converted, the system was cooled down, and the formed layers were separated. The apolar PNODAM-bound palladacycles were, not surprisingly, found back in the heptane layer. The polar DMA-layer did not contain any measurable amounts of palladium (<0.1 ppm, value obtained by inductively coupled plasma (ICP) MS), yet stayed catalytically active for freshly added substrates. Although its activity was slower than for the thermomorphic system, any activity in a phase that does not contain any polymers and thus palladacycles already shows that a palladacycle is not required for doing Heck catalysis. Other studies on this and related supramolecular non-covalent assemblies were also performed by Weck *et al*.[189-191]

The group of Van Koten studied NCN-pincer palladium dendrimers bound to a 'dendronized' polystyrene support.[192] The dendrons consist of propylamido-benzyl ether branching units with peripheral primary amine groups. After reaction with highly active succinimidyl ester-functionalized NCN-pincer palladium complexes, the first to third generation dendronized polymers were synthesized. Capping of the remaining unreacted free amines with a UV-active reagent (2,4-dinitrofluorobenzene) and measuring the UV absorbance concluded a loading of 91-93%, and thus an average number of 850 (G_1), 1700 (G_2), and 3400 (G_3) NCN-pincer metal centers per molecule respectively.

These so-called DenPol's (dendritic polymers) were tested in the earlier mentioned aldol condensation reaction of methyl isocyanate and benzaldehyde[6]. All generations showed a significantly lower activity than the parent propylamido-NCN palladium bromide, probably due to solubility problems and thus the more heterogeneous character of these DenPol's.[192] A more surprising observation, however, is that all DenPol catalysts, independent of the dendron generation, exhibit the same activity per palladium site for this reaction. Apparently, no interference between the various pincer metal sites takes place and therefore all the palladium centers seem to be kinetically equivalent. These results suggested that the pincer metal moieties are forced outwards, and no back-folding of groups occurs.

A collaboration between the groups of Van Koten and Frey resulted in the use of NCN-pincer palladium functionalized hyperbranched polymers for catalysis.[193] The main advantage of these polydisperse compounds compared to dendrimers, is their easy synthesis. In a single-step, one-pot procedure, a monomer can be converted into a hyperbranched polymer. Disadvantages are the fact that the reactive sites obtained after functionalization are randomly distributed throughout the whole molecule, and that, unlike dendrimers, the synthesis cannot be performed in a controllable way. Nanosized, hyperbranched polycarbosilane compounds functionalized with NCN-pincer palladium complexes were synthesized. The polydispersity index (PDI) of these compounds is 1.8, making these polymers candidates for applications in continuous membrane reactor catalysis.

The catalytic behavior of a monomeric NCN-pincer palladium complex as a control was compared with the hyperbranched polycarbosilane compound in the aldol reaction of

[6]Reaction conditions: 2.5 mol% [Pd], 10 mol% D*i*PEA, CH_2Cl_2, rt

benzaldehyde and methyl isocyanoacetate[7]. It was shown that the total turnover numbers per palladium site of the two tested compounds are almost equal, although the initial TOF (after one hour) of the monomer is about two times higher than the initial TOF of the hyperbranched polymer. Hajji wrote a comprehensive review about hyperbranched polymers in catalysis.[194]

SCS-pincer palladium complexes have also been attached to solid supports. Portnoy *et al.* synthesized aromatic polythioether dendrons which can serve as precursor to the SCS-pincer complex on Wang resin.[195] Metalation takes place with $PdCl_2(PhCN)_2$. Preliminary catalytic results show that $G_2(CO_2Me)$ resins are efficient and recyclable pre-catalysts for the Heck reaction.

1.4 Concluding remarks

In the broad field of supported palladium catalysis, the area of palladacycle-functionalized dendrimers is still in its infancy. For example, the only ligands supported on dendrimers are the ECE-pincer moieties (and its EC-half-pincer analogues) containing E = N, P or S donor atoms. Until now, organometallic palladadendrimers have mainly been used in two different domains by, coincidently, two Dutch research groups: (1) as (recyclable) catalysts (by Van Koten and co-workers) and (2) for the synthesis of self-assembled nanostructures (in the group of Reinhoudt).

In catalysis, the reason palladacycle-functionalized dendrimers are used is that the covalent Pd-C bond creates robust dendritic catalysts, which therefore increases the sustainability of the nanosized catalysts. However, so far only a fraction of the possibilities have been investigated yet. Ironically, most research has focused on Heck catalysis, for which it was shown recently that the catalytic species are Pd-nanoparticles rather than the palladacycles themselves. Aldol-condensations are another class of reactions that have been studied to some extent. These investigations have shown that the application of palladacyclic dendrimers in continuous flow membrane reactors is a promising approach for continuous production of, e.g., pharmaceutically active compounds.

[7] Reaction conditions: 1 mol% [Pd], 10 mol% D*i*PEA, CH_2Cl_2, rt

The coordination-based dendrimers of Reinhoudt's group have been used for visualizing individual nanoscopic assemblies, and for the introduction of redox- and optical active fragments. An interesting development along this line of research is the synthesis of water-soluble palladadendrimers.

Considering the application of palladadendrimers in catalysis, several developments may be foreseen. Whereas up to date mostly single catalytic transformations have been studied, a combination of dendritic palladacycles could lead to new and sustainable protocol for multi-step synthesis of fine chemicals. Such catalytic cascade or tandem reactions could either be accomplished by multiple-different palladacycles on a single dendritic object or otherwise by means of multiple dendritic objects carrying a single, yet different type of palladacyle each. One of the constituents of palladadendrimers in particular and of dendritic catalyst in general of which the overall effect on the catalytic properties is least well understood, is actually the dendritic backbone itself. It would therefore be of interest to study the effect of the nature and properties of the dendrimer backbone itself on catalysis in a more consistent manner.

To conclude, this review highlights the interesting properties of palladacycle-functionalized dendrimers, but also shows that a coming-of-age of these organometallic macromolecules and their application requires much more research effort.

1.5 References

(1) Buhleier, E.; Wehner, W.; Vögtle, F. *Synthesis* **1978**, 155-158.

(2) Tomalia, D. A.; Baker, H.; Dewald, J.; Hall, M.; Kallos, C.; Martin, S.; Roeck, J.; Ryder, J.; Smith, P. *Polym. J. Tokio* **1985**, *17*, 117-132.

(3) Tomalia, D. A.; Naylor, A. M.; Goddard III, W. A. *Angew. Chem. Int. Ed.* **1990**, *29*, 138-175.

(4) Tomalia, D. A.; Durst, H. D. *Top. Curr. Chem.* **1993**, *165*, 193-313.

(5) Newkome, G. R.; Yao, Z. Q.; Baker, G. R.; Gupta, V. K. *J. Org. Chem.* **1985**, *50*, 2003-2004.

(6) Newkome, G. R.; Yao, Z. Q.; Baker, G. R.; Gupta, V. K.; Russo, P. S.; Saunders, M. J. *J. Am. Chem. Soc.* **1986**, *108*, 849-850.

(7) Hawker, C. J.; Fréchet, J. M. J. *J. Am. Chem. Soc.* **1990**, *112*, 7638-7647.

(8) Hawker, C. J.; Fréchet, J. M. J. *J. Chem. Soc. Chem. Commun.* **1990**, *15*, 1010-1013.

(9) Wooley, K. J.; Hawker, C. J.; Frechet, J. M. J. *J. Am. Chem. Soc.* **1991**, *113*, 4252-4261.

(10) Fréchet, J. M. J. *Science* **1994**, *263*, 1710-1715.

(11) Hawker, C. J.; Wooley, K. L.; Fréchet, J. M. J. *J. Chem. Soc. Perkin Trans. 1* **1993**, 1287-1297.

(12) Van Hest, J. C. M.; Delnoye, D. A. P.; Baars, M. W. P. L.; van Genderen, M. H. P.; Meijer, E. W. *Science* **1995**, *268*, 1592-1595.

(13) Santo, M.; Fox, M. A. *J. Phys. Org. Chem.* **1999**, *12*, 293-307.

(14) Liu, M. J.; Kono, K.; Fréchet, J. M. J. *J. Controlled Release* **2000**, *65*, 121-131.
(15) Beezer, A. E.; King, A. S. H.; Martin, I. K.; Mitchell, J. C.; Twyman, L. J.; Wain, C. F. *Tetrahedron* **2003**, *59*, 3873-3880.
(16) Morgan, M. T.; Carnahan, M. A.; Immoos, C. E.; Ribeiro, A. A.; Finkelstein, S.; Lee, S. J.; Grinstaff, M. W. *J. Am. Chem. Soc.* **2003**, *125*, 15485-15489.
(17) Gupta, U.; Agashe, H. B.; Asthana, A.; Jain, N. K. *Biomacromolecules* **2006**, *7*, 649-658.
(18) Hu, J. J.; Cheng, Y. Y.; Ma, Y. R.; Wu, Q. L.; Xu, T. W. *J. Phys. Chem.B* **2009**, *113*, 64-74.
(19) Langer, R. *Nature* **1998**, *392*, 5-10.
(20) Liu, M. J.; Fréchet, J. M. J. *Pharmaceut. Sci. Tech. Today* **1999**, *2*, 393-401.
(21) Uhrich, K. E.; Cannizzaro, S. M.; Langer, R. S.; Shakesheff, K. M. *Chem. Rev.* **1999**, *99*, 3181-3198.
(22) Kolhe, P.; Misra, E.; Kannan, R. M.; Kannan, S.; Lieh-Lai, M. *Int. J. Pharmaceutics* **2003**, *259*, 143-160.
(23) Allen, T. M.; Cullis, P. R. *Science* **2004**, *303*, 1818-1822.
(24) Boas, U.; Heegaard, P. M. H. *Chem. Soc. Rev.* **2004**, *33*, 43-63.
(25) Dufes, C.; Keith, W. N.; Bilsland, A.; Proutski, I.; Uchegbu, J. F.; Schatzlein, A. G. *Cancer Res.* **2005**, *65*, 8079-8084.
(26) Kukowska-Latallo, J. F.; Candido, K. A.; Cao, Z. Y.; Nigavekar, S. S.; Majoros, I. J.; Thomas, T. P.; Balogh, L. P.; Khan, M. K.; Baker, J. R. *Cancer Res.* **2005**, *65*, 5317-5324.
(27) Lee, C. C.; Gillies, E. R.; Fox, M. E.; Guillaudeu, S. J.; Fréchet, J. M. J.; Dy, E. E.; Szoka, F. C. *Proc. Nat. Acad. Sci. U. S. A.* **2006**, *103*, 16649-16654.
(28) Patel, D.; Henry, J.; Good, T. *Biochim. Biophys. Acta-Gen. Subj.* **2006**, *1760*, 1802-1809.
(29) Pan, B. F.; Cui, D. X.; Sheng, Y.; Ozkan, C. G.; Gao, F.; He, R.; Li, Q.; Xu, P.; Huang, T. *Cancer Res.* **2007**, *67*, 8156-8163.
(30) Cheng, Y. Y.; Xu, T. W. *Eur. J. Med. Chem.* **2008**, *43*, 2291-2297.
(31) Gajbhiye, V.; Palanirajan, V. K.; Tekade, R. K.; Jain, N. K. *J. Pharm. Pharmacol.* **2009**, *61*, 989-1003.
(32) Helms, B. A.; Reulen, S. W. A.; Nijhuis, S.; de Graaf-Heuvelmans, P. T. H. M.; Merkx, M.; Meijer, E. W. *J. Am. Chem. Soc.* **2009**, *131*, 11683-11691.
(33) Hong, S.; Rattan, R.; Majoros, I. J.; Mullen, D. G.; Peters, J. L.; Shi, X. Y.; Bielinska, A. U.; Blanco, L.; Orr, B. G.; Baker, J. R.; Holl, M. M. B. *Bioconjugate Chem.* **2009**, *20*, 1503-1513.
(34) Roglin, L.; Lempens, E. H. M.; Meijer, E. W. *Angew. Chem. Int. Ed.* **2011**, *50*, 102-112.
(35) Castro, R.; Cuadrado, I.; Alonso, B.; Casado, C. M.; Moran, M.; Kaifer, A. E. *J. Am. Chem. Soc.* **1997**, *119*, 5760-5761.
(36) Zeng, F. W.; Zimmerman, S. C. *Chem. Rev.* **1997**, *97*, 1681-1712.
(37) Bosman, A. W.; Janssen, H. M.; Meijer, E. W. *Chem. Rev.* **1999**, *99*, 1665-1688.
(38) Landskron, K.; Ozin, G. A. *Science* **2004**, *306*, 1529-1532.
(39) Zeng, X. B.; Ungar, G.; Liu, Y. S.; Percec, V.; Dulcey, S. E.; Hobbs, J. K. *Nature* **2004**, *428*, 157-160.
(40) Rudzevich, Y.; Rudzevich, V.; Moon, C.; Schnell, I.; Fischer, K.; Bohmer, V. *J. Am. Chem. Soc.* **2005**, *127*, 14168-14169.
(41) Singh, B.; Florence, A. T. *Int. J. Pharmaceutics* **2005**, *298*, 348-353.
(42) Van de Coevering, R.; Klein Gebbink, R. J. M.; van Koten, G. *Prog. Polymer Sci.* **2005**, *30*, 474-490.
(43) Campidelli, S.; Perez, L.; Rodriguez-Lopez, J.; Barbera, J.; Langa, F.; Deschenaux, R. *Tetrahedron* **2006**, *62*, 2115-2122.
(44) Newkome, G. R.; Wang, P. S.; Moorefield, C. N.; Cho, T. J.; Mohapatra, P. P.; Li, S. N.; Hwang, S. H.; Lukoyanova, O.; Echegoyen, L.; Palagallo, J. A.; Iancu, V.; Hla, S. W. *Science* **2006**, *312*, 1782-1785.
(45) Boisselier, E.; Ornelas, C.; Pianet, I.; Aranzaes, J. R.; Astruc, D. *Chem. Eur. J.* **2008**, *14*, 5577-5587.
(46) Virboul, M. A. N.; Lutz, M.; Siegler, M. A.; Spek, A. L.; van Koten, G.; Klein Gebbink, R. J. M. *Chem. Eur. J.* **2009**, *15*, 9981-9986.
(47) Albrecht, M.; van Koten, G. *Angew. Chem. Int. Ed.* **2001**, *40*, 3750-3781.
(48) Krasteva, N.; Besnard, I.; Guse, B.; Bauer, R. E.; Mullen, K.; Yasuda, A.; Vossmeyer, T. *Nano Lett.* **2002**, *2*, 551-555.
(49) Rosi, N. L.; Mirkin, C. A. *Chem. Rev.* **2005**, *105*, 1547-1562.

(50) Shiddiky, M. J. A.; Rahman, M. A.; Shim, Y. B. *Anal. Chem.* **2007**, *79*, 6886-6890.
(51) Jiwpanich, S.; Sandanaraj, B. S.; Thayumanavan, S. *Chem. Commun.* **2009**, 806-808.
(52) Ornelas, C.; Ruiz, J.; Astruc, D. *Organometallics* **2009**, *28*, 4431-4437.
(53) Astruc, D.; Boisselier, E.; Ornelas, C. *Chem. Rev.* **2010**, *110*, 1857-1959.
(54) Knapen, J. W. J.; van der Made, A. W.; de Wilde, J. C.; van Leeuwen, P. W. N. M.; Wijkens, P.; Grove, D. M.; van Koten, G. *Nature* **1994**, *372*, 659-663.
(55) Kleij, A. W.; Gossage, R. A.; Klein Gebbink, R. J. M.; Brinkmann, N.; Reijerse, E. J.; Kragl, U.; Lutz, M.; Spek, A. L.; van Koten, G. *J. Am. Chem. Soc.* **2000**, *122*, 12112-12124.
(56) van Heerbeek, R.; Kamer, P. C. J.; van Leeuwen, P. W. N. M.; Reek, J. N. H. *Chem. Rev.* **2002**, *102*, 3717-3756.
(57) Twyman, L. J.; King, A. S. H.; Martin, I. K. *Chem. Soc. Rev.* **2002**, *31*, 69-82.
(58) Helms, B.; Fréchet, J. M. J. *Adv. Synth. Catal.* **2006**, *348*, 1125-1148.
(59) Mery, D.; Astruc, D. *Coord. Chem. Rev.* **2006**, *250*, 1965-1979.
(60) Gaikwad, A. V.; Boffa, V.; ten Elshof, J. E.; Rothenberg, G. *Angew. Chem. Int. Ed.* **2008**, *47*, 5407-5410.
(61) Gaab, M.; Bellemin-Laponnaz, S.; Gade, L. H. *Chem. Eur. J.* **2009**, *15*, 5450-5462.
(62) Yazerski, V. A.; Klein Gebbink, R. J. M. *Catalysis by Metal Complexes (2010)* **2010**, *33 (Heterogenized Homogeneous Catalysts for Fine Chemicals Production)*, 171-201.
(63) Newkome, G. R.; He, E.; Moorefield, C. N. *Chem. Rev.* **1999**, *99*, 1689-1746.
(64) Gorman, C. *Adv. Mater.* **1998**, *10*, 295-309.
(65) Andres, R.; de Jesús, E.; Flores, J. C. *New J. Chem.* **2007**, *31*, 1161-1191.
(66) Berger, A.; Klein Gebbink, R. J. M.; van Koten, G. *Top. Organomet. Chem.* **2006**, *20 (Dendrimer Catal.)*, 1-38.
(67) Astruc, D.; Chardac, F. *Chem. Rev* **2001**, *101*, 2991-3023.
(68) Majoral, J. P.; Caminade, A. M. *Chem. Rev.* **1999**, *99*, 845-880.
(69) Kreiter, R.; Kleij, A. W.; Klein Gebbink, R. J. M.; van Koten, G. *Dendrimers IV* **2001**, *217*, 163-199.
(70) Dahan, A.; Portnoy, M. *J. Pol. Sci. A-Pol. Chem.* **2005**, *43*, 235-262.
(71) Chase, P. A.; Klein Gebbink, R. J. M.; van Koten, G. *J. Organomet. Chem.* **2004**, *689*, 4016-4054.
(72) Kassube, J. K.; Gade, L. H. *Top. Organomet. Chem.* **2006**, *20 (Dendrimer Catal.)*, 39-59.
(73) Méry, D.; Astruc, D. *Coord. Chem. Rev.* **2006**, *250*, 1965-1979.
(74) Oosterom, G. E.; Reek, J. N. H.; Kamer, P. C. J.; van Leeuwen, P. W. N. M. *Angew. Chem. Int. Ed.* **2001**, *40*, 1828-1849.
(75) Astruc, D.; Chardac, F. *Chem. Rev.* **2001**, *101*, 2991-3023.
(76) Chase, P. A.; Klein Gebbink, R. J. M.; van Koten, G. *J. Organomet. Chem.* **2004**, *689*, 4016-4054.
(77) Kreiter, R.; Kleij, A. W.; Klein Gebbink, R. J. M.; van Koten, G. *Top. Curr. Chem.: Dendrimers IV* **2001**, *217*, 163-199.
(78) Dijkstra, H. P.; van Klink, G. P. M.; van Koten, G. *Acc. Chem. Res.* **2002**, *35*, 798-810.
(79) Ong, W.; McCarley, R. L. *Org. Lett.* **2005**, *7*, 1287-1290.
(80) Dahan, A.; Portnoy, M. *Org. Lett.* **2003**, *5*, 1197-1200.
(81) Reetz, M. T.; Lohmer, G.; Schwickardi, R. *Angew. Chem. Int. Ed.* **1997**, *36*, 1526-1529.
(82) Hurley, A.; Mohler, D. L. *Org. Lett.* **2000**, *2*, 2745-2748.
(83) Valerio, C.; Fillaut, J. L.; Ruiz, J.; Guittard, J.; Blais, J. C.; Astruc, D. *J. Am. Chem. Soc.* **1997**, *119*, 2588-2589.
(84) Breinbauer, R.; Jacobsen, E. N. *Angew. Chem. Int. Ed.* **2000**, *39*, 3604-3607.
(85) Dijkstra, H. P.; Slagt, M. Q.; McDonald, A.; Kruithof, C. A.; Kreiter, R.; Mills, A. M.; Lutz, M.; Spek, A. L.; Klopper, W.; van Klink, G. P. M.; van Koten, G. *Eur. J. Inorg. Chem.* **2003**, *5*, 830-838.
(86) Helms, B.; Fréchet, J. M. J. *Adv. Synth. Catal.* **2006**, *348*, 1125-1148.
(87) Hattori, H.; Fujita, K. I.; Muraki, T.; Sakaba, A. *Tetrahedron Lett.* **2007**, *48*, 6817-6820.
(88) Servin, P.; Laurent, R.; Gonsalvi, L.; Tristany, M.; Peruzzini, M.; Majoral, J. P.; Caminade, A. M. *Dalton Trans.* **2009**, 4432-4434.
(89) Hecht, S.; Fréchet, J. M. J. *Angew. Chem. Int. Ed.* **2001**, *40*, 74-91.

(90) Oosterom, G. E.; van Haaren, R. J.; Reek, J. N. H.; Kamer, P. C. J.; van Leeuwen, P. W. N. M. *Chem. Commun.* **1999**, 1119-1120.
(91) Tsuji, J. *In: Negishi E (ed) Handbook of Organopalladium Chemistry for Organic Synthesis* **2000** *Wiley, New York*.
(92) Tsuji, J. *Palladium Reagents and Catalysts: New Perspectives for the 21st Century* **2004**, *1st edition, Wiley, New York*.
(93) de Groot, D.; Eggeling, E. B.; de Wilde, J. C.; Kooijman, H.; van Haaren, R. J.; van der Made, A. W.; Spek, A. L.; Vogt, D.; Reek, J. N. H.; Kamer, P. C. J.; van Leeuwen, P. W. N. M. *Chem. Commun.* **1999**, 1623-1624.
(94) de Groot, D.; Reek, J. N. H.; Kamer, P. C. J.; van Leeuwen, P. W. N. M. *Eur. J. Org. Chem.* **2002**, *6*, 1085-1095.
(95) Heuze, K.; Mery, D.; Gauss, D.; Blais, J. C.; Astruc, D. *Chem. Eur. J.* **2004**, *10*, 3936-3944.
(96) Mizugaki, T.; Murata, M.; Ooe, M.; Ebitani, K.; Kaneda, K. *Chem. Commun.* **2002**, 52-53.
(97) Mansour, A.; Kehat, T.; Portnoy, M. *Org. Biomol. Chem.* **2008**, *6*, 3382-3387.
(98) Alper, H.; Arya, P.; Bourque, C.; Jefferson, G. R.; Manzer, L. E. *Can. J. Chem.* **2000**, *78*, 920-924.
(99) Zweni, P. P.; Alper, H. *Adv. Synth. Catal.* **2006**, *348*, 725-731.
(100) Antebi, S.; Arya, P.; Manzer, L. E.; Alper, H. *J. Org. Chem.* **2002**, *67*, 6623-6631.
(101) Lu, S. M.; Alper, H. *J. Am. Chem. Soc.* **2005**, *127*, 14776-14784.
(102) Lu, S. M.; Alper, H. *J. Am. Chem. Soc.* **2008**, *130*, 6451-6455.
(103) Reynhardt, J. P. K.; Alper, H. *J. Org. Chem.* **2003**, *68*, 8353-8360.
(104) Zweni, P. P.; Alper, H. *Adv. Synth. Catal.* **2004**, *346*, 849-854.
(105) Servin, P.; Laurent, R.; Romerosa, A.; Peruzzini, M.; Majoral, J. P.; Caminade, A. M. *Organometallics* **2008**, *27*, 2066-2073.
(106) Badetti, E.; Franc, G.; Majoral, J. P.; Caminade, A. M.; Sebastian, R. M.; Moreno-Manas, M. *Eur. J. Org. Chem.* **2011**, 1256-1265.
(107) Smith, G.; Chen, R.; Mapolie, S. *J. Organomet. Chem.* **2003**, *673*, 111-115.
(108) Smith, G. S.; Mapolie, S. F. *J. Mol. Catal. A-Chem.* **2004**, *213*, 187-192.
(109) Meder, M.; Galka, C. H.; Gade, L. H. *Monatshefte für Chemie* **2005**, *136*, 1693-1706.
(110) Siggelkow, B. A.; Gade, L. H. *Zeitschrift für Anorganische und Allgemeine Chemie* **2005**, *631*, 2575-2584.
(111) Meise, M.; Haag, R. *ChemSusChem* **2008**, *1*, 637-642.
(112) Janssen, M.; Müller, C.; Vogt, D. *Adv. Synth. Catal.* **2009**, *351*, 313-318.
(113) Huang, C. C.; Lin, Y. C.; Lin, P. Y.; Chen, Y. J. *Eur. J. Org. Chem.* **2006**, 4510-4518.
(114) Hoare, J. L.; Lorenz, K.; Hovestad, N. J.; Smeets, W. J. J.; Spek, A. L.; Canty, A. J.; Frey, H.; van Koten, G. *Organometallics* **1997**, *16*, 4167-4173.
(115) Hovestad, N. J.; Hoare, J. L.; Jastrzebski, J. T. B. H.; Canty, A. J.; Smeets, W. J. J.; Spek, A. L.; van Koten, G. *Organometallics* **1999**, *18*, 2970-2980.
(116) Astruc, D.; Lu, F.; Aranzaes, J. R. *Angew. Chem. Int. Ed.* **2005**, *44*, 7852-7872.
(117) Scott, R. W. J.; Wilson, O. M.; Crooks, R. M. *J. Phys. Chem. B* **2005**, *109*, 692-704.
(118) Jansen, J. F. G. A.; Debrabander-van den Berg, E. M. M.; Meijer, E. W. *Science* **1994**, *266*, 1226-1229.
(119) Niu, Y. H.; Yeung, L. K.; Crooks, R. M. *J. Am. Chem. Soc.* **2001**, *123*, 6840-6846.
(120) Ooe, M.; Mizugaki, T.; Ebitani, K.; Kaneda, K. *J. Am. Chem. Soc.* **2002**, *223*, 416-417.
(121) Chung, Y. M.; Rhee, H. K. *Catal. Lett.* **2003**, *85*, 159-164.
(122) Knecht, M. R.; Weir, M. G.; Frenkel, A. I.; Crooks, R. M. *Chem. Mat.* **2008**, *20*, 1019-1028.
(123) Carino, E. V.; Knecht, M. R.; Crooks, R. M. *Langmuir* **2009**, *25*, 10279-10284.
(124) Weir, M. G.; Knecht, M. R.; Frenkel, A. I.; Crooks, R. M. *Langmuir* **2010**, *26*, 1137-1146.
(125) Chandler, B. D.; Gilbertson, J. D. *Top. Organomet. Chem.* **2006**, *20 (Dendrimer Catal.)*, 97-120.
(126) Yeung, L. K.; Crooks, R. M. *Nano Letters* **2001**, *1*, 14-17.
(127) Li, Y.; El-Sayed, M. A. *J. Am. Chem. Soc.* **2001**, *222*, 335-339.
(128) Wu, L.; Li, Z. W.; Zhang, F.; He, Y. M.; Fan, Q. H. *Adv. Synth. Catal.* **2008**, *350*, 846-862.
(129) Bernechea, M.; de Jesús, E.; Lopez-Mardomingo, C.; Terreros, P. *Inorg. Chem.* **2009**, *48*, 4491-4496.

(130) Yeung, L. K.; Lee, C. T.; Johnston, K. P.; Crooks, R. M. *Chem. Commun.* **2001**, 2290-2291.
(131) Ornelas, C.; Aranzaes, J. R.; Salmon, L.; Astruc, D. *Chem. Eur. J.* **2008**, *14*, 50-64.
(132) Ornelas, C.; Ruiz, J.; Salmon, L.; Astruc, D. *Adv. Synth. Catal.* **2008**, *350*, 837-845.
(133) Ornelas, C.; Diallo, A. K.; Ruiz, J.; Astruc, D. *Adv. Synth. Catal.* **2009**, *351*, 2147-2154.
(134) Liu, G. X.; Puddephatt, R. J. *Organometallics* **1996**, *15*, 5257-5259.
(135) Chessa, G.; Canovese, L.; Gemelli, L.; Visentin, F.; Seraglia, R. *Tetrahedron* **2001**, *57*, 8875-8882.
(136) Angurell, I.; Rossell, O.; Seco, M.; Ruiz, E. *Organometallics* **2005**, *24*, 6365-6373.
(137) Vinogradov, S. A.; Lo, L. W.; Wilson, D. F. *Chem. Eur. J.* **1999**, *5*, 1338-1347.
(138) Lebedev, A. Y.; Cheprakov, A. V.; Sakadzic, S.; Boas, D. A.; Wilson, D. F.; Vinogradov, S. A. *ACS Appl. Mat. Interfaces* **2009**, *1*, 1292-1304.
(139) Rozhkov, V.; Wilson, D.; Vinogradov, S. *Macromolecules* **2002**, *35*, 1991-1993.
(140) Moulton, C. J.; Shaw, B. L. *J. Chem. Soc. Dalton Trans.* **1976**, *11*, 1020-1024.
(141) Van Koten, G.; Timmer, K.; Noltes, J. G.; Spek, A. L. *J. Chem. Soc. Chem. Commun.* **1978**, *6*, 250-252.
(142) Van Koten, G.; Jastrzebski, J. T. B. H.; Noltes, J. G.; Spek, A. L.; Schoone, J. C. *J. Organomet. Chem.* **1978**, *148*, 233-245.
(143) Creaserm, C. S.; Kaska, W. C. *Inorg. Chim. Acta* **1978**, *30*, L325-L326.
(144) Albrecht, M.; van Koten, G. *Angew. Chem. Int. Ed.* **2001**, *30*, 3750-3781.
(145) Dijkstra, H. P.; Ronde, N.; van Klink, G. P. M.; Vogt, D.; van Koten, G. *Adv. Synth. Catal.* **2003**, *345*, 364-369.
(146) Beletskaya, I. P.; Chuchurjukin, A. V.; Dijkstra, H. P.; van Klink, G. P. M.; van Koten, G. *Tetrahedron Lett.* **2000**, *41*, 1081-1085.
(147) Huck, W. T. S.; van Veggel, F. C. J. M.; Kropman, B. L.; Blank, D. H. A.; Keim, E. G.; Smithers, M. M. A.; Reinhoudt, D. N. *J. Am. Chem. Soc.* **1995**, *117*, 8293-8294.
(148) Dijkstra, H. P.; Steenwinkel, P.; Grove, D. M.; Lutz, M.; A.L, S.; van Koten, G. *Angew. Chem. Int. Ed.* **1999**, *38*, 2185-2188.
(149) Huck, W. T. S.; Snellink-Ruel, B.; van Veggel, F. C. J. M.; Reinhoudt, D. N. *Organometallics* **1997**, *16*, 4287-4291.
(150) Beletskaya, I. P.; Chuchuryukin, A. V.; van Koten, G.; Dijkstra, H. P.; van Klink, G. P. M.; Kashin, A. N.; Nefedov, S. E.; Eremenko, I. L. *Russ. J. Org. Chem.* **2003**, *39*, 1268-1281.
(151) Chanthateyanonth, R.; Alper, H. *Adv. Synth. Catal.* **2004**, *346*, 1375-1384.
(152) Dijkstra, H. P.; Meijer, M. D.; Patel, J.; Kreiter, R.; van Klink, G. P. M.; Lutz, M.; Spek, A. L.; Canty, A. J.; van Koten, G. *Organometallics* **2001**, *20*, 3159-3168.
(153) Rodríguez, G.; Lutz, M.; Spek, A. L.; van Koten, G. *Chem. Eur. J.* **2002**, *8*, 45-57.
(154) van de Coevering, R.; Kuil, M.; Alfers, A. P.; Visser, T.; Lutz, M.; Spek, A. L.; Klein Gebbink, R. J. M.; van Koten, G. *Organometallics* **2005**, *24*, 6147-6158.
(155) Dijkstra, H. P.; Chuchuryukin, A.; Suijkerbuijk, B. M. J. M.; van Klink, G. P. M.; Mills, A. M.; Spek, A. L.; van Koten, G. *Adv. Synth. Catal.* **2002**, *344*, 771-780.
(156) Dijkstra, H. P.; Kruithof, C. A.; Ronde, N.; van de Coevering, R.; J.; Vogt, D.; van Klink, G. P. M.; van Koten, G. *J. Org. Chem.* **2003**, *68*, 675-685.
(157) Ronde, N. J.; Totev, D.; Müller, C.; Lutz, M.; Spek, A. L.; Vogt, D. *Chemsuschem* **2009**, *2*, 558-574.
(158) Suijkerbuijk, B. M. J. M.; Lutz, M.; Spek, A. L.; van Koten, G.; Klein Gebbink, R. J. M. *Org. Letters* **2004**, *6*, 3023-3026.
(159) Suijkerbuijk, B. M. J. M.; Tooke, D. M.; Lutz, M.; Spek, A. L.; Jenneskens, L. W.; van Koten, G.; Klein Gebbink, R. J. M. *J. Org. Chem.* **2010**, *75*, 1534-1549.
(160) Suijkerbuijk, B. M. J. M.; Herreras-Martínez, S. D.; van Koten, G.; Klein Gebbink, R. J. M. *Organometallics,* **2008**, *27*, 534-542.
(161) van de Coevering, R.; Kuil, M.; Klein Gebbink, R. J. M.; van Koten, G. *Chem. Commun.* **2002**, *15*, 1636-1637.
(162) van de Coevering, R.; Alfers, A. P.; Meeldijk, J. D.; Martinez-Viviente, E.; Pregosin, P. S.; Klein Gebbink, R. J. M.; van Koten, G. *J. Am. Chem. Soc.* **2006**, *128*, 12700-12713.

(163) Kleij, A. W.; van de Coevering, R.; Klein Gebbink, R. J. M.; Noordman, A. M.; Spek, A. L.; van Koten, G. *Chem. Eur. J.* **2001**, *7*, 181-192.
(164) Ribaudo, F.; van Leeuwen, P. W. N. M.; Reek, J. N. H. *Top. Organomet. Chem.* **2006**, *20 (Dendrimer catal.)*, 39-59.
(165) van de Coevering, R.; Klein Gebbink, R. J. M.; van Koten, G. *Prog. Polym. Sci.* **2005**, *30*, 474-490.
(166) van Manen, H. J.; Nakashima, K.; Shinkai, S.; Kooijman, H.; Spek, A. L.; van Veggel, F. C. J. M.; Reinhoudt, D. N. *Eur. J. Inorg. Chem.* **2000**, 2533-2540.
(167) Huck, W. T. S.; van Veggel, F. C. J. M.; Reinhoudt, D. N. *Angew. Chem. Int. Ed.* **1996**, *35*, 1213-1215.
(168) Huck, W. T. S.; Prins, L. J.; Fokkens, R. H.; Nibbering, N. M. M.; van Veggel, F. C. J. M.; Reinhoudt, D. N. *J. Am. Chem. Soc.* **1998**, *120*, 6240-6246.
(169) van Manen, H. J.; Fokkens, R. H.; Nibbering, N. M. M.; van Veggel, F. C. J. M.; Reinhoudt, D. N. *J. Org. Chem.* **2001**, *66*, 4643-4650.
(170) Huck, W. T. S.; Rohrer, A.; Anilkumar, A. T.; Fokkens, R. H.; Nibbering, N. M. M.; van Veggel, F. C. J. M.; Reinhoudt, D. N. *New J. Chem.* **1998**, *22*, 165-168.
(171) Huisman, B. H.; Huck, W. T. S.; Friggeri, A.; van Manen, H. J.; Menozzi, E.; Vancso, G. J.; van Veggel, F. C. J. M.; Reinhoudt, D. N. *Angew. Chem. Int. Ed.* **1999**, *38*, 2248-2251.
(172) van Manen, H. J.; Auletto, T.; Dordi, B.; H., S.; Vancso, H. G. J.; van Veggel, F. C. J. M.; Reinhoudt, D. N. *Adv. Funct. Mater.* **2002**, *12*, 811-818.
(173) Friggeri, A.; van Manen, H. J.; Auletta, T.; Li, X. M.; Zapotoczny, S.; Schonherr, H.; Vancso, G. J.; Huskens, J.; van Veggel, F. C. J. M.; Reinhoudt, D. N. *J. Am. Chem. Soc.* **2001**, *123*, 6388-6395.
(174) Huck, W. T. S.; Hulst, R.; Timmerman, P.; van Veggel, F. C. J. M.; Reinhoudt, D. N. *Angew. Chem. Int. Ed.* **1997**, *36*, 1006-1008.
(175) van Manen, H. J.; Fokkens, R. H.; van Veggel, F. C. J. M.; Reinhoudt, D. N. *Eur. J. Org. Chem.* **2002**, *2002*, 18.
(176) van Manen, H. J.; van Veggel, F. C. J. M.; Reinhoudt, D. N. *Dendrimers IV* **2001**, *217*, 121-162.
(177) Kleij, A. W.; Klein Gebbink, R. J. M.; van den Nieuwenhuijzen, P. A. J.; Kooijman, H.; Lutz, M.; Spek, A. L.; van Koten, G. *Organometallics* **2001**, *20*, 634-647.
(178) Albert, J.; Cadena, J. M.; Granell, J. *Tetrahedron-Asymmetry* **1997**, *8*, 991-994.
(179) Slagt, M. Q.; Jastrzebski, J. T. B. H.; Klein Gebbink, R. J. M.; van Ramesdonk, H. J.; Verhoeven, J. W.; Ellis, D. D.; Spek, A. L.; van Koten, G. *Eur. J. Org. Chem.* **2003**, *2003*, 1692-1703.
(180) Bergbreiter, D. E.; Osburn, P. L.; Wilson, A.; Sink, E. M. *J. Am. Chem. Soc.* **2000**, *122*, 9058-9064.
(181) Bergbreiter, D. E.; Osburn, P. L.; Frels, J. D. *J. Am. Chem. Soc.* **2001**, *123*, 11105-11106.
(182) Bergbreiter, D. E.; Sung, S. D.; Li, J.; Ortiz, D.; Hamilton, P. N. *Org. Proc. Res. Devel.* **2004**, *8*, 461-468.
(183) Pollino, J. M.; Weck, M. *Organic Letters* **2002**, *4*, 753-756.
(184) Pollino, J. M.; Weck, M. *Synthesis* **2002**, *9*, 1277-1285.
(185) Pollino, J. M.; Nair, K. P.; Stubbs, L. P.; Adams, J.; Weck, M. *Tetrahedron* **2004**, *60*, 7205-7215.
(186) Bergbreiter, D. E.; Osburn, P. L.; Frels, J. D. *Adv. Synth. Catal.* **2005**, *347*, 172-184.
(187) Yu, K. Q.; Sommer, W.; Richardson, J. M.; Weck, M.; Jones, C. W. *Adv. Synth. Catal.* **2005**, *347*, 161-171.
(188) Sommer, W. J.; Yu, K. Q.; Sears, J. S.; Ji, Y. Y.; Zheng, X. L.; Davis, R. J.; Sherrill, C. D.; Jones, C. W.; Weck, M. *Organometallics* **2005**, *24*, 4351-4361.
(189) Yu, K. Q.; Sommer, W.; Weck, M.; Jones, C. W. *J. Catal.* **2004**, *226*, 101-110.
(190) Gerhardt, W. W.; Zucchero, A. J.; Wilson, J. N.; South, C. R.; Bunz, U. H. F.; Weck, M. *Chem. Commun.* **2006**, 2141-2143.
(191) South, C. R.; Higley, M. N.; Leung, K. C. F.; Lanari, D.; Nelson, A.; Grubbs, R. H.; Stoddart, J. F.; Weck, M. *Chem. Eur. J.* **2006**, *12*, 3789-3797.
(192) Suijkerbuijk, B. M. J. M.; Shu, L.; Klein Gebbink, R. J. M.; Schlüter, A.D.; van Koten, G. *Organometallics* **2003**, *22*, 4175-4177.
(193) Schlenk, C.; Kleij, A. W.; Frey, H.; van Koten, G. *Angew. Chem. Int. Ed.* **2000**, *39*, 3736-3736.
(194) Hajji, C.; Haag, R. *Top. Organomet. Chem.* **2006**, *20 (Dendrimer Catal.)*, 149-176.
(195) Dahan, A.; Weissberg, A.; Portnoy, M. *Chem. Commun.* **2003**, 1206-1207.

Chapter 2

SCS-pincer palladium-catalyzed auto-tandem catalysis using dendritic catalysts in semi-permeable compartments

Abstract

Novel monomeric and dendritic SCS-pincer palladium complexes **2**, **3** and **4** have been synthesized in good yields (60-89%) and high purity (palladium loading >97%). These complexes were successfully used as catalysts in the stannylation of cinnamyl chloride with hexamethylditin and in the auto-tandem catalysis consisting of this stannylation followed by an electrophilic addition with 4-nitrobenzaldehyde, showing similar reaction rates and selectivities for all complexes. Dendritic complex **4** has furthermore been used in the compartmentalized catalysis of single and auto-tandem reactions, allowing catalyst reuse for four consecutive runs.

Based on: Niels J. M. Pijnenburg, Harm P. Dijkstra, Gerard van Koten, Robertus J. M. Klein Gebbink, *Dalton Trans.,* ***2011,*** *40*, 8896-8905.

2.1 Introduction

Immobilization of homogeneous catalysts on a solid or macromolecular soluble support[1-7] allows for the separation of catalysts from reaction mixtures by (membrane) filtration techniques and enables catalyst recycling and continuous catalytic processes, e.g. in membrane reactors. The use of dendrimers as support permits control over the number of catalyst units on each single macromolecular entity. Dendrimers have excellent solubility properties and tend to dissolve better in organic solvents than their linear and cross-linked polymeric analogues.[8] The controlled, molecular synthesis of dendrimers provides excess to monodisperse materials, which further enhances their solubility and separation properties. The first example of a functionalized dendrimer containing multiple peripheral metal catalysts was published in 1994 by Van Koten and Van Leeuwen[9] and since then the field of dendrimer catalysis has further developed. Several comprehensive reviews on dendritic catalysts, their use in synthesis and their separation and reuse have been reported.[1,2,4,10-18]

The possibility of performing sequential or tandem catalysis, i.e. a sequence of chemical reactions in which every transformation is catalyzed, with a single or several dendritic catalysts has been pointed out in an early stage,[15] but no experimental reports on this topic have been published so far. We are interested in such systems, because the ability to carry out multiple sequential catalyzed reaction steps in combination with the possibility of separating and recycling the costly catalysts creates an interesting reaction setup in view of performing green chemistry. The various aspects of tandem catalysis are nicely compiled in a review by Fogg and Dos Santos.[19]

Recently the groups of Rothenberg and Vogt have reported on dendritic catalysts in combination with solution-phase compartmentalized catalysis in tailor-made membrane reactors for single reactions.[20-22] Also in heterogeneous[23] and enzyme catalysis[24] similar systems have been described. We have chosen to investigate a reaction setup that combines tandem catalysis with compartmentalized catalysis, and that furthermore does not require sophisticated membrane reactors, arriving at an elegant, green reaction setup.

Here, we set out to investigate the use of simple, commercially available, membrane dialysis bags filled with dendritic catalysts for tandem catalysis. Catalytic reactions can be performed using such semi-permeable compartments by inserting one or several of these

compartments in a single reaction mixture. After reaction the dialysis bag(s) can be easily removed from the reaction mixture and in principle be placed into a fresh reaction solution. Proofs of concept for such a 'teabag' approach have been reported earlier by us[25,26] and more recently by Gade.[27]

A prerequisite for the separation and recycling of dendritic catalysts is that the active catalytic centers should be tightly bound to the dendritic support to prevent catalyst leaching. Because of its robust metal-carbon bond, dendritic ECE-pincer complexes are good catalyst candidates in this respect. Many studies on ECE-pincer metal complexes (ECE = $C_6H_3(CH_2E)_2$-2,6]$^-$; E = NR_2, PR_2, SR, etc., *figure 2.1*) in which the metal ions are bound to the pincer ligand via a covalent M-C bond and two coordinative M-E bonds have been reported.[28-31] Amongst others, we have shown that dendritic ECE-pincer complexes can indeed be separated by membrane separation techniques and reused without significant metal leaching for several runs.[25,32]

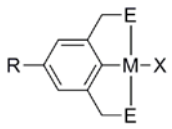

Figure 2.1: A pincer metal complex. M = metal (Ni, Pd, Pt, etc.), X = co-ligand (e.g. Cl, Br, I, MeCN, OH_2), E = electron donating groups (NMe_2, PPh_2, SPh, etc.).

In a recent collaboration with the group of Szabó, we have found that two independent reactions that are catalyzed by two different pincer metal complexes[33,34] (*figure 2.2*, *reaction 1 and 2*), can in fact be catalyzed in a consecutive, one pot manner by a single, different pincer metal complex[35,36] (*figure 2.2*, *reaction 3*). The stannylation of cinnamyl chloride with hexamethylditin to form cinnamyl trimethylstannane (*reaction 1*) is typically catalyzed by NCN-pincer Pd complexes and the homoallylation of 4-nitrobenzaldehyde by cinnamyl trimethylstannane to form trimethyl(1-(4-nitrophenyl)-2-phenyl-but-3-enyloxy)stannane (*reaction 2*), which after aqueous workup yields 1-(4-nitrophenyl)-2-phenyl-3-buten-1-ol, is usually catalyzed by PCP-pincer Pd complexes. In contrast, monomeric SCS- and PCS-pincer palladium complexes are able to catalyze both of those mechanistically different reactions. In this catalytic auto-tandem reaction (*reaction 3*) all three starting materials are present in the reaction mixture from the offset of the reaction and the reaction is carried out in one

pot. In the presence of 5 mol% SCS-pincer palladium catalyst, the homoallylic alcohol products are formed in 74% yield after 16 h at 40 ^{o}C.[35] A diastereomeric product ratio of 9:1 favoring the *anti* diastereomers was observed.

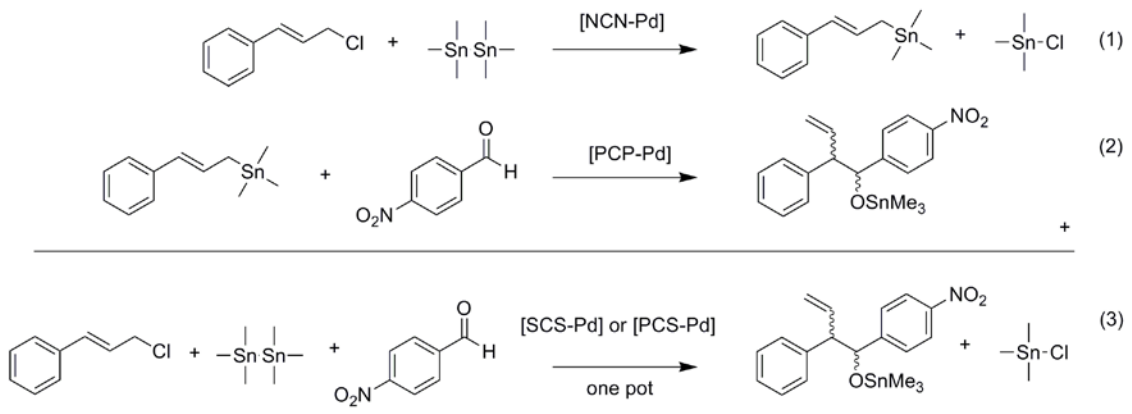

Figure 2.2: The NCN-pincer palladium-catalyzed stannylation of cinnamyl chloride to cinnamyl trimethylstannane (reaction 1) and the PCP-pincer palladium-catalyzed electrophilic cross-coupling of cinnamyl trimethylstannane and 4-nitrobenzaldehyde to trimethyl(1-(4-nitrophenyl)-2-phenylbut-3-enyloxy)stannane, which results in trimethyl(1-(4-nitrophenyl)-2-phenylbut-3-enyloxy)stannane after aqueous workup (reaction 2) can be combined to a SCS- or PCS-pincer palladium-catalyzed auto-tandem reaction where all substrates are present from the beginning of the reaction (reaction 3).

Here, we present our investigations on a dendrimer-supported version of the SCS-pincer Pd auto-tandem catalyst and have explored its use in a compartmentalized setup. The objectives of our investigations were twofold. First, a first generation dendritic catalyst was to be tested in solution and its activity compared to those of its monomeric and its zeroes generation dendritic analogues. For this purpose a series of four catalysts was prepared (*figure 2.3*). This series consists of two monomeric analogues (**1** and **2**) and two dendritic SCS-pincer palladium complexes (**3** and **4**). Compound **2** contains a *para*-functionalized trimethylsilyl group that resembles the connectivity of the pincer moieties to the dendritic scaffold. As a second objective, dendritic catalyst **4** was tested in a compartmentalized setup and reused several times to evaluate its stability and recyclability.

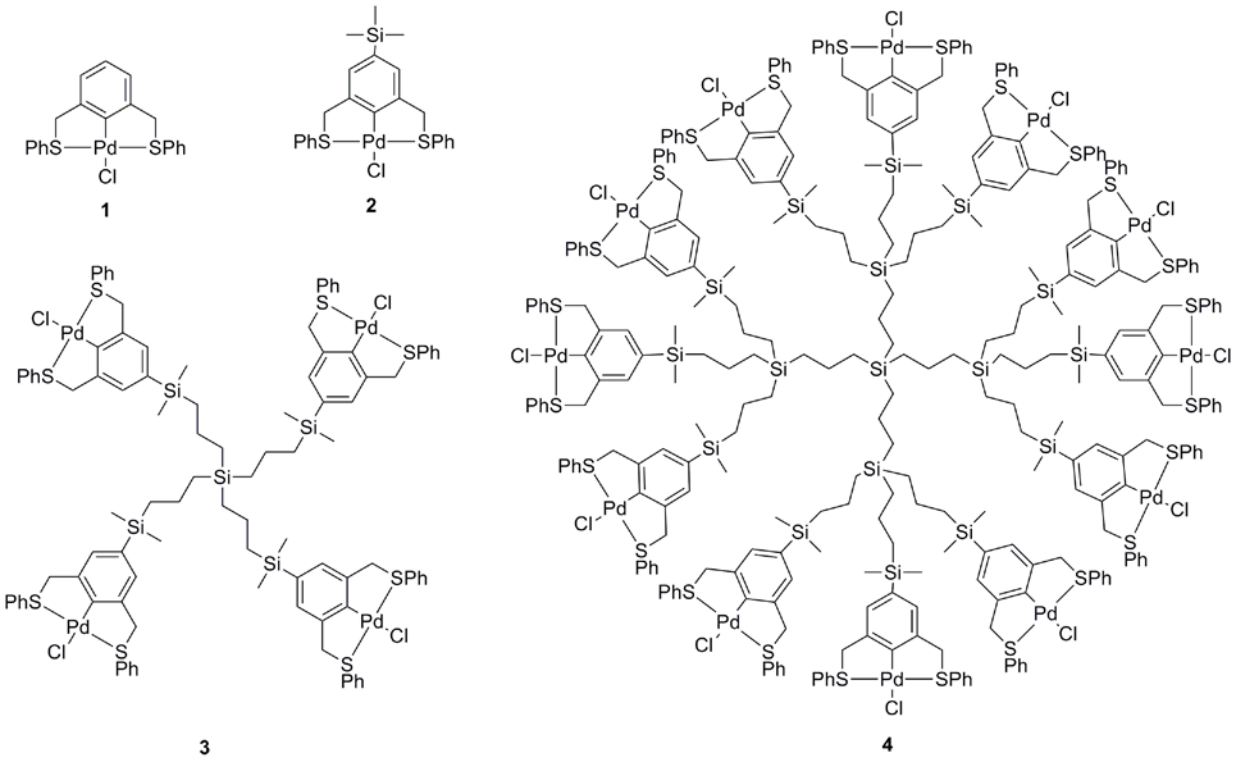

*Figure 2.3: Monomeric and dendritic SCS-pincer palladium complexes **1**-**4** used as catalyst in the tandem reaction.*

*2.2 Synthesis of compounds **1**-**4***

Parent SCS-pincer palladium complex **1** has been reported by Sillanpää and co-workers and was synthesized as described.[37] The trimethylsilyl-functionalized complex **2** was synthesized starting from the *para*-bromo functionalized pincer ligand precursor **5** in a two-step synthetic protocol (*figure 2.4*). Ligand precursor **5** was lithiated via lithium-halogen exchange by addition of 2 equiv. of *t*BuLi at -80 ^{o}C and subsequent treatment with trimethylsilyl chloride. After workup this procedure gave pincer ligand precursor **6** in 96% isolated yield. Palladation of **6** was achieved via direct C-H-activation with $[Pd(MeCN)_4](BF_4)_2$ in refluxing acetonitrile. The resulting cationic acetonitrile complex was treated with a saturated aqueous sodium chloride solution to replace the acetonitrile ligand by the stronger chloride ligand. Although cationic SCS-pincer Pd(MeCN) complexes have shown to be very reactive in the stannylation reaction[33] and in the tandem reaction,[35] our catalytic studies have been performed with the neutral SCS-pincer Pd-Cl complexes, because of the poor solubility

properties of the polycationic SCS-pincer Pd(MeCN) dendrimers and the improved storage properties of the Pd-Cl dendrimers.

The resulting SCS-pincer Pd complex was purified by column chromatography, and further treated with 100 equiv. of poly(vinylpyridine) (PVPy) in dichloromethane for 3 h. PVPy is known to intercept free palladium particles in solution and is regularly used in catalyst poisoning experiments.[38,39] By doing so, minute amounts of potentially catalytically active Pd(0) species were excluded from palladium complexes that were subsequently used in catalysis experiments. After this workup, **2** was obtained as an air and moisture stable orange-yellow solid in 89% yield.

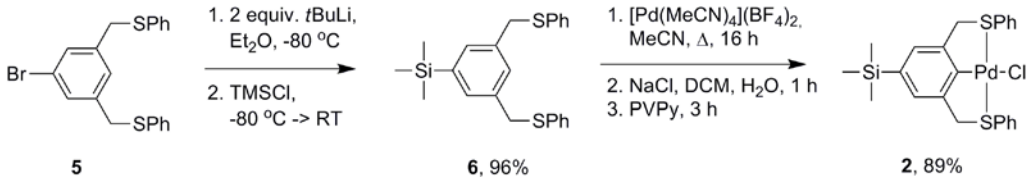

5 **6**, 96% **2**, 89%

*Figure 2.4: Synthesis of trimethylsilyl functionalized SCS-pincer palladium complex **2**.*

Dendritic complexes **3** and **4** were synthesized via a similar protocol as trimethylsilyl-pincer complex **2**. Instead of using trimethylsilyl chloride as the quenching agent for lithiated **5**, chloro-terminated carbosilane dendrimers **7** and **8** were used (*figure 2.5*). These dendritic scaffolds where synthesized according to a standard literature procedure via a repetitive Grignard/hydrosilylation reaction sequence starting from tetrachlorosilane and allylbromide.[40] An excess of lithiated **5** (1.2 equivalents per Si-Cl moiety) was used to ensure a complete conversion of all chlorosilyl groups in order to yield monodisperse dendritic materials. The excess of pincer ligand precursor (and eventual other low molecular weight contaminants) was removed by passive dialysis. After three dialysis cycles, the dendritic ligand precursors were isolated in good yields (76% for dendrimer **9**, and 61% for dendrimer **10**) and high purity (*vide infra*).

Dendrimers **9** and **10** were palladated by using an excess of $[Pd(MeCN)_4](BF_4)_2$ (1.2 equivalents per dendritic arm) in a refluxing mixture of acetonitrile and toluene. This solvent combination was used to improve the solubility of the dendritic ligands. A treatment with NaCl resulted in the chloride complexes. After passive dialysis and PVPy treatment, orange-

yellow powders were obtained in reasonable to good yields (83% for G_0 dendrimer **3**, 60% for G_1 dendrimer **4**).

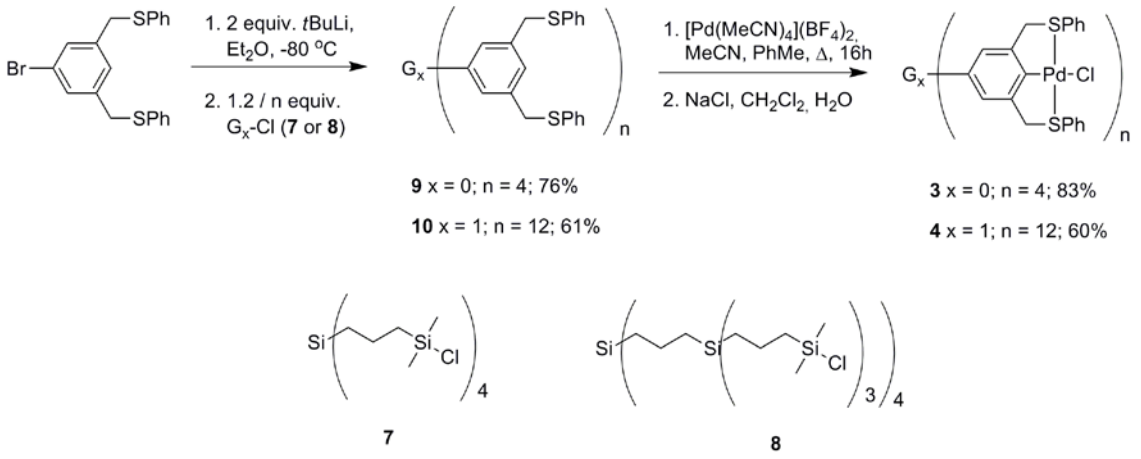

*Figure 2.5: Synthesis of carbosilane-based dendritic SCS-pincer palladium complexes **3** and **4**.*

The integrity and purity of palladium complexes **1**-**4** was verified by means of a combination of analytical techniques. ^{1}H NMR analysis of the complexes showed a single characteristic signal for the benzylic protons around 4.6 ppm. The introduction of the palladium center caused a large downfield shift for this signal compared to the corresponding pre-ligands, which show this resonance at 4.0 ppm. Besides the chemical shift of this signal, also its line width differs significantly for the palladium complexes compared to the pre-ligands. A sharp singlet was observed for the ligand precursors **6**, **9** and **10**, whereas a broad to very broad singlet was seen for the corresponding SCS-pincer palladium complexes **2**-**4**. This observation is in agreement with observations in the literature, and is caused by the flexible structure of SCS-pincer Pd complexes due to a combination of inversion of the conformation of the sulfur atoms, and puckering of the S-Pd-C chelate.[41,42] A similar shift of the benzylic signals was observed in the ^{13}C NMR spectra; for all reported species the signal corresponding to the benzylic carbon shifts from 39 ppm for the ligand precursor to 52 ppm for the palladium complex. ^{1}H as well as ^{13}C NMR spectra of complexes **7**-**10** did not show any residual ligand precursor signals. The dendritic ligands and complexes show broad signals for all observed protons, in agreement with their macromolecular nature.

G_0 ligand precursor **9** and complex **3** were successfully analyzed by MALDI-TOF MS. For **9**, a parent peak at *m*/*z* = 1714.69 was observed (theoretical value for $[M+H]^+$ is *m*/*z* = 1714.94). Analysis of complex **3** showed a distinct signal at *m*/*z* = 2478.73 for a tetra-palladium species

(theoretical value for $[M+Na]^+$ is 2479.19). No signals corresponding to species of lower palladium content or to the free ligand were observed. For the G_1 ligand **10** and G_1 complex **4** the conditions for a good mass analysis were not found. Changing to ESI-MS also did not result in a proper analysis.

Besides the absorption around 250 nm that is typical of compounds that contain aromatic groups, SCS-pincer palladium complexes show a characteristic UV absorption at 330 nm. The corresponding pre-ligands do not show an absorption in this region ($\varepsilon_{330} < 0.001$). This specific optical feature was therefore used to determine the Pd content of the isolated dendritic materials. Analytically pure trimethylsilyl functionalized complex **2** was used as a calibrant. Separate dilution series of monomeric complex **2** and dendritic complexes **3** and **4** in CH_2Cl_2 were prepared by using an equal concentration of palladium centers (theoretical value). The absorption at 330 nm for these dilution series was plotted against their theoretical Pd-concentration. The ratio of the slopes of these straights for **3** and **4** to the slope of the straight of **2** were taken as a measure of the percentage of palladium centers in the dendritic complexes. These experiments showed an average of 3.9 and 11.9 metalated arms per molecule respectively, thus showing a full palladium loading of both **3** and **4** (*table 2.1*).

*Table 2.1: Determination of the palladium content of complexes **3** and **4** based on absorption intensities (330 nm) of dilution series.*[a].

Catalyst	Slope of dilution series	R^2 value of dilution series	% of palladated arms	Calcd. nr. of palladated arms
2	0.0074700	0.9972	100	1
3	0.0072627	0.9988	97.22	3.9
4	0.0074227	0.9991	99.37	11.9

[a] *The dilution curve of complex **2** was used as a standard and the Pd-content of **3** and **4** were calibrated accordingly.*

Metalations of identical dendritic compounds bearing NCN-type pincer ligands were performed via stepwise lithiation of the pincer ligands with *t*-BuLi followed by transmetalation with a metal(II) precursor.[32] Although these reactions appeared to be high yielding for momomeric pincer complexes, for dendritic complexes no complete metal loading was achieved due to partial hydrolysis of the extremely sensitive lithio-intermediate.

Metalation percentages around 80-90% were generally observed for these NCN-pincer dendrimers. To the best of our knowledge, the present SCS-pincer dendrimers are the first to show full metalation for these types of structures.

2.3 *Catalysis with **1**-**4** in solution*

Dendrimers **3** and **4** and their mononuclear counterparts **1** and **2** were tested as catalysts in the stannylation reaction (*reaction 1*) and in the two-step tandem reaction (*reaction 3*). In both reactions, the substrates were combined in either THF or CH_2Cl_2 in equimolar amounts. These solutions were found to be stable for a prolonged time without catalyst: no blank reactions took place. The catalysts were added at 2 mol% palladium (i.e. 2 mol% of **1** or **2**, 0.5 mol% of **3** or 0.167 mol% of **4**). A nitrogen atmosphere was necessary because of the sensitivity towards hydrolysis of hexamethylditin, and due to the lability of the primary reaction product cinnamyl trimethylstannane.

*Table 2.2: Formation of cinnamyl trimethylstannane (%) in the stannylation of cinnamyl chloride as catalyzed by complexes **1**-**4**.*[a]

Catalyst	1 h, CH_2Cl_2	5 h, CH_2Cl_2	1 h, THF	5 h, THF
1	58	99	83	100
2	71	100	82	100
3	69	100	83	100
4	55	99	82	100

[a] *Conditions: 0.80 mmol cinnamyl chloride, 0.80 mmol hexamethylditin and 2 mol% Pd catalyst in 6 mL CH_2Cl_2 or THF, ambient temperature, N_2 atmosphere.*

Both the monomeric and the dendritic complexes were found to be excellent catalysts for the stannylation of cinnamyl chloride (*table 2.2*). Complete conversion was obtained in all cases in less than 5 h, showing very similar reaction kinetics. In CH_2Cl_2 the reactions were complete in 5 h, with a conversion of 55-71% in the first hour. In THF a similar trend was observed, although after 1 h the conversion is significantly higher (~83%).

In the tandem reaction (*reaction 3*) in THF, it was found that the overall activity after 24 and 72 h was very similar for compounds **1**-**4** (*table 2.3*). Initially, a fast decrease of cinnamyl chloride was observed within 5 h (*figure 2.6*), next to a fast increase of cinnamyl trimethylstannane. The second reaction step was much slower and reached full conversion only after several days. The dendritic catalysts **3** and **4** proved to be more effective than the monomeric catalysts in the first reaction step. For the overall tandem reaction, the 'head start' of the dendritic catalysts was averaged out due to the much longer reaction time that was required for the second reaction step. Overall, monomeric catalyst **1**, which lacks a trimethylsilyl group on the *para*-position with respect to the palladium center, appeared to be slightly slower than the other catalysts used. The ratio between *anti* and *syn* products at the end of the reaction showed a slight dependence on the catalyst, with the dendritic catalysts being somewhat more selective for the *anti* 1-(4-nitrophenyl)-2-phenylbut-3-en-1-olproducts. The *anti*/*syn* ratio varies from 5 for the monomeric species to 6 for the dendritic catalysts.

*Table 2.3: Substrate conversion, intermediate built-up, and product formation in tandem reaction (3) catalyzed by **1**-**4** in THF.*[a]

	Cinnamyl chloride (%)			Cinnamyl trimethylstannane (%)			1-(4-nitrophenyl)-2-phenylbut-3-en-1-ol(%)			
	1h	24h	72h	1h	24h	72h	1h	24h	72h	*Anti* / *Syn* ratio
1	37	1	0	38	61	21	25	38	79	5.0
2	44	1	0	36	50	6	20	49	94	5.2
3	29	0	0	39	58	12	32	42	88	5.7
4	15	0	0	53	56	6	32	44	94	6.0

[a] *Conditions: 0.80 mmol cinnamyl chloride, 0.80 mmol hexamethylditin, 0.80 mmol 4-nitrobenzaldehyde and 2 mol% Pd catalyst in 6 mL THF at ambient temperatures, N_2 atmosphere.*

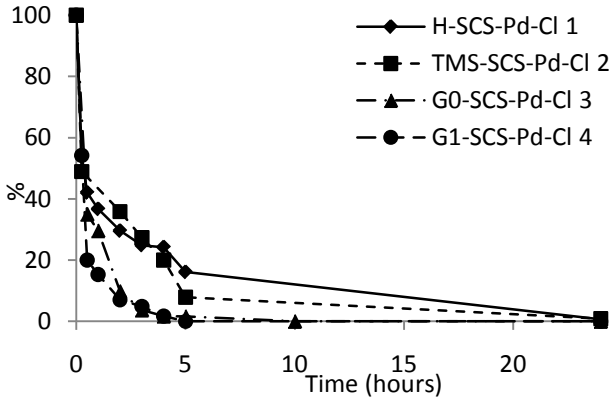

*Figure 2.6: Conversion of cinnamyl chloride to cinnamyl trimethylstannane catalyzed by Pd-catalysts **1**-**4** in the tandem reaction.*

*2.4 Compartmentalized catalysis with dendritic complex **4***

Next, the catalytic performance of first generation metallodendritic catalyst **4** was investigated in a compartmentalized setting. For this purpose, catalyst **4** was placed inside a semi-permeable compartment and tested in the stannylation reaction (1) and in tandem reaction (3). As the semi-permeable compartment a membrane dialysis bag (benzoylated regenerated cellulose dialysis tubing) was used. The mass weight cut-off (MWCO) of this membrane is 1000 Da, whereas the molecular weight of the dendritic catalyst is 7593 Da. As shown by UV/Vis analysis, no detectable dendrimer leaching took place in CH_2Cl_2 or THF for a week when the dendritic catalyst was placed inside such a membrane dialysis bag. For these studies a reaction vessel was used that is equipped with a glass raster at approximately 1 cm above the bottom of the reactor in order to protect the membrane dialysis bag from being damaged by the rotating stirring bar at the bottom of the reactor (*figure 2.7*).

Figure 2.7: Reactor used for compartmentalized (tandem) catalysis experiments. A dialysis membrane bag closed by two white clamps contains the catalyst solution.

2.4.1 Stannylation of cinnamyl chloride with hexamethylditin (reaction 1)

Initial studies with compartmentalized dendritic catalyst **4** were performed in the palladium-catalyzed stannylation reaction of cinnamyl chloride. To this end, a membrane dialysis bag containing a solution of dendritic catalyst **4** in THF was placed into a solution containing the substrates. After 24 h of reaction, the membrane dialysis bag was removed and placed into a second vessel containing a new batch of substrates in THF. The presence of the semi-permeable barrier had a large effect on the reaction rate. Not only was a significant lag phase in substrate conversion observed, the reaction also took considerably longer to go to completion (24 h) compared to the reaction under standard homogeneous conditions (5 h). Diffusion of substrates into the membrane bag and of products out of the membrane bag driven by osmotic pressure seems an obvious reason why a lower reaction rate was observed under compartmentalized conditions, as product sampling was carried out from the outer membrane phase.

The same catalyst batch was used in four consecutive runs by removal of the membrane dialysis bag from the reaction solution after 24 h and placement of the bag into a new batch of substrates. The compartmentalized catalyst remained active over the four runs, although the reaction rate steadily decreased in every run. Substrate conversions of 100%, 95%, 72%, and 61%, respectively, were observed for the four runs. The fourth run was prolonged to 72

h of reaction time and a conversion of 99% was observed at this time, indicating the endured activity of the dendritic catalyst.

The palladium contents of the outer membrane solution of these four runs were analyzed via ICP mass spectroscopy in order to probe possible palladium leaching from the membrane bag. Various amounts of palladium were found in all four runs (*table 2.4*). In the first run 13 ppm Pd was detected, corresponding to 5.2% of the total starting amount of palladium. In the second, third and fourth runs lower amounts of palladium were found. In these four runs, a total of 12.4% of the starting amount of palladium had leached through the membrane into the outer solution.

*Table 2.4: Pd ICP-MS analysis of the outer membrane solution in the consecutive formation of cinnamyl trimethylstannane using compartmentalized catalyst **4**.*

	Palladium (ppm)	Leaching (%)
Run 1	13	5.2
Run 2	10	4.0
Run 3	5	2.0
Run 4	3	1.2

After the fourth run, complex **4** was regained from the dialysis bag in 89% yield. NMR analysis showed that **4** was not regained unmodified. Analysis of the peaks corresponding to the benzylic protons showed that a significant amount of the SCS-pincer moieties (approximately 30%) no longer contained a palladium center and had been transformed in a preligand form. Apparently, significant amounts of palladium were released from the pincer ligand manifold during catalysis via overall protonolysis. The difference between the amount of Pd leaching as determined by ICP-MS and by NMR analysis (12.4% and 30% respectively) might be caused by agglomeration of released palladium into larger clusters inside the membrane dialysis bag or by adsorption of Pd by the membrane itself.

Possible leaching of dendritic catalyst **4** itself from the membrane bag was tested in the presence of each individual substrate in THF under catalytic conditions (i.e. 2 mol% Pd per substrate and identical concentration). In none of these experiments any palladium leaching was observed ([Pd] < 0.1 ppm). This leads to the conclusion that only under true catalytic conditions, i.e. in the presence of both substrates, palladium leaching took place.

2.4.2 Tandem stannylation and electrophilic addition (reaction 3)

After the single step stannylation reaction, the compartmentalized dendritic catalyst **4** was investigated in the tandem stannylation/homo-allylation reaction. The compartmentalized tandem reaction was found to progress slower than the stannylation reaction: NMR-monitoring of the reaction was carried out for one week whereupon the dialysis bag was transferred into a new batch of substrates.

In the first run, the stannylation reaction took place readily and went to completion within 24 h (*table 2.5*). The second step of the tandem reaction, i.e. the electrophilic substitution of nitrobenzaldehyde and cinnamyl trimethylstannane was found to progress at a much lower rate: noticeable amounts of cinnamyl trimethylstannane were still present after 2 days of reaction. In fact, also after a prolonged reaction time of one week the reaction had not gone to completion. At that point a steady state mixture of tandem products (60%) and cinnamyl trimethylstannane (40%) was observed. An *anti*/*syn* product ratio of 4.2 : 1 was found in this mixture, which is a somewhat lower ratio than for the homogeneous reaction (6.0 : 1).

*Table 2.5: Substrate conversion, intermediate built-up, and product formation in the tandem reaction (3) catalyzed by dendritic catalyst **4** inside a membrane dialysis bag in THF.*[a]

	Cinnamyl chloride (%)			Cinnamyl trimethylstannane (%)			1-(4-nitrophenyl)-2-phenylbut-3-en-1-ol(%)			
	1 h	24 h	168 h	1 h	24 h	168 h	1 h	24 h	168 h	*Anti* / *Syn* ratio
Run 1	48	0	0	39	56	36	13	44	64	4.2
Run 2	47	0	0	36	54	49	17	46	51	3.8
Run 3	88	14	4	5	59	43	7	29	53	1.9
Run 4	83	44	45	11	33	23	6	23	32	1.9

[a] *Conditions: 8.0 mmol cinnamyl chloride, 8.0 mmol hexamethylditin, 8.0 mmol 4-nitrobenzaldehyde and 2 mol% Pd catalyst inside a membrane dialysis bag in 60 mL THF at ambient temperatures and N_2 environment.*

Upon further use of the same compartmentalized catalyst in three additional consecutive runs by replacing the contents of the reaction vessel by a fresh batch of substrates after 1 week, it was found that the catalyst was active in all of these runs. This might be somewhat surprising taking into account that the electrophilic addition of the first run did not reach

complete conversion. Actually, a very similar reaction profile was found for the second run as for the first run. The rate of conversion and of product formation were almost identical in the first two runs (*table 2.5*). The amount of tandem products found in the second run was even slightly higher compared to the first run, which is most probably caused by the remaining amount of product in the dialysis bag present after the first run. The *anti*/*syn* ratio of the products in run 1 (4.2 : 1) and 2 (3.8 : 1) was found to be similar.

In the third run, the first step of the tandem reaction was considerably slower than in the first two runs. Consequently, the second step showed a reduced reaction rate in the initial stage. However, after one week the same amount of tandem product had formed as compared to the second run. In the fourth run a considerable decrease in reaction rate for both reaction steps was observed: half of the starting amount of cinnamyl chloride was still present after one week, and tandem product formation proceeded to only 37%. The *anti*/*syn* product ratio in run 3 and run 4 (1.9 : 1) differed significantly from that in the previous runs.

ICP-MS analysis was again carried out to probe the palladium concentration in the outer solutions after 1 week of reaction (*table 2.6*). The amount of palladium observed in these cases was higher than for the single step stannylation reaction, which might be caused by the longer reaction times that are necessary for the tandem catalysis reaction. In the first run a considerable 35.8 ppm of palladium leached out of the membrane bag, which corresponds to 14.3% of the total amount of palladium centers. Pd-leaching in the three subsequent runs decreased to 1.6 ppm in run 4.

*Table 2.6: Pd-analysis (ICP-MS analysis) of the outer membrane solution for four consecutive runs using complex **4**.*

	Palladium (ppm)	Leaching (%)
Run 1	35.8	14.3
Run 2	23.1	9.3
Run 3	5.7	2.3
Run 4	4.1	1.6

2.4.3 Optimization of reaction conditions

Preliminary results from mechanistical studies aimed at optimizing the conditions to perform compartmentalized auto-tandem catalysis showed a very fast tandem reaction takes place when three (or more) equivalents of cinnamyl chloride and hexamethylditin are used compared to 4-nitrobenzaldehyde.[43] Using these reagent excess conditions, dendritic SCS-pincer palladium complex **4** (2 mol% Pd) was investigated in a compartmentalized setup to explore the possibility of performing recyclable auto-tandem catalysis. This modification led to a dramatic improvement in reaction time: an almost full conversion to 1-(4-nitrophenyl)-2-phenylbut-3-en-1-olwas obtained in only three hours (*table 2.7*), whereas only 50% of product was synthesized in a week by using just one equivalent of cinnamyl chloride and hexamethylditin.

Table 2.7: Formation of secondary product and Pd ICP-MS analysis of the outer membrane solution for the compartmentalized tandem catalysis experiment after 3 hours of reaction.

	Product formation (%)	*anti*/*syn* ratio	Palladium (ppm)	Observed leaching (%)
Run 1	89	3.9	0	0
Run 2	96	4.0	0	0
Run 3	96	3.8	3	1
Run 4	92	3.7	8	3

The subsequent second, third and fourth runs also yielded almost quantitative amounts of 1-(4-nitrophenyl)-2-phenylbut-3-en-1-olin the same amount of time. When the contents of the (outer) reaction solutions were analyzed for palladium leaching by ICP/MS analysis (table 2.7), palladium leaching was found to be significantly diminished. No detectable amounts of palladium leaching were observed in the first two runs, whereas starting in the third run palladium leaching was observed to a very minor extent. Furthermore a constant *anti*/*syn* product ratio was observed for four consecutive runs. These optimized reaction conditions and their mechanistic implications will be the subject of *Chapter 3*.

2.5 Concluding remarks

In this paper, the synthesis of novel dendritic ECE-pincer palladium is described. For the first time, full metal loadings were obtained for these types of dendritic carbosilane compounds. Since the palladation of the SCS-pincer ligands in the present study was performed by a direct C-H activation in absence of reactive intermediates, a full metal loading for both the G_0 and the G_1 dendritic complexes could be achieved in a synthetic route that also contains less reaction steps than in the earlier report on NCN-pincer Pd-dendrimers.

The new dendritic SCS-pincer palladium complexes appear to be efficient catalysts for the stannylation of allyl chlorides by hexamethylditin (reaction 1) and for the auto-tandem reaction between cinnamyl chloride, hexamethylditin and 4-nitrobenzaldehyde to form 1-(4-nitrophenyl)-2-phenylbut-3-en-1-ol(reaction 3). This particular auto-tandem reaction was studied in a standard batch manner as well as in a compartmentalized manner. We found that compartmentalized tandem catalysis is indeed possible using simple commercially available dialysis bags using a “tea-bag” approach. These studies provide the first example for compartmentalized auto-tandem catalysis using a semi-permeable compartment in which a molecularly enlarged catalyst is retained. Upon reuse of a catalyst-loaded membrane bag, the catalytic reaction was found to take place with a similar reaction profile. However, upon further reuse, i.e. in a third and fourth catalytic run, the reaction rate slowed down, while still significant amounts of products were formed. On the other hand, complex **4** was used for one month in this recycling experiment, which shows an overall stability of the organometallic complex.

In addition, these studies showed an anticipated drawback of the membrane bag setup. When relying on passive diffusion for substrate and product transport, overall reaction rates tend to be low. The use of excess amounts of only two of the reaction substrates, however, was found to considerably speed up the compartmentalized tandem reaction.

For the particular palladium-catalyzed tandem reaction studied here, palladium leaching through the membrane was also observed. Obviously, this possesses a serious drawback in view of recyclability and reproducibility of the system. For further research more robust catalytic systems and/or different reaction conditions would have to lead to an improved recyclability. We will, furthermore, investigate other dendritic catalyst systems in order to further develop the concept of compartmentalized catalysis and compartmentalized tandem

reactions. At the same time, we are looking into the SCS-pincer palladium catalysts discussed here.[43] These complexes have earlier been found to be instable at high temperatures (>120 ^{o}C) in the presence of strong bases and are used in these conditions among others as precursor for Pd(0)-catalyzed Heck reactions.[44-46] In the current reactions, however, neither high temperatures nor strong bases were used, so palladium leaching from the pincer manifold was rather unexpected. To the best of our knowledge, this is the first example in which it has been found that SCS-pincer palladium complexes are instable under mild conditions, i.e. ambient temperature and non-acidic or non-basic conditions.

We are currently carrying out further mechanistic studies on this particular catalytic tandem reaction in which palladium is combined with ditin and tin halide species. These studies have already led to an optimized and very promising compartmentalized auto-tandem system that performs fast catalysis for this tandem reaction with very minor Pd(0) leaching.[43]

2.6 Experimental Section

General

All reactions were carried out using standard Schlenk techniques under an inert dinitrogen atmosphere unless stated otherwise. All solvents were carefully dried and distilled prior to use. All standard reagents were purchased commercially and used without further purification. Carbosilane dendrimers **7** and **8**,[40] SCS-pincer ligand **5**[47,48] and $[Pd(MeCN)_4](BF_4)_2$[49] were prepared according to literature procedures. All other reagents were purchased from Acros Organics and Sigma-Aldrich Chemical Co. Inc. and used as received. ^{1}H (300 MHz), ^{13}C (100 MHz) and ^{29}Si (60 MHz) NMR spectra were recorded on a Varian 400 MHz spectrometer at 25 ^{o}C, chemical shifts are given in ppm referenced to residual solvent resonances. UV/Vis spectra were recorded on a Cary 50 Scan UV/Visible spectrophotometer. MALDI-TOF MS spectra were acquired using a Voyager-DE Bio-Spectrometry Workstation mass spectrometer equipped with a nitrogen laser emitting at 337 nm. High resolution mass spectroscopy (HRMS) has been performed on a Waters LCT Premier XE Micromass instrument using the electrospray ionization (ESI) technique. GC analysis was carried out using a Perkin Elmer Clarus 500 GC equipped with an Alltech Econo-Cap EC-5 column.

3,5-bis-(phenylthiomethyl)phenyl)trimethylsilane ***6*** *(TMS-SCS-H)*

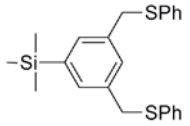

A solution of **5** (2.49 mmol, 1.00 g) in Et_2O (30 mL) was cooled to –80 °C whereupon a 1.6 M *t*BuLi solution in pentane (2.0 equiv., 4.98 mmol, 3.11 mL) was added slowly in 5 min. The solution immediately turned dark red. After stirring for another 5 min. at –80 °C trimethylsilyl chloride (1.1 equiv., 2.74 mmol, 348 μL) was added in one portion. The cooling bath was removed and the reaction mixture was allowed to reach ambient temperature. The solution turned pale yellow. After 30 minutes, all volatiles were evaporated and dichloromethane was added to the residue. This solution was washed with water (2x50 mL) and a saturated NaCl solution (2x50 mL), dried over $MgSO_4$ and concentrated, yielding **6** as a colorless syrup in 0.90 g (92%).

^{1}H NMR ($CDCl_3$, 300 MHz): δ 7.32-7.21 (m, 13H, CH_{arom}), 4.10 (s, 4H, CH_2), 0.21 (s, 9H, SiCH_3). ^{13}C NMR ($CDCl_3$, 75 MHz): δ 141.1, 137.3, 136.5, 133.0, 130.7, 130.3, 129.1, 126.7, 39.5, -0.8. ^{29}Si NMR ($CDCl_3$, 60 MHz): δ -3.76. ESI-HRMS for $C_{23}H_{26}S_2Si$ (m/z): $[M+Na]^+$ 417.1143 (calcd. 417.1108).

para-TMS SCS-pincer Pd complex ***2***

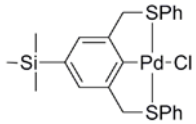

To a solution of **6** (1.27 mmol, 500 mg) in acetonitrile (30 mL) was added $[Pd(MeCN)_4](BF_4)_2$ (1.2 equiv., 1.52 mmol, 674 mg). The reaction mixture was stirred for 16 h at reflux temperature followed by filtration over Celite and evaporation of the solvent. A biphasic solution consisting of dichloromethane (10 mL) and a saturated aqueous solution of NaCl (10 mL) was added. The resulting mixture was stirred for 1 h. Subsequently, the organic phase was separated and the aqueous phase was washed with dichloromethane (2x20 mL). The combined organic fractions were washed with water, dried over $MgSO_4$ and evaporated to dryness. Column chromatography (CH_2Cl_2) was used for further purification of the product. Finally, the product is dissolved in dichloromethane and a large excess (~100 equiv.) of PVPy was added. After the solution has stirred for 2 h, the solution was filtered over Celite. After

evaporation of the dichloromethane, the product was obtained as yellow powder. Yield: 605 mg (89%).

^{1}H NMR (CD_2Cl_2, 300 MHz): δ 7.86 (m, 4H, C SPh_{ortho}), 7.41 (m, 6H, $SPh_{meta+para}$), 7.13 (s, 2H, $CH_{arom.pincer}$), 4.64 (br.s, 4H, SCH_2), 0.24 (s, 9H, $SiCH_3$). ^{13}C NMR ($CDCl_3$, 75 MHz): δ 149.7, 136.9, 132.8, 131.7, 130.0, 129.8, 127.2, 125,1, 52.1, -1.1. ^{29}Si NMR ($CDCl_3$, 60 MHz): δ -3.67. UV/Vis (CH_2Cl_2): λ_{max} = 331.0 nm. ESI-HRMS for $C_{23}H_{25}ClPdS_2Si$ (m/z): $[M-Cl]^+$ 499.0239 (calcd. 499.0210).

*G_0 dendritic SCS-pincer ligand **9***

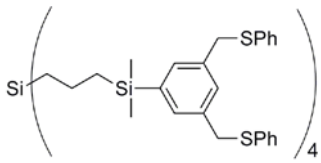

A solution of **5** (4.4 equiv., 1.87 mmol, 0.75 g) in Et_2O (40 mL) was cooled to -80 °C and a 1.6 M *t*BuLi solution in pentane (8.6 equiv., 3.65 mmol, 2.28 mL) was added dropwise in 5 min. The solution immediately turned dark red. The reaction was stirred for another 5 min at −80 °C. Next, carbosilane dendrimer **7** (1 equiv., 0.425 mmol, 0.242 g) was added in one portion. The cooling bath was removed and the reaction mixture was allowed to reach ambient temperature. The color turned to red/orange. Subsequently, MeOH (5 mL) was added to quench the excess lithio-pincer. Immediately, the solution turned pale yellow. After 30 min, all volatiles were evaporated and dichloromethane was added to the residue. This solution was washed with water (2x50 mL) and brine (2x50 mL), dried over $MgSO_4$ and concentrated. The resulting orange syrup was dissolved in 5 mL of a CH_2Cl_2 : MeOH mixture (1:1, *v/v*) and placed into a dialysis bag. This bag was placed into a beaker containing a mixture of CH_2Cl_2 : MeOH (500 mL; 1:1, *v/v*) and dialyzed for 2 h. This procedure was repeated twice. Finally, the contents of the dialysis bag were evaporated, yielding **9** as a pale orange syrup in 0.57 g (76%).

^{1}H NMR ($CDCl_3$, 300 MHz): δ 7.30-7.16 (m, 48H, CH_{arom}), 4.06 (s, 16H, SCH_2), 1.31 (m, 8H, $SiCH_2CH_2$), 0.74 (t, 8H, J = 6.2 Hz, $SiMe_2CH_2$), 0.56 (t, 8H, J = 6.2 Hz, $Si_{core}CH_2$), 0.17 (s, 24H, $SiMe_2$). ^{13}C NMR ($CDCl_3$, 75 MHz): δ 140.5, 137.1, 136.5, 133.1, 130.4, 130.1, 129.0, 126.7, 39.4, 20.7, 18.8, 17.7, -2.7. ^{29}Si NMR ($CDCl_3$, 60 MHz): δ 0.73, -3.82. MALDI-TOF MS for $C_{100}H_{116}S_8Si_5$ (m/z): $[M+H]^+$ 1714.7 (calcd. 1714.9).

*G_0 dendritic SCS-pincer Pd complex **3***

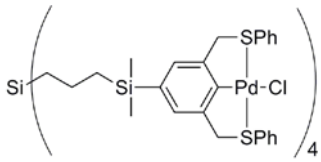

To a solution of compound **9** (0.32 mmol, 550 mg) in an acetonitrile/toluene mixture (20 mL, 1:1, *v/v*) was added $[Pd(MeCN)_4](BF_4)_2$ (5 equiv., 1.6 mmol, 740 mg). The reaction mixture was stirred for 16 h at reflux temperature. After removal of the solvent in vacuo a biphasic system consisting of dichloromethane (10 mL) and brine was added. The reaction mixture stirred for 1 h. Subsequently, the organic phase was separated and the aqueous phase was washed with dichloromethane (2x20 mL). The combined organic fractions were washed with water, dried over $MgSO_4$ and evaporated to dryness. The product was purified with column chromatography (CH_2Cl_2:EtOAc 4:1, *v/v*). Finally, the product is dissolved in dichloromethane and a large excess (~100 equiv.) of PVPy was added. After the solution has stirred for 2 h, the solution was filtered over Celite. After evaporation of the dichloromethane, the product was obtained as yellow powder. Yield: 650 mg (83%).

^{1}H NMR (CD_2Cl_2, 300 MHz): δ 7.83 (d, 16H, SPh_{ortho}), 7.39 (m, 24H, $SPh_{meta+para}$), 7.07 (s, 8H, CH_{pincer}), 4.62 (br. s, 16H, SCH_2), 1.31 (m, 8H, $SiCH_2CH_2$), 0.74 (t, 8H, J = 6.3 Hz, CH_2SiMe_2), 0.53 (t, 8H, J = 6.3 Hz, $Si_{core}CH_2$), 0.18 (s, 24H, $SiMe_2$). ^{13}C NMR ($CDCl_3$, 75 MHz): δ 149.2, 136.3, 132.8, 132.4, 131.4, 130.4, 127.9, 125,9, 52.3, 20.7, 18.8, 17.6, -2.9. ^{29}Si NMR ($CDCl_3$, 60 MHz): δ 0.62, -3.82. UV/Vis: 330.1 nm. MALDI-TOF MS for $C_{100}H_{112}Br_4Pd_4S_8Si_5$ (m/z): $[M + Na]^+$ 2478.73 (calcd. 2479.19).

*G_1 dendritic SCS-pincer ligand **10***

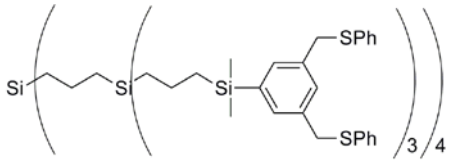

The used procedure of the synthesis of dendritic ligand **10** was similar to the one described for the compound **9**. For **10** 14 equiv. of **5** and 27 equiv. of *t*BuLi have been used. An orange-brown syrup was obtained in 61% yield (0.94 gram).

^{1}H NMR ($CDCl_3$, 300 MHz): δ 7.29-7.17 (m, 144H, $CH_{arom.}$), 4.03 (s, 48H, SCH_2), 1.33 (m, 32H, $SiCH_2CH_2$ (inner and outer)), 0.72 (bt, 24H, CH_2SiMe_2), 0.58 (m, 40H, $SiCH_2$), 0.13 (s, 72H,

$SiMe_2$). ^{13}C NMR ($CDCl_3$, 75 MHz): δ 140.5, 137.2, 136.7, 132.7, 130.8, 129.7, 128.7, 126.3, 39.4, 20.5, 20.2, 19.5, 18.9, 18.4, 17.8, -2.7. ^{29}Si NMR ($CDCl_3$, 59.6 MHz): δ 0.80 (core), 0.57 (middle), -3.75 (periphery).

*G_1 dendritic SCS-pincer Pd complex **4***

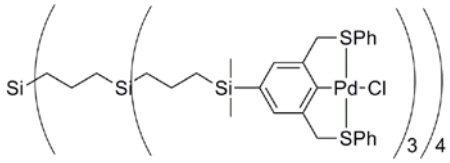

The used procedure for the synthesis of **4** was similar to the one described for the synthesis of **3**, but now 15 equivalents of $[Pd(MeCN)_4](BF_4)_2$ were used. The product appeared as an orange-yellow foam. Yield: 110 mg (60%).

^1H NMR (CD_2Cl_2, 300 MHz): δ. 7.86 (m, 48H, SPh_{ortho}), 7.45 (m, 72H, $SPh_{meta+para}$), 7.12 (bs, 24H, $CH_{arom,\ pincer}$), 4.61 (br. s, 16H, CH_2S), 1.37 (m, 32H, $SiCH_2CH_2$), 0.79 (m, 24H, CH_2SiMe_2), 0.60 (m, 40H, $SiCH_2$), 0.21 (s, 72H, $SiMe_2$). ^{13}C NMR ($CDCl_3$, 75 MHz): δ. 149.2, 136.0, 132.8, 131.9, 131.8, 130.1, 129.7, 127.0, 52.3, 20.7, 20.0, 19.7, 18.8, 18.4, 17.6, -2.8. ^{29}Si NMR ($CDCl_3$, 59.6 MHz): δ 0.77 (core), 0.57 (middle), -3.64 (periphery). UV/Vis: 330.1 nm

General protocol for the stannylation reaction with the catalyst present in solution

In a representative experiment, the appropriate catalyst (2 mol% [Pd], 0.016 mmol), was added to a solution of cinnamyl chloride (0.80 mmol, 122.1 mg, 113 μL), hexamethylditin (1.05 equiv., 0.84 mmol, 275 mg, 174 μL) and hexamethylbenzene (internal standard, 0.088 mmol, 14.4 mg) in 6 mL dry THF or CH_2Cl_2. The reaction stirred at room temperature in a nitrogen environment. Aliquots of 50 μL for NMR/GC analysis were regularly taken with an airtight syringe.

General protocol for the tandem coupling reaction with the catalyst present in solution

In a representative experiment, the appropriate catalyst (2 mol% [Pd], 0.016 mmol), was added to a solution of cinnamyl chloride (0.80 mmol, 122.1 mg, 113 μL), hexamethylditin (1.05 equiv., 0.84 mmol, 275 mg, 174 μL), 4-nitrobenzaldehyde (1.05 equiv., 0.84 mmol, 126.9 mg) and hexamethylbenzene (internal standard, 0.088 mmol, 14.4 mg) in 6 mL dry

THF. The reaction stirred at room temperature in a nitrogen environment. Aliquots of 50 µL for NMR/GC analysis were regularly taken with an airtight syringe.

*General protocol for the compartmentalized stannylation reaction with dendritic catalyst **4** present inside a membrane dialysis bag*

In a tailor-made reaction vessel, which is equipped with a stirring bar, a NS50 joint and a nitrogen inlet, dry THF (60 mL) was added. To the solvent were subsequently added cinnamyl chloride (8.0 mmol, 1.22 g, 1.13 mL), hexamethylditin (8.0 mmol, 2.75 g, 1.74 mL), and hexamethylbenzene (internal standard, 0.89 mmol, 144 mg). A dialysis bag (Aldrich, benzoylated cellulose membranes, MWCO = 1000 Da.) with 2.5 mL THF and 0.0133 mmol (2 mol% Pd) **4** was added to this solution. In regular intervals, samples of the outer solution were taken and analyzed by ^{1}H NMR.

*General protocol for the compartmentalized tandem coupling reaction with dendritic catalyst **4** present inside a membrane dialysis bag*

In a tailor-made reaction vessel, which is equipped with a stirring bar, a NS50 joint and a nitrogen inlet, dry THF (60 mL) was added. To the solvent were subsequently added cinnamyl chloride (8.0 mmol, 1.22 g, 1.13 mL), hexamethylditin (8.0 mmol, 2.75 g, 1.74 mL), 4-nitrobenzaldehyde (8.0 mmol, 1.21 g) and hexamethylbenzene (internal standard, 0.89 mmol, 144 mg). A dialysis bag (Aldrich, benzoylated cellulose membranes, MWCO = 1000 Da) with 2.5 mL THF and 0.0133 mmol (2% Pd) **4** that was closed by plastic clamps was added to this solution. In regular intervals, samples of the outer solution were taken and analyzed by ^{1}H NMR.

After the reaction has finished, the dialysis bag was directly placed in a fresh batch of substrates to start a new catalytic run.

2.7 References

1. Oosterom, G. E.; Reek, J. N. H.; Kamer, P. C. J.; van Leeuwen, P. W. N. M. *Angew. Chem. Int. Ed.* **2001,** *40*, 1828-1849.
2. van Heerbeek, R.; Kamer, P. C. J.; van Leeuwen, P. W. N. M.; Reek, J. N. H. *Chem. Rev.* **2002,** *102*, 3717-3756.
3. Dijkstra, H. P.; van Klink, G. P. M.; van Koten, G. *Acc. Chem. Res.* **2002,** *35*, 798-810.

4. Chase, P. A.; Klein Gebbink, R. J. M.; van Koten, G. *J. Organomet. Chem.* **2004,** *689*, 4016-4054.
5. Müller, C.; Nijkamp, M. G.; Vogt, D. *Eur. J. Inorg. Chem.* **2005**, 4011-4021.
6. Vankelecom, I. F. J. *Chem. Rev.* **2002,** *102*, 3779-3810.
7. Scarpello, J. T.; Nair, D.; dos Santos, L. M. F.; White, L. S.; Livingston, A. G. *J. Membrane Sci.* **2002,** *203*, 71-85.
8. Bosman, A. W.; Janssen, H. M.; Meijer, E. W. *Chem. Rev.* **1999,** *99*, 1665-1688.
9. Knapen, J. W. J.; van der Made, A. W.; de Wilde, J. C.; van Leeuwen, P. W. N. M.; Wijkens, P.; Grove, D. M.; van Koten, G. *Nature* **1994,** *372*, 659-663.
10. Astruc, D.; Chardac, F. *Chem. Rev.* **2001,** *101*, 2991-3023.
11. Kreiter, R.; Kleij, A. W.; Klein Gebbink, R. J. M.; van Koten, G. *Top. Curr. Chem.: Dendrimers IV* **2001,** *217*, 163-199.
12. Twyman, L. J.; King, A. S. H.; Martin, I. K. *Chem. Soc. Rev.* **2002,** *31*, 69-82.
13. Astruc, D.; Boisselier, E.; Ornelas, C. *Chem. Rev.* **2010,** *110*, 1857-1959.
14. de Jesús, E.; Flores, J. C. *Ind. Eng. Chem. Res.* **2008,** *47*, 7968-7981.
15. Berger, A.; Klein Gebbink, R. J. M.; van Koten, G. *Top. Organomet. Chem.* **2006,** *20 (Dendrimer Catal.)*, 1-38.
16. Mery, D.; Astruc, D. *Coord. Chem. Rev.* **2006,** *250*, 1965-1979.
17. Yazerski, V. A.; Klein Gebbink, R. J. M. *Catalysis by Metal Complexes (2010)* **2010,** *33 (Heterogenized Homogeneous Catalysts for Fine Chemicals Production)*, 171-201.
18. Pijnenburg, N. J. M.; Korstanje, T. J.; van Koten, G.; Klein Gebbink, R. J. M. *Palladacycles on Dendrimers and Star-Shaped Molecules, Wiley-VCH Verlag GmbH & Co. KGaA* **2008**, 361-398, *or* ***Chapter 1*** *of this thesis.*
19. Fogg, D. E.; dos Santos, E. N. *Coord. Chem. Rev.* **2004,** *248*, 2365-2379.
20. Gaikwad, A. V.; Boffa, V.; ten Elshof, J. E.; Rothenberg, G. *Angew. Chem. Int. Ed.* **2008,** *47*, 5407-5410.
21. Janssen, M.; Müller, C.; Vogt, D. *Adv. Synth. Catal.* **2009,** *351*, 313-318.
22. Janssen, M.; Wilting, J.; Müller, C.; Vogt, D. *Angew. Chem. Int. Ed.* **2010,** *49*, 7738-7741.
23. Sheldon, R. A.; van Bekkum, H. *Fine Chemicals Through Heteregeneous Catalysis* **2007**, 1st edition, Wiley, New York.
24. Grimes, M. T.; Drueckhammer, D. G. *J. Org. Chem.* **1993,** *58*, 6148-6150.
25. Albrecht, M.; Hovestad, N. J.; Boersma, J.; van Koten, G. *Chem. Eur. J.* **2001,** *7*, 1289-1294.
26. Arink, A. M.; van de Coevering, R.; Wieczorek, B.; Firet, J.; Jastrzebski, J. T. B. H.; Klein Gebbink, R. J. M.; van Koten, G. *J. Organomet. Chem.* **2004,** *689*, 3813-3819.
27. Gaab, M.; Bellemin-Laponnaz, S.; Gade, L. H. *Chem. Eur. J.* **2009,** *15*, 5450-5462.
28. Albrecht, M.; van Koten, G. *Angew. Chem. Int. Ed.* **2001,** *40*, 3750-3781.
29. Singleton, J. T. *Tetrahedron* **2003,** *59*, 1837-1857.
30. Selander, N.; Szabó, K. J. *Chem. Rev.* **2011,** *111*, 2048-2076.
31. Jensen, C. M.; Morales-Morales, D. *The Chemistry of Pincer Compounds* **2007,** *Elsevier Science Ltd.*
32. Kleij, A. W.; Gossage, R. A.; Klein Gebbink, R. J. M.; Brinkmann, N.; Reijerse, E. J.; Kragl, U.; Lutz, M.; Spek, A. L.; van Koten, G. *J. Am. Chem. Soc.* **2000,** *122*, 12112-12124.
33. Wallner, O. A.; Szabó, K. J. *Org. Lett.* **2004,** *6*, 1829-1831.
34. Solin, N.; Kjellgren, J.; Szabó, K. J. *J. Am. Chem. Soc.* **2004,** *126*, 7026-7033.
35. Gagliardo, M.; Selander, N.; Mehendale, N. C.; van Koten, G.; Klein Gebbink, R. J. M.; Szabó, K. J. *Chem. Eur. J.* **2008,** *14*, 4800-4809.
36. Li, J.; Siegler, M.; Lutz, M.; Spek, A. L.; Klein Gebbink, R. J. M.; van Koten, G. *Adv. Synth. Catal.* **2010,** *352*, 2474-2488.
37. Lucena, N.; Casabo, J.; Escriche, L.; Sanchez-Castello, G.; Teixidor, F.; Kivekas, R.; Sillanpää, R. *Polyhedron* **1996,** *15*, 3009-3018.
38. Weck, M.; Jones, C. W. *Inorg. Chem.* **2007,** *46*, 1865-1875.
39. Chen, J. S.; Vasiliev, A. N.; Panarello, A. P.; Khinast, J. G. *Appl. Catal. A Gen.* **2007,** *325*, 76-86.
40. van der Made, A. W.; van Leeuwen, P. W. N. M. *J. Chem. Soc. Chem. Commun.* **1992**, 1400-1401.
41. Dupont, J.; Beydoun, N.; Pfeffer, M. *J. Chem. Soc. Dalton Trans.* **1989**, 1715-1720.
42. Kruithof, C. A.; Dijkstra, H. P.; Lutz, M.; Spek, A. L.; Klein Gebbink, R. J. M.; van Koten, G. *Organometallics* **2008,** *27*, 4928-4937.
43. Pijnenburg, N. J. M.; Cabon, Y. H. M.; van Koten, G.; Klein Gebbink, R. J. M. ***Chapter 3*** *of this thesis.*
44. Bergbreiter, D. E.; Osburn, P. L.; Frels, J. D. *Adv. Synth. Catal.* **2005,** *347*, 172-184.
45. Yu, K. Q.; Sommer, W.; Richardson, J. M.; Weck, M.; Jones, C. W. *Adv. Synth. Catal.* **2005,** *347*, 161-171.

46. Sommer, W. J.; Yu, K. Q.; Sears, J. S.; Ji, Y. Y.; Zheng, X. L.; Davis, R. J.; Sherrill, C. D.; Jones, C. W.; Weck, M. *Organometallics* **2005,** *24*, 4351-4361.
47. Meijer, M. D.; Mulder, B.; van Klink, G. P. M.; van Koten, G. *Inorg. Chim. Acta* **2003,** *352*, 247-252.
48. Steenwinkel, P.; James, S. L.; Grove, D. M.; Veldman, N.; Spek, A. L.; van Koten, G. *Chem. Eur. J.* **1996,** *2*, 1440-1445.
49. Lai, T. W.; Sen, A. *Organometallics* **1984,** *3*, 866.

Chapter 3

Mechanistic studies on the SCS-pincer palladium-catalyzed tandem stannylation/electrophilic addition of allyl chlorides with hexamethylditin and benzaldehydes

Abstract

This chapter describes a mechanistic study of the SCS-pincer Pd-catalyzed auto-tandem reaction consisting of the stannylation of cinnamyl chloride with hexamethylditin, followed by an electrophilic addition of the primary tandem reaction product with 4-nitrobenzaldehyde to yield homoallylic alcohols as the secondary tandem products. This study pointed out that the anticipated stannylation product, cinnamyl trimethylstannane, is not a substrate for the second part of the tandem reaction.

These studies have provided insight in the catalytic behavior of SCS-pincer Pd(II) complexes in the auto-tandem reaction and on the formation and possible involvement of Pd(0) species during prolonged reaction times. The outcome of this study has led to optimized reaction conditions by which the overall tandem reaction proceeds through SCS-pincer Pd(II)-mediated catalysis, i.e. true auto-tandem catalysis. Accordingly, this study has provided the proper reaction conditions that allow the pincer catalysts to be recycled and reused.

3.1 Introduction

ECE-pincer palladium complexes have proven to be versatile catalysts that show unique catalytic properties due to (1) the strong Pd-C σ-bond that provides a stable ligand-metal manifold for catalysis and (2) the limitation of available coordination sites due to the tridentate nature of the ECE-pincer ligand. These properties modify the catalytic applications of palladium significantly.[1-6] Palladium pincer complexes serve as excellent catalysts for, among others, the stannylation of allylic chlorides, propargylic chlorides, allylic alcohols, phosphonates and epoxides using hexaalkylditin, as was published recently by Szabó and co-workers.[7,8] The same group also reported that palladium pincer complexes can act as catalysts for the addition of electrophiles like imines, sulfonimines, and aldehydes to allylstannanes.[9,10] Since some of the products of the stannylation reactions (e.g. allyl trialkylstannanes) can act as starting material for the electrophilic addition, studies have been performed to combine these two reactions in a one-pot procedure using two different orthogonal ECE-pincer palladium complexes[7] or in an auto-tandem system using a single SCS-pincer palladium complex catalyzing both reactions (SCS = $[2,6\text{-}(CH_2SPh)_2C_6H_3]^-$; *figure 3.1)*.[11]

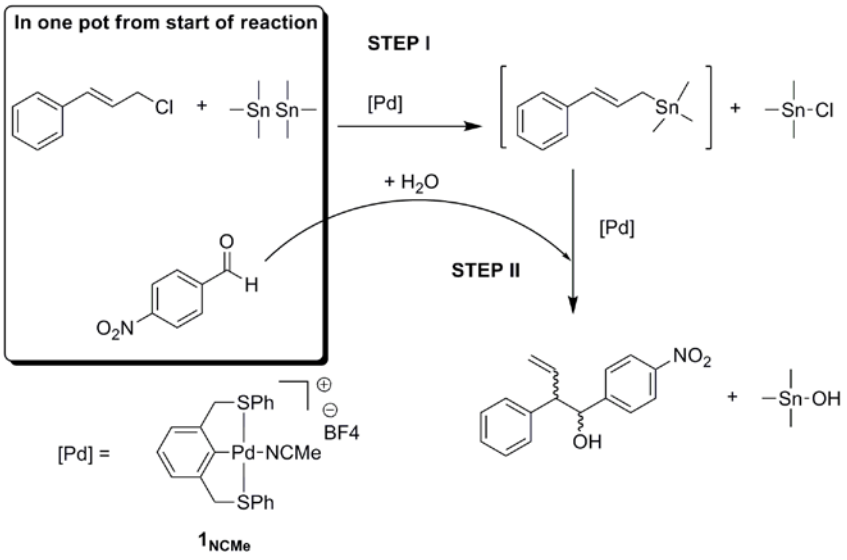

*Figure 3.1: Auto-tandem catalytic formation of 1-(4-nitrophenyl)-2-phenyl-3-buten-1-ol catalyzed by SCS-pincer Pd complex **1.MeCN**.*

A mechanism consisting of two catalytic cycles was proposed for this auto-tandem reaction (*figure 3.2*). This mechanism is a combination of the mechanisms of the two separate reactions.[7,9] First the SCS-pincer Pd(II) complex **1.MeCN** reacts with hexamethylditin to give the SCS-pincer Pd(II)-$SnMe_3$ complex **1.SnMe$_3$** (*figure 3.2, step A*). In the initial report [Pd(SCS)(MeCN)]BF_4 **1.MeCN** was used as the catalyst, while recently we have reported on the use of [Pd(SCS)Cl] **1.Cl** as catalysts.[12] Complex **1.SnMe$_3$** undergoes nucleophilic substitution with allyl chloride yielding allyltrimethylstannane and recovering the SCS-pincer Pd-halide complex **1.X** (step *B*). In the second cycle, the regained catalyst **1.X** undergoes a new transmetalation reaction in which it reacts with the formed allyl stannane leading to the formation of the reactive η^1-allylpalladium complex **1.η^1-allyl** (*step C*). This complex then acts as a nucleophile towards 4-nitrobenzaldehyde (*step D*). As the highest nucleophilicity resides on the γ-carbon atom of the allyl fragment of **1.η^1-allyl**, this reaction leads to the formation of a mixture of *syn* and *anti* homo-allylic alcohol products. After product dissociation **1.X** is regenerated in the last step (step E).

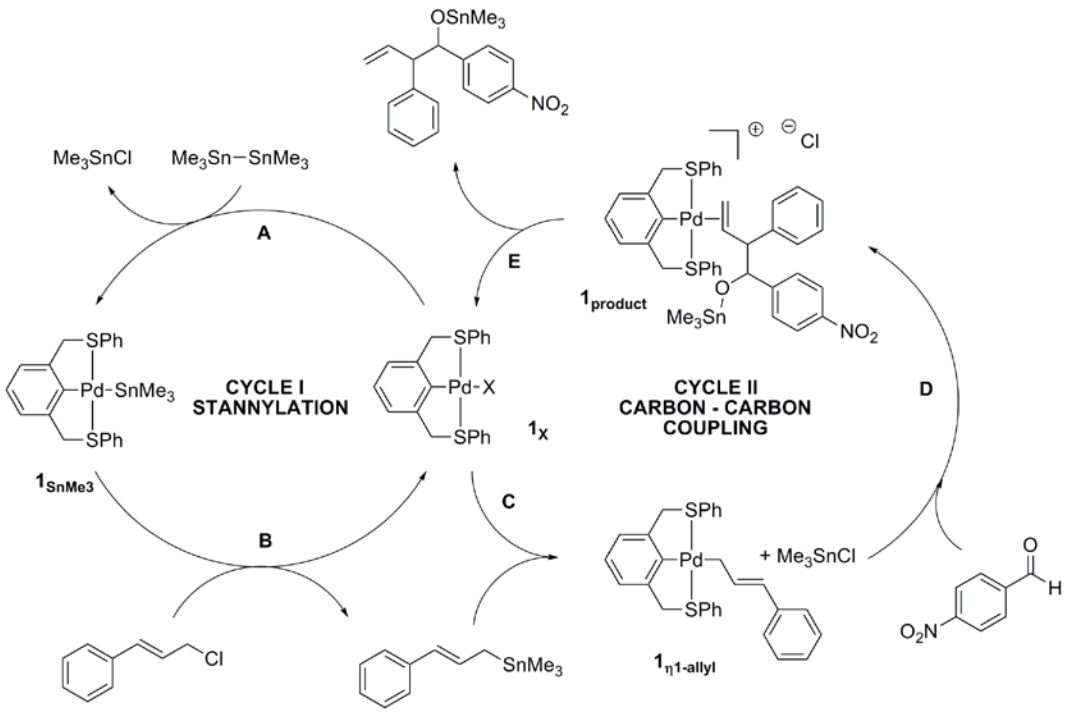

Figure 3.2: Proposed mechanism for the SCS-pincer Pd-catalyzed tandem stannylation/electrophilic substitution reaction between allyl chlorides, hexamethylditin and benzaldehydes (X = MeCN).[11]

Recent investigations on the recycling of dendritic SCS-pincer Pd-catalysts have raised questions concerning this Pd(II)-only mechanism. In these investigations the catalytic behavior of dendritic SCS-pincer palladium complexes in the tandem reaction was studied both in homogeneous solution and in a membrane dialysis bag.[12] In particular, in the compartmentalized dialysis bag experiments considerable palladium leaching was observed by ICP-MS and ^{1}H NMR analysis. It was found that after four consecutive runs approximately 30-40% of the pincer moieties of the dendritic catalyst did no longer contain a palladium center, indicating that Pd-leaching had occurred through release of palladium from the SCS-pincer ligands. These individual palladium centers will agglomerate to palladium nanoparticles, and penetration of the palladium nanoparticle through the dialysis bag may or may not occur, depending on the size of these nanoparticles. ICP-MS analysis of the outer membrane solutions showed a cumulative leaching of 27.5% Pd after four runs, similar to the observed amount of free ligands as analyzed by NMR analysis. This palladium leaching points to two important drawbacks in the compartmentalized auto-tandem catalysis setup. Firstly, leaching decreases the recycling efficiency of the dendritic catalyst, since the amount of catalytic centers in the dendritic catalyst decreases with each reuse. Secondly, if leaching takes place, it is unclear whether Pd(0) species play a role as catalyst and thus also contribute to the product formation. In case these species are catalytically active, this might have implications for several reaction parameters, including the overall activity and product selectivity, as was described by Jones *et al.* in their review on active species in palladium-catalyzed Heck and Suzuki-Miyaura reactions.[13] They demonstrated, e.g., that all catalytic activity in the Heck coupling of *n*-butyl acrylate with iodobenzene catalyzed by soluble polymer-supported SCS-pincer Pd complexes was caused by leached Pd(0) species and that the starting SCS-pincer Pd(II) complexes were inactive.[14]

Here, we report a more detailed study of this auto-tandem reaction to get insight in the catalytic behavior of SCS-pincer Pd(II) complexes and on the formation and possible involvement of Pd(0) species in catalysis. The aim of these studies was to find optimized reaction conditions where the formation of potentially active Pd(0) species can be avoided, in order to create a catalytic system in which SCS-pincer Pd(II) complexes are the only catalytically active species. Under such optimized conditions, the use of dendritic SCS-pincer palladium complexes in a compartmentalized setup would allow for their consecutive catalytic application without catalyst decomposition and, accordingly, under constant

operation conditions. In our present studies, we have used monomeric SCS-pincer Pd-Cl complexes in a series of kinetic experiments in combination with DFT calculations. These results have led to a more detailed mechanistic insight, which led to the development of improved conditions for running the tandem reaction of cinnamyl chloride with hexamethylditin and 4-nitrobenzaldehyde using dendritic SCS-pincer Pd(II) complexes in a compartmentalized reaction setup.

3.2 Kinetic reaction profile

An ideal tandem reaction consisting of two subsequent reactions deals with two rate constants: k_1 for reaction A + B → C, and k_2 for the subsequent reaction C + D → E (*figure 3.3*). In this simplified model it is assumed that all reagents are orthogonal, i.e. these do not react with each other in the absence of a catalyst. For the stannylation/electrophilic addition tandem reaction, this model can be used by assigning cinnamyl chloride as A, hexamethylditin as B, primary product cinnamyl trimethylstannane as C, 4-nitrobenzaldehyde as D and secondary product trimethyl(1-(4-nitrophenyl)-2-phenylbut-3-enyloxy)stannane (or its aqueous workup reaction product 1-(4-nitrophenyl)-2-phenyl-3-buten-1-ol) as E.

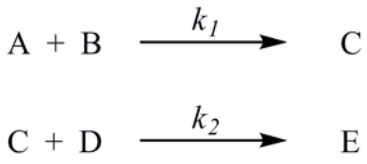

Figure 3.3: Simplified model for a tandem reaction with reagents A, B, and D and two subsequent reactions with rate constants k_1 and k_2.

The kinetic profile of this tandem reaction will vary with the values of the rate constants k_1 and k_2. With the input of the experimental data that were collected for the SCS-pincer palladium-catalyzed tandem reaction earlier by us,[12] we estimated $k_1 = 8 \cdot 10^{-3}$ mol s^{-1} and k_2

$= 4 \cdot 10^{-4}$ mol s^{-1}. By using these estimated values, a theoretical kinetic profile for this tandem reaction was calculated (*figure 3.4, see footnote*[8]).[15]

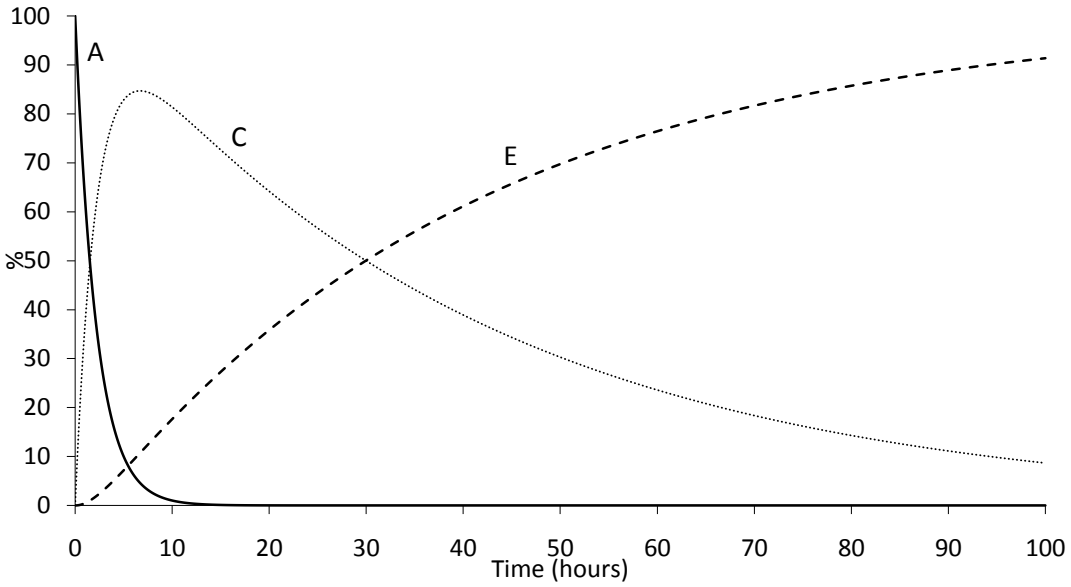

Figure 3.4: Theoretical kinetic profile for the tandem reaction with $k_1 = 8 \cdot 10^{-3}$ mol s^{-1} and $k_2 = 4 \cdot 10^{-4}$ mol s^{-1}. (A: cinnamyl chloride; C: cinnamyl trimethylstannane; E: trimethyl(1-(4-nitrophenyl)-2-phenylbut-3-enyloxy)stannane).

The experimental kinetic profile of the tandem reaction catalyzed by SCS-pincer Pd complex **1.Cl** reveals several differences between the theoretical and experimental kinetic profile for this reaction (*figure 3.5*). Similar reaction profiles were also observed for other monomeric SCS-pincer Pd complexes as well as for dendritic SCS-pincer Pd complexes,[12] thereby showing the single-site nature of each catalytic center in these dendritic complexes. For this reason the present studies were carried out with monomeric SCS-pincer Pd complex **1.Cl**.

The experimental kinetic profile shows that in the first 5 h of the reaction (*Part I* in *figure 3.5*) cinnamyl chloride is consumed relatively fast (84% conversion) and both the primary product cinnamyl trimethylstannane and the secondary product 1-(4-nitrophenyl)-2-phenylbut-3-en-1-olare formed in 50 and 34%, respectively. The formation of 1-(4-

[8] The theoretical kinetic profile for tandem reaction has been calculated using Microsoft Office Excel 2007 using:
$[A] = [A]_0 * \exp(-k_1 * t)$,
$[B] = [A]_0 * [k_1 / (k_2 - k_1)] * [\exp(-k_1 * t) - \exp(-k_2 * t)]$, and
$[C] = [A]_0 * \mathbf{[}1 + \mathbf{(}[k_1 * \exp(-k_2 * t) - k_2 * \exp(-k_1 * t)] / [k_2 - k_1]\mathbf{)]}$.[15]

nitrophenyl)-2-phenylbut-3-en-1-oldid not show the sinusoidal kinetic curve as predicted for the formation of a secondary product in a tandem reaction (*figure 3.4*). Instead, the instant formation of both the primary and secondary tandem products was observed; each of them being formed in substantial amounts already after as early as 15 min (typically around 20-30%). In the second part of the reaction (*Part II* in *figure 3.5*), the reaction progression suddenly stops, resulting in a period during which no change in the concentration of the starting material, primary and secondary product is observed. After 24 h, in the third and last part of the reaction (*Part III* in *figure 3.5*), the reaction catalysis starts again leading to a slow but complete conversion of the primary product, cinnamyl trimethylstannane to secondary product 1-(4-nitrophenyl)-2-phenylbut-3-en-1-olin 5 days.

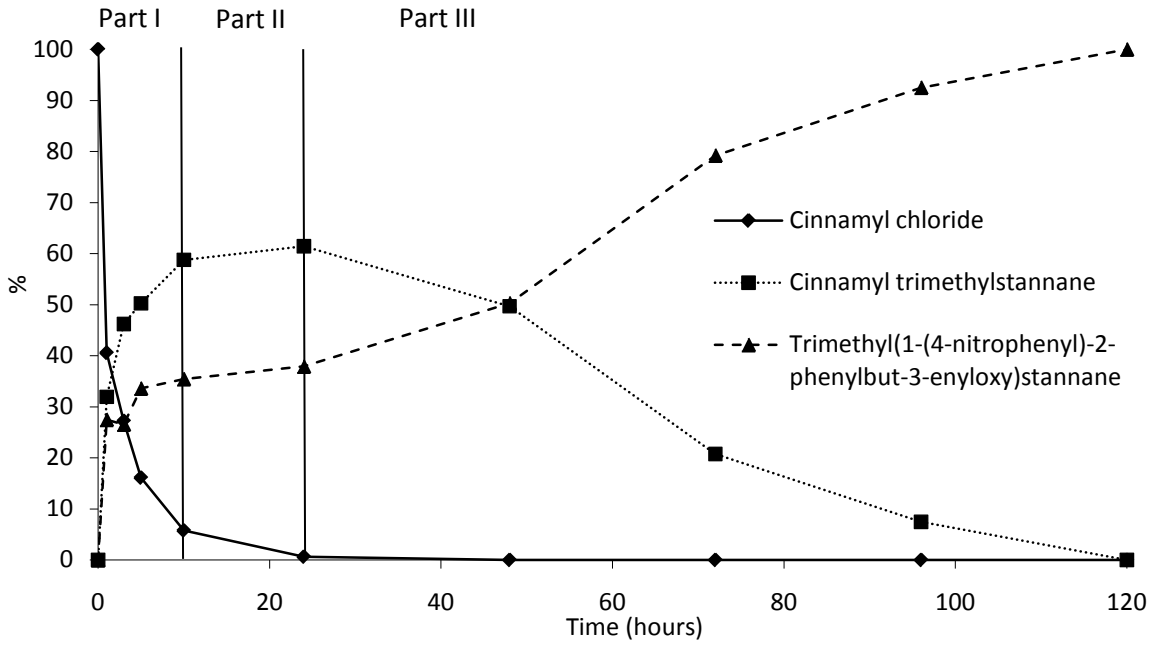

Figure 3.5: Experimental kinetic profile for the SCS-pincer Pd-catalyzed tandem reaction. Conditions: 0.80 mmol cinnamyl chloride, 0.80 mmol hexamethylditin, 0.80 mmol 4-nitrobenzaldehyde and 2 mol% Pd catalyst ***1.Cl*** *in 6 mL of THF (ambient temperatures, N_2 atmosphere).*

In conclusion, the observed reaction profile shows two distinct sections. One section (part I) that leads to close to complete consumption of starting material and rapid formation of both primary and approximately 35% of the secondary product trimethyl(1-(4-nitrophenyl)-2-phenylbut-3-enyloxy)stannane. The second section involves a combination of parts II and III, in which consumption of the primary product to form the secondary product goes through a

significant lag phase and ultimately leads to almost quantitative formation of trimethyl(1-(4-nitrophenyl)-2-phenylbut-3-enyloxy)stannane. These observations strongly suggest that instead of a single catalytically species, the involvement of at least two catalytically active species seem to be required to describe the experimental kinetic profile of the tandem reaction.

To investigate these findings in more detail, a series of kinetic experiments were performed. Firstly, the two individual reactions that form the tandem reaction were investigated independently to get more insight in the behavior of catalyst **1.Cl** in the separate reaction steps (*paragraph 3.3*). Secondly, control experiments were carried out in which the reactivity of the substrates with respect to each other and/or the catalyst was investigated (*paragraph 3.4*). The results of these experiments have allowed us to propose a new mechanism that explains the full experimental kinetic reaction profile as shown in *figure 3.5* (*paragraph 3.5*). This mechanism is corroborated by additional DFT calculations (*paragraph 3.6*).

3.3 Separate reaction steps

3.3.1 Reaction step 1: Stannylation

The conversion of cinnamyl chloride in the first step of the tandem reaction, i.e. the stannylation with hexamethylditin, was investigated using THF and CH_2Cl_2 as solvents and in the absence and presence of 4-nitrobenzaldehyde. In these experiments the loading of catalyst **1.Cl** was fixed at 2 mol%. The results of these experiments are depicted in *table 3.1*. This reaction exhibits a small solvent effect: reactions carried out in THF tend to be slightly faster than those in CH_2Cl_2. Furthermore, the stannylation of cinnamyl chloride in the absence of the benzaldehyde electrophile was remarkably faster than in the case where the electrophile was present. For the separate reaction, a complete conversion was found in both solvents after 10 h, whereas in the tandem setup approximately 20% cinnamyl chloride remained present at this time. The stannylations in the tandem reaction were completed only after 16 h of reaction time.

An NMR experiment was performed to get insight in the order of the catalyst in the stannylation reaction. A solution containing equimolar amounts of cinnamyl chloride and hexamethylditin (0.67 mmol) in CD_2Cl_2 was placed in a series of NMR tubes and solutions of a given concentration of SCS-pincer Pd complex **1.Cl** were added to reach a constant volume of 0.5 mL. Reaction progression was monitored at regular intervals (*figure 3.6*). We found that the kinetic order in catalyst is 1.7 for this reaction (determined at 10% substrate conversion; see the inset in *figure 3.6*). Even at a catalyst loading of 0.0625 mol%, the reaction progressed at a significant rate. A blank experiment without pincer palladium complex was found not to lead to any product formation.

Table 3.1: Conversion of cinnamyl chloride in the SCS-pincer Pd-catalyzed stannylation with hexamethylditin in the absence or presence of 4-nitrobenzaldehyde in THF or CH_2Cl_2.[a]

4-nitrobenzaldehyde	Solvent	Conversion of cinnamyl chloride (%)		
		1h	5h	24h
Absent	CH_2Cl_2	48	100	100
Absent	THF	72	100	100
Present	CH_2Cl_2	46	80	100
Present	THF	53	84	100

[a] *Conditions: 0.80 mmol cinnamyl chloride, 0.80 mmol hexamethylditin, 2 mol% **1.Cl** and, if present, 0.80 mmol 4-nitrobenzaldehyde in 6 mL solvent (ambient temperatures, N_2 atmosphere).*

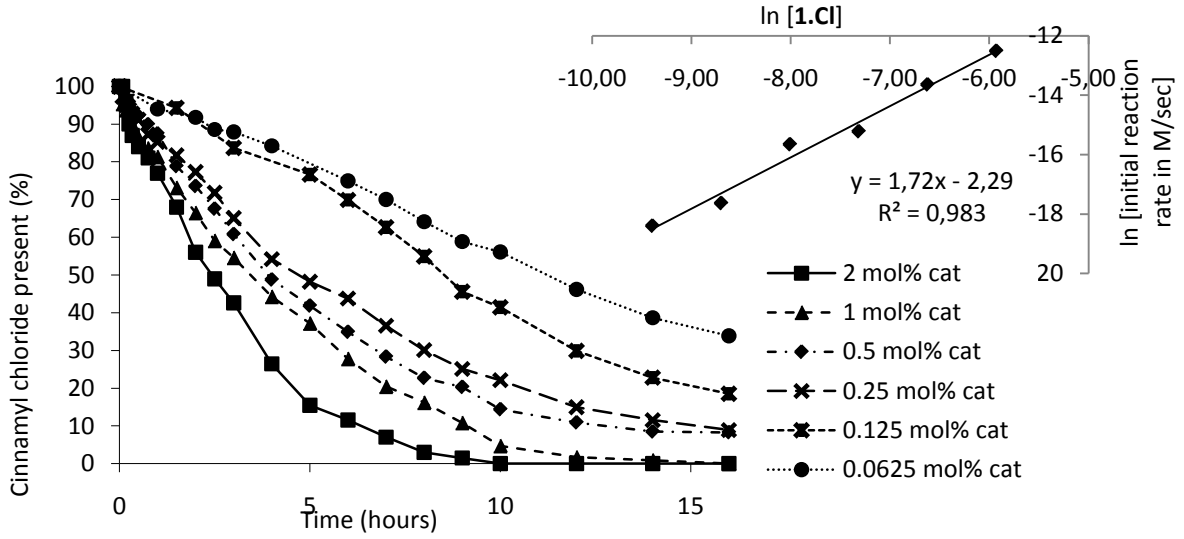

*Figure 3.6: The stannylation of cinnamyl chloride in time using different amounts of catalyst **1.Cl**.*
*Inset: ln ([**1.Cl**]) vs time of 10% cinnamyl chloride conversion.*

Poisoning experiments with mercury and polyvinylpyridine (PVPy) were performed to probe the involvement of Pd(0) species in this reaction. Mercury (Hg(0)) is known to intercept Pd(0) by amalgamation of palladium colloids or by adsorption of Pd(0) particles to the mercury surface.[16,17] PVPy binds free, unbound Pd atoms to the many pyridine ligands that are present in the polymer.[18,19] Upon addition of either of these poisons, no change in reactivity was observed. These observations rule out the involvement of Pd(0) in cycle I.

A closer examination of the separate stannylation reaction in the presence of **1.Cl** by ^{1}H NMR analysis showed that small but significant amounts of 1-phenyl-2-propenyl trimethylstannane, the branched isomer of cinnamyl trimethylstannane were formed in this reaction. Interestingly, the maximum amount of this species reached about 10% after 3 h, whereupon its concentration decreased again to form its more stable isomer cinnamyl trimethylstannane (*figure 3.7)*. Identification of 1-phenyl-2-propenyl trimethylstannane is based on the comparison with reported NMR data of the isolated compound.[20] An ^{1}H NMR spectrum recorded after 3 h of reaction time clearly shows typical signals for cinnamyl chloride, cinnamyl trimethylstannane, as well as 1-phenyl-2-propenyl trimethylstannane (*figure 3.8*).

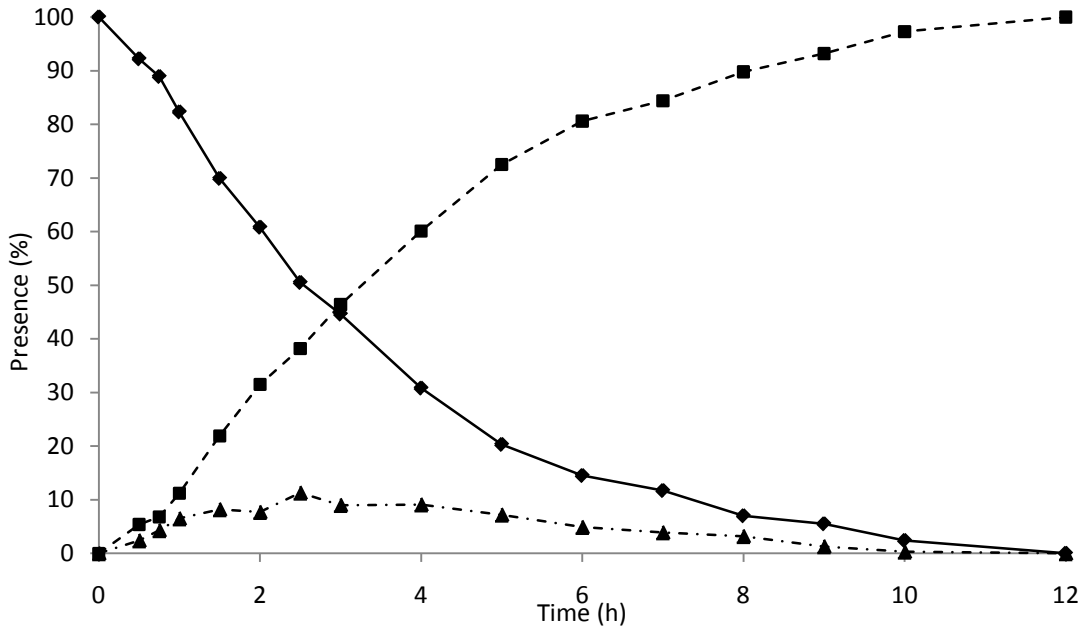

Figure 3.7: The reaction profile of the stannylation of cinnamyl chloride including the presence of 1-phenyl-2-propenyl trimethylstannane.

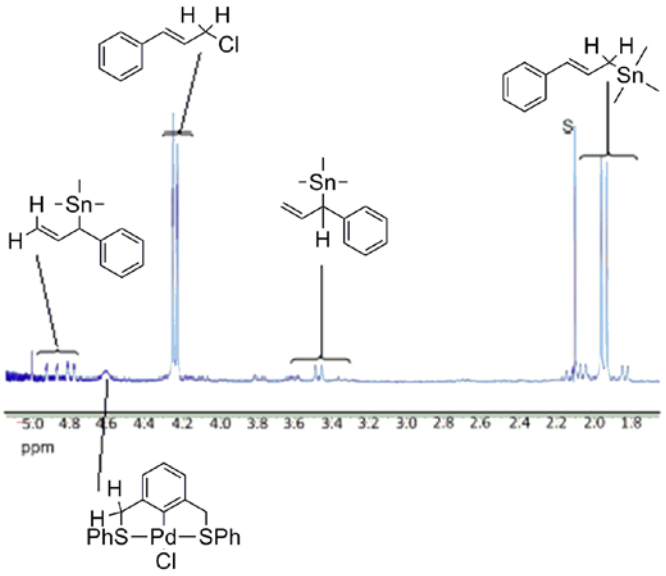

Figure 3.8: ^{1}H spectrum of a stannylation reaction of cinnamyl chloride with hexamethylditin in the presence of ***1.Cl*** *after 50% substrate conversion (S = solvent peak).*

3.3.2 Reaction step II: Electrophilic addition

In a separate experiment, the isolated primary tandem product cinnamyl trimethylstannane was reacted with 4-nitrobenzaldehyde and palladium pincer catalyst **1.Cl** in CH_2Cl_2 or THF in order to determine the kinetics of cycle II of the tandem in an independent manner. In literature this reaction has mainly been performed with PCP-pincer Pd complexes.[9,21] In collaboration with the group of Szabó, we have reported that this particular reaction also works with cationic SCS- and PCS-pincer Pd complexes as the second reaction of the same tandem reaction that is investigated here.[11] Surprisingly, when this second reaction step was investigated with the neutral SCS-pincer Pd complex **1.Cl**, no product formation was found to take place at all after 16 h. The only reaction that was observed, was the partial decomposition of cinnamyl trimethylstannane by Sn-C bond cleavage towards allylbenzene. Even when this experiment was performed at reflux temperatures no formation of homoallylic alcohol products was observed after 16 h.

In another experiment, the effect of adding additional trimethyltin chloride to the reaction mixture was investigated. Trimethyltin chloride is present in the tandem reaction mixture as a byproduct of the first reaction step (*figure 3.1*). Because the electrophilic addition reaction

was successful in the tandem reaction and not in the separate reaction, the presence of trimethyltin chloride in the reaction mixture might play a role. This appeared not to be the case, since also after addition of trimethyltin chloride no reaction between cinnamyl trimethylstannane and 4-nitrobenzaldehyde was observed after 16 h in the presence of catalytic amounts of **1.Cl**. Finally, a stoichiometric amount of catalyst **1.Cl** was used, but even under these conditions no carbon-carbon coupling occurred.

Under these conditions (i.e. using SCS-pincer Pd complex **1.Cl** in the presence or absence of trimethyltin chloride) the reaction mixtures became darker after one day, probably caused by slow decomposition of the pincer complex and formation of palladium colloids in the solution. After a long period of inactivity, product formation eventually was observed in all of these dark reaction mixtures. When this same reaction was performed using the same loading of $Pd(dba)_2$ or $Pd(PPh_3)_4$ as catalyst, the reaction proceeded within 1 h showing a full conversion towards secondary product 1-(4-nitrophenyl)-2-phenylbut-3-en-1-olin a *anti*/*syn* product ratio of 1.5:1.

The reactivity of 1-phenyl-2-propenyl trimethylstannane, the branched isomer of cinnamyl trimethylstannane, was investigated in a similar way. To a solution of independently synthesized 1-phenyl-2-propenyl trimethylstannane[20,22] stoichiometric amounts of 4-nitrobenzaldehyde and catalytic amounts (2 mol%) of SCS-pincer Pd complex **1.Cl** were added and the reaction was followed by NMR analysis. Immediate formation of the allylation product 1-(4-nitrophenyl)-2-phenylbut-3-en-1-olwas observed. After 3 h the reaction was complete and did not only yield the secondary tandem product but also cinnamyl trimethylstannane. The ratio between the tandem *anti* product, the tandem *syn* product, and cinnamyl trimethylstannane was 3.5 : 1 : 1.

Next, 1-phenyl-2-propenyl trimethylstannane was treated with SCS-pincer Pd-catalyst **1.Cl** only (i.e. no aldehyde was added) to determine whether the isomerization of 1-phenyl-2-propenyl trimethylstannane to cinnamyl trimethylstannane is catalyzed by the SCS-pincer Pd complex. After 16 h, large amounts of cinnamyl trimethylstannane were formed, whereas no 1-phenyl-2-propenyl trimethylstannane remained. Because of the unstable character of both isomers, decomposition products (amongst others allylbenzene) were also formed. Indeed, when 1-phenyl-2-propenyl trimethylstannane is stirred in CH_2Cl_2 without additives for 16 h, mainly decomposition products were detected. In addition, small amounts of cinnamyl trimethylstannane were observed while no starting material was recovered. This result is

remarkably different from the experiment in which SCS-pincer Pd–complex **1.Cl** was present. Apparently, SCS-pincer Pd complex **1.Cl** catalyzes the isomerization from 1-phenyl-2-propenyl trimethylstannane to its linear isomer cinnamyl trimethylstannane.

3.4 Control experiments

To get more insight in the reactivity and orthogonality of the used reagents in the tandem reaction, several experiments were performed in which the added equivalents of substrates and the presence or absence of the catalyst were varied. The outcome of these tests is summarized in *table 3.2*. Entries 1-3 show that Pd pincer complex **1.Cl** is required for the stannylation reaction: no blank reaction was observed. In the absence of **1.Cl**, also no reaction occurred between hexamethylditin and 4-nitrobenzaldehyde within 16 h (entry 4). The presence of hexamethylditin is also essential for the formation of the secondary product: no direct palladium-catalyzed coupling of cinnamyl chloride and 4-nitrobenzaldehyde occurred (entry 6). Addition of Pd-pincer complex **1.Cl** to a mixture of hexamethylditin and 4-nitrobenzaldehyde led to decomposition of 4-nitrobenzaldehyde (entry 7). When this experiment was repeated with another electrophile, i.e. 4-cyanobenzaldehyde, no decomposition was found implying the involvement of the nitro-group in the degradation. Using 4-cyanobenzaldehyde as the substrate in the palladium-catalyzed tandem reaction led to very similar reaction kinetics as described here for 4-nitrobenzaldehyde and the formation of the respective secondary tandem product 1-(4-cyanophenyl)-2-phenyl-3-buten-1-ol.

The use of a large excess of 4-nitrobenzaldehyde with respect to cinnamyl chloride and hexamethylditin led to the complete formation of secondary tandem product, but hardly speeded up the reaction (entry 8). Again a temporary state of reaction inactivity was observed, whereupon product formation proceeded gradually to completion after two days. When hexamethylditin was added in large excess, the stannylation was speeded up enormously (full reaction within 15 min), but the reaction did not proceed beyond the primary product cinnamyl trimethylstannane (entry 9), even when a similar excess of 4-nitrobenzaldehyde is used (entry 10). Interestingly no formation of the secondary tandem product was observed in these cases.

Table 3.2: *Control experiments on the reactivity and the orthogonality of the different reagents in the tandem reaction.*[a]

Exp. nr.	Equivalents of substrates			Cat	Products
	CC	HMDT	4NBA		
1	1	1	1	2%	Product 2[b]
2	1	1	0	-	-
3	1	1	1	-	-
4	0	1	1	-	-
5	1	1	0	2%	Product 1
6	1	0	1	2%	-
7	0	1	1	2%	-[c]
8	1	1	10	2%	Product 2[c]
9	1	10	1	2%	Product 1
10	1	10	10	2%	Product 1
11	10	10	1	2%	Product 2[d]
12	5	5	1	2%	Product 2[d]
13	3	3	1	2%	Product 2[d]
14	1.5	1.5	1	2%	Product 2[e]

[a] CC = cinnamyl chloride; HMDT = hexamethylditin; 4NBA = 4-nitrobenzaldehyde, Product 1 = cinnamyl trimethylstannane, Product 2 = trimethyl(1-(4-nitrophenyl)-2-phenylbut-3-enyloxy)stannane. All experiments were performed at 25 ^{o}C and followed in time by ^{1}H NMR analysis. [b] The reaction profile of this entry was similar to the one described in *figure 3.5*. [c] Decomposition of 4-nitrobenzaldehyde was observed. [d] Due to the excess of CC and HMDT, also 9 (entry 11), 4 (entry 12) or 2 (entry 13) equivalents of product 1 were formed respectively. Complete substrate conversion towards tandem product was observed in the first 5 h. [e] Reaction profile of this entry shows 70% product formation in the first 5 h, a plateau at 70% of product formation and finally a gradual completion of the reaction after 120 h.

In the presence of an excess of both cinnamyl chloride and hexamethylditin the tandem reaction went to completion in just a few hours (entries 11-14). *Figure 3.9* shows the reaction profile when three equivalents of cinnamyl chloride and hexamethylditin were used (entry 13). A threefold excess of these substrates with respect to 4-nitrobenzaldehyde therefore resulted in a remarkable 60-fold reaction rate increase (120 h vs 2 h to reach completion) and an entirely different reaction profile. In fact, the observed reaction profile

lacks a lag phase and looks much like the theoretical kinetic profile shown in *figure 3.4.* Only upon lowering the amounts of cinnamyl chloride and hexamethylditin to 1.5 equiv. with respect to 4-nitrobenzaldehyde a reaction plateau was again observed. In this case, product formation stopped after 5 h at 70% of secondary tandem product (compare 40% secondary tandem product formation at equimolar substrate ratio, *figure 3.5*) and only completed after 120 h.

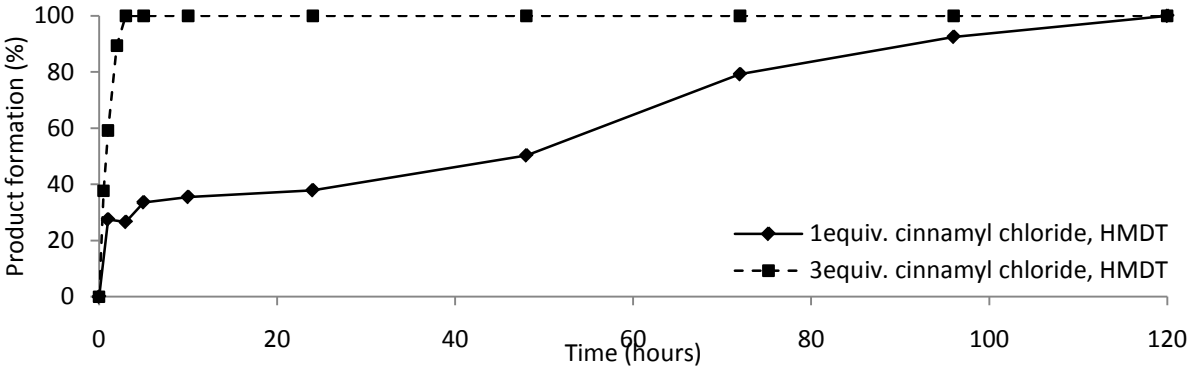

Figure 3.9: Secondary tandem product formation using 4-nitrobenzaldehyde and 1 or 3 equivalents of cinnamyl chloride and hexamethylditin respectively.

3.5 Discussion

The tandem reaction consisting of the SCS-pincer palladium-catalyzed stannylation of cinnamyl chloride by hexamethylditin and subsequent addition of 4-nitrobenzaldehyde to form homo-allylic alcohols shows that the mechanism of this catalytic auto-tandem reaction is more complex than was anticipated so far. Based on our experiments, we propose an alternative mechanism for the tandem reaction catalyzed by SCS-pincer Pd complex **1.Cl** that explains the unusual reaction kinetic profile of the reaction, including the high initial 1-(4-nitrophenyl)-2-phenylbut-3-en-1-olformation and the sudden halt of the formation of this secondary tandem product (*figure 3.10*). These observations could not be explained with the catalytic cycle described by Gagliardo *et al*. for cationic SCS-pincer Pd complexes **1.MeCN**.[11]

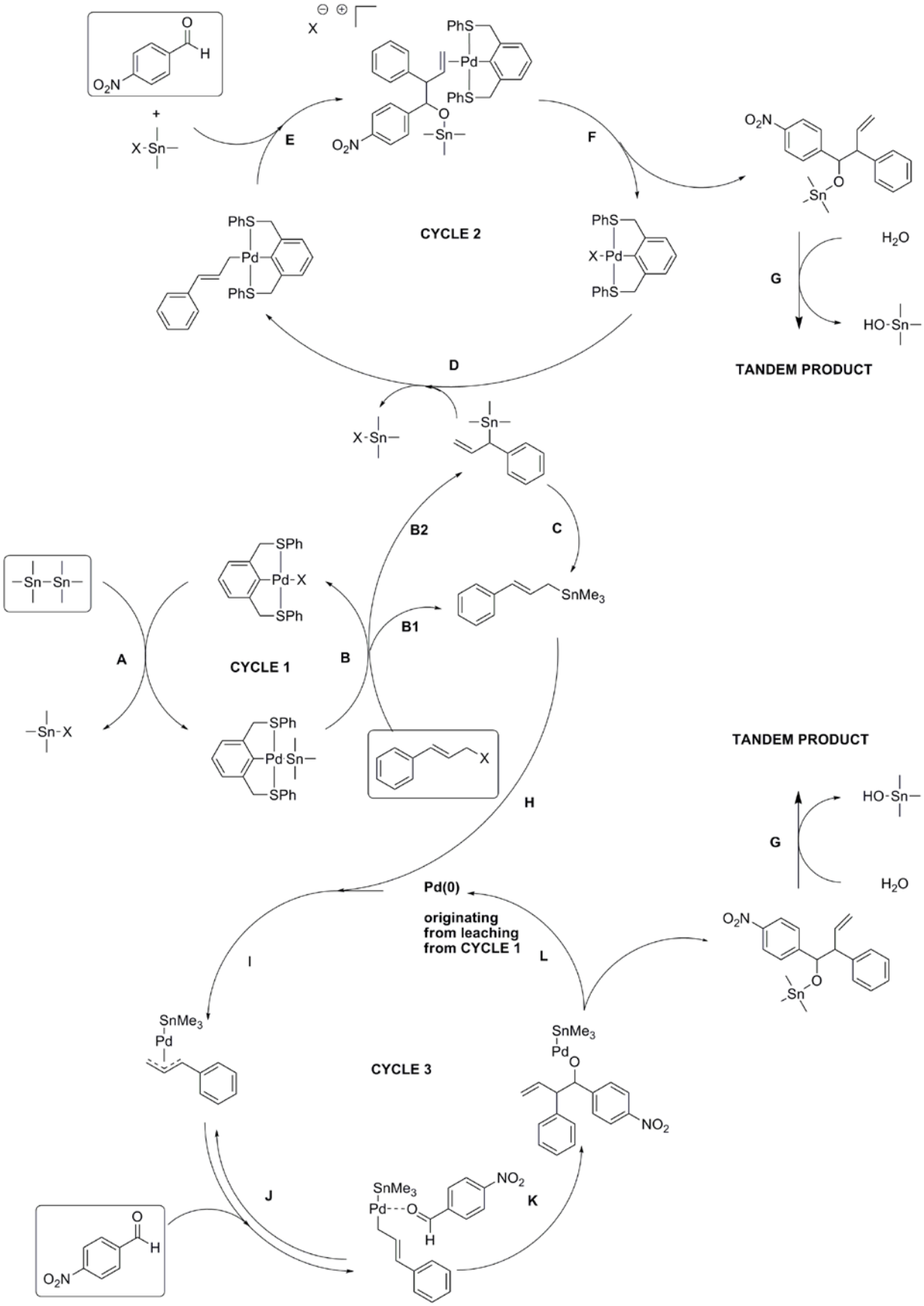

Figure 3.10: Proposed reaction mechanism for the tandem reaction between cinnamyl chloride, hexamethylditin and 4-nitrobenzaldehyde using SCS-pincer palladium complexes.

3.5.1. Cycle 1

In the mechanism shown in *figure 3.10*, SCS-Pd complex **1.Cl** is transmetalated in the first catalytic cycle by hexamethylditin leading to a palladium-tin species (*step A*), which can undergo substitution with allyl chlorides like cinnamyl chloride (*step B*). This reaction can either take place via an S_N2-type substitution leading to the linear product cinnamyl trimethylstannane (*step B1*), or via an S_N2'-type substitution leading to the branched product 1-phenyl-2-propenyl trimethylstannane (*step B2*). Experiments in which only the stannylation reaction was investigated showed that small amounts of the branched S_N2' substitution product are formed. This S_N2' product disappears again before the stannylation reaction goes to completion. It isomerizes in situ to the more stable conjugated cinnamyl trimethylstannane (*step C*) or it enters the second catalytic cycle. The S_N2 product cinnamyl trimethylstannane appeared unreactive and, therefore, does not enter the second catalytic cycle toward the benzaldehyde electrophile in separate reactions. We believe that the formation of 1-phenyl-2-propenyl trimethylstannane is the key to the unusual reaction profile that was observed for the tandem reaction.

As soon as the first reaction step is completed, i.e. all cinnamyl chloride and hexamethylditin have reacted, no 1-phenyl-2-propenyl trimethylstannane is present, because it has either reacted onward to the secondary tandem product or it has been converted to the more stable cinnamyl trimethylstannane. At this point, cycle II of the tandem reaction cannot take place, since the remaining cinnamyl trimethylstannane has proven to be unreactive in this reaction. This explains the sudden drop in activity at the end of part I of the reaction profile. It furthermore explains why higher amounts of cinnamyl chloride and hexamethylditin compared to 4-nitrobenzaldehyde lead to a reaction plateau at a higher percentage of secondary product (entry 14), or to a completed tandem reaction with a normal kinetic profile (*table 3.2*, entries 11-13).

For this stannylation reaction an order of 1.7 in palladium was found (*figure 3.6*), which suggests a certain degree of positive cooperativity of SCS-pincer Pd fragments in the rate limiting step of the reaction. Therefore catalysts showing a high local concentration of catalytic centers, e.g. dendritic catalysts, might show a higher reaction rate than their monomeric analogues. Indeed, earlier investigations by us (***Chapter 2***) show that the dendritic SCS-pincer Pd-complexes are more active catalysts for the stannylation of cinnamyl

chloride.[12] Here the monomeric catalyst showed 63% conversion of cinnamyl chloride after 1 h reaction, while the G_0 and the G_1 dendritic catalysts are significantly more active showing 71% and 85% conversion, respectively.

In conclusion, only when the first reaction step in the tandem is progressing, i.e. when distinct amounts of 1-phenyl-2-propenyl trimethylstannane are present, the second tandem step can take place, since this species is required to feed the second reaction step. As soon as the starting materials cinnamyl chloride and hexamethylditin become depleted, no further formation of 1-phenyl-2-propenyl trimethylstannane occurs which leads to a status quo in the kinetic reaction profile.

3.5.2 Cycle 2

While in our previous investigation we assumed that the second catalytic cycle starts with the formation of a Pd-η^1-allyl intermediate upon reaction of linear cinnamyl trimethylstannane with the (recovered) SCS-pincer Pd complex **1.Cl**,[11] we now propose that this catalytic cycle starts with a transmetalation between branched product 1-phenyl-2-propenyl trimethylstannane and the SCS-pincer Pd-halide complex. This leads to the formation of the η^1-allyl palladium species $\mathbf{1}_{\eta\text{1-allyl}}$ (*step D*). The attack on the carbonyl group of the benzaldehyde subsequently takes place from the nucleophilic γ-carbon, creating a tertiary homo-allylic alcohol that is coordinated to the Pd center in a η^2-allyl fashion via the allyl moiety (*step E*). In this step, the two prochiral reaction partners react to form a mixture of secondary reaction products favoring the *anti* products (*RS, SR*) above the *syn* products (*RR, SS*). The *anti* products are formed in excess due to the more advantageous spatial distribution of the substituents, which reduces steric hindrance in the transition state in step E. In the absence of available protons, the product is initially stabilized by the earlier released trimethyltin cation. Finally, the formed product is liberated from Pd (*step F*), whereupon protonation in the workup leads to the secondary tandem product 1-(4-nitrophenyl)-2-phenyl-3-buten-1-ol (*step G*).

3.5.3 Cycle 3

In the third cycle all further reactivity is proposed to be mediated by the in situ formation of Pd(0) species and not at all by SCS-Pd(II) complexes. The latter complexes only act as precursors for the formation of Pd nanoparticles. Although ECE-Pd complexes are known to be stable as long as the temperature is not raised to too high values in the presence of strong bases,[23,24] a dramatic color change of the tandem reaction mixtures was observed after one day at room temperature and visible Pd black formation occurred at room temperature after approximately two days.

We propose that Pd(0) formation is caused by an auto-decomposition of the SCS-pincer palladium-tin species **1.SnMe$_3$** in the first catalytic cycle. This species mainly reacts with cinnamyl chloride forming the primary reaction products cinnamyl trimethylstannane and 1-phenyl-2-propenyl trimethylstannane (*step B* in catalytic cycle I), but a small portion is proposed to be reduced to release a free Pd(0) atom (*step H*). The Pd(0) atoms that are formed in this way provide a starting point for a Pd(0)/Pd(II)-based catalytic cycle: cycle III.

In this cycle, the Pd(0) center is proposed to undergo oxidative addition with cinnamyl trimethylstannane forming a palladium(II) η^3-allyl intermediate similar to Pd(0)-catalyzed allylic substitution reactions of allyl halides[25] and Stille couplings.[26,27] It is widely accepted that this palladium(II) η^3-allyl intermediate has an electrophilic nature and reacts with nucleophiles.[28] Nevertheless it is well-known that η^3-allyl groups show exchange between (eventual) *syn* and *anti* substituents and that the intermediate of this process is a η^1-allyl metal complex.[29] Recently, Nakamura and Yamamoto found that bis-η^3-allylpalladium complexes can behave as nucleophiles and are able to react with electrophiles, like aldehydes.[30-32] Szabó and co-workers have performed extensive mechanistic studies on such palladium-catalyzed electrophilic allylation reactions that start from bis-η^3-allylpalladium complexes.[33-36] In these cases, the catalytic reaction proceeds because the aldehyde is able to coordinate to this bis-η^3-allylpalladium complex forming a η^3-allyl-η^1-allylpalladium intermediate. Subsequent nucleophilic attack of the η^1-allyl group on the carbon-oxygen double bond of the aldehyde produces a η^3-allyl-homoallyloxypalladium species. In this mechanism, one of the allyl ligands is a spectator ligand and therefore does not actively take part in the catalytic cycle. Its role is important in blocking one half of the coordination sphere and fine-tuning the activity of this reaction.[34]

In our case the nucleophilic reactivity might be explained by a similar mechanism that takes place on the surface of a Pd nanoparticle, a situation where also one half of the coordination sphere is blocked. A surface Pd(0) center might undergo oxidative addition with cinnamyl trimethylstannane forming a palladium(II) η^3-allyl intermediate (*step I*), whereupon coordination of 4-nitrobenzaldehyde to this intermediate might generate a nucleophilic η^1-allylpalladium intermediate (*step J*). This interaction likely is part of an equilibrium in which the palladium(II) η^3-allyl intermediate is favored. The η^1-allylpalladium intermediate can escape from the equilibrium by attacking the carbonyl center of the aldehyde leading to an alkoxypalladium species (*step K*). Via a reductive elimination, the catalytic cycle closes (*step L*) and the released product leads after protonation in the workup of this reaction to the secondary tandem product (*step G*). The *anti/syn* product ratio of this secondary product that has been formed via this Pd(0)/Pd(II) mechanism was found to be lower (1.5 : 1) than the product that has been exclusively formed via a Pd(II)-only mechanism (3.5-4.0 : 1).

3.6 DFT calculations

In the previous part, we demonstrated that the SCS-pincer palladium complex **1.Cl** does not catalyze the electrophilic addition of 4-nitrobenzaldehyde to cinnamyl trimethylstannane, whereas it successfully performs this reaction in the case of the isomeric substrate 1-phenyl-2-propenyl trimethylstannane. The most likely explanation for this behavior is that complex **1.Cl** is able to react with the branched 1-phenyl-2-propenyl trimethylstannane to form the (transient) key reactive η^1-allylpalladium intermediate, whereas this transformation cannot be achieved in the case of the cinnamyl trimethylstannane substrate.

A plausible, dissociative pathway for the reaction of complex **1.Cl** with an allylstannane moiety leading to a η^1-allylpalladium complex **1.η^1-allyl** is described in *figure 3.11*. It involves *(i)* dissociation of the chloride ligand from **1**, *(ii)* coordination of the double bond of the allylstannane substrate to the vacant site of the palladium center, and *(iii)* S_N2-type substitution of the chloride anion on the tin center, liberating the corresponding chlorostannane and forming **1.η^1-allyl**.

The viability of such a reaction pathway was tested using DFT calculations on a model system in which all methyl and phenyl groups of the pincer complex and the stannane substrates

were replaced by hydrogen atoms (R = R' = R'' = R''' = H). Preliminary results from these calculations indicate that the reaction is unlikely to proceed as it is strongly endothermic (ΔG^0 = + 12.6 kcal.mol^{-1}), but that the required transition state appears fairly accessible at room temperature ($\Delta G^{\dagger}$ = 20.6 kcal.mol^{-1}, *figure 3.12*).

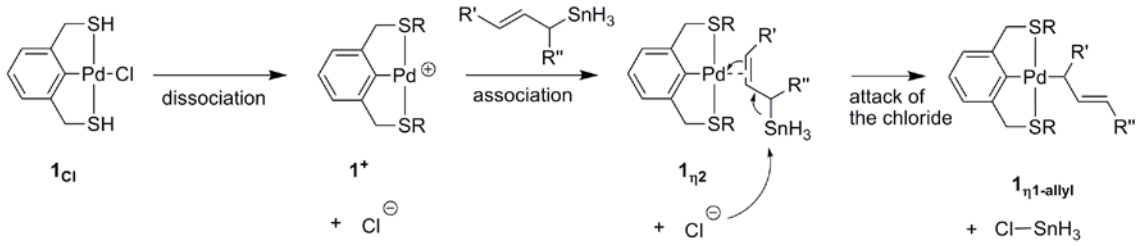

*Figure 3.11: Proposed dissociative pathway for the formation of a η^1-allylpalladium complex from an allylstannane moiety and complex **1.Cl**.*

In the real system, the position of the phenyl substituent of the allylstannane moiety appeared to have a crucial influence on the reactivity. This can be qualitatively rationalized using *figure 3.11*. For the cinnamyl trimethylstannane substrate (R' = Ph and R'' = H), the starting material is stabilized by delocalization of the allyl double bond with the phenyl ring, whereas the final product presents a hindered branched η^1-allyl fragment without delocalization between the double bond and the phenyl substituent. On the opposite, for the 1-phenyl-2-propenyl trimethylstannane substrate (R' = H, R'' = Ph), the starting material is branched and not stabilized by delocalization, whereas the product exhibits a non bulky linear η^1-allyl fragment, which is further stabilized by delocalization of the double bond with the phenyl group.

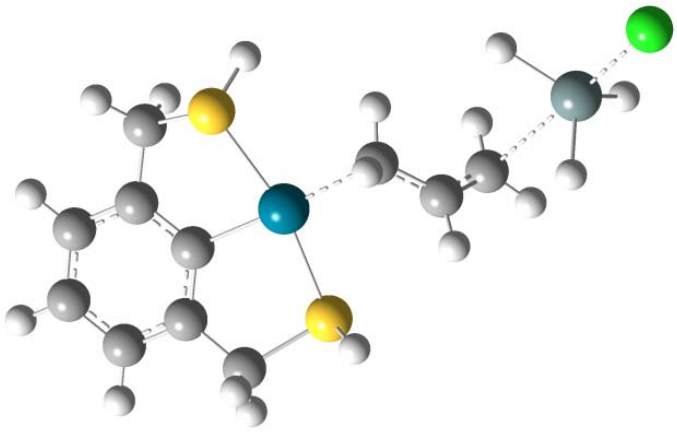

Figure 3.12: Transition state of the formation of a η^1-allylpalladium complex by nucleophilic attack of a chloride anion on the tin atom of an allylstannane coordinated to a palladium-pincer cation through an S_N2-type mechanism.

This qualitative reasoning is reflected in the overall reaction energy as computed by DFT for both isomers. In the case of the cinnamyl trimethylstannane substrate, the transformation depicted in *figure 3.11* is strongly endothermic (ΔG^0 = 16.4 kcal mol^{-1}) and therefore would be difficult to achieve using the current reaction conditions. For 1-phenyl-2-propenyl trimethylstannane, however, the overall reaction is almost athermic (ΔG^0 = 2.6 $kcal.mol^{-1}$) and should consequently be able to proceed smoothly. Therefore, we conclude that our DFT results are in agreement with the hypothesis and our experimental results that 1-phenyl-2-propenyl trimethylstannane is able to react with SCS-pincer Pd-catalyst **1.Cl** to form a Pd-allyl intermediate, whereas cinnamyl trimethylstannane is unreactive towards this complex.

3.7 Conclusions

The SCS-pincer Pd-catalyzed auto-tandem reaction consisting of the stannylation of cinnamyl chloride followed by the electrophilic addition of 4-nitrobenzaldehyde to form 1-(4-nitrophenyl)-2-phenylbut-3-en-1-olwas studied. In our study, we have found that when palladium pincer complex **1.Cl** is used as the catalyst both cinnamyl trimethylstannane, and its branched isomer 1-phenyl-2-propenyl trimethylstannane is formed in the first reaction step. The branched isomer turned out to be the active substrate in the second pincer-

catalyzed reaction step, the electrophilic addition of 4-nitrobenzaldehyde towards the secondary tandem product. These findings were corroborated by DFT calculations.

The consequence of this behavior is that as soon as the first catalytic cycle has finished because all substrates for the stannylation reaction have reacted, no branched product 1-phenyl-2-propenyl trimethylstannane is present in the reaction mixture. Since the linear isomer cinnamyl trimethylstannane is not reacting via the Pd(II)-catalyzed second catalytic cycle, but via another mechanism (catalytic cycle 3), this second cycle is no longer fed, and as a consequence the electrophilic addition of 4-nitrobenzaldehyde can no longer take place. This means that the total reaction progress stops and a plateau in the kinetic reaction profile is observed.

Addition of more equivalents of cinnamyl chloride and hexamethylditin with respect to 4-nitrobenzaldehyde leads to higher amounts of branched isomer 1-phenyl-2-propenyl trimethylstannane. Formation of the secondary tandem product 1-(4-nitrophenyl)-2-phenylbut-3-en-1-olgoes to completion using three, or more equivalents of cinnamyl chloride and hexamethylditin, because under these conditions the second catalytic cycle is continuously fed. The reaction rate enormously improves from one week using one equivalent of cinnamyl chloride and hexamethylditin to only 2 h using three equivalents of these substrates, thereby showing normal reaction kinetics for a tandem reaction. Consequently, the tandem reaction takes place rapidly via a Pd(II)-only mechanism. Under these conditions, a mechanism that makes use of the cinnamyl trimethylstannane product that is also formed in cycle I and of Pd(0) particles leached from the palladium pincer (cycle III) does not take part to this tandem reaction, which improves reaction rate, product selectivity and prevents Pd-leaching from the SCS-pincer Pd complexes.

For further catalytic application of this reaction, it is advised to use an excess of cinnamyl chloride and hexamethylditin compared to 4-nitrobenzaldehyde to guarantee a Pd(II)-only mechanism. In this way, this auto-tandem reaction was successfully performed in a compartmentalized way using a dendritic SCS-pincer Pd-catalyst for four runs in a high catalytic rate (89, 96, 96 and 92% for the respective runs) showing no palladium leaching for the first two runs.[12]

3.8 Experimental section

General

All reactions were carried out using standard Schlenk techniques under an inert dinitrogen atmosphere unless stated otherwise. All solvents were carefully dried and distilled prior to use. All standard reagents were purchased commercially and used without further purification. ^{1}H (300 MHz), ^{13}C (100 MHz) and ^{29}Si (60 MHz) NMR spectra were recorded on a Varian 400 MHz spectrometer at 25 ^{o}C, chemical shifts are given in ppm referenced to residual solvent resonances. ICP-MS analyses were carried out by Kolbe Mikroanalytisches Laboratorium (Mülheim a.d. Ruhr, Germany). GC analysis was carried out using a Perkin Elmer Clarus 500 GC equipped with an Alltech Econo-Cap EC-5 column.

Synthesis of cinnamyl trimethylstannane

In CH_2Cl_2 (30 mL) were added cinnamyl chloride (8.0 mmol, 1.2 g, 1.1 mL), hexamethylditin (8.0 mmol, 2.8 g, 1.7 mL) and SCS-pincer Pd complex **1.Cl** (1 mol%, 37 mg). After a few hours, quantitative conversion towards cinnamyl trimethylstannane was observed. The solution was separated from the catalyst via flash chromatography on neutral alumina using hexanes as eluent. The fractions that contained product were collected and PVPy (100 equiv.) was added. After stirring for one hour, the colorless solution was filtered and concentrated under vacuum leading to pure cinnamyl trimethylstannane in 46% yield.

Analytical data were in accordance with the data published by Fong et al.[37]

Synthesis of 1-phenyl-2-propenyl trimethylstannane

To $CDCl_3$ (3 mL) were added cinnamyl chloride (0.80 mmol, 122 mg, 0.113 mL), hexamethylditin (0.80 mmol, 275 mg, 0.174 mL) and SCS-pincer Pd complex **1.Cl** (1 mol%, 3.7 mg). After a few hours, quantitative conversion towards cinnamyl trimethylstannane was observed. The solution was separated from the catalyst via flash chromatography on neutral alumina using hexanes as eluent. The fractions that contained product were collected and PVPy (100 equiv.) was added. After stirring for one hour, the colorless solution was filtered and concentrated under vacuum leading to pure cinnamyl trimethylstannane in 35% yield.

A solution of cinnamyl trimethylstannane (approximately 0.1 M) in $CDCl_3$ was placed into a NMR tube. Irradiation of this tube with a high pressure mercury UV lamp for 2 h at a

distance of 2 cm to the lamp in a cooled water bath (to compensate for the heat caused by the lamp), leads to complete conversion of cinnamyl trimethylstannane to 1-phenyl-2-propenyl trimethylstannane. This NMR tube was directly used for further investigations. Analytical data were in accordance with the data published by Takuwa.[20]

General protocol for the tandem reaction

SCS-pincer palladium complex (2 mol%, 0.016 mmol, 7.4 mg), was added to a solution of cinnamyl chloride (0.80 mmol, 122.1 mg, 113 μL), hexamethylditin (0.80 mmol, 275 mg, 174 μL), 4-nitrobenzaldehyde (0.80 mmol, 126.9 mg) and hexamethylbenzene (internal standard, 0.088 mmol, 14.4 mg) in 6 mL dry THF. The reaction stirred at room temperature in a nitrogen environment. Aliquots of 50 μL for NMR/GC analysis were regularly taken with an airtight syringe.

Protocol for the first reaction step of the tandem: stannylation

The general protocol for the tandem reaction was followed, but no 4-nitrobenzaldehyde was added. The reaction was performed in 6 mL dry THF or 6 mL dry CH_2Cl_2 and analyzed by NMR and GC.

Variation on the concentration of catalyst in the first reaction step of the tandem

In a NMR tube, a solution of cinnamyl chloride (67 μmol, 10.2 mg, 9.4 μL), hexamethylditin (67 μmol, 21.8 mg, 13.8 μL) and hexamethylbenzene (internal standard, 7.4 μmol, 1.2 mg) in 0.5 mL of CD_2Cl_2 was added. Subsequently a solution of SCS-pincer palladium complex **1.Cl** in 0.1 mL CD_2Cl_2 was introduced to the NMR-tube. A series of solutions were made containing 2%, 1%, 0.5%, 0.25%, 0.125% or 0.0625% of catalyst **1.Cl**. The experiments were performed inside a Varian 300 MHz spectrometer at 25 ^{o}C.

Poisoning experiments for the first reaction step of the tandem

The general protocol for the stannylation was followed. Polyvinylpyridine (2% cross linked, 100 equiv., 80 mmol, 8.4 g) or mercury (2 drops) were added to the reaction mixture. Analysis has been performed by NMR and GC analysis.

Protocol for the second reaction step of the tandem: electrophilic addition

In this experiment, SCS-pincer palladium complex **1.Cl** (2 mol%, 0.016 mmol, 7.4 mg), was added to a solution of cinnamyl trimethylstannane (0.80 mmol, 225 mg), 4-nitrobenzaldehyde (0.80 mmol, 126.9 mg) and hexamethylbenzene (internal standard, 0.088 mmol, 14.4 mg) in 6 mL dry THF. The reaction stirred at room temperature in a nitrogen environment. Aliquots of 50 μL for NMR/GC analysis were regularly taken with an airtight syringe.

Catalysis using 1-phenyl-2-propenyl trimethylstannane

A solution of 1-phenyl-2-propenyl trimethylstannane (0.25 mmol, 70 mg) in $CDCl_3$ (0.5 mL) is prepared. To this solution is added 4-nitrobenzaldehyde (0.25 mmol, 38 mg) and SCS-pincer palladium complex (**1.Cl**, ~5%, few mg). Limitations in the accuracy of the used analytical balances cause that the catalyst loading could not exactly be determined. The experiments were performed inside a Varian 300 MHz spectrometer at 25 ^{o}C.

DFT calculations

All calculations were run in gas phase at the DFT level on the software G03W using the B3LYP functional and the basis set H/C/S/Cl 6-31G*, Pd/Sn LANL2DZ.[38] All geometries were optimized using the regular convergence criteria (keywords opt for intermediates and opt = qst3 for transition states). Intermediates were characterized by the absence of imaginary vibrations in a frequency calculation. Transition states were characterized by the presence of a single imaginary vibration in a frequency calculation. The following simplifications were applied: 1) the phenyl groups of the pincer moieties were replaced by H atoms, 2) the trimethyltin group was replaced by a stannyl group (SnH_3).

3.9 References

1. Albrecht, M.; van Koten, G. *Angew. Chem. Int. Ed.* **2001,** *40*, 3750-3781.
2. Singleton, J. T. *Tetrahedron* **2003,** *59*, 1837-1857.
3. Slagt, M. Q.; Rodriguez, G.; Grutters, M. M. P.; Klein Gebbink, R. J. M.; Klopper, W.; Jenneskens, L. W.; Lutz, M.; Spek, A. L.; van Koten, G. *Chem. Eur. J.* **2004,** *10*, 1331-1344.
4. Szabó, K. J. *Synlett* **2006**, 811-824.
5. Selander, N.; Szabó, K. J. *Chem. Rev.* **2011**, *111*, 2048-2072.

6. Pijnenburg, N. J. M.; Korstanje, T. J.; van Koten, G.; Klein Gebbink, R. J. M. *Palladacycles on Dendrimers and Star-Shaped Molecules, Wiley-VCH Verlag GmbH & Co. KGaA* **2008**, 361-398, *or* ***Chapter 1*** *of this thesis*.
7. Wallner, O. A.; Szabó, K. J. *Org. Lett.* **2004,** *6*, 1829-1831.
8. Selander, N.; Szabó, K. J. *Dalton Trans.* **2009**, 6267-6279.
9. Solin, N.; Kjellgren, J.; Szabó, K. J. *J. Am. Chem. Soc.* **2004,** *126*, 7026-7033.
10. Aydin, J.; Kumar, K. S.; Sayah, M. J.; Wallner, O. A.; Szabó, K. J. *J. Org. Chem.* **2007,** *72*, 4689-4697.
11. Gagliardo, M.; Selander, N.; Mehendale, N. C.; van Koten, G.; Klein Gebbink, R. J. M.; Szabó, K. J. *Chem. Eur. J.* **2008,** *14*, 4800-4809.
12. Pijnenburg, N. J. M.; Dijkstra, H. P.; van Koten, G.; Klein Gebbink, R. J. M. *Dalton Trans.* **2011,** *40,* 8896-8905, *or* ***Chapter 2*** *of this thesis*.
13. Phan, N. T. S.; van der Sluys, M.; Jones, C. W. *Adv. Synth. Catal.* **2006,** *348*, 609-679.
14. Weck, M.; Jones, C. W. *Inorg. Chem.* **2007,** *46*, 1865-1875.
15. Laidler, K. J. *Reaction Kinetics* **1987,** *3rd edition, Harper & Row, New York*.
16. Widegren, J. A.; Finke, R. G. *J. Mol. Catal. A. Chem.* **2003,** *198*, 317-341.
17. Paal, C.; Hartmann, W. *Berichte der Deutschen Chemische Gesellschaft* **1918,** *51*, 711-737.
18. Yu, K. Q.; Sommer, W.; Weck, M.; Jones, C. W. *J. Catal.* **2004,** *226*, 101-110.
19. Yu, K. Q.; Sommer, W.; Richardson, J. M.; Weck, M.; Jones, C. W. *Adv. Synth. Catal.* **2005,** *347*, 161-171.
20. Takuwa, A.; Kanaue, T.; Yamashita, K.; Nishigaichi, Y. *J. Chem. Soc. Perkin Trans. 1* **1998**, 1309-1314.
21. Wallner, O. A.; Szabó, K. J. *Chem. Eur. J.* **2006,** *12*, 6976-6983.
22. Takuwa, A.; Kanaue, T.; Nishigaichi, Y.; Iwamoto, H. *Tetrahedron Lett.* **1995,** *36*, 575-578.
23. Bergbreiter, D. E.; Osburn, P. L.; Frels, J. D. *Adv. Synth. Catal.* **2005,** *347*, 172-184.
24. Sommer, W. J.; Yu, K. Q.; Sears, J. S.; Ji, Y. Y.; Zheng, X. L.; Davis, R. J.; Sherrill, C. D.; Jones, C. W.; Weck, M. *Organometallics* **2005,** *24*, 4351-4361.
25. de Meijere, A.; Brase, S. *J. Organometal. Chem.* **1999,** *576*, 88-110.
26. Stille, J. K. *Angew. Chem. Int. Ed.* **1986,** *25*, 508-523.
27. Casado, A. L.; Espinet, P. *J. Am. Chem. Soc.* **1998,** *120*, 8978-8985.
28. Tsuji, J. *In: Negishi E (ed) Handbook of Organopalladium Chemistry for Organic Synthesis* **2000** *Wiley, New York.*
29. Crabtree, R. H. *The Organometallic Chemistry of the Transition Metals* **2005,** *Fourth Edition, Wiley-Interscience*, 131-136.
30. Nakamura, H.; Iwama, H.; Yamamoto, Y. *Chem. Commun.* **1996**, 1459-1460.
31. Nakamura, H.; Bao, M.; Yamamoto, Y. *Angew. Chem. Int. Ed.* **2001,** *40*, 3208-3214.
32. Yamamoto, Y.; Nakamura, H. *Top. Organomet. Chem.* **2005,** *14*, 211-239.
33. Wallner, O. A.; Szabó, K. J. *J. Org. Chem.* **2003,** *68*, 2934-2943.
34. Szabó, K. J. *Chem. Eur. J.* **2004,** *10*, 5269-5275.
35. Solin, N.; Kjellgren, J.; Szabó, K. J. *Angew. Chem. Int. Ed.* **2003,** *42*, 3656-3658.
36. Solin, N.; Kjellgren, J.; Szabó, K. J. *J. Am. Chem. Soc.* **2004,** *126*, 7026-7033.
37. Fong, C. W.; Kitching, W. *J. Organometal. Chem.* **1970,** *22*, 107-&.
38. Frisch, M. J.; Trucks, G. W.; Schlegel, H. B.; Scuseria, G. E.; Robb, M. A.; Cheeseman, J. R.; Scalmani, G.; Barone, V.; Mennucci, B.; Petersson, G. A.; Nakatsuji, H.; Caricato, M.; Li, X.; Hratchian, H. P.; Izmaylov, A. F.; Bloino, J.; Zheng, G.; Sonnenberg, J. L.; Hada, M.; Ehara, M.; Toyota, K.; Fukuda, R.; Hasegawa, J.; Ishida, M.; Nakajima, T.; Honda, Y.; Kitao, O.; Nakai, H.; Vreven, T.; Montgomery, J. A., Jr.;; Peralta, J. E.; Ogliaro, F.; Bearpark, M.; Heyd, J. J.; Brothers, E.; Kudin, K. N.; Staroverov, V. N.; Kobayashi, R.; Normand, J.; Raghavachari, K.; Rendell, A.; Burant, J. C.; Iyengar, S. S.; Tomasi, J.; Cossi, M.; Rega, N.; Millam, J. M.; Klene, M.; Knox, J. E.; Cross, J. B.; Bakken, V.; Adamo, C.; Jaramillo, J.; Gomperts, R.; Stratmann, R. E.; Yazyev, O.; Austin, A. J.; Cammi, R.; Pomelli, C.; Ochterski, J. W.; Martin, R. L.; Morokuma, K.; Zakrzewski, V. G.; Voth, G. A.; Salvador, P.; Dannenberg, J. J.; Dapprich, S.; Daniels, A. D.; Farkas, O.; Foresman, J. B.; Ortiz, J. V.; Cioslowski, J.; Fox, D. J. *Gaussian 09, Revision A.02; Gaussian Inc.: Wallingford CT, 2009.*

Chapter 4

The role of the dendritic support in the catalytic performance of peripheral pincer Pd complexes

Abstract

To investigate the effects of the dendrimer backbone on catalysis, a series of monomeric and dendritic SCS-pincer Pd complexes was synthesized and tested in two different Pd(II)-catalyzed reactions. To this end, the three novel polar PAMAM dendrimer-immobilized SCS-pincer Pd complexes **3**, **4**, and **5**, and the two apolar carbosilane dendrimer-immobilized complexes **7** and **8** were compared to three monomeric analogues **1**, **2** and **6**. These complexes were investigated in the cross-coupling reaction between vinyl epoxide and styrylboronic acid and the auto-tandem reaction of cinnamyl chloride, hexamethylditin, and 4-nitrobenzaldehyde. The differences in catalytic rate and product selectivity for these complexes are described and discussed. For the cross-coupling reaction, the PAMAM dendrimer-immobilized complexes were found to give similar reaction rates, but higher product selectivities than their monomeric counterparts. The carbosilane complexes showed lower reaction rates and similar product selectivities. These observations are explained in view of dendrimer aggregation and peripheral group backfolding.

Based on: Niels J. M. Pijnenburg, Martin Lutz, Maxime A. Siegler, Anthony L. Spek, Gerard van Koten, Robertus J. M. Klein Gebbink, *New J. Chem.,* ***2011, DOI:*** *10.1039/C1NJ20366E.*

4.1 Introduction

Dendrimer-immobilized catalysts combine the benefits of homogeneous catalysis, namely high activity, a well-understood catalyst description and mild reaction conditions, with the key benefit of heterogeneous catalysis: the recyclability of the catalyst.[1] Since the first report appeared by Van Koten and Van Leeuwen,[2] the field of dendrimer-immobilized catalysts has expanded enormously. Several comprehensive reviews have been published that provide an overview on dendrimer-immobilized organometallic catalysts, thereby focusing on the recyclability and the differences of these dendritic catalysts in terms of reaction rate and/or selectivity compared to their monomeric, non-dendritic counterparts.[3-8]

Most dendritic catalysts consist either of a single catalytic unit connected to the focal point of a dendritic wedge to increase steric bulk around the reaction center, or of multiple catalytic units that are connected to the periphery of a dendritic support. The role of the dendritic support on the overall catalytic performance of both types of dendritic catalysts is not negligble.[9] Except for electronic effects that may result from the covalent connection of the dendrimers to the organometallic catalyst, steric effects seem to play a more pronounced role. In close proximity of the dendritic backbone, the chemical micro-environment near the catalytic center may significantly alter.[10] Limited accessibility due to additional steric bulk around a catalytic center might impede substrate binding and therefore is an important reason for dendritic effects to be observed on catalytic reaction rates or product selectivities.

Several examples that reveal positive dendritic effects in terms of a higher product selectivity for dendritic catalysts in comparison to non-dendritic catalysts have been reported.[11-15] In these cases the increased steric crowding around the catalytic reaction center seems to hamper the formation of sterically unfavored (often branched) isomers in favor of less sterically demanding (often linear) isomers, thus improving the selectivity. Positive dendritic effects on reaction rate and product yield have also been observed.[16-20]

The origins of these effects are diverse. For example, in a recent paper Snelders *et al.* observed that higher generations of oligocationic dendritic ligands can stabilize the mono-ligated active species in the Suzuki-Miyaura cross-coupling reaction of aryl chlorides with phenyl boronic acids.[18] On the other hand, cooperation between two or multiple catalytic centers might be favored in case of peripherally immobilized catalysts. Jacobsen *et al*.

reported a positive effect for the Co-salen-catalyzed hydrolytic kinetic resolution of epoxides, a reaction known to be second order in Co.[20] The Kharasch addition, an atom transfer radical reaction, performed by immobilized NCN-pincer nickel catalysts by Kleij *et al.* is another example, although this has led to a negative dendritic effect.[19]

The choice of the type of dendritic support used for the dendrimer immobilization of a catalyst is often not specifically stated, and sometimes even seems quite randomly chosen. Experience in the research group, dendrimer availability and price, rather than arguments based on chemical properties are often important parameters for the selection of the dendritic support used for catalyst immobilization. As a result, only few reports detail the specific effects of the use of a different dendrimer support on one and the same reaction catalyzed by identical catalytic sites.[15,21] In addition, obtaining a balanced overview of such effects by combining data from different literature reports is difficult. For these reasons, we set out to study the catalytic performance of dendrimer-immobilized catalysts by maintaining a single catalyst type and instead changing the dendritic support.

In this study, two abundantly used but chemically different types of dendrimers have been used as supports for catalyst immobilization: polyamidoamine (PAMAM) dendrimers and carbosilane (CS) dendrimers.[22] PAMAM dendrimers are possibly the most frequently used types of dendrimers in materials science, biotechnology applications and catalysis and are commercially available. These polar dendrimers consist of an ethylenediamine core that has been reacted through a divergent synthesis protocol with methyl acrylate and ethylenediamine to create higher generations of dendrimers.[23-25] Carbosilane dendrimers on the other hand are apolar dendrimers that consist of C-Si and C-C bonds. The central silicon atom and other peripheral silicon centers act as the branching points in these dendrimers. Because of their chemical inertness these dendrimers are often used in catalysis.[26,27] Carbosilane dendrimers are usually synthesized in a divergent manner in an iterative two-step protocol using alternate allylation and hydrosilylation steps.[28]

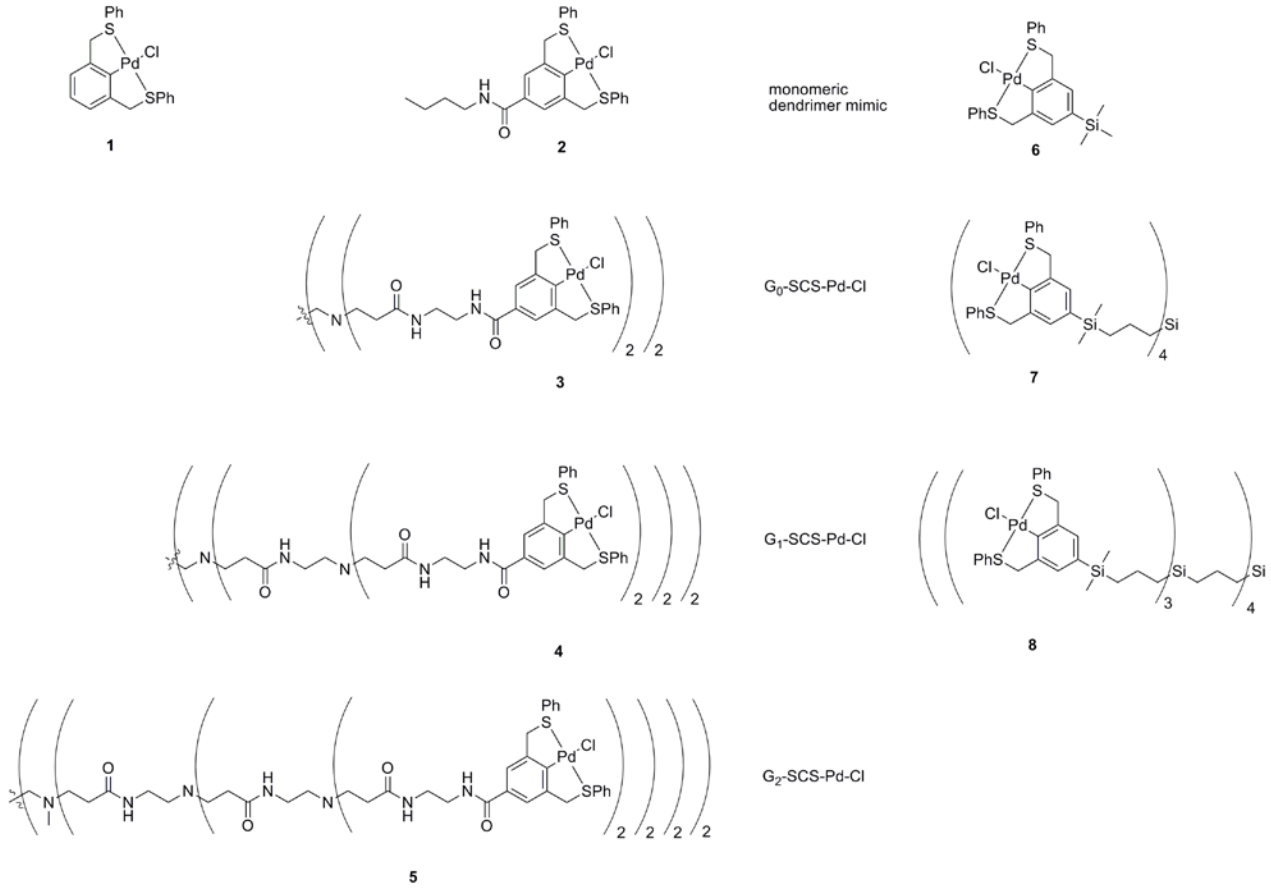

*Figure 4.1: Monomeric and dendritic SCS-pincer Pd complexes **1**-**8** comprizing either PAMAM or carbosilane dendritic scaffolds.*

We have studied two SCS-pincer Pd-catalyzed reactions with a series of different SCS-pincer Pd-catalysts. This series consist of the 'parent' SCS-pincer Pd complex **1**, two monomeric *para*-substituted SCS-pincer Pd complexes (**2** and **6**) as models for the dendrimer-supported complexes, and a series of PAMAM (**3**-**5**) and CS (**7** and **8**) dendrimer-supported pincer Pd complexes (*figure 4.1*). This series of eight different SCS-pincer Pd complexes was tested in two different Pd-catalyzed reactions: 1) the cross-coupling of vinyl epoxide with styrylboronic acid,[29] and 2) an auto-tandem reaction consisting of the stannylation of cinnamyl chloride followed by allylation of 4-nitrobenzaldehyde resulting in functionalized allylic alcohols (after aqueous workup, *figure 4.2*).[30] In both reactions, different reaction products can be formed; either a linear/branched or a *syn*/*anti* product mixture. In this way, not only the catalytic reaction rate, but also the product profile can be used to parameterize the effect of the dendritic supporting scaffold on the performance of the SCS-pincer Pd-catalysts.

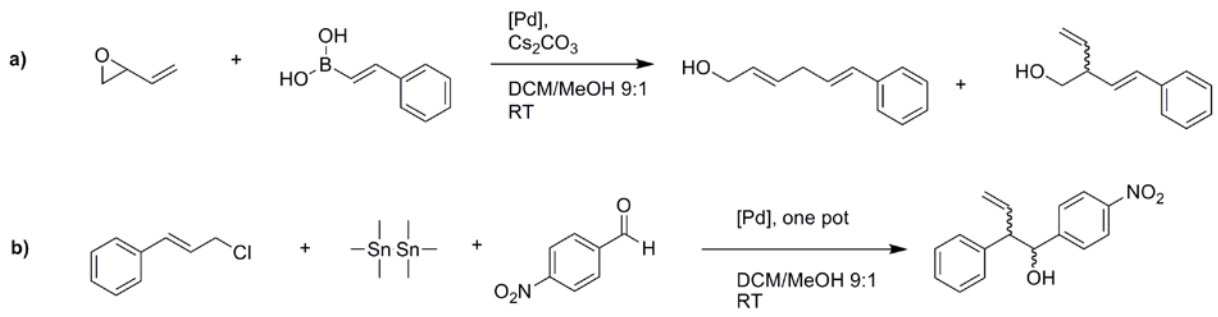

Figure 4.2: SCS-pincer Pd-catalyzed reactions: a) cross-coupling between vinyl epoxide and styrylboronic acid, and b) auto-tandem reaction between cinnamyl chloride, hexamethylditin, and 4-nitrobenzaldehyde.

4.2 Synthesis and analysis of SCS-pincer Pd complexes

4.2.1 Synthesis

Monomeric pincer complex **2** and dendritic pincer complexes **3**-**5** were synthesized via an amide coupling between a primary amine (i.e. *n*-butylamine or commercially available amino-terminated PAMAM dendrimers) and an activated ester pincer derivative. This coupling reaction is based on an earlier reported protocol in which an NCN-Pd-pincer active ester compound was used to connect NCN-pincer Pd complexes to various amines via a robust amide linkage.[31]

The activated ester functionalized SCS-pincer Pd complex **13** was synthesized starting from commercially available 1-bromo-3,5-dimethylbenzene (*figure 4.3*). Bromination of this xylene via a light-induced reaction using *N*-bromosuccinimide (NBS) in methyl acetate, prevents the use of the more commonly published, but very environmentally unfriendly NBS bromination in carbon tetrachloride.[32] The resulting 1-bromo-3,5-bis-(bromomethyl)benzene **9** was reacted under basic conditions with thiophenol to yield SCS-pincer preligand **10**.[33] Subsequently, ligand **10** was lithiated upon addition of two equivalents of *t*BuLi at -80 ^{o}C in diethylether. Quenching of this mixture by addition of (gaseous) carbon dioxide at -80 ^{o}C,[34] and protonation by addition of water lead to carboxylic acid **11** in 71% yield. This amphiphilic compound is hardly soluble in organic solvents, therefore the next synthetic step was performed in suspension. EDC coupling (EDC = 1-ethyl-3-(3-dimethylamino-propyl)carbo-diimide; a water soluble carbodiimide) of **11** with *N*-hydroxysuccinimide (NHS) in the

presence of triethylamine yielded active ester **12** in good yields. Palladation of **12** was carried out using $[Pd(MeCN)_4](BF_4)_2$ in refluxing acetonitrile. After treatment of the resulting cationic SCS-pincer Pd-MeCN complex with sodium chloride for 1 h, the resulting *para*-succinimidyl ester functionalized SCS-pincer Pd complex **13** was isolated as an air-stable yellow powder. In a last step, a solution of **13** was treated with 100 equivalents of cross linked (polyvinyl)pyridine (PVPy) for 3 h. This last step was performed to chelate Pd(0) particles that might still be present as byproducts after the introduction of the palladium centers.[35] These particles could potentially lead to undesired competition in catalysis, therefore care was taken to avoid these particles in the final batch of **13**. After treatment with PVPy beads, active ester SCS-pincer complex **13** was obtained in 78% yield as a pale yellow powder.

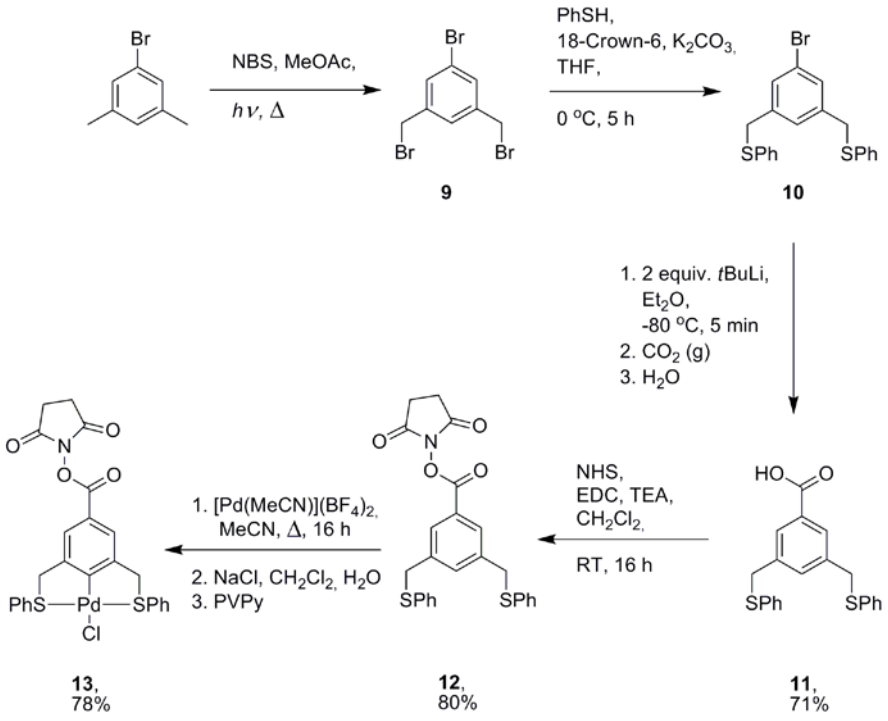

*Figure 4.3: Synthesis of succinimidyl ester functionalized SCS-pincer Pd complex **13**.*

Next, compound **13** was used to couple SCS-pincer Pd complexes to primary amines in dichloromethane or in a mixture of dichloromethane and methanol under ambient conditions (*figure 4.4)*. The latter solvent was used to improve the solubility of the dendritic products. As it turned out, **13** did not undergo nucleophilic substitution by methanol under these conditions. Using *n*-butylamine as nucleophile lead to monomeric complex **2** in 82%

yield. Succinimidyl ester **13** was connected in the same way to the peripheral groups of commercially available PAMAM dendrimers leading to dendritic complexes **3**-**5**. A slight excess of 1.25 equivalents of pincer complex **13** per dendritic arm was used in this protocol. The resulting dendritic complexes were purified from the succinimide byproduct via passive dialysis and the dendritic products were isolated in good yields (66-78%) as yellow powders. The solubility of these dendrimers is not very high in most common organic solvents. Polar aprotic solvents like DMF and DMSO and a mixture of dichloromethane and methanol are the only tested solvents in which these complexes showed good solubility. These dendritic catalysts were not found to be soluble in pure dichloromethane nor in pure methanol.

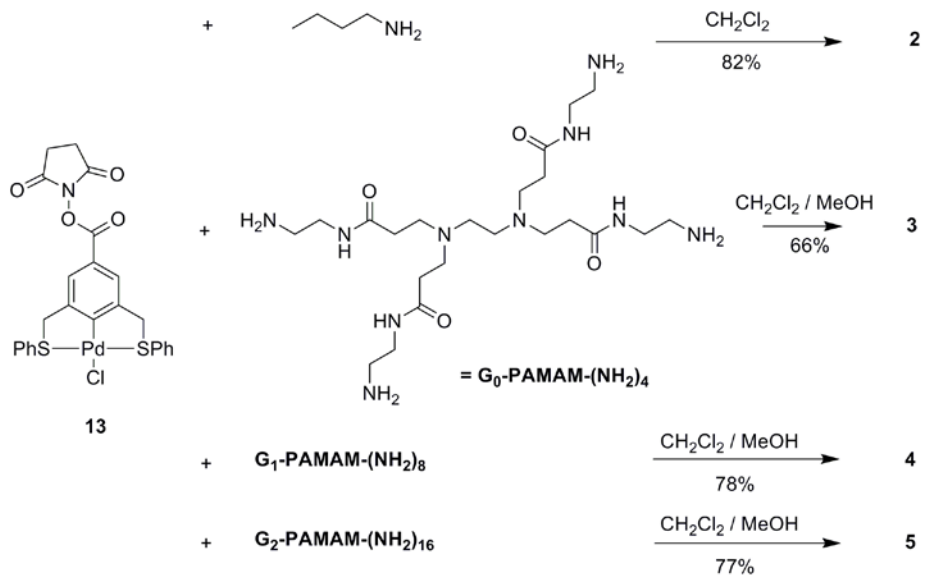

*Figure 4.4: Synthesis of monomeric complex **2** and dendritic complex **3**-**5** by active ester chemistry.*

The synthesis of *para*-TMS SCS-pincer Pd complex **6** and carbosilane dendrimers **7** and **8** has been published earlier by us,[35] and will not be detailed here.

4.2.2 Analysis

*X-ray structures of **1**, **13** and **2***

Single crystals of **2** and the bromide analogues of **1** and **13** suitable for X-ray crystal structure determinations were obtained by slow vapor diffusion of diethylether into dichloromethane solutions at room temperature. In the crystal structures of $\mathbf{1_{Br}}$ and $\mathbf{13_{Br}}$ occupational disorder

between bromine and chlorine was found on the halogen positions. The bromine of the metal complex has been partially for **13$_{Br}$**, or largely for **1$_{Br}$**, exchanged by chlorine from the dichloromethane solvent. This exchange has been reported before, by among others Kruithof[36] and Bergbreiter.[37] The molecular structures of **1**, **13$_{Br}$**, and **2** are displayed in *figure 4.5* and typical bond lengths and angles are shown in *table 4.1.* The Pd-center is found in a typical pincer-type distorted square planar geometry in all structures: S(1)–Pd(1)–S(2) was found to be 170.56(3)° for **1**, 168.26(3) for **13$_{Br}$**, and 168.17(3)° for **2**. The observed Pd-C1 bond length for **1**, **13$_{Br}$** and **2** (1.981(3), 1.972(3) and 1.986(3) Å. respectively) was found to be equidistant to those in earlier published complexes and also other bond lengths and angles are very close to the corresponding bond lengths and angles for earlier published SCS-pincer Pd complexes.[36-40] The five-membered palladacycles in these complexes are puckered in opposite directions with torsion angles Pd(1)–S(1)–C(7)–C(2) and Pd(1)–S(2)–C(14)–C(6) of 31.75(19)° and 14.05(19)° for **1**, -20.2(3)° and 2.5(3)° for **13$_{Br}$** and 29.31(19)° and 25.8(2)° for **2**, respectively. The orientation of the phenyl ring on S(2) for **13$_{Br}$** is orientated almost parallel to the local C2 axis, whereas that on S(1) is perpendicular to it. For complex **1** and **2** the orientation of both phenyl rings is approximately perpendicular towards the local axis of symmetry. In **2** the N-H of the amide moiety acts as hydrogen bond donor with the metal-coordinated chlorine as acceptor. This hydrogen bonding results in a one-dimensional chain along the crystallographic *b* axis (not shown), comparable to *para*-OH functionalized SCS-pincer Pd complexes by Mehendale.[40]

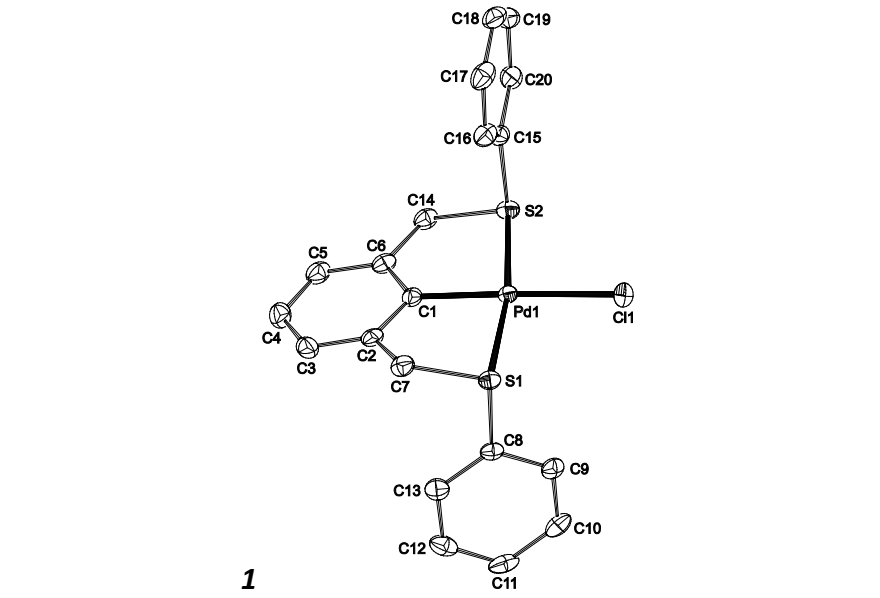

1

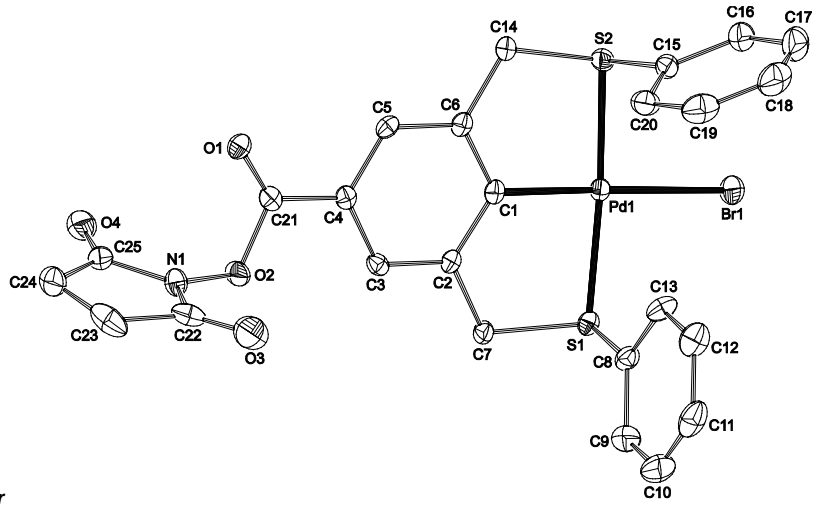

13$_{Br}$

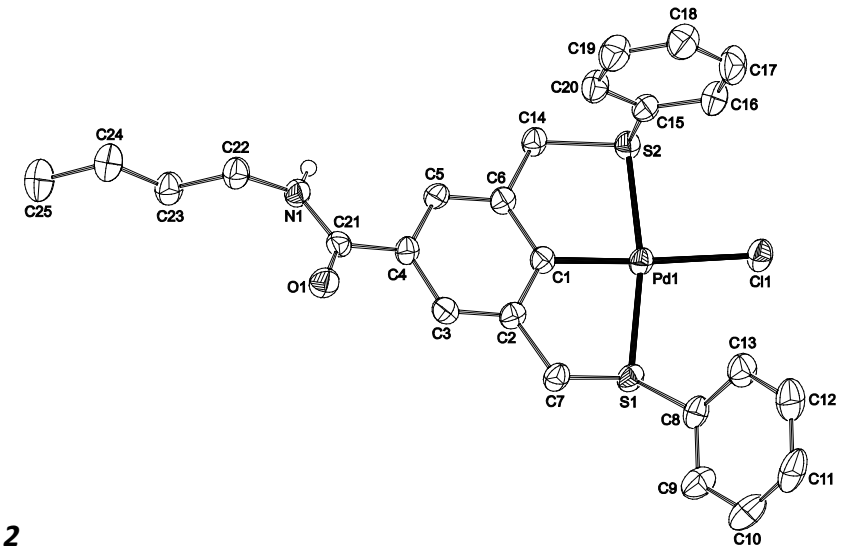

2

*Figure 4.5: ORTEP representations of the molecular structures of **1**, **13$_{Br}$**, and **2**. Displacement ellipsoids are drawn at the 50% probability level. C-H hydrogen atoms are omitted for clarity. Of the disordered halogen ligands in **1** and **13$_{Br}$** only the major form is shown.*

*Table 4.1: Selected bond lengths [Å], angles [°] and torsion angles [°] for crystal structures **1**, **13$_{Br}$** and **2**.*

	1	**13$_{Br}$**	**2**
Pd1-C1	1.981(3)	1.972(3)	1.986(3)
Pd1-S1	2.3002(7)	2.2956(9)	2.2996(7)
Pd1-S2	2.2946(7)	2.2963(10)	2.2980(7)
C1-Pd1-S1	85.59(8)	86.04(11)	83.39(8)
C1-Pd1-S2	84.97(8)	85.83(11)	85.09(8)
S1-Pd1-S2	170.56(3)	168.26(3)	168.17(3)
Pd1-S1-C7-C2	31.75(19)	-20.2(3)	29.31(19)
Pd1-S2-C14-C6	14.05(19)	2.5(3)	25.8(2)
Pd1-S1-C8-C9	70.4(2)	178.2(3)	-172.5(2)
Pd1-S2-C15-C16	-9.3(2)	107.5(3)	82.4(2)

*Analysis of PAMAM dendrimers **3**, **4** and **5***

To get insight in the integrity and catalyst loading of dendritic complexes **3**-**5**, a variety of analytical techniques have been applied. The smallest PAMAM dendrimer complex, i.e. G_0 compound **3**, was successfully characterized by ESI-MS. Signals contributed to the $[M–2Cl]^{2+}$ fragment with *m*/*z* = 1201.0618 (calcd. *m*/*z* = 1201.0865) and to the $[M\text{-}3Cl+Na+ x\ MeCN]^{2+}$ (*x* = 2-4) fragments were identified. For the higher generation dendritic compounds **4** and **5**, no correct mass spectra could be obtained. Due to their macroscopic size these compounds could neither be detected by ESI-MS nor by MALDI-TOF MS.

Proton and carbon NMR analysis showed shifts of the signals of the most peripheral CH_2 groups of the PAMAM dendrimer after coupling (^{1}H NMR: from 2.8 ppm to 3.4 ppm; ^{13}C NMR from 41 ppm to 39 ppm). Nearly identically IR spectra for **3**, **4**, and **5**, together with negative ninhydrin tests[41] performed after the coupling reaction of succinimidyl ester functionalized SCS-pincer Pd complex **13** with the G_x-PAMAM-NH_2 dendrimers, hinting at the absence of primary amine groups, conclude that for all generations PAMAM dendrimers a complete coupling reaction has taken place leading to fully metalated dendrimers **3**-**5**.

4.3 Catalytic results

4.3.1 Cross-coupling of vinyl epoxide with styrylboronic acid

The ECE-pincer Pd-catalyzed cross-coupling of vinyl epoxides with boronic acids (reaction (1), *figure 4.2*) has been introduced by Kjellgren *et al*[29] and has been studied in a later stage by Bonnet using SCS-pincer Pd complexes.[42] This reaction allows for a range of vinyl epoxides to be coupled to various boronic acids using NCN- and SeCSe-pincer Pd-Cl complexes. These reactions proceed via either an S_N2 or S_N2' mechanism and lead to a mixture of linear and branched products in a ratio of 2.3 for $N^{Me}CN^{Me}$-pincer Pd complexes[29] and 3.8 for $S^{iPr}CS^{iPr}$-pincer Pd complexes.[42]

The dendritic catalysts **3**, **4**, and **5** do not dissolve in the THF/water mixture used by Kjellgren[29] and Bonnet.[42] For this reason, a mixture of CH_2Cl_2/MeOH (9:1, *v*/*v*) was used for the catalytic tests; in this solvent mixture the reaction substrates and catalysts are fully soluble, and reproducible catalytic results were obtained. In the reaction setup, two equivalents of cesium carbonate were used as base and 2 mol% of Pd was used as catalyst in 2 mL CH_2Cl_2/MeOH. Without catalyst (blank reaction) no product formation was observed. The linear product 6-phenylhexa-2,5-dien-1-ol and the branched product 4-phenyl-2-vinylbut-3-en-1-ol were observed as major reaction products. In addition, fractions of styrene (hydrolysis product) and 1,4-diphenylbuta-1,3-diene (homocoupling product) were found. After 3 h of reaction time, the formation of 60-63% cross-coupling products, 34-38% styrene, and 2-3% 1,4-diphenylbuta-1,3-diene were typically found for all tested catalysts. The amount of hydrolysis product that was found is higher than reported in literature,[29] and is likely caused by the change of reaction medium from THF/H_2O to CH_2Cl_2/MeOH.

The conversion of styrylboronic acid in reaction (1) in time catalyzed by the different SCS-pincer Pd complexes is depicted in *figure 4.6a-c* for the PAMAM-based catalysts **1**-**5**, for the series of carbosilane dendrimers **1** and **6**-**8**, and for the respective G_0 and G_1 PAMAM and CS dendrimers. Furthermore, the ratio between linear and branched cross-coupling product is shown in *figure 4.6d* for all catalysts.

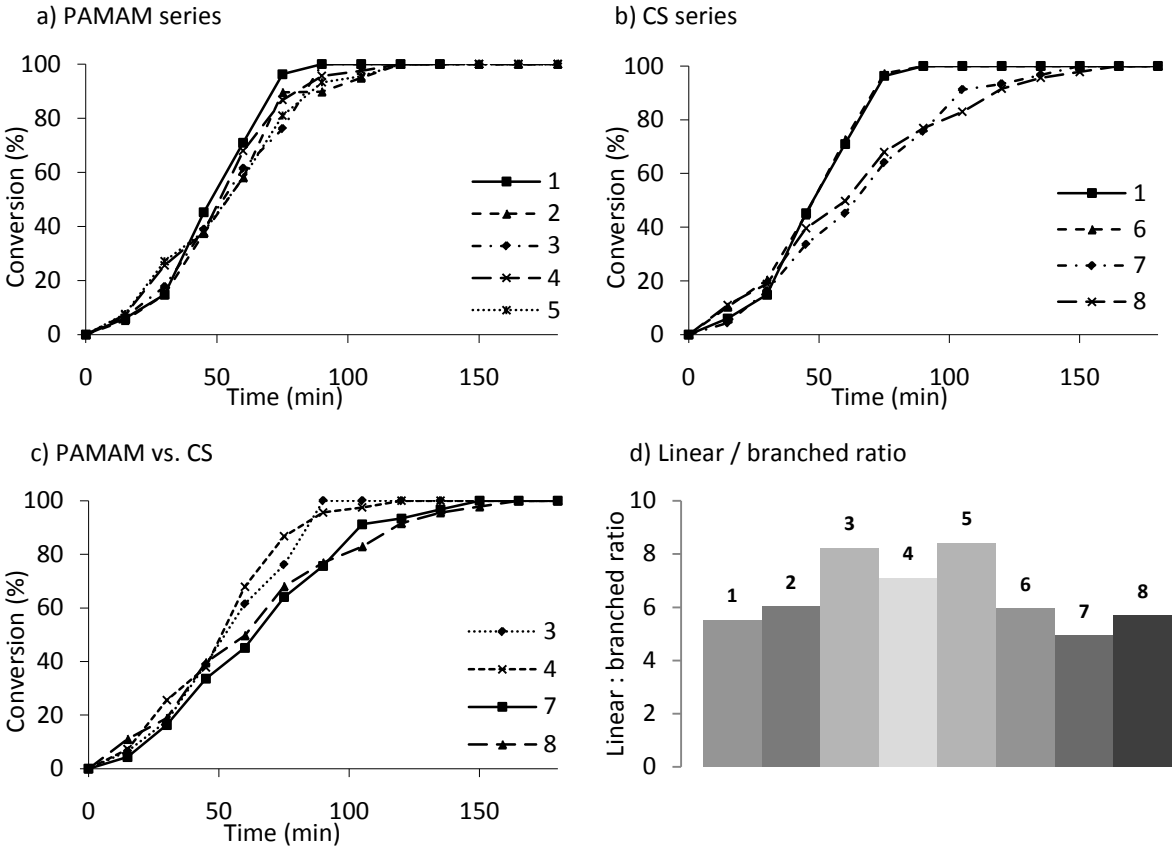

Figure 4.6: a, b, c) Conversion of styrylboronic acid in the SCS-pincer Pd-catalyzed cross-coupling with vinyl epoxide at constant Pd-concentration. d) Linear/branched product ratio of this coupling using different SCS-pincer Pd complexes.

In this particular reaction, the effect of either the presence or the absence of a PAMAM-scaffold on the reaction rate appears to be minimal (*figure 4.6a*). For all tested generations of PAMAM dendrimers (catalysts **3**-**5**) and for monomeric catalyst **2** the observed overall reaction rates are identical, and somewhat lower than for parent catalyst **1**. Dendrimers **4** and **5** did show a somewhat higher conversion after 30 minutes, but this difference was cancelled out after about 1 h. The linear/branched selectivity increases significantly from 5.5-6.0 for the monomeric catalysts **1** and **2** to 7.0-8.5 for the dendritic PAMAM catalysts **3**, **4** and **5** (*figure 4.6d*). There seems to be no direct relation with the size of the dendrimer or the number of SCS-pincer Pd-units per dendrimer and the observed l/b ratio, as this ratio increases from **2** to **3** (6.0 and 8.2 respectively), then decreases again for **4**, and reaches a maximum of 8.4 for **5**. Amongst these catalysts, monomeric catalyst **2** shows the lowest l/b ratio, which hints at a positive influence of the dendritic catalyst structure on the l/b ratio.

Carbosilane dendrimers **7** and **8** showed a somewhat higher initial reaction rate than the monomeric catalysts **1** and **6**. However, after 1 h the monomeric catalysts are significantly faster than dendritic catalysts **7** and **8**. These dendritic catalysts showed a different overall reaction profile than all other catalysts tested here. While the other catalysts displayed a fairly S-type reaction profile, catalysts **7** and **8** showed a more linear reaction profile in which the overall reaction rate considerably dropped compared to monomeric catalysts **1** and **6** (*figure 4.6b*). The l/b selectivity for catalysts **1**, **6**, **7**, and **8** showed only small differences and all appeared close to the observed ratio for parent catalysts **1** of 5.5. TMS-appended catalyst **6** showed in fact the highest l/b selectivity (5.9) amongst the carbosilane series. The selectivity decreases for **7** to 4.9 and then increases back for **8** close to the selectivity of **6**.
When the catalytic performance of the polar PAMAM dendrimers **3** and **4** was compared to the apolar carbosilane dendrimers **7** and **8**, the PAMAM dendrimers were found to be superior by showing a higher reaction rate and a higher l/b ratio (*figure 4.6c+d*).

4.3.2 Tandem catalysis

Next, the dendritic catalysts were tested in auto-tandem reaction 2 (*figure 4.2*). Starting from a mixture of the three reaction substrates cinnamyl chloride, hexamethylditin and 4-nitrobenzaldehyde, a mixture of stereoisomers of the 1-(4-nitrophenyl)-2-phenylbut-3-en-1-ol product was obtained. The ratio of *anti* (*RS* and *SR*) and *syn* (*RR* and *SS*) products depends on the particular catalyst that is used in the reaction.
In these experiments, three equivalents of cinnamyl chloride and hexamethylditin were used with respect to the amount of 4-nitrobenzaldehyde. These substrate ratios were used because earlier studies have shown that only under these conditions the tandem reaction operates through a Pd(II) cycle and that the formation and participation of Pd(0) is excluded.[43] Again, a mixture of CH_2Cl_2 and MeOH (9:1, *v*/*v*) has been used as solvent system and no reaction was observed in the absence of catalysts.

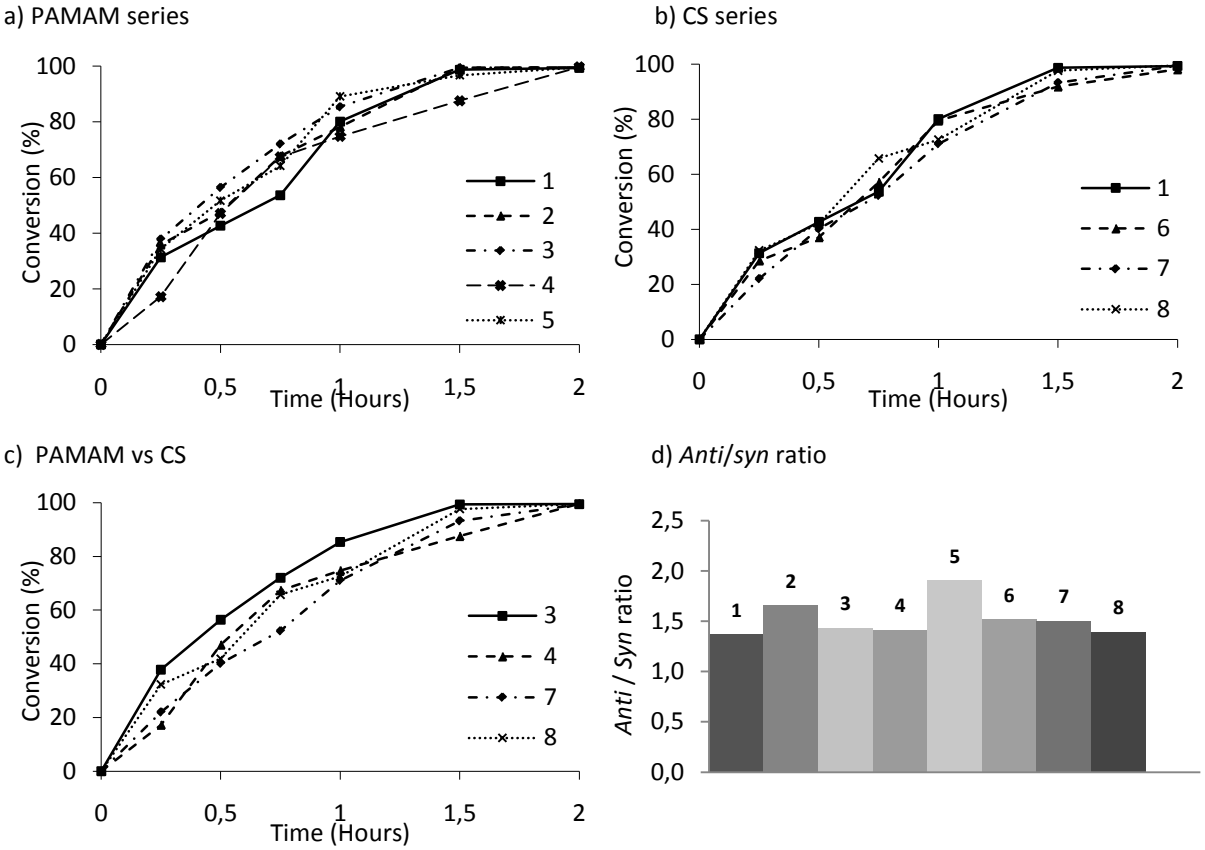

Figure 4.7: a, b, c) Conversion of cinnamyl chloride in the SCS-pincer Pd-catalyzed auto-tandem reaction with hexamethylditin and 4-nitrobenzaldehyde at constant Pd-concentration. d) Linear/branched product ratio of this coupling using different SCS-pincer Pd complexes.

Figure 4.7 depicts the conversion of the cinnamyl chloride substrate using the eight different SCS-pincer palladium complexes **1**-**8**. The conversion of this substrate appeared to be almost independent of the catalyst used (*figure 4.7a-c)*. In all cases, the conversion of cinnamyl chloride is complete within 2 h and all kinetic curves seemingly follow a first order type reaction profile. Amongst the dendritic catalysts, G_0-PAMAM dendrimer **3** seems to be the most active one (*figure 4.7c*). Also for the second step in this tandem reaction (i.e. the formation of the reaction product 1-(4-nitrophenyl)-2-phenylbut-3-en-1-ol) all eight tested catalysts, whether monomeric, dendritic, polar or apolar, showed very similar reaction profiles. The *anti*/*syn* ratio of the tandem products appeared to be between 1.4 and 1.5 for all catalysts (*figure 4.7d)*. Exceptions are monomeric catalyst **2** that shows a slightly higher *anti*/*syn* ratio of 1.6 and the PAMAM G_2 catalyst **5** that showed a significantly higher *anti*/*syn* ratio of 1.9.

4.4 Discussion and conclusions

In this paper two series of dendritic catalysts were studied: one series is based on the polar PAMAM scaffold (catalysts **3**-**5**) and the other series on the apolar CS scaffold (catalysts **7**-**8**). Together with monomeric catalysts **1**, **2** and **6**, which are the parent catalyst **1** and two monomeric catalysts that are electronically equivalent to the PAMAM-based (catalyst **2**) and the CS-based catalysts (catalyst **6**), these dendritic catalysts have been tested in two different Pd-catalyzed reactions to investigate whether the dendritic support itself plays a role in the catalytic parameters of these reactions.

For the Pd-catalyzed cross-coupling of vinyl epoxide with styrylboronic acid (*reaction 1*) small but significant rate and selectivity differences between monomeric catalysts, polar PAMAM and apolar CS dendritic catalysts have been found. Because the three monomeric catalysts **1**, **2** and **6** showed very similar characteristics for this reaction, these differences are not caused by remote electronic effects on the catalytic center, but rather by steric effects. The PAMAM-based dendritic catalysts showed a very similar reaction rate compared to the monomeric catalysts, while the carbosilane-based dendritic catalysts were found to be considerable slower than their monomeric counterparts. The product selectivity in this cross-coupling reaction showed another trend. Here, the monomeric catalysts and the carbosilane dendrimers showed a linear/branched product ratio around 5-6, whereas the PAMAM dendrimers showed a noticeably higher l/b ratio of 8-9: a small, but significant positive dendritic effect.

We believe that these small effects can be explained by taking the solubility and the conformational behavior of the dendritic supports into account. These considerations lead us to propose that under the reaction conditions dendrimer aggregation takes place for the carbosilane dendrimers and peripheral group backfolding occurs in PAMAM dendrimers, which lead to the observed catalytic behavior of the dendritic catalysts.

The apolar carbosilane catalysts are soluble in the dichloromethane/methanol (9:1, *v*/*v*) solvent mixture, which may be considered as rather polar on the basis of the dielectric constants of these solvents (ε = 9.1 for CH_2Cl_2, and 33 for CH_3OH). It is known that the introduction of apolar polymers into polar solvents leads to polymer entanglement. In this way, macroscopic clusters of these polymeric materials are formed in order to minimize the Gibbs free energy of the mixture.[44,45] These materials show a tendency to self-assembly into

clusters that are solvated by the least polar solvent system, dichloromethane in our case. From the catalytic point of view, the accumulation of dendritic catalysts by means of self-assembled clusters is likely to lead to a decreased number of accessible catalyst sites, and therefore a lower reaction rate for the cross-coupling catalyzed by the CS-based catalysts. For the polar PAMAM dendrimers no accumulation in the reaction medium is expected and therefore the observed reaction rates are comparable to those of monomeric catalysts.

The differences in product selectivity in the cross-coupling reaction can be explained by the role of peripheral group backfolding. With respect to PAMAM dendrimers, carbosilane dendrimers are relatively small, rigid and sterically crowded. For this reason no backfolding of peripheral groups is taking place for these type of dendrimers (see Elshakre *et al.*[22] for a structural study between carbosilane and PAMAM dendrimers). The observed selectivity of these carbosilane based catalysts is therefore similar to the tested monomeric catalysts: the catalysts on the outside of the self-assembled clusters possess a similar local reaction environment as the monomeric catalysts and accordingly lead to a similar product selectivity. At the same time, catalytic moieties located on the inside of a cluster are not reached by the substrates, and therefore do not take part in catalysis and hence do not affect product selectivity.

Because of the relatively long dendritic arms and the possibility to form hydrogen bonds, backfolding of the peripheral groups towards the interior of the PAMAM-dendrimers is a well-known phenomenon.[22,46-48] The peripheral catalysts that are brought closely to the crowded center of the dendrimer, are expected to experience a different and more crowded reaction environment than monomeric catalysts or peripherally located catalysts. In the catalytic cycle as published by Szabó,[29] the formation of the branched isomers takes place via a (direct) S_N2 attack of a SCS-pincer Pd-allyl intermediate on vinyl epoxide, whereas for the linear isomers in this step a (conjugated) S_N2' attack on vinyl epoxide occurs (*figure 4.8*). Because of steric crowding in the dendrimer interior, the S_N2 transition state will be higher in energy than the S_N2' transition state when the reaction takes place at a backfolded catalytic moiety. Accordingly, formation of the linear product isomer is even more favored than formation of the branched product isomer under backfolding conditions. This leads to an overall increase in the linear : branched product ratio, even though reaction kinetics are likely slower at a backfolding catalytic site.

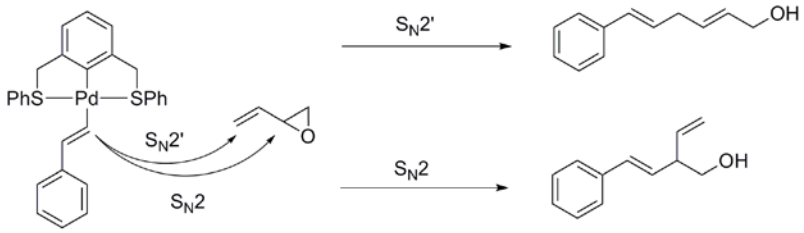

Figure 4.8: The product formation step in the catalytic cycle of the cross-coupling as proposed by Szabó[29]

For the auto-tandem reaction between cinnamyl chloride, hexamethylditin and 4-nitrobenzaldehyde (reaction 2) the differences in the reaction characteristics between the various catalysts were smaller than for the cross-coupling reaction. The structural arguments for these differences, i.e. accumulation of apolar carbosilane dendrimers and backfolding of PAMAM dendrimers, still hold for the tandem reaction as it was carried out in the same solvent system, but do not seem to have a large impact on the reaction characteristics of this reaction. The most striking observation for this tandem reaction is the improved selectivity of the largest PAMAM-dendrimer **5** compared to all other tested catalysts. This positive dendritic effect might again be caused by increased steric crowding because of partial backfolding of the catalysts to the dendrimer interior. A closer look at the mechanism of the tandem reaction[43] shows that the SCS-pincer Pd-η^1-allyl intermediate attacks the electrophilic 4-nitrobenzaldehyde to form both *syn* and *anti* products (*figure 4.9*). The distinction between the formation of these products is the relative orientation of the two reaction partners in the transition state. Due to the large 4-nitrobenzyl-group, the orientation is always favored to a positioning that leads to an *anti* product, since in all cases these diastereoisomers are observed in excess. In a sterically crowded environment, this effect is likely enhanced leading to a higher selectivity for dendritic catalyst **5**.

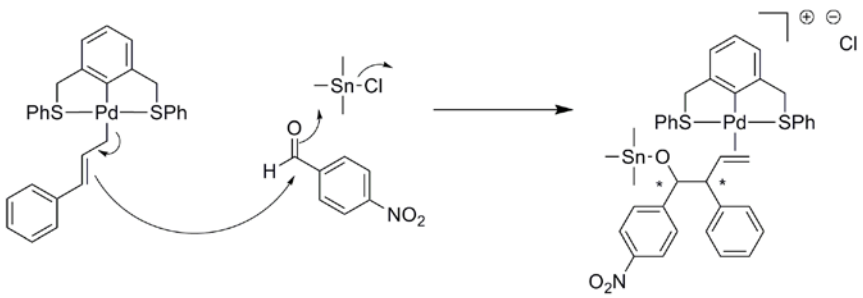

Figure 4.9: The product formation step in the catalytic cycle of the cross-coupling as proposed by us.[43]

In conclusion, the role of the dendritic support in dendrimer-immobilized homogeneous catalysis has been investigated for a series of dendritic catalysts in which the dendritic backbone was varied. For one of the catalytic reactions that was studied the change in dendritic support had a clear effect, whereas for the other reaction the effect was minor. These observations indicate that the role of the dendritic support in 'directing' a catalytic reaction seems very much dependent on the specific reaction intrinsic. It would therefore be of interest to explore reactions that have been proven to show a positive dendritic effect with regards to selectivity or reaction rate, with entirely different dendritic scaffolds than in the original studies. Further studies, using either very apolar or very polar substrates might also enhance the observed effects that have been discussed here and eventually might lead to a more rational choice of the dendrimer support to be used in homogeneous catalysts.

4.5 Experimental section

General

All reactions were carried out using standard Schlenk techniques under an inert dinitrogen atmosphere unless stated otherwise. All solvents were carefully dried and distilled prior to use. All standard reagents were purchased commercially and used without further purification. Compounds **9** (synthesis described by Amijs *et al.*[32]., analytical data present in Paugam *et al.*[49]), **10**[33] and $[Pd(MeCN)_4](BF_4)_2$[50] were prepared according to literature procedures. The PAMAM dendrimers were purchased by Dendritech as solutions in MeOH (G_0: 39.36%, *w*/*w*, G_1: 45.10%, *w*/*w*, G_2: 30.17%, *w*/*w*) and used as received. All other reagents were purchased from Acros Organics and Sigma-Aldrich Chemical Co. Inc. and used as received. ^1H (300 MHz) and ^{13}C (100 MHz) NMR spectra were recorded on Varian spectrometers at 25 ^oC, chemical shifts are given in ppm referenced to residual solvent resonances. UV/Vis spectra were recorded on a Cary 50 Scan UV/Visible spectrophotometer. IR spectra (ATR) were measured with a Perkin Elmer Spectrum One FT-IR instrument. High resolution mass spectroscopy (HRMS) has been performed on a Waters LCT Premier XE Micromass instrument using the electrospray ionization (ESI) technique. GC analysis was carried out using a Perkin Elmer Clarus 500 GC equipped with an Alltech Econo-Cap EC-5 column.

3,5-Bis-(phenylsulfidomethyl)benzoic acid ***11***

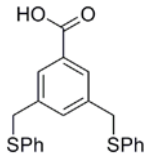

To a cooled solution (-80 °C) of 3,5-bis-(phenylthiomethyl)bromobenzene (**10**, 2.00 g, 4.98 mmol) in Et_2O (60 mL) was added a 1.6 M *t*BuLi solution in hexanes (2.0 equiv., 6.23 mmol, 9.97 mL). The resulting yellow mixture was stirred for 5 min. Then, dry CO_2 (large excess) was bubbled through the solution. Immediately a white precipitation was formed. The suspension was allowed to reach room temperature and water (1 mL) was added resulting in a clear solution. Then, the volatiles were removed and the resulting slurry was taken up in dichloromethane (100 mL) and extracted with an aqueous 4M HCl solution (3x100 mL). The organic fractions were collected and evaporated in vacuo. The resulting syrup was redissolved in CH_2Cl_2 (3 mL) and precipitated by slow addition of hexanes. The supernatant was removed to yield a white powder (1.30 g, 71%).

^{1}H NMR (DMSO-d_6, 300 MHz): δ 13.02 (bs, 1H, COO*H*), 7.79 (s, 2H, Ar*H*), 7.61 (s, 1H, Ar*H*), 7.32-7.21 (m, 6H, *m*,*p*-*S*Ph), 7.19-7.16 (m, 4H, *o*-SPh), 4.28 (s, 4H, CH_2). ^{13}C NMR (DMSO-d_6, 100 MHz) δ 167.6, 139.1, 136.2, 134.2, 131.6, 129.7, 129.3, 129.1, 126.8, 36.9. IR (ATR): ν_{OH} 2605 cm^{-1}, ν_{CO} 1687 cm^{-1}. ESI-HRMS for $C_{21}H_{18}O_2S_2$ (m/z): [M + Na^+] 389.0667 (calcd. 389.0646).

2,5-Dioxopyrrolidin-1-yl-3,5-bis-(phenylthiomethyl)benzoate ***12***

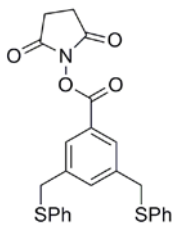

Benzoic acid **11** (1.00 g, 2.97 mmol) was dissolved in dichloromethane (40 mL). Subsequently triethylamine (1.2 equiv., 0.50 mL, 3.57 mmol), 1-ethyl-3-(3-dimethylaminopropyl)-carbodiimide (EDC, 1.2 equiv., 0.68 g, 3.57 mmol) and *N*-hydroxysuccinimide (NHS, 1.2 equiv., 0.41 g, 3.57 mmol) were added to the solution and the reaction mixture was stirred for 16 h. Water (40 mL) was added to the reaction and the resulting biphasic solution was extracted. The organic phase was washed with water (4x40 mL) to get rid of the formed urea

product. The product was purified via column chromatography (hexanes : THF 2:1, *v*/*v*) resulting in a white powder (1.09 g, 80%).

^{1}H NMR ($CDCl_3$, 300 MHz): δ 7.86 (s, 2H, Ar*H*), 7.47 (s, 1H, Ar*H*), 7.30-7.17 (m, 10H, SPh), 4.05 (s, 4H, SCH_2), 2.87 (s, 4H, C(=O)CH_2) . ^{13}C NMR ($CDCl_3$, 100 MHz) δ 164.7, 156.9, 134.6, 131.1, 130.6, 126.1, 125.3, 124.8, 122.5, 120.9, 34.2, 21.2. ESI-HRMS for $C_{25}H_{21}NO_4S_2$ (m/z): $[M + Na]^+$ 486.0829 (calcd. 486.0810).

*SCS-pincer Pd complex **13***

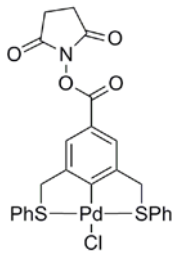

To a solution of SCS-pincer ligand **12** (1.36 g, 2.93 mmol) in acetonitrile (40 mL) was added $[Pd(MeCN)_4](BF_4)_2$ (1.1 equiv., 1.43 g, 3.23 mmol). The yellow solution was stirred for 16 hours at reflux temperature, whereupon the solvent was evaporated. Subsequently, the resulting solids were suspended by adding acetone (40 mL). NaCl (large excess) was added and the suspension was stirred for 1 h. The reaction mixture was filtered and the volatiles were removed in vacuo. The resulting solids were redissolved in CH_2Cl_2 (50 mL) and extracted with water (50 mL). The organic fractions were dried over $MgSO_4$, filtered and treated with polyvinylpyridine (PVPy; approximately 100 equiv.) to scavenge eventual present Pd(0) impurities. The PVPy was removed by filtration and the resulting clear solution was concentrated. The product slowly precipitates from the solution and was collected by decantation of the supernatant. This solution was concentrated and the precipitated product was collected again. This cycle was repeated five times. The solid fractions were collected and yielded 1.38 g (78%) of a pale yellow powder.

^{1}H NMR (CD_2Cl_2, 300 MHz): δ 7.79-7.72 (m, 6H, *o*-SPh + ArH), 7.43-7.37 (m, 6H, *m*,*p*-SPh), 4.70 (bs, 4H, SCH_2), 2.84 (s, 4H, C(=O)CH_2) . ^{13}C NMR (CD_2Cl_2, 100 MHz) δ 169.5, 162.1, 150.8, 132.1, 131.6, 130.4, 130.0, 129.9, 123.6, 121.8, 52.5, 25.9. ESI-HRMS for $C_{25}H_{20}ClNO_4PdS_2$ (m/z): $[2M\text{-}Cl]^+$ = 1172.9449 (calcd. = 1172.9440). UV/Vis (CH_2Cl_2): λ_{max} = 330.1 nm.

*SCS-pincer Pd complex **2***

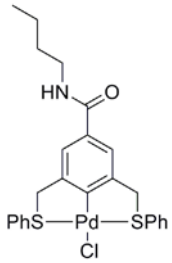

Active ester complex **13** (28.3 mg, 46.9 µmol) and butylamine (1.0 equiv., 4.6 µL, 46.9 µmol) were dissolved in CH_2Cl_2 (2 mL). The reaction mixture was stirred for 2 h. After performing a ninhydrin test on TLC to confirm that no primary amines were present in the solution,[41] the reaction was stopped by diluting it with 10 mL CH_2Cl_2 and a similar volume of water. This biphasic mixture was extracted and the organic phase was washed two more times with water and brine (2x10 mL). The organic fraction was dried over $MgSO_4$, filtered and concentrated in vacuo yielding a yellow solid (21.6 mg, 82%).

^{1}H NMR (CD_2Cl_2, 300 MHz): δ 7.85 (m, 4H, *o*-SPh), 7.47-7.43 (m, 8H, Ar*H* + *m*,*p*-SPh), 6.39 (t,^3J = 4.5 Hz, 1H, N*H*), 4.67 (bs, 4H, SCH_2), 3.38 (q, ^3J = 6.9 Hz, 2H, NCH_2), 1.57 (m, 2H, NCH$_2$CH_2), 1.42 (m, 2H, CH$_3$CH_2), 0.97 (t, ^3J = 7.2 Hz, CH_3). ^{13}C NMR (CD_2Cl_2, 100 MHz) δ 174.2, 149.9, 132.2, 131.8, 130.2, 130.0, 129.9, 123.8, 120.8, 52.4, 40.1, 31.9, 20.4, 14.0. ESI-HRMS for $C_{25}H_{26}ClNOPdS_2$ (m/z): $[M\text{-}Cl+MeCN]^+$ = 567.0720 (calcd. = 567.0765). UV/Vis (CH_2Cl_2): λ_{max} = 330.1 nm. IR (ATR): ν_{max} 3344 m, 3056 w, 2957 m, 2929 m, 2857 m, 1652 s, 1586 m, 1533 s, 1477 m, 1438 s, 1317 m, 1274 m, 1245 s, 1023 s, 902 m, 754 s, 740 s, 685 s.

*Synthesis of dendritic catalysts **3**, **4** and **5***

General procedure:

To a mixture of CH_2Cl_2 and MeOH (1:1, *v*/*v*; 10 mL) was added G_x-PAMAM-NH_2 dendrimer (solution in MeOH, purchased by Dendritech) and 1.25 equiv. of **13** per dendritic arm. This solution was stirred at room temperature. At regular intervals, a ninhydrin test on TLC was performed to check the remainder of primary amines in the solution.[41] The reaction was stopped when primary amines were no longer detected. The dendritic compound was purified by passive dialysis. To this end, the reaction mixture was concentrated to 5 mL and placed into a dialysis bag. This bag was placed into a beaker containing a mixture of CH_2Cl_2 :

MeOH (200 mL; 1:1 *v/v*) and dialyzed for 2 h. This procedure was repeated twice. The contents of the dialysis bag were removed from the bag and evaporated to dryness to yield the PAMAM-G_x-(SCS-Pd-Cl)$_n$ materials.

PAMAM-G_0-(SCS-Pd-Cl)$_4$ ***3***

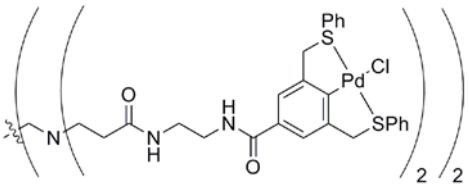

Yield: 110 mg (66%). ^{1}H NMR (CD_2Cl_2/CD_3OD 1:1, *v*/*v*): δ 7.77 (m, 16H, *o*-SPh), 7.45 (s, 8H, Ar*H*), 7.38-7.32 (m, 24H, *m*,*p*-SPh), 4.60 (bs, 16H, SCH_2), 3.40-3.30 (m, 16H, NHCH_2CH_2NH), 2.62 (m, 8H, NCH_2CH$_2$C(=O)), 2.40 (s, 4H, NCH_2CH_2N), 2.26 (m, 8H, NCH$_2$CH_2C(=O)). ^{13}C NMR (CD_2Cl_2/CD_3OD 1:1) δ 173.9, 168.1, 150.0, 132.2, 131.7, 131.1, 130.3, 129.8, 129.1, 121.1, 52.4, 50.9, 49.9, 40.2, 39.1, 33.4. UV/Vis (CH_2Cl_2): λ_{max} = 330.1 nm. IR (ATR): ν_{max} = 3287 br, 3056 m, 2926 m, 2854 m, 1634 s, 1580 m, 1532 s, 1471 m, 1440 s, 1322 m, 1254 s, 1024 m, 908 m, 742 s, 685 s. ESI-HRMS for $C_{104}H_{108}Cl_4N_{12}O_8Pd_4S_8$ (m/z): $[M\text{-}2Cl]^{2+}$ = 1201.0618 (calcd. = 1201.0865).

PAMAM-G_1-(SCS-Pd-Cl)$_8$ ***4***

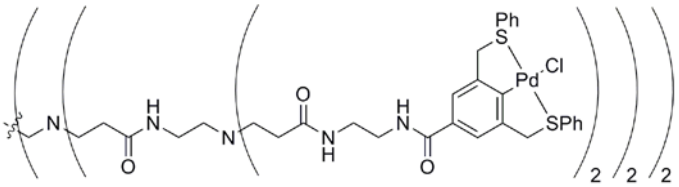

Yield: 140 mg (78%). ^{1}H NMR (CD_2Cl_2/CD_3OD 1:1, *v*/*v*): δ 7.79 (m, 32H, *o*-SPh), 7.48 (bs, 16H, ArH), 7.39 (m, 48H, *m*,*p*-SPh), 4.65 (bs, 32H, SCH_2), 3.44-3.16 (m, 32H, NHCH_2CH_2NH), 2.87 (m, 8H, NHCH_2CH$_2$N), 2.70 (m, 24H, NCH_2CH$_2$C(=O)), 2.48 (s, 12H, NCH_2CH_2N + NHCH$_2$CH_2N), 2.30 (m, 24H, NCH$_2$CH_2C(=O)). ^{13}C NMR (CD_2Cl_2/CD_3OD 1:1) δ 174.0, 170.0 (two signals), 150.1, 132.2, 131.6, 131.2, 130.2, 129.8 (two signals), 121.1, 52.3, 50.0 (two signals), 49.2 (two signals), 40.1, 39.1, 37.6, 33.7. UV/Vis (CH_2Cl_2): λ_{max} = 330.1 nm. IR (ATR): ν_{max} = 3287 br, 3053 m, 2934 m, 2823 m, 1635 s, 1580 m, 1526 s, 1471 m, 1440 s, 1320 m, 1251 s, 1024 m, 907 m, 740 s, 685 s.

PAMAM-G_2-(SCS-Pd-Cl)$_{16}$ ***5***

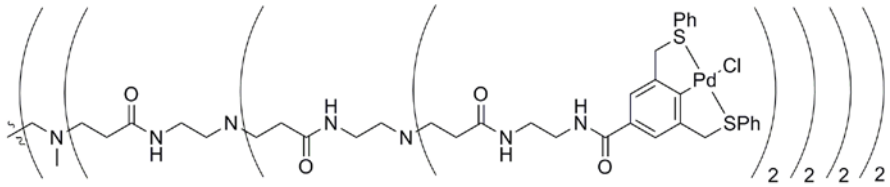

Yield: 140 mg (77%). ^{1}H NMR (CD_2Cl_2/CD_3OD 1:1, *v*/*v*): δ 7.76 (m, 64H, *o*-SPh), 7.47 (bs, 32H, ArH), 7.36 (m, 96H, *m*,*p*-SPh), 4.63 (bs, 64H, SCH_2), 3.40-3.16 (m, 64H, NHCH_2CH_2NH), 2.87 (m, 24H, NHCH_2CH$_2$N), 2.68 (m, 56H, NCH_2CH$_2$C(=O)), 2.48 (bs, 28H, NCH_2CH_2N + NHCH$_2$CH_2N), 2.28 (m, 56H, NCH$_2$CH_2C(=O)). ^{13}C NMR (CD_2Cl_2/CD_3OD 1:1) δ 174.1, 168.1 (three signals), 150.1, 132.0, 131.8, 131.2, 130.3, 129.8 (two signals), 121.2, 52.4, 50.1 (three signals), 49.3 (three signals), 40.2 (two signals), 39.1, 37.6, 33.8 (three signals). UV/Vis (CH_2Cl_2): λ_{max} = 330.1 nm. IR (ATR) ν_{max} = 3287 br, 3059 m, 2965 m, 2926 m, 1634 s, 1580 m, 1532 s, 1470 m, 1440 s, 1323 m, 1253 s, 1024 m, 908 m, 742 s, 686 m.

*X-ray crystal structure determination of compounds **1**, **13** and **2***

X-ray intensities were measured on a Nonius KappaCCD diffractometer with rotating anode (λ = 0.71073 Å) up to a resolution of $(\sin\theta/\lambda)_{max}$ = 0.65 Å^{-1}. Integration was performed with EvalCCD[51] (compounds **1**, **13**) or HKL2000[52] (compound **2**). The structures were solved with automated Patterson methods using DIRDIF-08[53] (**1**, **13**) or Direct Methods using SHELXS-97[54] (**2**). Least squares refinement was performed with SHELXL-97[54] on F^2 of all reflections. Structure calculations and checking for higher symmetry was performed with PLATON.[55] Further details are given in *table 4.2*.

Compound **1.** The position of the halogen was partially occupied by bromine (26% occupancy) and chlorine (74% occupancy). The anisotropic displacement parameters of chlorine and bromine were constrained to the same values. The Pd-halogen distances were restrained to the expectation values of 2.4 Å (chlorine) and 2.5 Å (bromine). All hydrogen atoms were located in difference Fourier maps and refined with a riding model.

Compound **13.** The crystal was cracked with a 4.7° rotation about an arbitrary axis relating the two fragments. Refinement was performed on a HKLF5 file.[56] The position of the halogen was partially occupied by bromine (66% occupancy) and chlorine (34% occupancy). The

anisotropic displacement parameters of chlorine and bromine were constrained to the same values. The Pd-halogen distances were restrained to the expectation values of 2.4 Å (chlorine) and 2.5 Å (bromine). All hydrogen atoms were located in difference Fourier maps and refined with a riding model.

Compound **2.** All hydrogen atoms were located in difference Fourier maps. The N-H hydrogen atom was refined freely with isotropic displacement parameters, C-H hydrogen atoms were refined with a riding model.

Table 4.2: Experimental details of the crystal structure determinations

	1	**13**	**2**
formula	$C_{20}H_{17}Br_{0.26}Cl_{0.74}PdS_2$	$C_{25}H_{20}Br_{0.66}Cl_{0.34}NO_4PdS_2$	$C_{25}H_{26}ClNOPdS_2$
fw	475.09	633.73	562.44
crystal size [mm^3]	0.40x0.08x0.08	0.37x0.25x0.06	0.30x0.15x0.04
crystal color	yellow	pale yellow	yellow
T [K]	110(2)	110(2)	150(2)
crystal system	monoclinic	orthorhombic	monoclinic
space group	$P2_1/c$ (no. 14)	$Pca2_1$ (no. 29)	$P2_1/c$ (no. 14)
a [Å]	9.8035(7)	8.6141(2)	15.8584(2)
b [Å]	18.0936(12)	12.4476(2)	9.8059(2)
c [Å]	10.0847(5)	22.2620(4)	16.2730(3)
β [°]	97.542(3)	-	113.3804(7)
V [$Å^3$]	1773.35(19)	2387.04(8)	2322.76(7)
Z	4	4	4
d_{calcd} [g/cm^3]	1.779	1.763	1.608
μ [mm^{-1}]	1.988	2.129	0.841
abs. corr. type	analytical	multi-scan	multi-scan
abs. corr. range	0.53-0.91	0.70-0.88	0.84-1.12
refl. measured / unique	25006 / 4063	30099 / 5863	28291 / 5286
parameters / restraints	221 / 2	312 / 3	285 / 0
R1/wR2 [I>2σ(I)]	0.0271 / 0.0511	0.0296 / 0.0558	0.0350 / 0.0851
R1/wR2 [all refl.]	0.0452 / 0.0556	0.0374 / 0.0578	0.0493 / 0.0932
S	1.070	1.133	1.055
Flack x[57]	-	-0.011(10)	-
$\rho_{min/max}$ [$e/Å^3$]	-0.60 / 0.59	-0.50 / 0.69	-1.05 / 1.02

General protocol for the cross-coupling of vinyl epoxide with styrylboronic acid

A catalyst solution (2 mol% Pd, 0.016 mmol Pd centers) in a mixture of CH_2Cl_2 and MeOH (9:1, *v/v*, 2 mL) was added to a solution of vinyl epoxide (1.0 equiv., 0.80 mmol, 64 μL), styrylboronic acid (1.0 equiv., 0.80 mmol, 118.4 mg), Cs_2CO_3 (2.0 equiv., 1.6 mmol, 521 mg),

and hexamethylbenzene (internal standard, 0.111 mmol, 14.4 mg) in a mixture of CH_2Cl_2 and MeOH (9:1, *v/v*, 18 mL). The reaction mixture was stirred at room temperature in a nitrogen environment. Aliquots of 50 μL for NMR/GC analysis were taken at regular time intervals with an airtight syringe.

General protocol for the stannylation/electrophilic addition tandem reaction

A catalyst solution (2 mol% Pd, 0.016 mmol Pd centers) in a mixture of CH_2Cl_2 and MeOH (9:1, *v*/*v*, 2 mL) was added to a solution of cinnamyl chloride (3.0 equiv., 2.40 mmol, 0.34 mL), hexamethylditin (3.0 equiv., 2.40 mmol, 0.50 mL), 4-nitrobenzaldehyde (1.0 equiv., 0.80 mmol, 121 mg), and hexamethylbenzene (internal standard, 0.088 mmol, 14.4 mg) in a mixture of CH_2Cl_2 and MeOH (9:1, *v*/*v*, 10 mL). The reaction stirred at room temperature in a nitrogen environment. Aliquots of 50 μL for NMR/GC analysis were taken at regular time intervals with an airtight syringe.

4.6 References

1. Dijkstra, H. P.; van Klink, G. P. M.; van Koten, G. *Acc. Chem. Res.* **2002,** *35*, 798-810.
2. Knapen, J. W. J.; van der Made, A. W.; de Wilde, J. C.; van Leeuwen, P. W. N. M.; Wijkens, P.; Grove, D. M.; van Koten, G. *Nature* **1994,** *372*, 659-663.
3. Astruc, D.; Chardac, F. *Chem. Rev.* **2001,** *101*, 2991-3023.
4. Kreiter, R.; Kleij, A. W.; Klein Gebbink, R. J. M.; van Koten, G. *Top. Curr. Chem.: Dendrimers IV* **2001,** *217*, 163-199.
5. Chase, P. A.; Klein Gebbink, R. J. M.; van Koten, G. *J. Organomet. Chem.* **2004,** *689*, 4016-4054.
6. Kassube, J. K.; Gade, L. H. *Top. Organomet. Chem.* **2006,** *20 (Dendrimer Catal.)*, 39-59.
7. Berger, A.; Klein Gebbink, R. J. M.; van Koten, G. *Top. Organomet. Chem.* **2006,** *20 (Dendrimer Catal.)*, 1-38.
8. Andres, R.; de Jesús, E.; Flores, J. C. *New J. Chem.* **2007,** *31*, 1161-1191.
9. Helms, B.; Fréchet, J. M. J. *Adv. Synth. Catal.* **2006,** *348*, 1125-1148.
10. Bosman, A. W.; Janssen, H. M.; Meijer, E. W. *Chem. Rev.* **1999,** *99*, 1665-1688.
11. Gatard, S.; Kahlal, S.; Mery, D.; Nlate, S.; Cloutet, E.; Saillard, J. Y.; Astruc, D. *Organometallics* **2004,** *23*, 1313-1324.
12. Zhang, J. L.; Zhou, H. B.; Huang, J. S.; Che, C. M. *Chem. Eur. J.* **2002,** *8*, 1554-1562.
13. Benito, J. M.; de Jesús, E.; de la Mata, F. J.; Flores, J. C.; Gomez, R. *Chem. Commun.* **2005**, 5217-5219.
14. Ropartz, L.; Haxton, K. J.; Foster, D. F.; Morris, R. E.; Slawin, A. M. Z.; Cole-Hamilton, D. J. *J. Chem. Soc. Dalton Trans.* **2002**, 4323-4334.
15. Ribourdouille, Y.; Engel, G. D.; Richard-Plouet, M.; Gade, L. H. *Chem. Commun.* **2003**, 1228-1229.
16. Dahan, A.; Portnoy, M. *Org. Lett.* **2003,** *5*, 1197-1200.
17. Servin, P.; Laurent, R.; Gonsalvi, L.; Tristany, M.; Peruzzini, M.; Majoral, J. P.; Caminade, A. M. *Dalton Trans.* **2009**, 4432-4434.
18. Snelders, D. J. M.; van Koten, G.; Klein Gebbink, R. J. M. *J. Am. Chem. Soc.* **2009,** *131*, 11407-11416.
19. Kleij, A. W.; Gossage, R. A.; Klein Gebbink, R. J. M.; Brinkmann, N.; Reijerse, E. J.; Kragl, U.; Lutz, M.; Spek, A. L.; van Koten, G. *J. Am. Chem. Soc.* **2000,** *122*, 12112-12124.

20. Breinbauer, R.; Jacobsen, E. N. *Angew. Chem. Int. Ed.* **2000,** *39*, 3604-3607.
21. Kassube, J. K.; Gade, L. H. *Adv. Synth. Catal.* **2009,** *351*, 739-749.
22. Elshakre, M.; Atallah, A. S.; Santos, S.; Grigoras, S. *Comp. Theor. Polymer Sci.* **2000,** *10*, 21-28.
23. Tomalia, D. A.; Naylor, A. M.; Goddard, W. A. *Angew. Chem. Int. Ed.* **1990,** *29*, 138-175.
24. Labieniec, M.; Watala, C. *Centr. Eur. J. Biol.* **2009,** *4*, 434-451.
25. Esfand, R.; Tomalia, D. A. *Drug Discovery Today* **2001,** *6*, 427-436.
26. Frey, H.; Schlenk, C. *Dendrimers II* **2000,** *210*, 69-129.
27. van Koten, G.; Jastrzebski, J. T. B. H. *J. Mol. Catal. A Chem.* **1999,** *146*, 317-323.
28. van der Made, A. W.; van Leeuwen, P. W. N. M. *J. Chem. Soc. Chem. Commun.* **1992**, 1400-1401.
29. Kjellgren, J.; Aydin, J.; Wallner, O. A.; Saltanova, I. V.; Szabó, K. J. *Chem. Eur. J.* **2005,** *11*, 5260-5268.
30. Gagliardo, M.; Selander, N.; Mehendale, N. C.; van Koten, G.; Klein Gebbink, R. J. M.; Szabó, K. J. *Chem. Eur. J.* **2008,** *14*, 4800-4809.
31. Suijkerbuijk, B. M. J. M.; Slagt, M. Q.; Klein Gebbink, R. J. M.; Lutz, M.; Spek, A. L.; van Koten, G. *Tetrahedron Lett.* **2002,** *43*, 6565-6568.
32. Amijs, C. H. M.; van Klink, G. P. M.; van Koten, G. *Green Chem.* **2003,** *5*, 470-474.
33. Meijer, M. D.; Mulder, B.; van Klink, G. P. M.; van Koten, G. *Inorg. Chim. Acta* **2003,** *352*, 247-252.
34. Slagt, M. Q.; Klein Gebbink, R. J. M.; Lutz, M.; Spek, A. L.; van Koten, G. *J. Chem. Soc. Dalton Trans.* **2002**, 2591-2592.
35. Pijnenburg, N. J. M.; Dijkstra, H. P.; van Koten, G.; Klein Gebbink, R. J. M. *Dalton Trans.* **2011,** *40,* 8896-8905, *or* ***Chapter 2*** *of this thesis*.
36. Kruithof, C. A.; Dijkstra, H. P.; Lutz, M.; Spek, A. L.; Klein Gebbink, R. J. M.; van Koten, G. *Organometallics* **2008,** *27*, 4928-4937.
37. Bergbreiter, D. E.; Frels, J. D.; Rawson, J.; Li, J.; Reibenspies, J. H. *Inorg. Chim. Acta* **2006,** *359*, 1912-1922.
38. van Manen, H. J.; Nakashima, K.; Shinkai, S.; Kooijman, H.; Spek, A. L.; van Veggel, F. C. J. M.; Reinhoudt, D. N. *Eur. J. Inorg. Chem.* **2000**, 2533-2540.
39. Cervantes, R.; Castillejos, S.; Loeb, S. J.; Ortiz-Frade, L.; Tiburcio, J.; Torrens, H. *Eur. J. Inorg. Chem.* **2006**, 1076-1083.
40. Mehendale, N. C.; Lutz, M.; Spek, A. L.; Klein Gebbink, R. J. M.; van Koten, G. *J. Organomet. Chem.* **2008,** *693*, 2971-2981.
41. Kaiser, E.; Colescot, R. L.; Bossinge, C. D.; Cook, P. L. *Anal. Biochem.* **1970,** *34*, 595-&.
42. Bonnet, S.; Lutz, M.; Spek, A. L.; van Koten, G.; Klein Gebbink, R. J. M. *Organometallics* **2010,** *29*, 1157-1167.
43. Pijnenburg, N. J. M.; Cabon, Y. H. M.; van Koten, G.; Klein Gebbink, R. J. M. ***Chapter 3*** *of this thesis*.
44. Ravve, A. *Principles of Polymer Chemistry* **2000,** *2nd edition, Kluwer Academic, New York*.
45. Teegarden, D. M. *Polymer Chemistry: Introduction to a Indispensable Science* **2004,** *NSTA, Arlington, Virginia*.
46. Boas, U.; Christensen, J. B.; Heegaard, P. M. H. *J. Mat. Chem.* **2006,** *16*, 3786-3798.
47. Opitz, A. W.; Wagner, N. J. *J. Polymer Sci. B-Polymer Phys.* **2006,** *44*, 3062-3077.
48. Ballauff, M.; Likos, C. N. *Angew. Chem. Int. Ed.* **2004,** *43*, 2998-3020.
49. Paugam, M. F.; Bien, J. T.; Smith, B. D.; Chrisstoffels, L. A. J.; de Jong, F.; Reinhoudt, D. N. *J. Am. Chem. Soc.* **1996,** *118*, 9820-9825.
50. Lai, T. W.; Sen, A. *Organometallics* **1984,** *3*, 866.
51. Duisenberg, A. J. M.; Kroon-Batenburg, L. M. J.; Schreurs, A. M. M. *J. Appl. Cryst.* **2003,** *36*, 220-229.
52. Otwinowski, Z.; Minor, W. *Macromol. Cryst. A* **1997,** *276*, 307-326.
53. Beurskens, P. T.; Admiraal, G.; Beurskens, G.; Bosman, W. P.; Garcia-Granda, S.; Gould, R. O.; Smits, J. M. M.; Smykalla, C. *The DIRDIF08 program system, Technical Report of the Crystallography Laboratory, University of Nijmegen, The Netherlands* **2008**
54. Sheldrick, G. M. *Acta Cryst.* **2008,** *A64*, 112-122.
55. Spek, A. L. *Acta Cryst.* **2009,** *D65*, 148-155.
56. Herbst-Irmer, R.; Sheldrick, G. M. *Acta Cryst.* **1998,** *B54*, 443-449.
57. Flack, H. D. *Acta Cryst.* **1983,** *A39*, 876-881.

Chapter 5

Support-related product formation by PEG-copolymer-supported SCS-pincer palladium catalysts

Abstract

Based on copolymers comprised of ethylene oxide and allyl glycidyl ether, two precisely tailored linear polymers exhibiting fully identical chemical composition and high loading of SCS-pincer palladium complexes were prepared. One catalytically active conjugate had a distinctive random, the other a diblock structure. These structures allowed us to investigate the pure effect of the soluble polymeric support on the catalytic behavior of the pincer complexes. Together with the parent monomeric SCS-pincer palladium catalyst, the immobilized pincer catalysts were employed for the cross-coupling of vinyl oxirane with styrylboronic acid. The overall reactivity of these supported catalysts slightly decreased compared to the parent monomeric catalyst. More surprisingly, both conjugates showed an increase in selectivity compared to the monomeric Pd complex, and in particular the diblock structure showed an almost doubled l/b product selectivity compared to the random copolymer. These observations are explained based on the geometric requirements of the S_N2 and S_N2' reaction paths that lead to the respective products.

5.1 Introduction

The use of functional polymers as soluble supports in organic synthesis and homogeneous catalysis represents an important research area. Besides the widely used insoluble, solid polymer supports, their soluble counterparts have attracted particular interest, as they promise to overcome the main drawback of heterogenized catalysis, i.e., disadvantageous reaction kinetics.[1-4] To date, poly(ethylene glycol) monomethyl ether with a molecular weight of 5000 g/mol (MPEG-5000) is the most widely utilized soluble polymeric support for catalysts (and supported reagents) due to its chemical inertness and excellent solubility in both organic and aqueous media. Due to these features, combined with its established biocompatibility, PEG is also the reference polymer for pharmaceutical and biomedical application. However, the loading capacity of PEG is limited by a maximum of two functional end groups. In this context, dendrimers and hyperbranched polymers such as poly(glycerol) represent a promising class of soluble macromolecular supports, because of their high number of functional groups accessible for the attachment of reagents or catalysts.[5-9]

The immobilization of homogeneous catalysts on the periphery of dendrimers has been the subject of intense research.[10-14] ECE-pincer metal complexes are perfect candidates for this purpose, because of their robust metal-carbon σ-bond, high chemical stability and adjustable covalent anchoring groups. In particular, ECE-pincer Pd-catalysts have proven to be excellent catalysts for a variety of organic reactions,[15-18] including aldol condensations, Michael reactions, allylations of electrophiles, stannylation and borylation reactions, and cross-coupling reactions, e.g. the epoxide opening of vinyl epoxides and boronic acids.[19,20] It is known by an earlier investigation of us that the (polymeric/dendritic) support may influence either in a negative or in a positive sense several catalytic parameters of a supported catalyst, like e.g. reaction rate and product selectivity.[21] This is due to steric and electronic alteration of the catalytic centers as a result of interactions with the polymer support.[22] Positive dendritic effects that reveal a higher product selectivity compared to monomeric catalysts were reported by (among others) the research groups of Che,[23] Gomez,[24] Cole-Hamilton,[25] and Klein Gebbink.[21,26] These effects were also reported in the case when dendrimer encapsulated nanoparticles (DENs) were used as catalysts.[27,28]

Despite the predominance of PEG-supported systems only few approaches have been reported with PEG derivatives presenting an increased number of functional groups, as for example is the case in dendronized PEGs.[29,30] In one single paper by Elias and Vigalok a diblock copolymer based on PEG has been employed for micellar catalysis.[31] So far, only poly(2-oxazoline) block copolymers developed in the group of Nuyken and recently also the block copolymers obtained by ring opening metathesis polymerization have been employed to provide a segment determining solution properties and a segment for the covalent linkage of multiple catalytic units.[32-35]

Considering the desired features of soluble supports, it is surprising that so far, to the best of our knowledge, neither block nor random copolymers based on ethylene oxide (EO) and suitable epoxide comonomers have been described yet, as those multifunctional PEGs (mf-PEGs) embody tailor-made polymers with good control over molecular weight, offer an adjustable number of functional groups and at the same time provide the assembly with solubility characteristics of PEG.[36-41]

In the present study we have used examples of block and random copolymers derived from anionic ring opening copolymerization of EO and allyl glycidyl ether (AGE), that represent an outstanding modular synthetic platform, for which a large variety of compositions and molecular weights are accessible (*figure 5.1*). In addition, a broad range of functionalities can be introduced via modification of the pendant allyl ethers with a respective functional ω-thiol, employing thiol-ene coupling (TEC), a type of reaction that possesses 'click' characteristics.[42] The key feature of these multifunctional-PEGs is the random distribution of functional groups at the backbone and therefore a constant average spacing between neighboring catalyst-moieties, guaranteeing that systematic studies are not influenced by inhomogeneity effects in the polymer backbone.[43] In the current study the precise control of the EO/AGE copolymer system was utilized for the synthesis of two PEG-based SCS-pincer conjugates exhibiting virtually identical chemical composition. One conjugate is based on a diblock copolymer, $P(EO)_{113}$-*b*-$P(G\text{-}Pd)_7$ while the other is a random copolymer structure, $P(EO_{110}$-*co*-$(G\text{-}Pd)_8)$.

5.2 Results

In a straightforward procedure (*figure 5.1*) the random copolymer P(EO-*co*-AGE) was prepared via anionic ring opening copolymerization of EO and AGE initiated with the cesium salt of 2-methoxyethanol. Albeit EO and AGE differ in electronic and steric properties AGE is strictly randomly incorporated throughout the polymerization, as previously demonstrated by the combination of advanced real-time ^{1}H NMR kinetics, analysis of thermal behavior by differential scanning calorimetry and analysis of triad sequence distribution via ^{13}C NMR.[43] The diblock copolymer $P(EO)_{113}$-*b*-$P(AGE)_{11}$ was synthesized by employing the cesium salt of MPEG-5000 as macroinitiator for the homopolymerization of AGE (*figure 5.1*). Size exclusion chromatography (SEC) analysis demonstrated good control of molecular weight and narrow molecular weight distributions. ^{1}H NMR spectroscopy showed good adjustment of the AGE ratio via the initial monomer feed. TEC was performed with AIBN as a radical initiator and cysteamine hydrochloride to obtain the multiamino functional PEG derivatives $P(EO)_{113}$-*b*-$P(G\text{-}NH_2)_7$ and $P(EO_{110}$-*co*-$(G\text{-}NH_2)_8)$. The obtained primary amino groups were accessible for active ester coupling with succinimidyl ester functionalized SCS-pincer Pd complexes, affording the diblock copolymer $P(EO)_{113}$-*b*-$P(G\text{-}Pd)_7$ and its exact random analogue $P(EO_{110}$-*co*-$(G\text{-}Pd)_8)$ SCS-pincer PEG conjugates with high catalyst loadings of ~ 0.7 mmol/g (*table 5.1*).[43] ^{1}H NMR analysis of side chain and pincer signals demonstrated full conversion of amino groups into stable benzamides. Remaining free pincer catalyst was entirely removed via dialysis, as evidenced by SEC and NMR. ^{1}H NMR spectroscopy showed virtually identical chemical composition for both SCS-pincer loaded PEG derivatives. Most importantly, the combination of TEC conversion and catalyst linkage via active ester coupling maintained the precisely designed macromolecular structures with low PDIs (1.17 and 1.20).

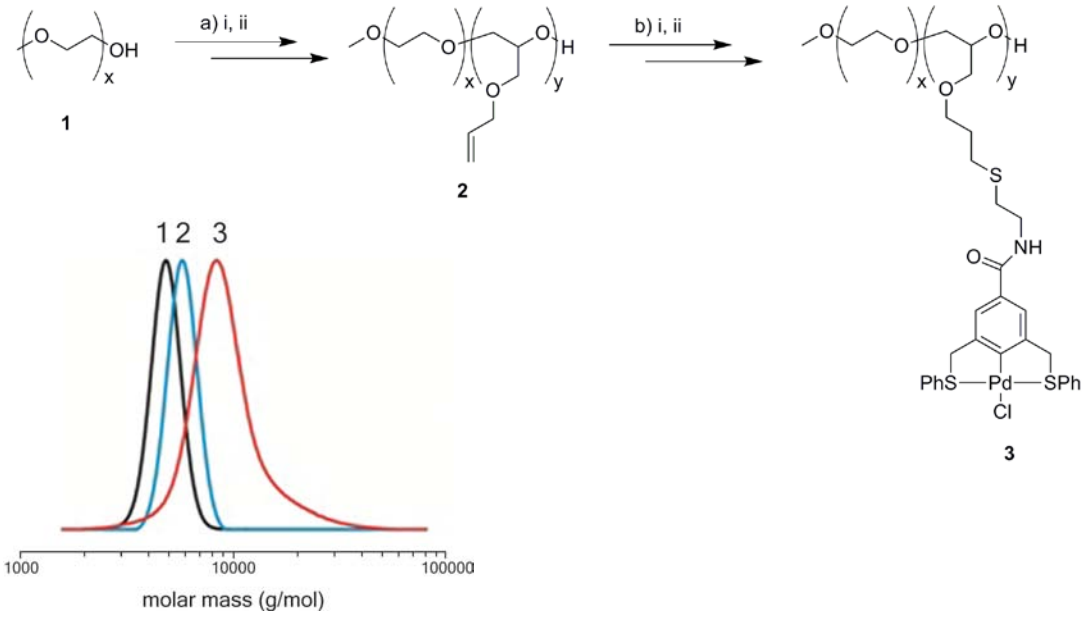

Figure 5.1: Synthesis and corresponding size exclusion chromatograms of SCS-pincer-functionalized diblock copolymer $P(EO)_{113}$-b-$P(G\text{-}Pd)_7$ starting from MPEG-5000 (x = 113). a) i: CsOH/benzene, vacuo, 90 °C. ii: AGE, toluene, 40 °C. b) i: $HS(CH_2)_2NH_2$, AIBN, DMF, 70 °C; ii: DMF, NHS-SCS-pincer Pd-Cl, 50 °C. Synthesis of random structure in analogy with a) ii: AGE/EO, DMSO, THF, 40 °C.

Table 5.1: Characterization data for random and diblock copolymers comprised of ethylene oxide and allyl glycidyl ether, amino functionalized derivatives and pincer-conjugates obtained from ^{1}H NMR and SEC.

	composition (NMR) [a]	M_n (NMR) (g/mol) [a]	M_n (SEC) (g/mol) [b]	M_w/M_n [b]
1	$P(EO)_{113}$-b-$P(AGE)_{11}$	6200	5700	1.02
2	$P(EO)_{113}$-b-$P(G\text{-}NH_2)_7$	6600	N/A*	N/A*
3	$P(EO)_{113}$-b-$P(G\text{-}Pd)_7$	9600	8400	1.17
4	$P(EO_{103}$-ran-$AGE_{11})$	5800	4400	1.07
5	$P(EO_{110}$-ran-$(G\text{-}NH_2)_8)$	6000	N/A*	N/A*
6	$P(EO_{110}$-ran-$(G\text{-}Pd)_8)$	10200	7000	1.20

[a] determined from ^{1}H NMR (300 MHz), [b] M_n determined by SEC-RI in DMF * strong interactions with column material.

Together with the parent monomeric SCS-pincer palladium catalyst, the polymer supported catalysts have been employed for the cross-coupling of vinyl oxirane with styrylboronic acid (*figure 5.2*).[19] This palladium-catalyzed reaction leads to the formation of a mixture of the

linear 6-phenylhexa-2,5-dien-1-ol **1** and the branched 4-phenyl-2-vinylbut-3-en-1-ol **2** products. Besides cross-coupling products also significant amounts of hydrolysis products (styrene) and minute amounts of homo-coupling products (1,4-diphenylbuta-1,3-diene) were found.

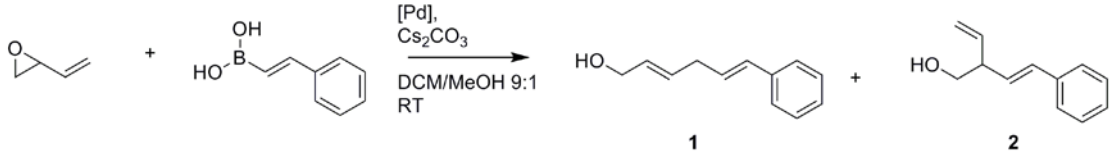

*Figure 5.2: The palladium-catalyzed cross-coupling of vinyl oxirane with styrylboronic acid leads to linear product **1** and branched product **2**.*[19]

Both polymer-immobilized catalysts $P(EO)_{113}$-*b*-$P(G\text{-}Pd)_7$ and $P(EO_{110}$-*co*-$(G\text{-}Pd)_8)$ showed a lower conversion of the starting materials than the monomeric SCS-pincer Pd-catalyst, which gave complete reaction within 1.5 h (*figure 5.3*). In contrast, the polymer-supported catalyst achieved conversions of approximately 80% within 5 h. When the diblock copolymer was compared to the randomly distributed polymer, their reaction rates were rather similar. The overall decrease in reactivity is most likely caused by the increased steric crowding around the metal center in both immobilized systems, leading to a decreased accessibility of the substrates.

The formation of cross-coupling, hydrolysis, and homo-coupling products was found to be constant at 60:38:2 %, respectively, for all tested catalyst systems similar to earlier investigations.[21] The product ratio between the linear cross-coupling product **1** and the branched cross-coupling product **2** dramatically changed, when the polymer-supported catalysts were used (*figure 5.3*). For the parent complex a linear to branched ratio of 5.5 was reported, while for the pincer catalyst supported on the random copolymer the selectivity increased to 8.1. The diblock copolymer SCS-pincer conjugate showed a further selectivity improvement, resulting in an l/b ratio of 14.9, which is almost threefold higher than for the monomeric complex. The structure of the soluble polymer support apparently controlled the selectivity of the Pd-catalyzed cross-coupling reaction. The regioselectivity observed when these pincer complexes were used as catalysts was found to be entirely different from the case where $Pd_2(dba)_3$ is used as catalyst precursor (l/b ratio of 1.5),[19] which is a clear

indication that the catalytically active species in our conditions is a molecular palladium complex.

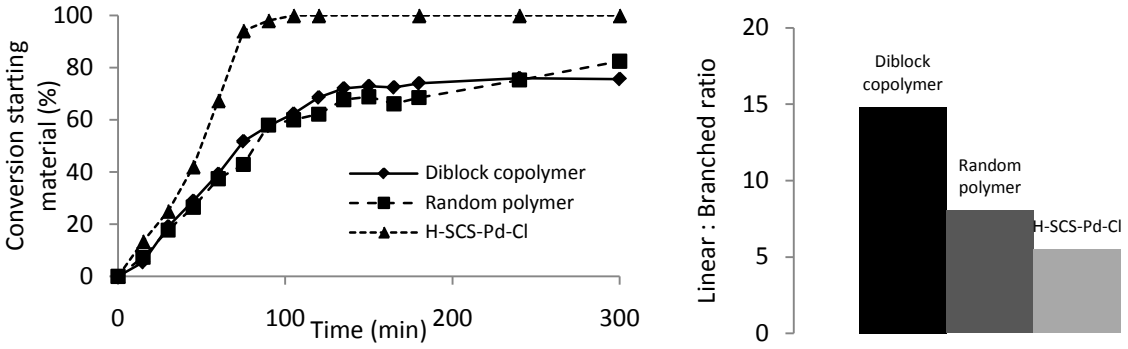

Figure 5.3: Graphs showing conversion of styrylboronic acid in the SCS-pincer Pd-catalyzed cross-coupling with vinyl oxirane (left graph) and the l/b product ratio of the formed cross-coupling products (right graph). In this reaction 0.80 mmol vinyl oxirane, 0.80 mmol styrylboronic acid and 1.6 mmol cesium carbonate were used in CH_2Cl_2/MeOH (20 mL, 9:1, v/v) together with 2 mol% of catalytic centers.

Transmission electron microscopy images obtained via drop casting of the $P(EO)_{113}$-*b*-$P(G\text{-}Pd)_7$ block copolymer catalyst directly from the reaction solution (CH_2Cl_2/MeOH 9:1) showed the formation of aggregates in the size range of 10 nm (*figure 5.4*). For the random copolymer structure the formation of separate domains or defined superstructures is not expected and was not observed. A CH_2Cl_2/MeOH solvent mixture was specifically chosen in the catalytic reactions, because both the polymeric catalysts and the monomeric pincer complex showed excellent solubility. We, therefore, concluded that the change in product selectivity by the polymer-supported catalysts is unlikely to be the result of the solution properties of the catalysts, but must be due to the polymeric micro-structure at the catalytic sites. The random PEG copolymer structure exhibits equidistant average spacing between the catalytic sites at the PEG backbone, whereas in the diblock copolymer the catalytic sites are closely packed in the functional polymer segment, which most probably results in steric constraints. In the catalytic cycle of this reaction,[19] a η^1-vinyl-Pd intermediate resulting from the transmetalation of the SCS-pincer Pd-Cl complex with styrylboronic acid is proposed. Next, this vinyl functionality is transferred to the vinyl epoxide substrate in an S_N2 or S_N2' type reaction. When steric crowding around the vinyl-Pd intermediate increases as is the

case for the diblock copolymer, the sterically least hindered reaction pathway, i.e. the S_N2' attack on the terminal olefin of vinyl oxirane, would be favored, leading to an increased amount of linear product **1**.

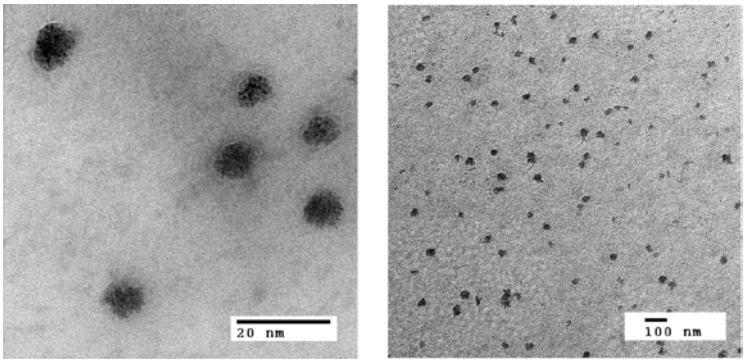

Figure 5.4: Transmission electron microscopy images of diblock copolymer supported conjugate $P(EO)_{113}$-b-$P(G\text{-}Pd)_7$ obtained by drop casting from the reaction solvent.

5.3 Conclusions

In summary, activated ester SCS-pincer complexes in combination with a multifunctional PEG copolymer support represent a highly promising platform for tailor-made soluble polymer supported catalysts. These new catalytically active PEG conjugates, comprised of EO and AGE with identical chemical composition, demonstrated controlled access to “high capacity PEG” catalysts and the possibility to investigate the pure influence of polymeric structure on the activity and selectivity of a covalently attached catalytic center. Further in depth systematic experiments with various PEG based supports and SCS-pincers are currently under investigation to gain deeper insight into the support-determined structure-activity and selectivity relationships of these soluble supported catalysts.

5.4 Experimental Section

General

All reactions were carried out using standard Schlenk techniques under an inert dinitrogen atmosphere unless stated otherwise. All solvents were carefully dried and distilled prior to use. All standard reagents were purchased commercially and used without further purification. ^{1}H NMR spectra (300 MHz) and ^{13}C NMR spectra (75.5 MHz) were recorded using a Bruker AC300 or a Bruker AMX400 (Mainz) or on a Varian 400 MHz spectrometer (Utrecht). All spectra were referenced internally to residual proton signals of the deuterated solvent. For SEC measurements in DMF (containing 1 g/L of lithium bromide as an additive) an Agilent 1100 Series was used as an integrated instrument, including a PSS HEMA column ($10^6/10^5/10^4$ g/mol), a UV (275 nm) and a RI detector. Calibration was carried out using poly(ethylene oxide) standards provided by Polymer Standards Service. GC analysis was carried out using a Perkin Elmer Clarus 500 GC equipped with an Alltech Econo-Cap EC-5 column.

Succinimidyl ester functionalized SCS-pincer Pd-catalyst

The synthesis was performed using the procedure presented by Suijkerbuijk as described earlier.[21,44]

Synthesis of SCS-pincer copolymer conjugates

MPEG-b-PAGE block copolymer synthesis

MPEG-5000 (10 g, 2.0 mmol, 1 equiv.), cesium hydroxide monohydrate (302 mg, 3.6 mmol, 0.9 equiv.) and benzene (30 mL) were added in a dry Schlenk flask under argon atmosphere. Stirring at 60 °C for 30 min and evacuation at 90 °C for 3 h afforded the partially deprotonated macroinitiator. After dissolution in 50 mL of toluene and addition of allyl glycidyl ether (AGE, 6.84 g, 30.0 mmol, 15 equiv.) polymerization was performed at 40 °C overnight under an argon atmosphere. Addition of methanol and acidic ion-exchange resin, filtration, precipitation in cold diethyl ether afforded the pure block copolymer in 86% yield.

Copolymerization of ethylene oxide (EO) and AGE

Cesium hydroxide monohydrate (373 mg, 2.22 mmol, 1 equiv.) were suspended in benzene in a dry Schlenk flask under argon atmosphere and 2-methoxyethanol (169 mg, 2.22 mmol, 1 equiv.) were added. Stirring at 60 °C for 30 min and evacuation at 90 °C for 3 h afforded the cesium alkoxide. DMSO (10 mL) and THF (40 mL) were added in the evacuated flask. After dissolution the flask was cooled to -40 °C and EO (10 mL, 200 mmol, 90 equiv.) were cryo-transferred from a graduated ampule. AGE (2.5 g, 22.2 mmol, 10 equiv.) was added via a syringe. The mixture was warmed up to 40 °C and polymerization was performed overnight. Polymerization was terminated by addition of methanol and acidic ion-exchange resin. Dialysis (MWCO = 1000 g/mol) in ethanol was performed after filtration. The polymer was dried at 40 °C in vacuo to give pale yellow substance in good yield (88%)

Thiol-ene functionalization reaction

$P(EO_{110}$-co-$AGE_{12})$ (2 g, 2.4 mmol C=C, 1 equiv.), AIBN (295 mg, 1.8 mmol, 0.75 equiv.) and cysteamine hydrochloride (2.7 g, 24 mmol, 10 equiv.) were dissolved in 15 mL DMF. After three freeze-pump-thaw cycles the reaction mixture was stirred at 75 °C overnight. Dialysis (MWCO = 1000 g/mol) against DMF followed by ethanol and drying at 40 °C in vacuo gave the PEG derivative in good yields (>80%).

The procedure for the diblock copolymer was identical.

SCS-pincer coupling reaction

The multiamino functional polymer (40 mg, 65 µmol, 1 equiv.), the succinimidinyl-SCS-pincer Pd-Cl (50 mg, 77 µmol, 1.2 equiv.) and DiPEA (42 mg, 325 µmol, 5 equiv.) were dissolved in 2 mL dry DMF and stirred at 50 °C overnight. After dialysis (MWCO = 1000 g/mol) against DMF followed by $CHCl_3$ the solution was concentrated in vacuo. Precipitation in diethyl ether afforded the pure pincer polymer conjugates as glassy yellow materials. (> 80%).

General protocol for the cross-coupling of vinyl oxirane with styrylboronic acid

A catalyst solution (2 mol% Pd, 0.016 mmol/number of Pd centers present in molecule: 7.4 mg of HSCSPdCl, 10.8 mg of $P(EO_{110}$-ran-$(G\text{-}Pd)_8)$ (8.5 µmol), and 16.6 mg of $P(EO)_{113}$-b-$P(G\text{-}Pd)_7$ (12.1 µmol) in a mixture of CH_2Cl_2 and MeOH (9:1, v/v, 2 mL)) was added to a solution of vinyl oxirane (1.0 equiv., 0.80 mmol, 64 µL), styrylboronic acid (1.0 equiv., 0.80 mmol, 118.4

mg), cesium carbonate (2.0 equiv., 1.6 mmol, 521 mg) and hexamethylbenzene (internal standard, 0.111 mmol, 14.4 mg) in a mixture of CH_2Cl_2 and MeOH (9:1, 18 mL). The reaction stirred at room temperature in a nitrogen environment. Aliquots of 50 μL for NMR/GC analysis were regularly taken with an airtight syringe.

5.5 References

(1) Bergbreiter, D. E.; Tian, J. H.; Hongfa, C. *Chem. Rev.* **2009**, *109*, 530-582.
(2) Bergbreiter, D. E. *Chem. Rev.* **2002**, *102*, 3345-3384.
(3) Dickerson, T. J.; Reed, N. N.; Janda, K. D. *Chem. Rev.* **2002**, *102*, 3325-3344.
(4) Gravert, D. J.; Janda, K. D. *Chem. Rev.* **1997**, *97*, 489-510.
(5) Astruc, D.; Chardac, F. *Chem. Rev.* **2001**, *101*, 2991-3024.
(6) Majoral, J.-P.; Caminade, A.-M. *Chem. Rev.* **1999**, *99*, 845-880.
(7) Kassube, J. K.; Gade, L. H. *Stereoselective Dendrimer Catalysis*; Springer Verlag Heidelberg Germany, 2006 Vol. 20.
(8) Haag, R. *Chem. Eur. J.* **2001**, *7*, 327-335.
(9) Hebel, A.; Haag, R. *J. Org. Chem.* **2002**, *67*, 9452-9455.
(10) Oosterom, G. E.; Reek, J. N. H.; Kamer, P. C. J.; van Leeuwen, P. W. N. M. *Angew. Chem. Int. Ed.* **2001**, *40*, 1828-1849.
(11) van Heerbeek, R.; Kamer, P. C. J.; van Leeuwen, P. W. N. M.; Reek, J. N. H. *Chem. Rev.* **2002**, *102*, 3717-3756.
(12) Chase, P. A.; Klein Gebbink, R. J. M.; van Koten, G. *J. Organomet. Chem.* **2004**, *689*, 4016-4054.
(13) de Jesús, E.; Flores, J. C. *Ind. Eng. Chem. Res.* **2008**, *47*, 7968-7981.
(14) van de Coevering, R.; Klein Gebbink, R. J. M.; van Koten, G. *Progr. Polymer Sci.* **2005**, *30*, 474-490.
(15) Albrecht, M.; van Koten, G. *Angew. Chem. Int. Ed.* **2001**, *40*, 3750-3781.
(16) Singleton, J. T. *Tetrahedron* **2003**, *59*, 1837-1857.
(17) Selander, N.; Szabó, K. J. *Chem. Rev.* **2011**, *111*, 2048-2072.
(18) Pijnenburg, N. J. M.; Korstanje, T. J.; van Koten, G.; Klein Gebbink, R. J. M. *Palladacycles on Dendrimers and Star-Shaped Molecules, Wiley-VCH Verlag GmbH & Co. KGaA* **2008**, 361-398, *or* ***Chapter 1*** *of this thesis*.
(19) Kjellgren, J.; Aydin, J.; Wallner, O. A.; Saltanova, I. V.; Szabó, K. J. *Chem. Eur. J.* **2005**, *11*, 5260-5268.
(20) Bonnet, S.; Lutz, M.; Spek, A. L.; van Koten, G.; Klein Gebbink, R. J. M. *Organometallics* **2010**, *29*, 1157-1167.
(21) Pijnenburg, N. J. M.; Lutz, M.; Siegler, M.; Spek, A. L.; van Koten, G.; Klein Gebbink, R. J. M. *New. J. Chem.* **2011**, accepted, or **Chapter 4** of this thesis
(22) Helms, B.; Fréchet, J. M. J. *Adv. Synth. Catal.* **2006**, *348*, 1125-1148.
(23) Zhang, J. L.; Zhou, H. B.; Huang, J. S.; Che, C. M. *Chem. Eur. J.* **2002**, *8*, 1554-1562.
(24) Benito, J. M.; de Jesús, E.; de la Mata, F. J.; Flores, J. C.; Gomez, R. *Chem. Commun.* **2005**, 5217-5219.
(25) Ropartz, L.; Haxton, K. J.; Foster, D. F.; Morris, R. E.; Slawin, A. M. Z.; Cole-Hamilton, D. J. *J. Chem. Soc. Dalton Trans.* **2002**, 4323-4334.
(26) Snelders, D. J. M.; van Koten, G.; Klein Gebbink, R. J. M. *J. Am. Chem. Soc.* **2009**, *131*, 11407-11416.
(27) Oh, S. K.; Niu, Y. H.; Crooks, R. M. *Langmuir* **2005**, *21*, 10209-10213.
(28) Niu, Y. H.; Yeung, L. K.; Crooks, R. M. *J. Am. Chem. Soc.* **2001**, *123*, 6840-6846.
(29) Benaglia, M.; Annunziata, R.; Cinquini, M.; Cozzi, F.; Ressel, S. *J. Org. Chem.* **1998**, *63*, 8628-8629.
(30) Annunziata, R.; Benaglia, M.; Cinquini, M.; Cozzi, F. *Chem. Eur. J.* **2000**, *6*, 133-138.
(31) Elias, S.; Vigalok, A. *Adv. Synth. Catal.* **2009**, *351*, 1499-1504.
(32) Persigehl, P.; Jordan, R.; Nuyken, O. *Macromolecules* **2000**, *33*, 6977-6981.
(33) Kotre, T.; Zarka, M. T.; Krause, J. O.; Buchmeiser, M. R.; Weberskirch, R.; Nuyken, O. *Macromol. Symp.* **2004**, *217*, 203-214.

(34) Rossbach, B. M.; Leopold, K.; Weberskirch, R. *Angew. Chem. Int. Ed.* **2006**, *45*, 1309.
(35) Pawar, G. M.; Weckesser, J.; Blechert, S.; Buchmeiser, M. R. *Beilstein J. Org. Chem.* **2010**, *6*, 8.
(36) Taton, D.; Le Borgne, A.; Sepulchre, M.; Spassky, N. *Macromol. Chem. Phys.* **1994**, *195*, 139.
(37) Pang, X.; Jing, R.; Huang, J. *Polymer* **2008**, *49*, 893.
(38) Wurm, F.; Nieberle, J.; Frey, H. *Macromolecules* **2008**, *41*, 1909.
(39) Mangold, C.; Wurm, F.; Obermeier, B.; Frey, H. *Macromol. Rapid Commun.* **2009**, *31*, 258.
(40) Obermeier, B.; Wurm, F.; Frey, H. *Macromolecules* **2010**, *43*, 2244.
(41) Mangold, C.; Wurm, F.; Obermeier, B.; Frey, H. *Macromolecules* **2010**, *43*, 8511-8518.
(42) Posner, T. *Chem. Ber.* **1905**, *38*, 646.
(43) Obermeier, B.; Frey, H. *Bioconjugate Chem.* **2011**, *22*, 436-444.
(44) Suijkerbuijk, B. M. J. M.; Slagt, M. Q.; Klein Gebbink, R. J. M.; Lutz, M.; Spek, A. L.; van Koten, G. *Tetrahedron Lett.* **2002**, *43*, 6565-6568.

Chapter 6

Monomeric and dendritic second generation Grubbs- and Hoveyda-Grubbs-type catalysts for compartmentalized olefin metathesis

Abstract

In this paper the synthesis and characterization of monomeric and dendritic Grubbs II and Hoveyda-Grubbs II-based catalysts are reported. These complexes have been synthesized via a route based on the connection of monomeric or dendritic *N*-alkyl-*N'*-mesitylimidazol-2-ylidene pre-ligands to Grubbs I or Hoveyda-Grubbs I complexes. The immobilization of a modified Grubbs II type catalyst on a carbosilane dendrimer has been successfully carried out. Together with monomeric second generation Grubbs and Hoveyda-Grubbs-analogues and several commercially available olefin metathesis catalysts, this soluble, homogeneous tetrameric catalyst was tested in the ring closing metathesis of diethyl diallylmalonate. The immobilized complex proved to be a good catalyst that outperforms its monomeric analogue in this reaction at room temperature, whereas it was found to be slightly slower at reflux temperature. Attempts to use the dendritic Grubbs catalyst in a compartmentalized manner did not succeed, which is proposed to be due to the moisture sensitivity of the dendritic catalyst.

6.1 Introduction

Olefin metathesis is nowadays widely used for the synthesis of complex cyclic and acyclic molecules with potential pharmaceutical, biomedical and food applications.[1-4] Further industrial applications for olefin metathesis lie in polymer chemistry,[5] for example, in the synthesis of polymers like polynorbornene or polydicyclopentadiene.[6] Four of the most successful olefin metathesis catalysts are the ruthenium-based first and second generation Grubbs and Hoveyda-Grubbs catalysts **A**-**D** (*figure 6.1*).[7-10]

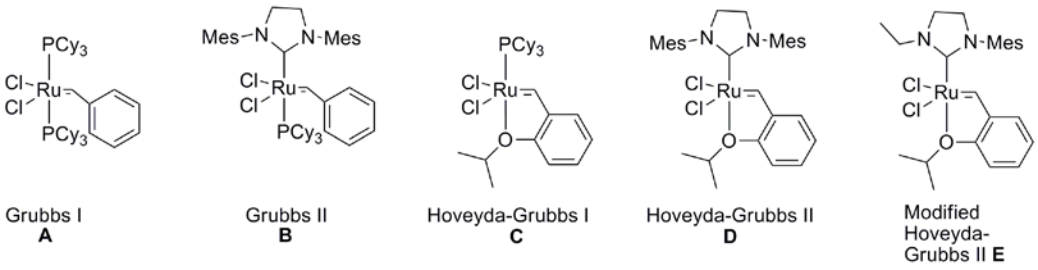

Figure 6.1: Various first and second generation Grubbs and Hoveyda-Grubbs catalysts.

Immobilization of these metathesis catalysts to polymeric supports in order to enable catalyst separation and catalyst reuse has been accomplished via a number of different approaches, as was nicely reviewed by Buchmeiser.[11] For the immobilization of the ruthenium-based catalysts **A**-**D** insoluble supports like polystyrene (PS),[12,13] and poly(vinylpyridine) (PVPy)[14] based resins, monolithic silica rods,[15-17] as well as inorganic supports like silica and alumina[18,19] are frequently used as supporting materials. In many of these examples the heterogenized metathesis catalysts have been reused successfully in ring closing metathesis (RCM), ring opening metathesis polymerization (ROMP), and other metathesis reactions.

Examples of the immobilization of metathesis catalysts on soluble supports have also been described.[10,20-24] In most cases the immobilization of a Hoveyda-Grubbs II catalyst was accomplished via the alkylidene ligand. Separation and reuse of these soluble, immobilized metathesis catalysts was accomplished by means of nanofiltration, fluorous extraction, or solvent-induced precipitation.

In an ongoing research program on immobilized homogeneous catalysis, we are interested in developing the concept of compartmentalized catalysis through the use of molecular weight enlarged homogeneous catalysts. These enlarged catalysts can be separated based on their size using nano-filtration reactors[25,26] or through a so-called tea bag approach.[27-29] In the latter approach the enlarged homogeneous catalyst is placed inside a semi-permeable compartment and is introduced into a reaction mixture. In this setup, catalysis can take place inside the membrane compartment while the formed product can diffuse out from the membrane compartment into the outer solution. After reaction completion, the compartment containing the immobilized catalyst can be easily removed from the reaction mixture and in principle be reused.

In ***Chapter 2*** of this thesis[30] we presented the first example of compartmentalized auto-tandem catalysis through the use of carbosilane dendrimer-immobilized pincer Pd complexes. These dendritic pincer Pd complexes were successfully reused in several consecutive runs in a stannylation/electrophilic addition sequence leading to homo-allylic alcohols.[30] We are currently interested in extending the scope of compartmentalized homogeneous catalysis towards olefin metathesis, being one of the most useful methods for carbon-carbon coupling. The combination of dendrimer-immobilized olefin metathesis catalysts with other molecular weight enlarged catalysts in multiple semi-permeable compartments is envisioned to lead to compartmentalized orthogonal tandem catalysis, in which several reaction steps are each catalyzed by different compartmentalized catalysts.[31]

The immobilization of Hoveyda-Grubbs type catalysts on carbosilane dendrimers was earlier reported by Hoveyda and co-workers.[10] In this case, immobilization of the ruthenium catalysts was accomplished via the alkylidene ligand leading to recyclable olefin metathesis catalysts. These complexes have also been used to reveal the “boomerang” (release/return) mechanism of this class of complexes.[32] It was postulated that the catalyst is first released from its (dendritic) support before it enters the catalytic cycle. When substrate conversion reaches completion, the complex returns to the support by coordination of the immobilized 2-isopropoxybenzylidene to the ruthenium center. Interestingly, Plenio and co-workers recently showed that catalyst return might not take place at all for the small fraction of catalysts that is actually involved in RCM.[33,34]

Regardless of the existence of the ‘return’ part in the boomerang mechanism, these dendritic catalysts would not have been suitable for our compartmentalized catalysis

purpose. After release from the dendritic support, the molecular catalytic species would be able to diffuse through the membrane along with the reaction substrate and product. The return of the permeated ruthenium center to its dendritic alkylidene ligand would then be very improbable, which would lead to ruthenium leaching and ultimately to a lower recyclability of the immobilized catalyst. Accordingly, this would violate the compartmentalized nature of the enlarged catalysts. For these reasons, we have opted to immobilize metathesis catalysts via the NHC ligand to dendritic supports.

Here, we present the synthesis of new dendritic NHC ligand immobilized second generation Grubbs- and Hoveyda-Grubbs-type catalysts **2** and **4**, and of their monomeric analogues **1** and **3** (*figure 6.2*). These homogeneous metathesis catalysts were investigated in the RCM of diethyl diallylmalonate and compared to well-known metathesis catalysts **A**, **B** and **D**. Finally, dendritic homogeneous catalyst **2** was used in compartmentalized metathesis catalysis.

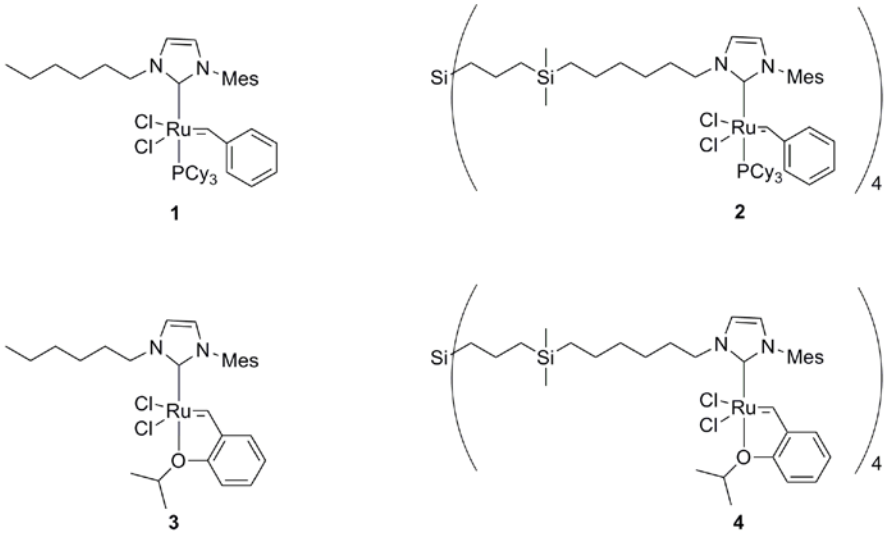

*Figure 6.2: Monomeric and dendritic second generation Grubbs and Hoveyda-Grubbs-type catalysts **1**-**4**.*

6.2 Synthesis

The series of modified monomeric and dendritic (Hoveyda-)Grubbs II-type catalysts **1**-**4** were synthesized via a synthetic route based on Blechert's method for the synthesis of 3-methyl-1-mesitylimidazol-2-ylidene and 3-ethyl-1-mesitylimidazol-2-ylidene derived catalysts (*figure*

6.3).[35] The NHC ligands used for **1**-**4** contain either a *n*-hexyl group or are connected to a dendritic carbosilane core via an *n*-hexyl linker.

The monomeric preligand **5** was synthesized in a one-step procedure starting from 1-mesitylimidazole (*figure 6.3*).[36] Upon treatment of 1-mesitylimidazole with 1-chlorohexane in refluxing toluene, 3-hexyl-1-mesitylimidazolium iodide **5** was formed in 64% isolated yield. Sodium iodide was added to the reaction mixture to generate 1-iodohexane in situ via a Finkelstein reaction in order to assist the nucleophilic substitution by the weak 1-mesitylimidazole nucleophile.[37] In the first step of the synthesis of mononuclear complexes **1** and **3**, preligand **5** was treated with potassium *tert*-butoxide to create the corresponding free NHC ligand in situ. Next, a solution of either Grubbs I catalyst **A** or Hoveyda-Grubbs I catalyst **C** was added to the toluene solution containing the NHC ligand to form complex **1** or **3**, respectively. Similar to related complexes,[38,39] the synthesis of complex **1** was found to take place at room temperature and the complex could be purified by means of column chromatography using neutral alumina under inert conditions in 80% yield. The resulting brown complex was found to be more air and moisture sensitive than commercially available Grubbs II catalyst **B** and was therefore stored under inert conditions.

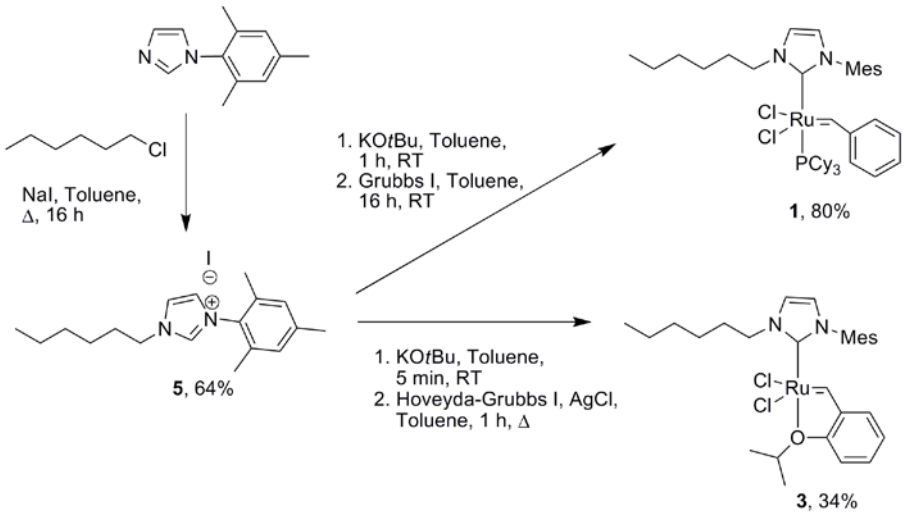

*Figure 6.3: Synthesis of modified monomeric Grubbs II and Hoveyda-Grubbs II complexes **1** and **3**.*

In the case of complex **2** the metalation step did not take place at room temperature and therefore harsher conditions (i.e. higher temperatures) were necessary. When using these elevated temperatures a side reaction occurred, which seriously decreased the overall yield

of the metalation. Under these reaction conditions, the 3-hexyl-1-mesityl NHC ligand showed a strong tendency to dimerize to form enetetramines (*figure 6.4*). The absence of a second mesitylene group on the NHC scaffold influences this Wanzlick equilibrium[40-42] in a negative way.[43] In this respect, the often used 1,3-dimesitylimidazol-3-ylidene ligands are known to be thermodynamically stable at room temperature and can be stored in solution.[44] Higher temperatures in synthetic protocols and/or the use of other ligands can lead to undesired dimerization though. In the use of NHC's as ligands in transition metal-carbene complexes, this side reaction has been reported frequently.[45,46]

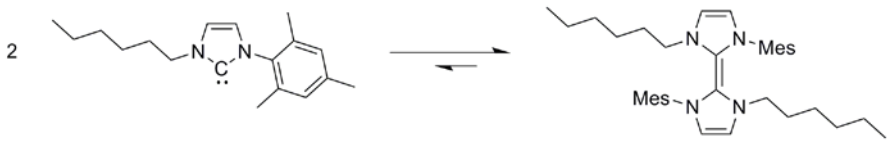

Figure 6.4: Wanzlick equilibrium between two carbenes and an enetetramine.

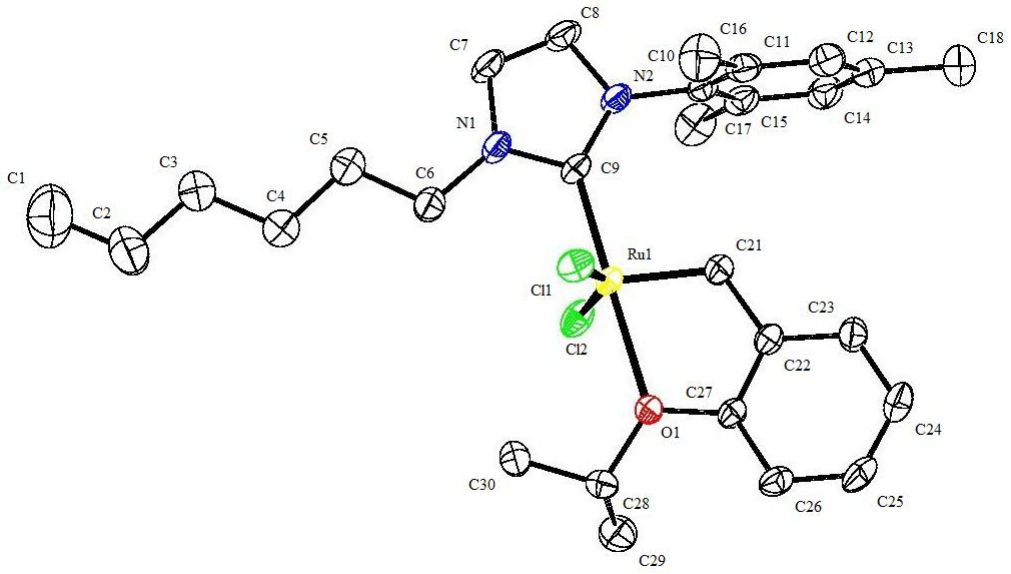

*Figure 6.5: ORTEP representation of the molecular structure of **3**. Displacement ellipsoids are drawn at the 50% probability level. Hydrogen atoms and disordered solvent molecules are omitted for clarity.*

*Table 6.1: Selected bond lengths (Å) and angles (°) for complex **3**, Hoveyda-Grubbs II complex **D**,[10] and Blechert's modified Hoveyda-Grubbs catalyst **E** that contains a 3-ethyl-1-mesitylimidazol-2-ylidene ligand.[35]*

	3	**D**	**E**
Ru(1) - C(9)	1.983(2)	1.981	1.966
Ru(1) - C(21)	1.834(2)	1.828	1.817
Ru(1) - O(1)	2.2764(16)	2.2612	2.269
N(1) - C(9)	1.369(3)	1.351	1.341
N(2) - C(9)	1.363(3)	1.350	1.344
Ru(1) - C(9) - N(1)	121.73(18)	120.8	118.4
Ru(1) - C(9) - N(2)	134.49(18)	131.6	134.4
C(9) - Ru(1) - C(21)	100.27(10)	101.5	102.46
O(1) - Ru(1) - C(9)	179.36(8)	176.2	177.46
Cl(1) - Ru(1) - Cl(2)	151.62(3)	156.5	151.11

Complex **3** was purified by column chromatography and was isolated in 34% yield. Crystals of **3** suitable for X-ray diffraction were obtained by hexane diffusion into a CH_2Cl_2 solution of the complex. The molecular geometry of the ruthenium center in **3** is close to square pyramidal (*figure 6.5*), as previously observed for the 'parent' Hoveyda-Grubbs II complex **D**[10] and Blechert's modified Hoveyda-Grubbs catalyst **E** (*figure 6.1*) that contains a related 3-ethyl-1-mesitylimidazol-2-ylidene ligand.[35] The C(9)-Ru(1)-O(1) bond angle of **3** (179 °) is slightly larger than the corresponding angle in complexes **D** (176 °) and **E** (177 °). Another interesting observation is that the Ru(1)-C(9)-N(1) bond angle for **3** (122 °) is closer to the same angle in **D** (121 °) than in **E** (118 °). Related to this observation, the Ru(1)-C(9)-N(2) bond angle in **3** (134 °) is closer to the angle in **E** (134 °) than in **D** (132 °). Other bond lengths and angles are very similar for the three complexes and a selection of bond lengths and angles is shown in *table 6.1*. The orientation of the methyl groups of the isopropoxy-moiety in **3** was found to be in accordance with the orientation in **D** and **E**. The hexyl chain of complex **3** is fully stretched in the solid state, i.e. the distance C(1)-C(6) is 6.31 Å, which corresponds to the most common distance of 6.3 Å for hexyl groups.[47]

Dendritic ligands **6** and **7** were obtained via a synthetic route starting from chlorodimethylsilyl-terminated carbosilane dendrimers **8** (G_0) and **9** (G_1)[48] and 6-chlorohex-1-yne (*figure 6.6*). In the first two steps of this route, an elongated chloroalkyl-terminated carbosilane dendrimer was synthesized. In the first step, 6-chlorohex-1-yne was deprotonated with LDA in THF at -78 °C. The chlorodimethylsilyl-terminated carbosilane dendrimers **8** or **9** were then added to these cold solutions to afford oligosilylalkynyl compounds **10** and **11**, respectively. Because of their instability towards oxygen and moisture, these silylalkynyl dendrimers were reduced immediately using Pd/C-mediated hydrogenation to afford the stable silylalkyl dendrimers **12** (G_0) and **13** (G_1). Treatment of these dendrimers with 1-mesitylimidazole in the presence of sodium iodide furnished the dendritic preligands **6** and **7**. These tetra- and dodecacationic dendritic compounds were characterized via ^{1}H, ^{13}C NMR and ESI-HRMS analysis.

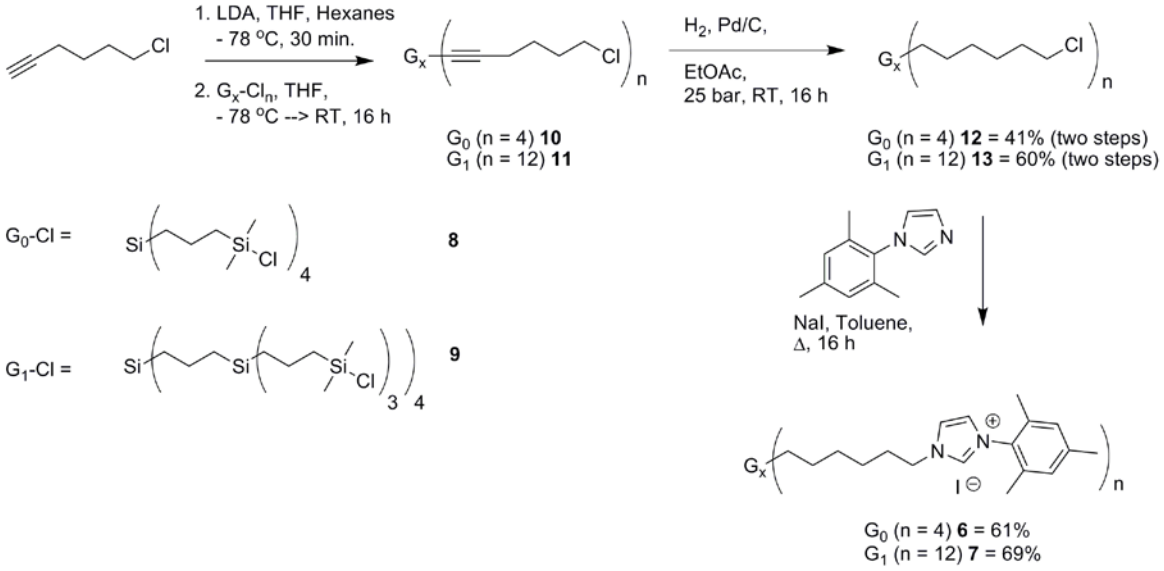

Figure 6.6: Synthesis of G_0 and G_1 dendritic mesitylimidazolium ligands.

The dendritic oligo-imidazolium ligands **6** and **7** exhibited a very poor solubility in toluene, benzene, and hexanes, which are the typical solvents used for the deprotonation of imidazolium ligands and the in situ metalation with first generation (Hoveyda)-Grubbs complexes to afford second generation (Hoveyda)-Grubbs complexes (*figure 6.7*). Clear solutions of the G_0 preligand could be obtained by placing a toluene solution of **6** into an ultrasonic bath for a period of 1 h. The metalation of **6** via deprotonation with potassium

tert-butoxide and treatment with Grubbs I complex **A** at room temperature successfully gave tetranuclear complex **2**. This novel dendritic modified Grubbs II type complex was characterized by means of ^{1}H, ^{13}C, and ^{31}P NMR. Monitoring of the benzylidene proton during the metalation reaction by means of ^{1}H NMR showed that Grubbs complex **A** fully converted into the dendritic complex **2**. The benzylidene proton signal displayed a clear shift from 20.02 to 19.80 ppm. ^{31}P NMR analysis showed a single phosphorus resonance at 34.6 ppm for **2**, while for Grubbs complex **A** this signal is found at 36.6 ppm. Furthermore, compound **2** was successfully analyzed by MALDI-TOF MS. A parent peak at *m/z* = 3703.0 was observed (calculated value for $[M+Na]^{+}$ is *m/z* = 3703.8). No signals corresponding to species of lower ruthenium content or to the free ligand were observed.

The formation of dendritic G_0 modified Hoveyda-Grubbs II complex **4** proved troublesome for several other reasons besides solubility. Because of the dendritic nature of the preligand, the peripheral groups are in close proximity. Therefore, enetetramine formation using dendritic NHC ligands is an even bigger issue than in the case of a monomeric NHC ligand (*vide supra*), which can be considered as a negative dendritic effect. Upon treatment of dendritic preligand **6** with potassium *tert*-butoxide and subsequent addition of a toluene solution of Hoveyda-Grubbs I complex **C**, a mixture of products was observed after 16 h at reflux temperature. According to integral analysis in ^{1}H NMR only approximately 25% of the dendritic arms was successfully loaded with a ruthenium center in this procedure. This corresponds to an average of one single ruthenium center introduced per four dendritic arms. Probably the other 75% of the dendritic carbene moieties underwent dimerization to enetetramines. A signal attributed to the imidazolium protons of the enetetramine was indeed observed as a pseudo-singlet at 5.51 ppm, which is close to the reported values for similar enetetramine compounds.[49,50] The ruthenium loading was not improved by a longer reaction time or by dilution of the dendritic ligand. Performing the reaction at lower temperatures rather than at reflux temperatures also did not lead to higher conversions. In addition, the use of KHMDS as base did not lead to improved ruthenations. Due to the low ruthenium loading of the dendritic Hoveyda-Grubbs materials obtained from this procedure and their likely dispersity, these were not included in the catalytic testings.

The ruthenation of G_1 dendritic ligand **7** was attempted in a similar manner as for dendritic ligand **6**. As mentioned earlier, the solubility of **7** in toluene, benzene, and hexanes was found to be poor. For the G_0 ligands an ultrasonic treatment led to a clear solution after 1 h,

but unfortunately this method did not lead to any solubility of G_1 ligand **7**. Addition of potassium *tert*-butoxide in an attempt to induce solubility upon deprotonation also did not lead to a clear solution. Therefore, disappointingly, our attempts to synthesize dendritic G_1 complexes were unsuccessful.

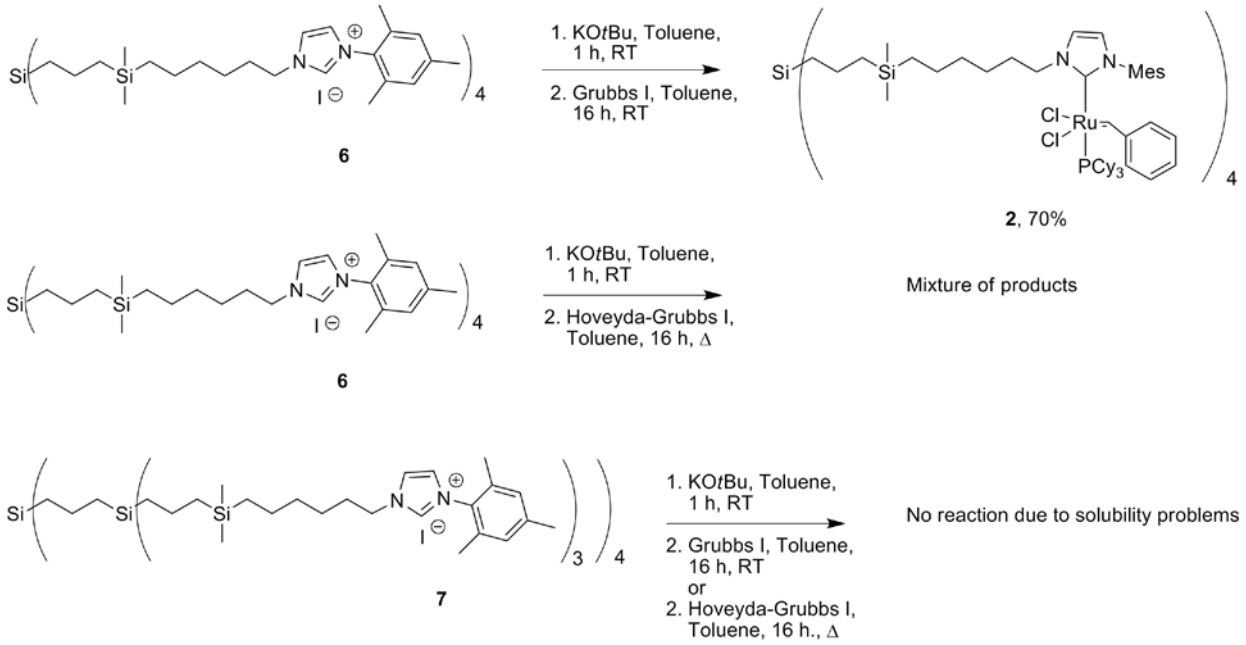

Figure 6.7: Synthesis of dendritic G_0 modified Grubbs II catalysts and attempted synthesis of dendritic G_0 modified Hoveyda-Grubbs II catalysts and dendritic G_1 modified (Hoveyda-)Grubbs catalysts.

6.3 Catalysis

The mononuclear complexes **1** and **3** and tetranuclear dendritic complex **2** were tested as catalysts in the ring closing metathesis (RCM) reaction of diethyl diallylmalonate to form diethyl cyclopent-3-ene-1,1-dicarboxylate (*figure 6.8*). The activity of these complexes in the reaction was compared experimentally to the activity of commercially available Grubbs catalysts **A** and **B** and Hoveyda-Grubbs catalysts **D** in this reaction. The reactions were performed in dichloromethane at room temperature and at reflux temperature using 5 mol% ruthenium (i.e. 5 mol% catalyst for all monomeric compounds and 1.25 mol% catalyst for dendritic compound **2**).

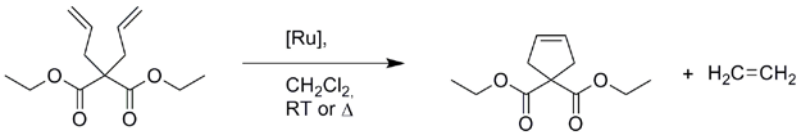

Figure 6.8: RCM of diethyl diallylmalonate to diethyl cyclopent-3-ene-1,1-dicarboxylate.

Comparison of the various Grubbs-type catalysts showed that all catalysts gave complete substrate conversion at room temperature and at reflux temperature, except for catalyst **3** at room temperature (*table 6.2*; *figure 6.9a+b*). At room temperature the commercially available Grubbs and Hoveyda-Grubbs catalysts gave very fast initial conversions, as was reported earlier.[8,51] In our setup, Grubbs I (**A**) showed 90% conversion only after 24 min., while Grubbs II (**B**) and Hoveyda-Grubbs II (**D**) showed 90% conversion after 91 and 146 min., respectively. Complexes **1** and **2** gave full conversions, but in somewhat lower reaction rates. Dendritic catalyst **2** showed a faster conversion than its monomeric analogue **1** (294 min. and 401 min. for 90% conversion respectively), and especially the difference in initial rate was found to be striking (35% and 17% conversion after 15 min. respectively). In fact, the initial rate of dendritic catalyst **2** is closer to the initial rate of catalysts **B** and **D** than to those of **1** and **3**. Hoveyda-Grubbs-based catalyst **3** was found to be the least active catalyst among those tested. In fact, this was the only catalyst that did not show a complete reaction after 24 h. At this time, a conversion of 87% was reached.

At reflux temperatures, the reaction rates for all tested catalysts increase substantially (*figure 6.9c+d*). For the three commercially available catalysts and catalysts **1** and **2** very high conversions (74-95%) were observed after only 15 min. All tested commercial catalysts showed 90% conversion in only 17-25 min. Compound **1** was able to compete with these catalysts by showing 90% conversion after 35 min. At these slightly elevated temperatures, its dendritic analogue **2** was found to be slower than **1**, whereas it was faster at ambient temperatures. Also the initial rate of dendritic catalyst **2** was somewhat lower than its monomeric analogue, although still 74% conversion was achieved within 15 min. The time for **2** to reach 50% of substrate conversion was 10 min, whereas it took slightly more than 1 h to reach 90% conversion. Again, catalyst **3** was found to be much slower than all other tested catalysts: after 15 min 38% of diethyl diallylmalonate conversion was observed, while it took more than 3 h before 90% of ring-closure was achieved.

Table 6.2: Comparison of the initial rate (conversion in % after 15 min) and the 50% and 90% substrate conversion times in the ruthenium-catalyzed RCM reaction of diethyl diallylmalonate.[a]

Catalyst	Conversion after 15 min. (%)		50% conversion (min.)		90% conversion (min.)	
	RT	Reflux	RT	reflux	RT	Reflux
Grubbs I **A**	82	88	10	8	24	21
Grubbs II **B**	40	95	24	8	91	17
Hoveyda-Grubbs II **D**	46	85	20	9	146	25
1	17	80	122	10	401	35
2	35	74	75	10	294	64
3	16	38	90	26	n.d.[b]	193

[a] Reaction conditions: 0.16 mmol diethyl diallylmalonate in 6 mL CH_2Cl_2 using 5 mol% Ru. [b] After 24 h 87% conversion was found.

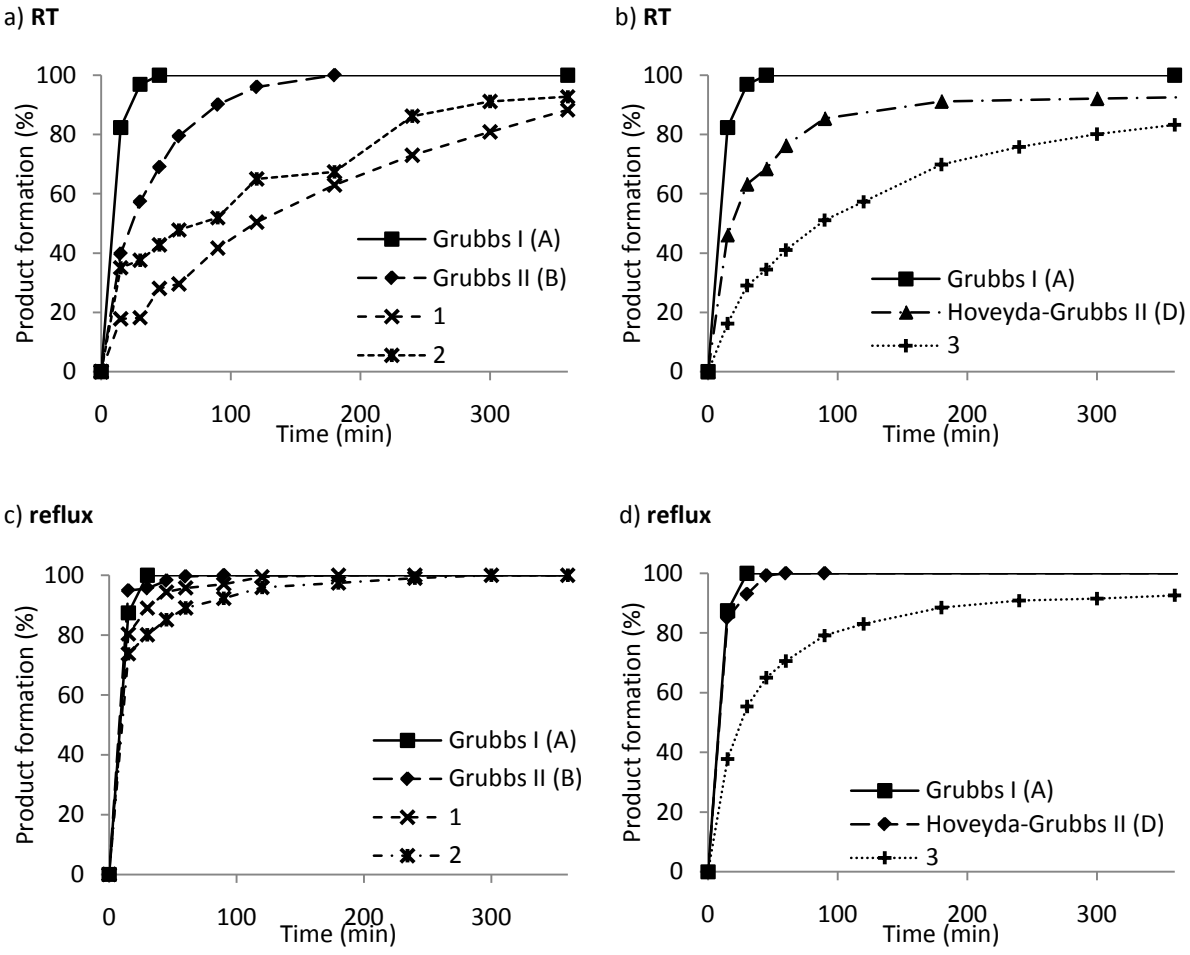

*Figure 6.9: Kinetic profiles of the RCM reaction of diethyl diallylmalonate: a) Grubbs I catalyst **A** and Grubbs II-type catalysts **B**, **1** and **2** at ambient temperature; b) Grubbs I catalyst **A** and Hoveyda-Grubbs II-type catalysts **D** and **3** at ambient temperature; c) **A**, **B**, **1** and **2** at 40 °C; d) **A**, **D** and **3** at 40 °C (for reaction conditions: see table 6.2).*

6.4 Recycling experiments

Next, dendritic catalyst **2** was used in the RCM of diethyl diallylmalonate in a compartmentalized reaction setup. In this experiment, a CH_2Cl_2 solution (5 mL) of the dendritic catalyst was placed in a closed dialysis bag. This dialysis bag was placed into a vessel containing a CH_2Cl_2 solution (90 mL) of diethyl diallylmalonate. The dialysis membrane had a mass weight cut off (MWCO) of 1000 Da, thereby allowing the substrates to permeate through the membrane, but keeping dendritic compound **2** (3703 Da) inside the dialysis bag. Agitation of the reaction mixture was brought about by means of a magnetic stirring bar at the bottom of the vessel.

Unfortunately, in this compartmentalized setup hardly any substrate conversion was observed. After 6 h, only 2% of the starting material had been reacted, whereas after a full week only 16% of the diallylmalonate was converted into the cyclopent-3-ene product. The most probable reason for this inactivity is that the presence of minute amounts of water at the surface of the dialysis bag could not be totally excluded in this reaction setup. The dialysis bags were purchased in an aqueous solution to prevent the membrane to dry. For our RCM purposes, the presence of water should be carefully avoided, as it is known that this might lead to catalyst deterioration.[52,53] Therefore these bags were pretreated by washing them consecutively in dry, degassed solutions of methanol and CH_2Cl_2 for 1 h each before use in the RCM experiment. Apparently, these pretreatments could not fully preclude the presence of small amounts of water.

Next, recycling of the dendritic catalyst was tested in a non-compartmentalized manner, i.e. by means of catalyst precipitation after reaction completion. Using dendritic catalyst **2** under catalytic conditions at room temperature, full conversion was observed after 12 h. At that time, the reaction solution was concentrated to approximately 10% of its original volume (9 mL) and hexanes (90 mL) were added. The formed precipitate was filtered under nitrogen from the colorless solution and redissolved in CH_2Cl_2 (90 mL). Then, a new batch of diethyl diallylmalonate was added and the reaction was followed in time. Disappointingly, in this second run no product formation was observed at all. Apparently, either at the end of the first run or during workup catalyst deterioration had taken place.

6.5 Discussion

6.5.1 Synthetic considerations

The immobilization of a (Hoveyda)-Grubbs catalyst to a dendritic support can in principle take place at either of the multiple ligands that coordinate to the ruthenium center of modified first and second generation (Hoveyda)-Grubbs catalysts. These ligands include: 1) the phosphine ligand (for catalysts **A**, **B** and **C**), 2) the halogen ligands (for catalysts **A**-**D**), 3) the alkylidene ligand (for catalysts **A**-**D**), and 4) the *N*-heterocyclic carbene (NHC) ligand (for catalysts **B** and **D**). Synthetic difficulties, loss in catalytic activity and halogen scrambling are three reasons why the first two sites of immobilization have only occasionally been reported.[12,54,55] Immobilization via the alkylidene ligand to (mainly) Hoveyda-Grubbs II catalyst **D** has been reported more often,[10,20,21,24,32,56-61] but is not applicable for our purpose (*vide supra*). Therefore, immobilization of the Ru centers via the NHC ligands to the dendritic support was the method of choice in our study.

We have opted for a facile immobilization manner via the NHC ligands, i.e. by the use of *N*-alkyl-*N'*-mesitylimidazol-2-ylidene ligands through the replacement of one of the mesitylene groups by an alkyl group. This method has been investigated before by other research groups,[17,35,62-65] and has the advantage of a straightforward synthetic route towards the NHC-Ru compounds from commercially available starting materials. Limitations in this method are the consequences on catalyst stability and activity that result from the presence of a single mesitylene moiety on the NHC ligand of the resulting Ru-compounds, which e.g. enhances the chance for (inter- or intramolecular) ligand dimerization during carbene ruthenation. In particular in the case of dendritic NHC ligands, enetetramine byproduct formation was observed, and as a result significantly hampered, i.e. low yielding, metalation reactions that lead to mixtures of products were yielded. Especially because of the use of high temperatures that were required for the ruthenation step of the NHC ligand with Hoveyda-Grubbs catalyst **C**, byproduct formation was found to be troublesome. When Grubbs catalyst **A** was used for this metalation, no signs of enetetramine formation were observed, probably because this synthetic step was successfully performed at ambient temperatures. Dendritic ligands showed higher amounts of enetetramine formation (a negative dendritic effect), since for these ligands the carbene ligands are in close proximity

by definition. The more frequently used 1,3-dimesitylimidazol-2-ylidene ligands are known to be thermodynamically stable, and therefore rather inert toward this dimerization.[44]

Among others, the groups of Blechert,[13] Buchmeiser,[15,66] Hoveyda,[57] Grubbs[22,23,67] and Weck[68] have also reported on NHC-immobilized ruthenium-based metathesis catalysts. In these cases, a hydroxymethyl-functionalized 1,3-dimesitylimidazol-2-ylidene ligand was used to accomplish a covalent linkage to the support. Initially, we also made attempts to synthesize dendritic Hoveyda-Grubbs type catalysts using this hydroxyl-modified NHC ligand, through the formation of a siloxane bond with the carbosilane dendrimer. However, the formed siloxane bonds turned out to be very susceptible towards hydrolysis and partially deteriorated during aqueous workup. Modifications in the synthesis and purification routes did not lead to NHC-modified dendrimers of sufficient purity.

Immobilization of NHC ligands via one of the two mesitylene groups was reported by Grubbs[67] and by Gilbertson.[69] The Hoveyda-Grubbs II catalyst was successfully immobilized onto silica gel and peptide chains respectively in this way. The rather elaborate synthetic route towards mesitylene-functionalized imidazolium preligands may be considered as a drawback in this approach, but in retrospection the increased thermodynamic stability and catalytic advantages of these 1,3-dimethylimidazol-2-ylidene based systems might have outweighed the synthetic disadvantages.

6.5.2 Catalytic considerations

Comparison of the novel Grubbs and Hoveyda-Grubbs-type catalysts **1**-**3** in the RCM of diethyl diallylmalonate has led to a number of interesting observations. When dendritic catalyst **2** is compared to its monomeric analogue **1**, the dendritic catalyst appears to be slightly more active at room temperature (93% versus 89% conversion after 6 h). This effect is even more clear upon comparison of the initial rates of **2** and **1** (35% versus 17% conversion after 15 minutes). An explanation for this observation could be that the dendritic scaffold in **2** causes a certain degree of steric crowding, which might compensate for the decreased steric bulk around the NHC-Ru moiety due to the lack of one mesitylene group; accordingly, a higher initial catalytic rate was observed for **2** compared to **1**. At reflux temperature monomeric catalyst **1** slightly outperforms dendritic catalyst **2**, possibly due to

the faster deactivation of the dendritic catalyst, which cancels out advantageous steric effects. For the modified Hoveyda-Grubbs catalyst **3** a lower activity was observed as compared to catalyst **1** (*figure 6.10c*). Still, this novel catalyst showed reasonable to good catalytic activity towards diethyl diallylmalonate with 80% conversion after 5 h at ambient temperatures and a complete conversion after 5 h at 40 °C.

Besides these observations, a lower overall reactivity in the RCM of diethyl diallylmalonate was observed for the novel complexes **1**-**3** compared to commercially available Grubbs catalysts **A**, **B** and **D**. The replacement of one of the mesitylene moieties by an alkyl group and the use of a saturated imidazolium-based NHC ligand instead of an unsaturated imidazolinium-based ligand, like in Grubbs II catalysts, makes the ruthenium center less sterically crowded and more electron rich,[70-72] resulting in a somewhat lower activity. Similar effects have recently also been reported by other research groups. Verpoort and co-workers reported on a comparison of catalyst **B** to, among others, a modified Grubbs II complex bearing a 3-octyl-1-mesityl-NHC ligand in the ROMP of 1,5-cyclooctadiene.[63] Also Blechert *et al.* observed somewhat lower reaction yields of modified Grubbs II or Hoveyda-Grubbs II complexes that contain 3-methyl-1-mesityl-NHC or 3-ethyl-1-mesityl-NHC ligands in the cross metathesis of different olefin substrates compared to catalysts **B** and **D**.[35] These complexes, however, sometimes show entirely different product selectivities than the more active complexes **B** and **D**. Finally, Fürstner showed that the RCM of diethyl diallylmalonate was significantly slower than when performed with catalyst **B**, but could be successfully performed in three successive runs by using second generation ruthenium benzylidene metathesis catalysts bearing hydroxyalkyl chains on their NHC ligands.[17]

6.6 Conclusions

Summarizing, we have presented the synthesis and application of new monomeric and dendritic (Hoveyda-)Grubbs-type ruthenium catalysts that contain a 3-alkyl-1-mesityl-NHC ligand. In the RCM reaction of diethyl diallylmalonate these catalysts showed good conversions, but the catalytic rate was found to be considerably lower than for commercially available olefin metathesis catalysts. The dendritic catalyst **2** showed a higher activity compared to its monomeric analogue at room temperature and a somewhat lower activity

at reflux temperatures. Complex **2** was found to be too moisture-sensitive to be successfully applied in compartmentalized catalysis. By changing to the more stable Hoveyda-Grubbs-type catalysts and by using a different type of NHC ligand, e.g. a 1,3-dimesitylimidazol-2-ylidene ligand for these complexes, a catalytic system would be created that is more active and would be less affected by the presence of minute amounts of water in the reaction mixture. The immobilization of the catalyst to the dendritic support could then either take place via the imidazolium ring or via one of the two mesitylene groups of the NHC ligand. With such improved dendritic Hoveyda-Grubbs catalysts the way would be paved for the first example of successful compartmentalized olefin metathesis. This will be the subject of further investigations.

6.7 Experimental section

General

All reactions were carried out using standard Schlenk techniques under an inert dinitrogen atmosphere unless stated otherwise. All solvents were carefully dried and distilled prior to use. All standard reagents were purchased commercially and used without further purification. 1-Mesitylimidazole was synthesized according to a procedure described by Liu et al.[36] Carbosilane dendrimers **8** and **9** were synthesized according to Van der Made's procedure.[48] All other reagents were purchased from Acros Organics and Sigma-Aldrich Chemical Co. Inc. and used as received. ^{1}H (400 MHz), ^{13}C (100 MHz), and ^{31}P (121 MHz) NMR spectra were recorded on a Varian 400 MHz spectrometer at 25 ^{o}C, chemical shifts are given in ppm referenced to residual solvent resonances. High resolution mass spectroscopy (HRMS) has been performed on a Waters LCT Premier XE Micromass instrument using the electrospray ionization (ESI) technique. MALDI-TOF MS spectra were acquired using a Voyager-DE Bio-Spectrometry Workstation mass spectrometer equipped with a nitrogen laser emitting at 337 nm. GC analysis was carried out using a Perkin Elmer Clarus 500 GC equipped with an Alltech Econo-Cap EC-5 column.

3-Hexyl-1-mesitylimidazolium iodide ***5***

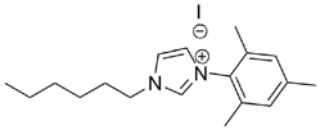

1-Mesitylimidazole (50 mg, 0.270 mmol), 1-chlorohexane (37 µL, 0.270 mmol) and sodium iodide (0.081 g, 0.540 mmol) were dissolved in toluene (2 mL) and the mixture was stirred at 110 ^{o}C for 16 h. A syrup precipitated and was separated from the liquid phase by decantation. The syrup was washed with hexanes (3 x 5 mL), redissolved in CH_2Cl_2 (5 mL) and filtered through a glass filter. The solvent was evaporated in vacuo to afford a white solid in 64% yield (64 mg).

^{1}H NMR ($CDCl_3$): δ 10.23 (s, 1H, NC*H*N), 7.63 (s, 1H, C$H_{imid.}$), 7.19 (s, 1H, C$H_{imid.}$), 7.02 (s, 2H, C$H_{mesitylene}$), 4.68 (t, 2H, CH_2N, ^{3}J = 7.2 Hz), 2.35 (s, 3H, *p*-CH_3), 2.09 (s, 6H, *o*-CH_3), 2.05-1.98 (m, 2H, NCH_2CH_2), 1.43-1.28 (m, 6H, CH_2), 0.88 (t, 3H, CH_3, ^{3}J = 6.8 Hz); ^{13}C NMR ($CDCl_3$): δ 141.6, 138.1, 134.4, 130.8, 130.1, 123.6, 123.2, 50.9, 31.3, 30.7, 26.0, 22.6, 21.4, 18.0, 14.1; IR (cm^{-1}): 3057 (m), 2955 (s), 2928 (s), 2858 (m), 1608 (w), 1561 (s), 1544 (s), 1201 (s). ESI-HRMS (*m/z*): calcd. for $C_{18}H_{27}N_2$ $[M\text{-}I]^+$ 271.2174, found 271.2168.

(3-hexyl-1-mesitylimidazolium)Cl_2Ru(=CHC_6H_5)(PCy_3) ***1***

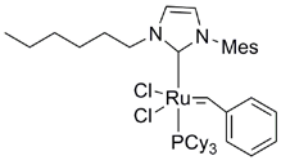

3-Hexyl-1-mesitylimidazolium iodide **5** (100 mg, 0.25 mmol) was dissolved 10 mL toluene (10 mL). Potassium *tert*-butoxide (189 µl of a 20 wt% solution in dry THF, 0.30 mmol, 1.2 equiv.) was added and the reaction mixture was stirred for one hour at room temperature. Via a cannula a solution of Grubbs I catalyst **A** (234.4 mg, 0.30 mmol, 1.2 equiv.) in toluene (70 mL) was added, whereupon the reaction mixture was stirred for 16 h. at room temperature. Next, the mixture was filtered and the filtrate was concentrated in vacuo at room temperature. Purification was performed by column chromatography with neutral alumina under nitrogen pressure using hexanes/diethyl ether (9/1) as eluents. This yielded a brown solid in 80% yield (163 mg).

^{1}H NMR (C_6D_6): δ 19.77 (s, 1H, Ru=C*H*Ar), 8.17 (m, 2H, Ru=CHArH_{ortho}), 7.12 (s, 1H, C$H_{imid.}$), 6.94 (m, 3H, Ru=CHAr$H_{meta+para}$), 6.55 (s, 1H, C$H_{imid.}$), 6.15 (m, 2H, C$H_{arom,\ mesityl}$), 4.64 (t, 2H, ^{3}J

= 7.6 Hz, NC*H*$_2$,), 2.55 (m, 2H, NCH$_2$C*H*$_2$), 2.12 (s, 3H, Ar-*para*-C*H*$_3$), 2.07-1.04 (m, 45H, aliphatic C*H* and C*H*$_2$), 0.86 (t, 3H, ^3J = 6.8 Hz, CH$_2$C*H*$_3$). ^{13}C NMR (C_6D_6): δ 292.4, 188.8, 148.4, 138.2, 136.5, 130.2, 129.7, 129.2, 128.4, 125.5, 122.8, 121.6, 50.9, 36.0, 31.9, 30.6, 30.0, 28.1, 27.1, 26.9, 22.8, 20.9, 18.5, 14.1. ^{31}P NMR (C_6D_6): δ 34.7. ESI-HRMS (m/z): calcd. for $C_{43}H_{65}Cl_2N_2PRu$ $[M-H]^+$ 811.3234, found 811.3194.

(3-hexyl-1-mesitylimidazolium)Cl$_2$Ru(=CHC$_6$H$_4$-ortho-OiPr) ***3***

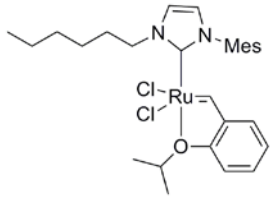

3-Hexyl-1-mesitylimidazolium iodide **5** (69 mg, 0.170 mmol) and KO*t*Bu (23 mg, 0.170 mmol) were suspended in toluene (5 mL) and the mixture was stirred for 5 min. In a different flask, Hoveyda-Grubbs I catalyst **C** (69 mg, 0.114 mmol) was dissolved in toluene (5 mL) and added to the first mixture. Finally, silver(I) chloride (49 g, 0.340 mmol) was added and the mixture was stirred at reflux temperature for 1 h. The suspension turned from brown to brown-green. Then, the mixture was filtered through a glass filter and the filtrate was concentrated to dryness in vacuo. The resulting brown solid was purified by column chromatography over silica (eluent gradient used: CH_2Cl_2/hexanes (9:1, *v*/*v*) to pure CH_2Cl_2). Crystals for X-ray diffraction were obtained by diffusion of hexanes into a CH_2Cl_2 solution of the pure solid. Green-brown crystals appeared in 34% yield (34 mg).

^{1}H NMR ($CDCl_3$): δ 16.44 (s, 1H, Ru=C*H*Ar), 7.50 (m, 1H, C*H*$_{arom., styrene}$), 7.24 (m, 1H, C*H*$_{imid.}$), 7.10 (s, 2H, C*H*$_{arom., mesityl}$), 7.00-6.90 (m, 3H, C*H*$_{arom., styrene}$), 6.89 (s, 1H, C*H*$_{imid.}$), 5.19 (septet, 1H, ^3J = 5.0 Hz, OC*H*), 4.90 (t, 2H, ^3J = 7.6 Hz, NC*H*$_2$), 2.50 (s, 3H, Ar-*para*-C*H*$_3$), 2.23-2.18 (m, 2H, NCH$_2$C*H*$_2$), 2.02 (s, 6H, Ar-*ortho*-C*H*$_3$), 1.81 (d, 6H, ^3J = 5.0 Hz, CHC*H*$_3$), 1.60 (m, 2H, NCH$_2$CH$_2$C*H*$_2$), 1.50-1.35 (m, 4H, aliphatic CH$_2$), 0.95 (t, 3H, ^3J = 7.6 Hz, CH$_2$C*H*$_3$); ^{13}C NMR ($CDCl_3$): δ 288.8, 172.4, 152.8, 144.6, 139.8, 137.6, 129.3, 129.2, 124.6, 122.8, 122.4, 121.4, 113.1, 75.3, 52.4, 31.6, 31.0, 29.9, 27.0, 22.9, 22.2, 21.5, 18.3, 14.3. ESI-HRMS (*m/z*): calcd. for $C_{28}H_{38}Cl_2N_2ORu$ $[M]^+$ 590.1407, found 590.1403.

Tetrakis-(3-((6-chlorohex-1-ynyl)dimethylsilyl)propyl)silane ***10***

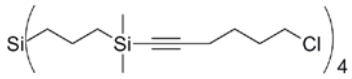

6-Chloro-1-hexyne (0.47 mL, 3.85 mmol) was dissolved in THF (20 mL) and cooled to -78 °C. Upon the dropwise addition of a 2M solution of LDA in THF / hexanes (1.97 mL, 3.94 mmol, 1.03 equiv.) the solution turned dark yellow. After 30 min. at -78 °C, a solution of $Si(CH_2CH_2CH_2SIMe_2Cl)_4$ (**8**, 0.50 g, 0.87 mmol) in THF (5 mL) was added dropwise. The mixture was allowed to reach room temperature and was stirred for a further 16 h. After this period all volatiles were removed in vacuo. The residue was dissolved in CH_2Cl_2 (50 mL) and washed with an aqueous saturated NH_4Cl solution (3 x 50 mL). The organic phase was dried over anhydrous $MgSO_4$, filtered and concentrated to afford an orange syrup. This moisture-sensitive product has been used without further purification in the next synthesis step.

^{1}H NMR ($CDCl_3$): δ 3.57 (t, 8H, ^3J = 6.8 Hz, CH_2Cl), 2.27 (t, 8H, ^3J = 6.8 Hz, C≡C-CH_2), 1.90 (m, 8H, CH_2CH$_2$Cl), 1.68 (m, 8H, C≡C-CH$_2$CH_2), 1.39 (m, 8H, SiCH$_2$CH_2), 0.69-0.57 (m, 16H, SiCH_2), -0.11 (s, 24H, SiCH_3); ^{13}C NMR ($CDCl_3$): δ 107.0, 84.7, 44.7, 31.7, 26.0, 21.4, 19.4, 18.7, 17.2, -1.2.

Tetrakis-(3-((6-chlorohexyl)dimethylsilyl)propyl)silane ***12***

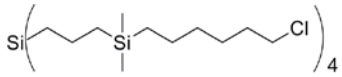

Tetrakis-(3-((6-chlorohex-1-ynyl)dimethylsilyl)propyl)silane **10** (1.20 g, 1.35 mmol) and Pd on charcoal (10 wt% Pd, 28 mg, 0.270 mmol, 20 mol%) were suspended 20 mL of absolute EtOH (20 mL) and placed in a 50 mL autoclave (Parr-4590 micro-reactor). After evacuation and purging the autoclave with hydrogen, the mixture was stirred at room temperature under a pressure of 25 bar of H_2 for 5 h. Then, the solution was filtered over Celite and the solvent was removed in vacuo. The resulting orange syrup was purified by flash chromatography over silica gel using CH_2Cl_2 as eluent. A colorless syrup was obtained in 41% yield (0.50 g) over two steps.

^{1}H NMR ($CDCl_3$): δ 3.53 (t, 8H, ^3J = 6.8 Hz, CH_2Cl), 1.75 (m, 8H, CH_2CH$_2$Cl), 1.42 (m, 8H, CH_2CH$_2$CH$_2$Cl), 1.37-1.22 (m, 24H), 0.59-0.50 (m, 16H, SiCH_2), 0.46 (m, 8H, SiCH_2), -0.05 (s, 24H, SiCH_3); ^{13}C NMR ($CDCl_3$): δ 45.4, 33.1, 32.8, 26.8, 24.0, 20.5, 18.8, 17.8, 15.6, -3.0.

Tetrakis-(3-((6-(3-mesitylimidazolium)hexyl)dimethylsilyl)propyl)silane iodide ***6***

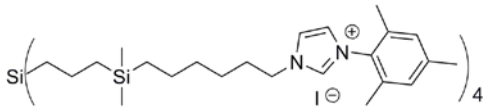

Tetrakis-(3-((6-chlorohexyl)dimethylsilyl)propyl)silane **12** ***(***0.50 g, 0.55 mmol) and 1-mesitylimidazole (0.45 g, 2.42 mmol, 4.4 equiv.) were dissolved in toluene (6 mL). Sodium iodide (0.66 g, 4.40 mmol, 8 equiv.) was added and the suspension was stirred at 110 ^{o}C for 18 h. During this period, a biphasic mixture was obtained. The upper solution was removed and the remaining syrup was washed several times with hexanes. The syrup was dissolved in CH_2Cl_2 whereupon a white solid precipitated. These inorganic salts were removed by filtration and the filtrate was concentrated in vacuo yielding a pale yellow solid in 61% yield (0.68 g).

^{1}H NMR ($CDCl_3$): δ 10.10 (s, 4H, NC*H*N), 7.99 (s, 4H, C$H_{imid.}$), 7.25 (s, 4H, C$H_{imid.}$), 6.98 (s, 8H, CH_{arom}), 4.66 (t, 8H, ^{3}J = 6.8 Hz, NCH_2), 2.33 (s, 12H, Ar-*para*-CH_3), 2.06 (s, 24H, Ar-*ortho*-CH_3), 2.05-1.93 (m, 8H, NCH_2CH_2), 1.40-1.20 (m, 32H, aliphatic CH_2), 0.60-0.50 (m, 16H, $SiMe_2CH_2$), 0.45 (m, 8H, $Si_{core}CH_2$), 0.06 (s, 24H, SiCH_3); ^{13}C NMR ($CDCl_3$): δ 141.4, 137.8, 134.4, 130.9, 130.2, 130.1, 123.8, 50.8, 33.4, 30.9, 26.2, 24.1, 21.4, 20.5, 18.8, 18.0, 17.8, 15.6, -2.9. IR (cm^{-1}): 3054 (w), 2915 (s), 2854 (m), 1608 (w), 1563 (w), 1545 (w), 1246 (s), 1201 (s), 1067 (s). ESI-HRMS (*m/z*): calcd. for $C_{92}H_{152}I_3N_8Si_5$ $[M\text{-}I]^+$ 1890.8146, found 1890.8818, calcd. for $C_{92}H_{152}I_2N_8Si_5$ $[M\text{-}2I]^{2+}$ 881.9551, found 881.9565, calcd. for $C_{92}H_{152}IN_8Si_5$ $[M–3I]^{3+}$ 545.6686, found 545.6622.

Dendrimer ***2***

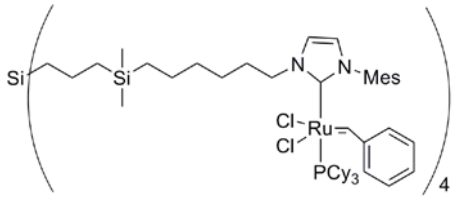

Imidazolium salt **6** (100 mg, 50 µmol) was dissolved in toluene (8 mL) using an ultrasonic agitation bath. A solution of potassium *tert*-butoxide in THF (20 wt%, 107 µL, 200 µmol, 4.0 equiv.) was added dropwise to the solution. The reaction mixture was stirred for 1 h at room temperature, whereupon a solution of Grubbs I catalyst **A** (153 mg, 200 µmol, 4.0 equiv.) in toluene (40 mL) was added slowly. The reaction mixture was stirred for 16 h. at room temperature, upon which its color changed from purple to purple-brown. After filtration, all

volatiles were removed in vacuo at room temperature. The resulting brown residue was washed with Et_2O several times and purified by column chromatography under an inert nitrogen atmosphere (neutral alumina, hexanes/ethyl acetate 2:1, *v*/*v*) to yield a dark brown solid in 70% yield (124 mg).

^{1}H NMR (C_6D_6): δ 19.80 (s, 4H, Ru=C*H*Ar), 8.19 (m, 8H, Ru=CHArH_{ortho}), 7.15 (s, 4H, C$H_{imid.}$), 6.98 (m, 12H, Ru=CHAr$H_{meta+para}$), 6.59 (s, 4H, C$H_{imid.}$), 6.21 (m, 8H, C$H_{arom, mesityl}$), 4.75 (m, 8H, NCH_2,), 2.62 (m, 8H, NCH_2CH_2), 2.16 (s, 12H, Ar-*para*-CH_3), 2.10-1.08 (m, 188H, aliphatic C*H* and CH_2), 0.90-0.60 (m, 24H, $SiCH_2$), 0.67-0.60 (m), 0.18 (bs, 24H, SiCH_3). ^{13}C NMR (C_6D_6): δ 291.2, 188.0, 151.9, 138.2, 136.8, 136.5, 130.5, 129.5, 129.2, 125.5, 123.0, 120.7, 50.6, 36.0, 35.4, 31.9, 29.9, 28.1, 27.1, 27.0, 26.7, 26.4, 22.9, 19.2, 18.6, 18.1, 14.2, -3.1. ^{31}P NMR (C_6D_6): δ 34.7. MALDI-TOF MS: (*m/z)* calcd. for $C_{192}H_{304}Cl_8N_8P_4Ru_4Si_5Na$ $[M+Na]^+$ 3703.8, found 3703.0.

Tetrakis-(tris-(3-((6-chlorohex-1-ynyl)dimethylsilyl)propyl)silane ***11***

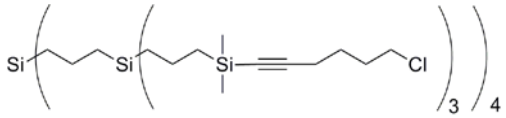

6-Chloro-1-hexyne (1.1 mL, 9.2 mmol, 14 equiv.) was dissolved in THF (40 mL) and cooled to -78 °C. A 2M solution of LDA in THF/hexanes (4.60 mL, 9.2 mmol, 14 equiv.) was added dropwise to the first solution and stirred for 30 min. at -78 °C. Then a solution of dendrimer **9** (1.91 g, 0.66 mmol) in THF (10 mL) was added dropwise at the same temperature. After addition, the mixture was allowed to reach room temperature and was stirred for another 16 h. The solvent was evaporated in vacuo and the resulting residue was dissolved in CH_2Cl_2 (50 mL) and washed with an aqueous saturated NH_4Cl solution (3 x 50 mL). The organic phase was dried over anhydrous $MgSO_4$, filtered and concentrated to afford an orange syrup. This air-sensitive product has been used without further purification in the next synthesis step.

^{1}H NMR ($CDCl_3$): δ 3.61 (t, ^3J = 6.6 Hz, 24H, CH_2Cl), 2.30 (m, 24H, C≡CCH_2), 1.93 (m, 24H, CH_2CH_2Cl), 1.73 (m, 24H, C≡CCH_2CH_2), 1.43-1.25 (m, 32H, $SiCH_2CH_2$), 0.73-0.63 (m, 64H, SiCH_2), 0.16 (s, 72H, Si-CH_3). ^{13}C NMR ($CDCl_3$): δ 105.8, 83.9, 43.7, 31.1, 25.6, 21.5, 20.9, 19.6, 19.3, 19.0, 18.4, 17.0, -1.3.

Tetrakis-(tris-(3-((6-chlorohexyl)dimethylsilyl)propyl)silane ***13***

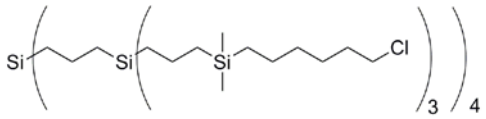

Dendrimer **11** (1.65 g, 0.57 mmol) and Pd on charcoal (10 wt% Pd, 118 mg, 0.11 mmol, 20 mol%) was suspended in ethyl acetate (20 mL) and placed in a 50 mL autoclave (Parr-4590 micro-reactor). After evacuation and purging the autoclave with hydrogen, the mixture was stirred at room temperature under a pressure of 25 bar of H_2 for 16 h. Then the solution was filtered through Celite and the solvent was evaporated. The residue was redissolved in CH_2Cl_2 (5 mL) and placed into a dialysis bag. This bag was placed into a beaker containing a mixture of CH_2Cl_2/MeOH (500 mL; 9:1, *v*/*v*) and dialyzed for 2 h. This procedure was repeated twice. Finally, the contents of the dialysis bag were evaporated, yielding **13** as a pale yellow syrup (60% over two steps, 1.02 g).

^{1}H NMR ($CDCl_3$): δ 3.51 (t, ^3J = 6.6 Hz, 24H, CH_2Cl), 1.79 (m, 24H, CH_2CH$_2$Cl), 1.42-1.18 (m, 104H, CH_2), 0.58-0.34 (m, 88H, SiCH_2), -0.05 (s, 72H, SiCH_3). ^{13}C NMR ($CDCl_3$): δ 45.4, 33.2, 32.9, 26.9, 24.0, 20.6, 18.8, 18.4, 18.1, 17.9, 17.6, 15.6, -3.0.

Tetrakis-(tris-(3-((6-(3-mesitylimidazolium)hexyl)dimethylsilyl)propyl)silane iodide ***7***

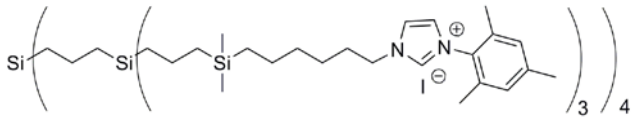

Dendrimer **13** (500 mg, 0.170 mmol), 1-mesitylimidazole (442 mg, 2.38 mmol, 14 equiv.) and sodium iodide (612 mg, 4.08 mmol, 24 equiv.) were dissolved in toluene (6 mL). This mixture was refluxed for 72 h. In this period, the product precipitated from the solution as a syrup. The supernatant was removed by careful decantation and the syrup was washed with hexanes (3 x 10 mL). Then the syrup was dissolved in CH_2Cl_2 whereupon inorganic sodium salts precipitated from the solvent. The solution was filtered and the filtrate was concentrated in vacuo. The product was further purified via passive dialysis in CH_2Cl_2/MeOH (500 mL; 9:1, *v*/*v*; 3 cycles of 2 h.) yielding a pale yellow solid in 69% (740 mg).

^{1}H NMR ($CDCl_3$): δ 9.98 (s, 12H, NC*H*N), 8.18 (s, 12H, C$H_{imid.}$), 7.28 (s, 12H, C$H_{imid.}$), 6.97 (s, 24H, C$H_{arom.}$), 4.67 (m, 24H, NCH_2), 2.32 (s, 72H, Ar-*para*-CH_3), 2.07 (s, 36H, Ar-*ortho*-CH_3), 1.42-1.18 (m, 128H, aliphatic CH_2), 0.65-0.38 (m, 88H, SiCH_2), -0.05 (s, 72H, SiCH_3). ^{13}C NMR ($CDCl_3$): δ 141.3, 137.0, 134.3, 130.8, 130.0, 124.3, 123.7, 50.5, 33.3, 30.9, 26.1, 24.0, 21.3,

20.4, 18.7, 18.0, 17.9, 17.8, 17.7, 17.4, 15.6, -3.3. ESI-HRMS (*m/z*): calcd. for $C_{288}H_{480}I_9N_{24}Si_{17}$ $[M-3I]^{3+}$ 1964.5259, found 1964.6520, calcd. for $C_{288}H_{480}I_8N_{24}Si_{17}$ $[M-4I]^{4+}$ 1441.6683, found 1441.6671, calcd. for $C_{288}H_{480}I_7N_{24}Si_{17}$ $[M-5]^{5+}$ 1127.9538, found 1127.7056. Also peaks for $[M-6I]^{6+}$, $[M-7I]^{7+}$ and $[M-8I]^{8+}$ have been successfully identified.

*Crystallographic data of complex **3***

X-ray intensities were measured on a Nonius Kappa CCD diffractometer with rotating anode (graphite monochromator, λ = 0.71073 Å[3]) at a temperature of 110 K. The integration of the data was performed with EvalCCD. For absorption correction and scaling the program SADABS was used. The structures were solved with automated Patterson Methods (DIRDIF-08) and refined with SHELXL-97 against F^2 of all reflections. Non-hydrogen atoms were refined freely with anisotropic displacement parameters. Hydrogen atoms were located in difference Fourier maps or introduced in calculated positions and refined with a riding model. Geometry calculations and checking for higher symmetry was performed with the PLATON program.[73] Further details are given in *table 6.3*.

*Table 6.3: Details of the X-ray crystal structure determinations of complex **3**.*

formula	$C_{28}H_{38}Cl_2N_2ORu$	temp [K]	150
Fw	590.57	V [Å^3]	3023.46(6)
Cryst. color	Brown	Z	4
Cryst. size [mm^3]	0.06 x 0.33 x 0.36	D_x [g/cm^3]	1.2974(1)
Cryst. syst	Monoclinic	μ [mm^{-1}]	0.716
space group	P21/c	reflections collected/unique	66907/6917
a [Å]	15.06929(4)	$(\sin\theta/\lambda)_{max}$ [Å^{-1}]	0.3
b [Å]	12.7795(2)	parameters/ restraints	313/not given
c [Å]	16.1807(2)	R1/wR2 [$I > 2\sigma(I)$]	5684
α [°]	90	R1/wR2 [all reflections]	0.0333/0.0976
β [°]	104.002(1)	S	1.11
γ [°]	90	$\rho_{min/max}$ [e/ Å^3]	-0.45, 1.03

Protocol for the RCM of diethyl diallylmalonate with the catalyst present in solution

In a representative experiment, the appropriate catalyst (5 mol% [Ru], 8 μmol), was added to a solution of diethyl diallylmalonate (0.16 mmol, 38.4 mg, 39 μL) and hexamethylbenzene (internal standard, 0.032 mmol, 5.2 mg) in dry CH_2Cl_2 (6 mL). The reaction stirred at room temperature or at 40 ^{o}C in an inert nitrogen atmosphere. Aliquots of 50 μL for GC analysis were regularly taken with an airtight syringe.

*Protocol for the RCM of diethyl diallylmalonate with dendritic catalyst **2** present in a dialysis bag*

In a tailor-made reaction vessel, which is equipped with a stirring bar, a NS50 joint and a nitrogen inlet, dry CH_2Cl_2 (90 mL) was added. To the solvent were subsequently added diethyl diallylmalonate (2.4 mmol, 580 mg, 580 μL) and hexamethylbenzene (internal standard, 0.48 mmol, 78 mg). A closed dialysis bag (Aldrich, benzoylated cellulose membranes, MWCO = 1000 Da.) filled with a solution of **2** (30 μmol, 1.25 mol%, 5 mol% Ru) in CH_2Cl_2 (5 mL) was placed in this solution. At regular intervals, samples of the outer solution were taken and analyzed by GC. After the reaction had finished, the dialysis bag containing the catalyst was directly placed in a fresh batch of substrates to start a new catalytic run. Again, at regular intervals, samples of the outer solution were taken and analyzed by GC.

*Protocol for the RCM of diethyl diallylmalonate with dendritic catalyst **2** present in a dialysis bag, recycling of **2** by means of precipitation*

In a tailor-made reaction vessel, which is equipped with a stirring bar, a NS50 joint and a nitrogen inlet, dry CH_2Cl_2 (60 mL) was added. To the solvent were subsequently added diethyl diallylmalonate (2.4 mmol, 580 mg, 580 μL), hexamethylbenzene (internal standard, 0.48 mmol, 78 mg) and **2** (30 μmol, 1.25 mol%, 5 mol% Ru). At regular intervals, samples of the outer solution were taken and analyzed by GC. After the reaction had finished, the solution was concentrated in vacuo to 10% of its original volume. Dry hexanes (60 mL) were added, whereupon a brown precipitate formed. This precipitate was isolated via filtration under a nitrogen environment and redissolved in CH_2Cl_2 (60 mL) whereupon a new batch of substrate and internal standard was added. At regular intervals, samples of the solution were taken and analyzed by GC.

6.8 References

(1) Trnka, T. M.; Grubbs, R. H. *Acc. Chem. Res.* **2001**, *34*, 18-29.
(2) Grubbs, R. H. *Tetrahedron* **2004**, *60*, 7117-7140.
(3) Vougioukalakis, G. C.; Grubbs, R. H. *Chem. Rev.* **2010**, *110*, 1746-1787.
(4) Grela, K. *Beilstein J. Org. Chem.* **2010**, *6*, 1089-1090.
(5) Mol, J. C. *J. Mol. Catal. A Chem.* **2004**, *213*, 39-45.
(6) Benito, J. M.; de Jesús, E.; de la Mata, F. J.; Flores, J. C.; Gomez, R. *Chem. Commun.* **2005**, 5217-5219.
(7) Schwab, P.; Grubbs, R. H.; Ziller, J. W. *J. Am. Chem. Soc.* **1996**, *118*, 100-110.
(8) Scholl, M.; Ding, S.; Lee, C. W.; Grubbs, R. H. *Org. Lett.* **1999**, *1*, 953-956.
(9) Kingsbury, J. S.; Harrity, J. P. A.; Bonitatebus, P. J.; Hoveyda, A. H. *J. Am. Chem. Soc.* **1999**, *121*, 791-799.
(10) Garber, S. B.; Kingsbury, J. S.; Gray, B. L.; Hoveyda, A. H. *J. Am. Chem. Soc.* **2000**, *122*, 8168-8179.
(11) Buchmeiser, M. R. *Chem. Rev.* **2009**, *109*, 303-321.
(12) Nguyen, S. T.; Grubbs, R. H. *J. Organomet. Chem.* **1995**, *497*, 195-200.
(13) Schurer, S. C.; Gessler, S.; Buschmann, N.; Blechert, S. *Angew. Chem. Int. Ed.* **2000**, *39*, 3898-3905.
(14) Mennecke, K.; Grela, K.; Kunz, U.; Kirschning, A. *Synlett* **2005**, 2948-2952.
(15) Sinner, F. M.; Buchmeiser, M. R. *Angew. Chem. Int. Ed.* **2000**, *39*, 1433-1439.
(16) Mayr, M.; Mayr, B.; Buchmeiser, M. R. *Angew. Chem. Int. Ed.* **2001**, *40*, 3839-3843.
(17) Prühs, S.; Lehmann, C. W.; Fürstner, A. *Organometallics* **2004**, *23*, 280-287.
(18) Coperet, C. *New J. Chem.* **2004**, *28*, 1-10.
(19) Sommer, W. J.; Weck, M. *Coord. Chem. Rev.* **2007**, *251*, 860-873.
(20) Connon, S. J.; Dunne, A. M.; Blechert, S. *Angew. Chem. Int. Ed.* **2002**, *41*, 3835-3838.
(21) Varray, S.; Lazaro, R.; Martinez, J.; Lamaty, F. *Organometallics* **2003**, *22*, 2426-2435.
(22) Gallivan, J. P.; Jordan, J. P.; Grubbs, R. H. *Tetrahedron Lett.* **2005**, *46*, 2577-2580.
(23) Hong, S. H.; Grubbs, R. H. *J. Am. Chem. Soc.* **2006**, *128*, 3508-3509.
(24) Yao, Q. W. *Angew. Chem. Int. Ed.* **2000**, *39*, 3896-3902.
(25) Dijkstra, H. P.; van Klink, G. P. M.; van Koten, G. *Acc. Chem. Res.* **2002**, *35*, 798-810.
(26) Janssen, M.; Müller, C.; Vogt, D. *Dalton Trans.* **2010**, *39*, 8403-8411.
(27) Albrecht, M.; Hovestad, N. J.; Boersma, J.; van Koten, G. *Chem. Eur. J.* **2001**, *7*, 1289-1294.
(28) Arink, A. M.; van de Coevering, R.; Wieczorek, B.; Firet, J.; Jastrzebski, J. T. B. H.; Klein Gebbink, R. J. M.; van Koten, G. *J. Organomet. Chem.* **2004**, *689*, 3813-3819.
(29) Gaab, M.; Bellemin-Laponnaz, S.; Gade, L. H. *Chem. Eur. J.* **2009**, *15*, 5450-5462.
(30) Pijnenburg, N. J. M.; Dijkstra, H. P.; van Koten, G.; Klein Gebbink, R. J. M. *Dalton Trans.* **2011**, *accepted*, *or **Chapter 2** of this thesis*.
(31) Fogg, D. E.; dos Santos, E. N. *Coord. Chem. Rev.* **2004**, *248*, 2365-2379.
(32) Kingsbury, J. S.; Hoveyda, A. H. *J. Am. Chem. Soc.* **2005**, *127*, 4510-4517.
(33) Vorfalt, T.; Wannowius, K. J.; Thiel, V.; Plenio, H. *Chem. Eur. J.* **2010**, *16*, 12312-12315.
(34) Vorfalt, T.; Wannowius, K. J.; Plenio, H. *Angew. Chem. Int. Ed.* **2010**, *49*, 5533-5536.
(35) Vehlow, K.; Mächling, S.; Blechert, S. *Organometallics* **2006**, *25*, 25-28.
(36) Liu, J.; Chen, J.; Zhao, J.; Zhao, Y.; Li, L.; Zhang, H. *Synthesis* **2003**, *17*, 2661-2666.
(37) Finkelstein, H. *Berichte Der Deutschen Chemischen Gesellschaft* **1910**, *43*, 1528-1532.
(38) Süssner, M.; Plenio, H. *Angew. Chem. Int. Ed.* **2005**, *44*, 6885-6888.
(39) Jordan, J. P.; Grubbs, R. H. *Angew. Chem. Int. Ed.* **2007**, *46*, 5152-5155.
(40) Wanzlick, H. W.; Schikora, E. *Angew. Chem. Int. Ed.* **1960**, *72*, 494-494.
(41) Wanzlick, H. W.; Schikora, E. *Chemische Berichte-Recueil* **1961**, *94*, 2389-2393.
(42) Denk, M. K.; Hatano, K.; Ma, M. *Tetrahedron Lett.* **1999**, *40*, 2057-2060.
(43) Denk, M. K.; Thadani, A.; Hatano, K.; Lough, A. J. *Angew. Chem. Int. Ed.* **2003**, *36*, 2607-2609.
(44) Arduengo, A. J.; Dias, H. V. R.; Harlow, R. L.; Kline, M. *J. Am. Chem. Soc.* **1992**, *114*, 5530-5534.
(45) Trnka, T. M.; Morgan, J. P.; Sanford, M. S.; Wilhelm, T. E.; Scholl, M.; Choi, T. L.; Ding, S.; Day, M. W.; Grubbs, R. H. *J. Am. Chem. Soc.* **2003**, *125*, 2546-2558.
(46) Hitchcock, P. B. *J. Chem. Soc. Dalton Trans.* **1979**, 1314-1317.
(47) Search performed in the *Cambridge Structural Database.* http://www.ccdc.cam.ac.uk/products/csd
(48) van der Made, A. W.; van Leeuwen, P. W. N. M. *J. Chem. Soc. Chem. Commun.* **1992**, 1400-1401.
(49) Taton, T. A.; Chen, P. *Angew. Chem. Int. Ed.* **1996**, *35*, 1011-1013.

(50) Murphy, J. A.; Zhou, S. Z.; Thomson, D. W.; Schoenebeck, F.; Mahesh, M.; Park, S. R.; Tuttle, T.; Berlouis, L. E. A. *Angew. Chem. Int. Ed.* **2007**, *46*, 5178-5183.
(51) Louie, J.; Bielawski, C. W.; Grubbs, R. H. *J. Am. Chem. Soc.* **2001**, *123*, 11312-11313.
(52) Dinger, M. B.; Mol, J. C. *Organometallics* **2003**, *22*, 1089-1095.
(53) Dinger, M. B.; Mol, J. C. *Eur. J. Inorg. Chem.* **2003**, 2827-2833.
(54) Nieczypor, P.; Buchowicz, W.; Meester, W. J. N.; Rutjes, F. P. J. T.; Mol, J. C. *Tetrahedron Lett.* **2001**, *42*, 7103-7105.
(55) Krause, J. O.; Nuyken, O.; Würst, K.; Buchmeiser, M. R. *Chem. Eur. J.* **2004**, *10*, 777-784.
(56) Yao, Q. W.; Zhang, Y. L. *J. Am. Chem. Soc.* **2004**, *126*, 74-75.
(57) Kingsbury, J. S.; Garber, S. B.; Giftos, J. M.; Gray, B. L.; Okamoto, M. M.; Farrer, R. A.; Fourkas, J. T.; Hoveyda, A. H. *Angew. Chem. Int. Ed.* **2001**, *40*, 4251-4256.
(58) Yao, Q. W.; Motta, A. R. *Tetrahedron Lett.* **2004**, *45*, 2447-2451.
(59) Dowden, J.; Savovic, J. *Chem. Commun.* **2001**, 37-38.
(60) Randl, S.; Buschmann, N.; Connon, S. J.; Blechert, S. *Synlett* **2001**, 1547-1550.
(61) Zaman, S.; Abell, A. D. *Tetrahedron Lett.* **2009**, *50*, 5340-5343.
(62) Vehlow, K.; Wang, D.; Buchmeiser, M. R.; Blechert, S. *Angew. Chem. Int. Ed.* **2008**, *47*, 2615-2618.
(63) Ledoux, N.; Allaert, B.; Pattyn, S.; vander Mierde, H.; Vercaemst, C.; Verpoort, F. *Chem. Eur. J.* **2006**, *12*, 4654-4661.
(64) Kumar, P. S.; Würst, K.; Buchmeiser, M. R. *J. Am. Chem. Soc.* **2009**, *131*, 387-395.
(65) Lichtenheldt, M.; Wang, D. R.; Vehlow, K.; Reinhardt, I.; Kuhnel, C.; Decker, U.; Blechert, S.; Buchmeiser, M. R. *Chem. Eur. J.* **2009**, *15*, 9451-9457.
(66) Mayr, M.; Buchmeiser, M. R.; Würst, K. *Adv. Synth. Catal.* **2002**, *344*, 712-719.
(67) Allen, D. P.; van Wingerden, M. M.; Grubbs, R. H. *Org. Lett.* **2009**, *11*, 1261-1264.
(68) Sommer, W. J.; Weck, M. *Adv. Synth. Catal.* **2006**, *348*, 2101-2113.
(69) Xu, G. P.; Gilbertson, S. R. *Org. Letters* **2005**, *7*, 4605-4608.
(70) Scholl, M.; Trnka, T. M.; Morgan, J. P.; Grubbs, R. H. *Tetrahedron Lett.* **1999**, *40*, 2247-2250.
(71) Cavallo, L.; Correa, A.; Costabile, C.; Jacobsen, H. *J. Organomet. Chem.* **2005**, *690*, 5407-5413.
(72) Sanford, M. S.; Love, J. A.; Grubbs, R. H. *J. Am. Chem. Soc.* **2001**, *123*, 6543-6554.
(73) Spek, A. L. *J. Appl. Cryst.* **2003**, *36*, 7-13.

Addendum

Towards compartmentalized orthogonal tandem catalysis

Introduction

The possibility to carry out multiple syntheses in a single reaction approach is a long-standing wish of synthetic chemists. The advantages of performing sequential reactions in the same reaction vessel are obvious, because workup procedures towards the intermediate products can be eliminated, which results in considerable environmental and economic advantages through savings of time, energy, solvent, and waste. In these 'one-pot' approaches product losses from isolation or purification of intermediate products can be decreased. At the same time, reactions yielding relatively unstable products can be included in the reaction sequence because these species are immediately used in a consecutive reaction step.

The overall reaction design of a tandem process becomes more complicated when one or several reaction steps are catalyzed by a (transition metal) catalyst. These catalysts should not interfere with reagents of the other reactions and, in turn, the catalyst's activity should not be altered by any of these reagents. The same applies for (disadvantageous) catalyst-catalyst interactions. Comprehensive reviews on tandem catalysis have recently been written by Fogg[1], Wasilke,[2] and Shindoh[3] and mainly show catalytic systems that deal with so-called auto-tandem catalysis, i.e. multiple mechanistically different catalytic steps performed by a single catalyst. An example is the palladium-catalyzed stannylation and electrophilic substitution recently reported by our group.[4,5] In contrast, only few reports describe homogeneous orthogonal tandem catalysis. In orthogonal tandem catalysis several mechanistically different catalytic steps are performed by a number of different catalysts in one pot. Again, an important prerequisite for orthogonal tandem catalysis is that the different catalysts do not interfere with each other and are not affected by any of the other reagents. Loones *et al.* reported on a successfully applied orthogonal tandem catalytic

reaction in which the palladium-catalyzed amination of 2,3-dibromopyridine with various amidines was followed by an intramolecular copper-catalyzed amination of the resulting product into a polycyclic dipyrido[1,2-a:2',3'-d]imidazole (*figure 1, top*).[6] Another, elegant example of orthogonal tandem catalysis was published by Jeong *et al*., who reported on a palladium-catalyzed allylation of an alkyne and an alkene followed by a rhodium-catalyzed Pauson-Khand reaction to form cyclopentenones (*figure 1, bottom*).[7]

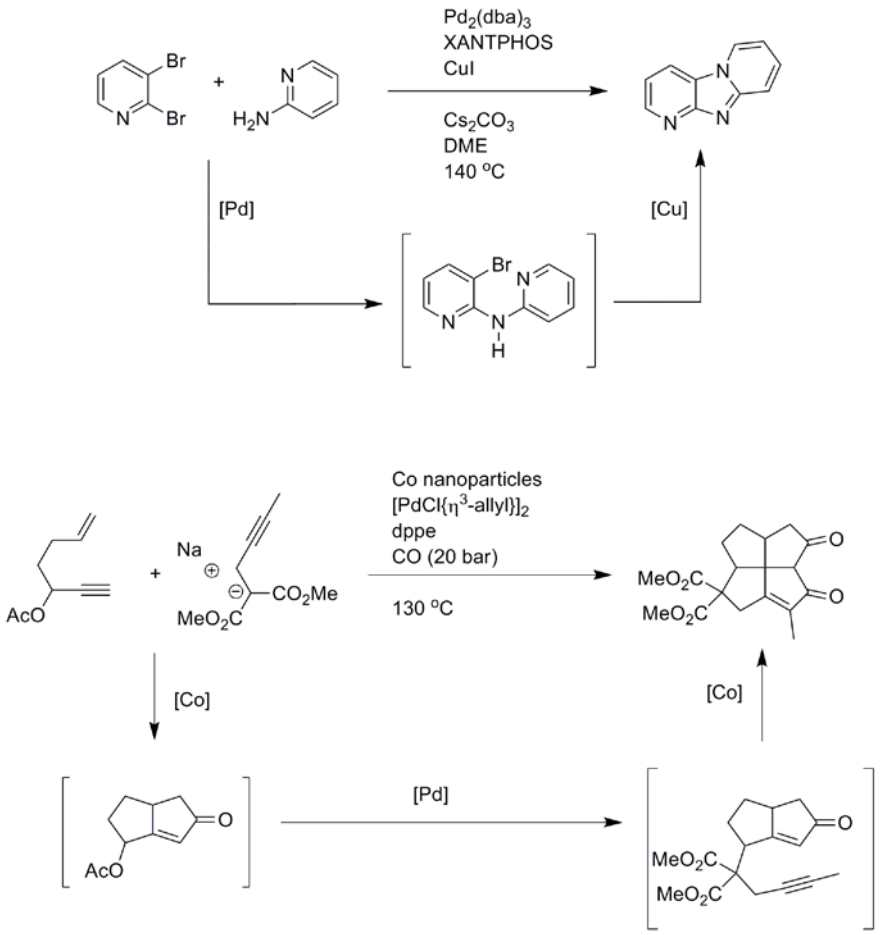

Figure 1: Earlier examples of orthogonal tandem catalysis.[6,7]

To be able to apply orthogonal tandem catalysis more regularly in organic synthesis, general solutions to the earlier mentioned prerequisites should be found. Obvious approaches are the search for the shortest possible contact time (exposure) between catalysts and reagents, substrates and products, and the restriction of a particular catalytic activity to a particular location only. A combination of these approaches was reported by Lectka *et al.*, who carried out several reaction steps using sequentially-linked 'reaction columns' that contain silica-immobilized (organo)catalysts.[8-10] The group of Ley has developed a similar setup by using

modular flow reactors that operate in combination with a variety of immobilized reagents and scavenger materials to achieve multi-component, multistep coupling reactions, e.g. for the synthesis of the natural product oxomaritidine.[11-14] Clean products were obtained without the need for intermediate work-up.

An alternative and homogeneous approach towards orthogonal tandem catalysis could be realized by using soluble immobilized catalysts in semi-permeable compartments in order to connect catalytic activity to location. These solution compartments can be added to or removed from the reaction vessel, thereby reducing unwanted side reactions and increasing the number of potentially feasible reaction steps in an orthogonal tandem catalytic reaction sequence. Furthermore, such an approach would open possibilities for catalyst recycling and for the design of continuous processes in e.g. membrane reactors (*figure 2*).

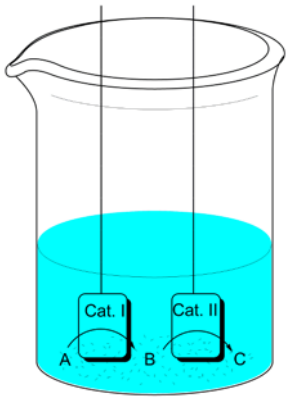

Figure 2: A schematic representation for a setup suitable for compartmentalized orthogonal tandem catalysis

In this thesis several examples of compartmentalized catalysis using dendritic-Pd and -Ru catalysts have been described.[5,15] Extending on these examples, we have investigated an orthogonal tandem catalytic reaction sequence that is based on the combination of the individual steps that are catalyzed by these dendritic-Pd and -Ru catalysts or by the corresponding mononuclear species. To this purpose a two-step sequence consisting of a ruthenium-catalyzed ring-closing metathesis and a palladium-catalyzed cross-coupling was investigated (*figure 3*). In this reaction, 2-(but-3-enyl)-3-vinyloxirane **1** is ring-closed to 7-oxabicyclo[4.1.0]hept-4-ene **2** by a ruthenium-based olefin metathesis catalyst, whereupon **2** acts as the substrate for a cross-coupling with styrylboronic acid **3** to result in a mixture of 2-styrylcyclohex-3-enol **4** and 4-styrylcyclohex-2-enol **5**.

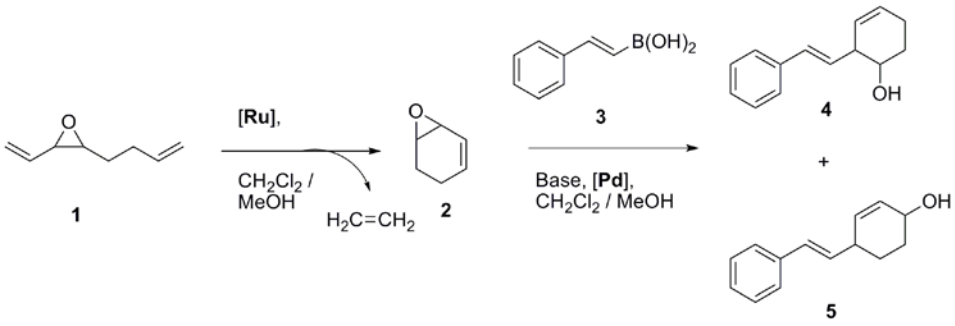

*Figure 3: Tandem reaction consisting of a ruthenium-catalyzed ring-closing metathesis of 2-(but-3-enyl)-3-vinyloxirane **1**, followed by a palladium-catalyzed cross-coupling with styrylboronic acid **3** leading to 2-styrylcyclohex-3-enol **4** and 4-styrylcyclohex-2-enol **5**.*

Here, we present our preliminary results on the combination of these two reaction steps into one homogeneous orthogonal tandem reaction. First, the two individual reaction steps were investigated using the respective mononuclear catalysts under normal conditions. Subsequently the separate reactions were studied in a compartmentalized setting using recyclable metallo-dendritic catalysts. Finally, these two reactions were combined.

Results

*Ring-closing metathesis of 2-(but-3-enyl)-3-vinyloxirane **1***

A racemic mixture of 2-(but-3-enyl)-3-vinyloxirane **1** was reacted in a ruthenium-catalyzed ring-closing metathesis reaction in a solvent mixture of CH_2Cl_2 : MeOH (9:1, *v*/*v*) at 40 °C. The respective catalysts used in this reaction are the same as presented in ***Chapter 6*** for the RCM of diethyl diallylmalonate. These catalysts comprise first and second generation Grubbs catalysts **6** and **7**, respectively, Hoveyda-Grubbs II catalyst **8**, mononuclear catalysts **9** and **10**, and metallo-dendritic Grubbs II type catalyst **11** (*figure 4*)**.**

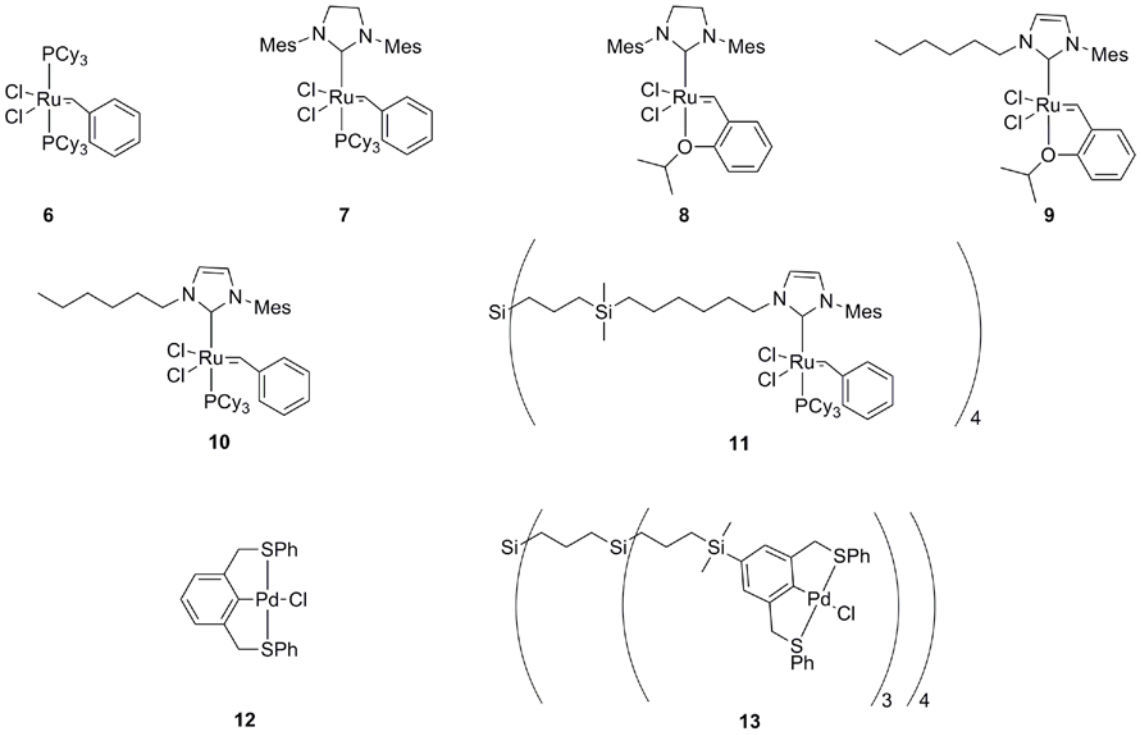

Figure 4: Mononuclear and metallo-dendritic ruthenium- and palladium-based catalysts applied for the tandem reaction shown in figure 3.

For the *trans* isomer of 2-(but-3-enyl)-3-vinyloxirane **1** no reaction was observed with any of these catalysts. It seems that the two allyl fragments in the *trans*-isomer of this substrate are too far apart to allow for a successful ring-closing reaction. The *cis*-isomer of **1**, on the other hand, shows an entirely different reactivity in the RCM reaction and leads to the formation of *cis*-7-oxabicyclo[4.1.0]hept-4-ene $\mathbf{2}_{cis}$. This result shows that because the two allyl fragments in $\mathbf{1}_{cis}$ are located on the same side of the oxirane plane, they are accessible to undergo olefin metathesis by the ruthenium-based metathesis catalyst. In the catalyst screening for the RCM of $\mathbf{1}_{cis}$ to $\mathbf{2}_{cis}$ large differences in reaction rates were observed, because the activity of the different catalysts influences the equilibria for the various RCM and ROMP reactions.[16,17] Fogg recently showed that olefin substrates often first undergo metathesis oligomerization, whereupon the formed oligomers lead to the RCM product. This product, in its turn, can be the substrate for subsequent ROMP reactions leading to higher molecular weight olefinic products.

First and second generation Grubbs catalysts **6** and **7** showed relatively low amounts of RCM product formation over time. The kinetic profile shows 15-25% product formation after 30 minutes, which remained relatively constant in the next 5 h. Subsequently, the amount of

the RCM product decreased. Hoveyda-Grubbs catalyst **8** showed a good conversion of 68% to $\mathbf{2}_{cis}$ after 3 h, which represents by far the highest RCM activity for the catalysts tested here. When the reaction was allowed to continue for another 12 h the amount of product decreased to 30%, which was taken as an indication that ROMP of the RCM product took place. The modified mononuclear and metallo-dendritic Grubbs II type catalysts **9**, **10**, and **11** disappointingly showed low conversions of 14, 2, and 7%, respectively after 3 h. No ROMP byproducts were observed in these cases. Because of the low activity of **11**, no studies regarding catalyst reuse or compartmentalized catalysis were performed.

*Cross-coupling of cis-7-oxabicyclo[4.1.0]hept-4-ene $\mathbf{2}_{cis}$ and styrylboronic acid **3** to styrylcyclohexenols **4** and **5***

For the palladium-catalyzed cross-coupling, the two substrates $\mathbf{2}_{cis}$ and **3**, D*i*PEA and a SCS-pincer palladium catalyst **12** (2 mol% Pd; *figure 4*) were added to a CH_2Cl_2 : MeOH solvent mixture. Two different products were formed (79% conversion after 3 h), i.e. an 1 : 1.1 mixture of the direct addition product 2-styrylcyclohex-3-enol **4** and the conjugate addition product 4-styrylcyclohex-2-enol **5.** Attempts to separate these isomers were unsuccessful.
Next, the dendritic SCS-pincer palladium complex **13**[5] (*figure 4*) was used to explore the recyclability of this catalyst and to perform compartmentalized catalysis in a semi-permeable membrane dialysis bag. A catalyst solution placed in a dialysis bag was immersed in a solution containing substrates $\mathbf{2}_{cis}$, **3** and D*i*PEA. The used membrane was a benzoylated regenerated cellulose membrane with a MWCO of 1000 Da., thereby preventing the metallo-dendritic catalyst (MW = 7593 Da.) to pass, but allowing permeation of all reactants, reagents and reaction products. After 24 h, the membrane dialysis bag was removed and placed into a solution with a new batch of substrates. It was found that the catalyst showed a similar activity and selectivity during all runs (*table 1*). To investigate possible occurrence of palladium leaching from the catalyst to the outer solution, aliquots of the different outer solutions were analyzed by ICP-MS analysis. No palladium could be detected indicating that the observed amount of palladium had been lower than the detection limit of the spectrometer. This result points out that a stable reaction setup was obtained containing a

metallo-dendritic catalyst, which can be recycled for multiple runs without affecting product formation and product selectivity.

*Table 1: Results of the compartmentalized palladium-catalyzed cross-coupling of cis-7-oxabicyclo[4.1.0]hept-4-ene **2**$_{cis}$ and styrylboronic acid **3** to 2-styrylcyclohex-3-enol **4** and 4-styrylcyclohex-2-enol **5**.*[a]

Run	Yield (formation of **4** + **5**, after 24 h, %)	Product ratio (mol. ratio **5**/**4**)	Amount of Pd in outer solution (ppm)
1	84	1.2	<1
2	91	1.2	<1
3	78	1.2	<1

[a] *Reaction carried out under ambient conditions.*

Ruthenium-catalyzed RCM and palladium-catalyzed cross-coupling reactions in one pot

Subsequently, the two reactions presented in the previous paragraphs were investigated in an orthogonal tandem, one-pot procedure. As a first approach, all reagents for the RCM and the cross-coupling reaction, i.e. racemic 2-(but-3-enyl)-3-vinyloxirane **1**, styrylboronic acid **3**, and D*i*PEA, and the two mononuclear catalysts **8** and **12** were combined in one vessel containing a solvent mixture of CH_2Cl_2 and MeOH (9:1, *v*/*v*) and the mixture was stirred at 40 °C for 5 h. ^{1}H NMR analysis of the reaction mixture after workup showed that the RCM reaction had not taken place, but that the palladium-catalyzed cross-coupling of 2-(but-3-enyl)-3-vinyloxirane **1**$_{rac}$ with styrylboronic acid **3** did occur indeed affording products **14** and **15** in a 1.3 : 1 ratio in a combined conversion of 63% (*figure 5*). Also these reaction products were found to be unsusceptible for ruthenium-catalyzed cross-coupling reactions.

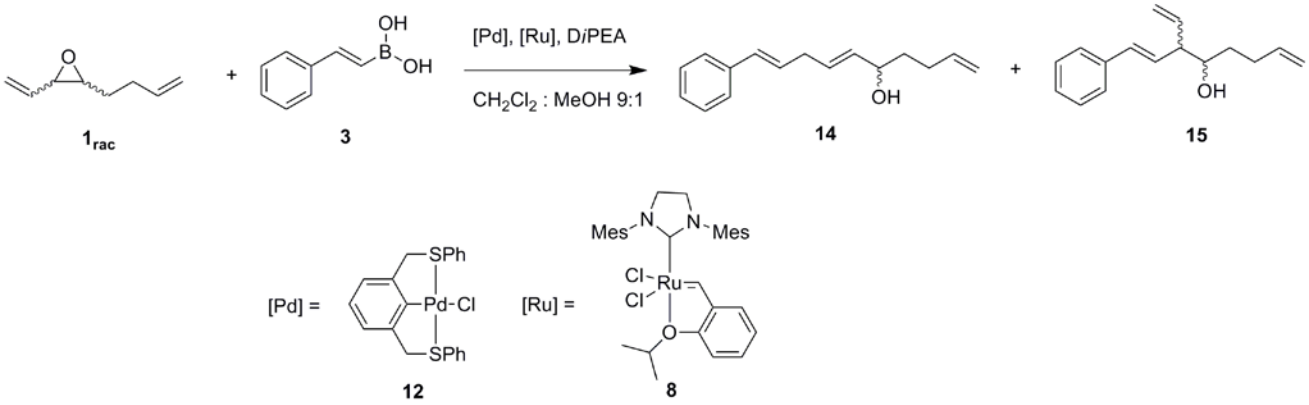

Figure 5: One-pot reaction of 2-(but-3-enyl)-3-vinyloxirane ***1****$_{rac}$ with styrylboronic acid* ***3*** *using Pd catalyst* ***12*** *and Ru catalyst* ***8****.*

In order to investigate the origin for the lack of RCM activity in the reaction mixture, a series of test reactions were performed in which substrates or reagents that are involved in the cross-coupling step were systematically added to the RCM reaction of *cis*-2-(but-3-enyl)-3-vinyloxirane **1**$_{cis}$ with catalyst **8** (5 mol%). It was found that the RCM reaction was not affected by either the addition of styrylboronic acid **3** or SCS-pincer complex **12**. However, the presence of D*i*PEA did block the reaction as well as the presence of other bases like cesium carbonate, triethylamine and cesium fluorate.

Because of these observations we decided to perform the two parts of the tandem reaction in one pot by subsequent addition of the reactants; i.e. the reagents of the second reaction were added not before the first reaction had finished. In other words, after the RCM reaction had stopped, styrylboronic acid **3**, D*i*PEA, and SCS-pincer Pd-catalyst **12** were added. The formation and consumption of the intermediate product **2**$_{cis}$ is depicted in *figure 6.* It shows that *cis*-2-(but-3-enyl)-3-vinyloxirane **1**$_{cis}$ was successfully ring closed to *cis*-7-oxabicyclo[4.1.0]hept-4-ene **2**$_{cis}$ in 53% conversion, 50% in the first 15 min., and that the reaction did not progress any further after this point in time (**1**$_{trans}$ did not undergo the ring-closing reaction, *vide supra*). After 180 min., boronic acid **3**, D*i*PEA, and SCS-pincer Pd-catalyst **12** were added and immediately the intermediate product **2**$_{cis}$ reacted with styrylboronic acid **3** to a mixture of 2-styrylcyclohex-3-enol **4** and 4-styrylcyclohex-2-enol **5** (l/b ratio 1 : 1.3). This reaction went to completion in 120 min. The conversion of the total reaction (starting from **1**$_{cis}$ via primary product **2**$_{cis}$ to products **4** and **5**) was found to be 53%. After the addition of the reactants for the palladium-catalyzed cross-coupling reaction, **1**$_{trans}$ (which is unable to react via RCM to **2**$_{trans}$, *vide supra*) as well as the non-reacted starting

material $\mathbf{1}_{cis}$ also reacted with styrylboronic acid **3**. This led to a mixture of products **14** and **15** in a product ratio of 1.5 : 1. The resulting mixture of **4**, **5**, **14**, and **15** was concentrated, but could not be separated via column chromatography. ^{1}H NMR spectra of sufficient quality were obtained to identify the separate reaction products.

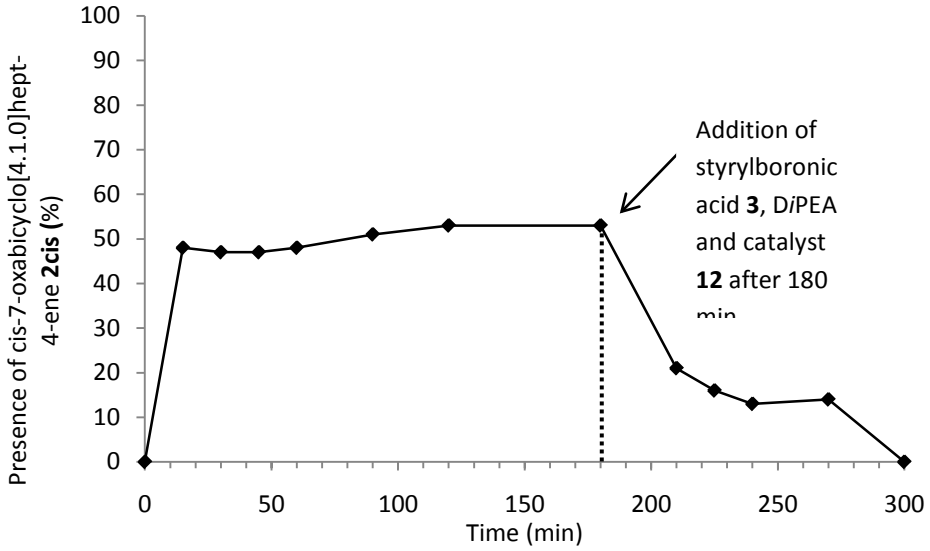

Figure 6: The presence of cis-7-oxabicyclo[4.1.0]hept-4-ene $\mathbf{2}_{cis}$ *in the reaction mixture being a product of the RCM of cis-2-(but-3-enyl)-3-vinyloxirane* $\mathbf{1}_{cis}$ *and a substrate for the cross-coupling with styrylboronic acid* ***3****.*

Discussion

In our search for a compartmentalized catalytic orthogonal tandem reaction, a new Ru/Pd mediated olefin-metathesis/cross-coupling tandem reaction was investigated. In a compartmentalized setup the robust dendritic SCS-pincer palladium complex **12** was recycled successfully for three consecutive runs in the cross-coupling of *cis*-7-oxabicyclo[4.1.0]hept-4-ene $\mathbf{2}_{cis}$ with styrylboronic acid **3** to form linear and branched products **4** and **5** without any palladium leaching or decreased activity. In addition, a one-pot orthogonal tandem reaction comprising a ruthenium-catalyzed RCM reaction and the cross-coupling of the in situ formed $\mathbf{2}_{cis}$ with styrylboronic acid **3** was successfully applied by stepwise addition of reagents and catalysts to yield the tandem products **4** and **5** in 53% yield.

The full concept of compartmentalized orthogonal tandem catalysis or one-pot tandem catalysis could, however, not be tested. The experiments described in this addendum show

that either the moisture sensitivity, the low RCM activity, or the lack of compatibility of the (dendritic) ruthenium-based catalysts and the base in the reaction mixture were found to frustrate the compartmentalized RCM of *cis*-2-(but-3-enyl)-3-vinyloxirane $\mathbf{1}_{cis}$ and, therefore, the compartmentalized orthogonal tandem catalysis. The commercially available Hoveyda-Grubbs II catalyst **8** was found to be more active in this particular RCM reaction and far less moisture sensitive than dendritic Grubbs catalyst **11**. However, its molecular size is simply not large enough for compartmentalized catalysis. Ideally, a dendritic Hoveyda-Grubbs II catalyst could have overcome these problems, but synthetic difficulties prevented the formation of such a Hoveyda-Grubbs II catalyst analogue.[15]

These issues can be formulated as the main drawback of the concept of compartmentalized orthogonal tandem catalysis. In many cases, it can be questioned whether the number of additional synthetic steps and compromises that are required to create a robust, soluble, immobilized catalyst outweigh the additional benefits of a setup that minimizes the amount of workup and makes catalyst recycling possible. The example displayed here clearly shows that special care should be taken regarding, firstly, the robustness of the dendritic catalysts and, secondly, the orthogonality of the catalysts towards all substrates present in the reaction mixture. By using consecutive compartmentalized catalysis, i.e. by addition of compartmentalized catalysts in a subsequent way, the latter problem can be partly overcome by regulation (or minimization) of the contact times between the catalyst and an activity-reducing reagent. If both prerequisites are fulfilled, a benign way of performing homogeneous catalysis is obtained. Additional studies on compartmentalized orthogonal tandem catalysis should explore whether this advanced form of homogenous catalysis is a realistic target.

Experimental section

General

All reactions were carried out using standard Schlenk techniques under an inert dinitrogen atmosphere unless stated otherwise. All solvents were carefully dried and distilled prior to use. All standard reagents were purchased commercially and used without further purification. Racemic 2-(but-3-enyl)-3-vinyloxirane $\mathbf{1}_{rac}$ was synthesized according to Breen's

procedure,[18] *cis*-7-oxabicyclo[4.1.0]hept-4-ene $\mathbf{2}_{cis}$ was alternatively synthesized via oxidation of 1,3-cyclohexadiene as performed by Jin.[19] The non-commercial ruthenium olefin catalysts **9**, **10** and **11** were described by us in an earlier manuscript.[15] The monomeric SCS-pincer palladium pincer **12** has been synthesized according to Sillanpää,[20] whereas the synthesis of dendritic SCS-pincer palladium pincer **13** was published earlier by us.[5] All other reagents were purchased from Acros Organics and Sigma-Aldrich Chemical Co. Inc. and used as received. ^{1}H (300 MHz), and ^{13}C (100 MHz) NMR spectra were recorded on a Varian 400 MHz spectrometer at 25 ^{o}C, chemical shifts are given in ppm referenced to residual solvent resonances. High-resolution mass spectroscopy (HRMS) has been performed on a Waters LCT Premier XE Micromass instrument using the electrospray ionization (ESI) technique. GC analysis was carried out using a Perkin Elmer Clarus 500 GC equipped with an Alltech Econo-Cap EC-5 column.

Spectroscopic data of new compounds

2-Styrylcyclohex-3-enol **4**:

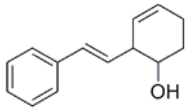

^{1}H NMR ($CDCl_3$, 300 MHz): δ 7.44-7.24 (m, 5H, C*H*$_{arom}$), 6.57 (d, 1H, Ph-C*H*=CH, ^{3}J = 15.9 Hz), 6.15 (dd, 1H, Ph-CH=C*H*, ^{3}J = 15.9 Hz, ^{3}J = 8.4 Hz), 5.81 (m, 1H, CH=C*H*-CHOH), 5.55 (m, 1H, C*H*=CH-CHOH) 3.75 (m, 1H, C*H*OH), 2.92 (m, 1H, C*H*), 2.27-2.02 (m, 2H, CH_2), 2.01-1.97 (m, 2H, CH_2). O*H* proton was not observed. ^{13}C NMR ($CDCl_3$, 100 MHz): δ 137.3, 132.7, 131.4, 128.8, 127.9, 127.7, 127.3, 126.5, 71.3, 49.0, 29.1, 24.4. ESI-MS: (*m/z*) 183.1159 ([M-OH]$^{+}$, calcd : 183.1174).

4-Styrylcyclohex-2-enol **5**:

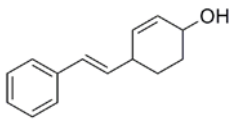

^{1}H NMR ($CDCl_3$, 300 MHz): δ 7.41-7.24 (m, 5H, C*H*$_{arom}$), 6.43 (d, 1H, Ph-C*H*=CH, ^{3}J = 15.9 Hz), 6.16 (dd, 1H, Ph-CH=C*H*, ^{3}J = 15.9 Hz, ^{3}J = 7.5 Hz), 5.85 (m, 2H, C*H*=C*H*-CHOH), 4.29 (m, 1H, CHO*H*), 3.04 (m, 1H, C*H*), 2.18-2.03 (m, 2H, CH_2), 1.62 (m, 2H, CH_2). O*H* proton was not

observed. ^{13}C NMR ($CDCl_3$, 100 MHz): δ 137.6, 133.2, 132.6, 131.2, 129.9, 128.8, 127.4, 126.3, 66.3, 38.9, 31.0, 26.7. ESI-MS: (*m/z*) 183.1138 ($[M-OH]^+$, calcd : 183.1174).

10-Phenyldeca-1,6,9-trien-5-ol **14**

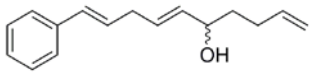

^1H NMR ($CDCl_3$, 300 MHz): δ 7.46-7.25 (m, 5H, CH_{arom}), 6.41 (d, 1H, Ph-C*H*=CH, ^3J = 15.6 Hz), 6.24 (m, 1H, Ph-CH=C*H*), 5.93-5.78 (m, 3H, CH_{olefin}), 5.18-4.98 (m, 2H, CH=CH_2), 4.23 (m, 1H, C*H*OH), 2.95 (m, 2H, CH-CH_2-CH), 2.21 (m, 2H, CH_2=CH-CH_2), 1.68 (m, 2H, CHOH-CH_2). O*H* proton was not observed.

1-Phenyl-3-vinylocta-1,7-dien-4-ol **15**

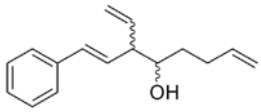

^1H NMR ($CDCl_3$, 300 MHz): δ 7.46-7.25 (m, 5H, CH_{arom}), 6.41 (d, 1H, Ph-CH=CH, ^3J = 15.6 Hz), 6.24 (m, 1H, Ph-CH=C*H*), 5.93-5.78 (m, 2H, 2x C*H*=CH_2), 5.18-4.98 (m, 4H, 2x CH=CH_2), 3.48 (m, 1H, C*H*OH), 3.17 (m, 1H, CH-C*H*-CHOH), 2.21 (m, 2H, CH_2=CH-CH_2), 1.68 (m, 2H, CHOH-CH_2). O*H* proton was not observed.

Protocol for the RCM of 2-(but-3-enyl)-3-vinyloxirane ***1**$_{rac}$* *using ruthenium catalysts in solution*

To a mixture of CH_2Cl_2 and MeOH (9:1, *v*/*v*, 6.0 mL) were added a racemic mixture of 2-(but-3-enyl)-3-vinyloxirane **1$_{rac}$** (0.60 mmol, 78 µL), hexamethylbenzene (internal standard, 0.12 mmol, 19.5 mg) and a ruthenium containing olefin metathesis catalyst **6**-**11** (5 mol%, 0.03 mmol Ru centers). The runs were carried at room temperature or reflux temperature and followed by GC analysis in time.

Protocol for the cross-coupling of cis-7-oxabicyclo[4.1.0]hept-4-ene ***2**$_{cis}$* *and styrylboronic acid* ***3*** *using palladium catalysts in solution*

To a mixture of CH_2Cl_2 and MeOH (9:1, *v*/*v*, 6.0 mL) were added *cis*-7-oxabicyclo[4.1.0]hept-4-ene **2$_{cis}$** (0.60 mmol, 54 µL), styrylboronic acid **3** (0.60 mmol, 81 mg), a base (D*i*PEA or Cs_2CO_3, 2 equiv., 1.2 mmol), hexamethylbenzene (internal standard, 0.12 mmol, 19.5 mg)

and SCS-pincer palladium catalyst **12**. The runs were carried at room temperature or reflux temperature and followed by GC analysis in time.

Protocol for the compartmentalized cross-coupling of *cis*-7-oxabicyclo[4.1.0]hept-4-ene $\mathbf{2}_{cis}$ *to styrylboronic acid **3** using dendritic catalyst **13***

In a reaction vessel a mixture of CH_2Cl_2 and MeOH (9:1, *v*/*v*, 100 mL) was added. To the solvent were subsequently added *cis*-7-oxabicyclo[4.1.0]hept-4-ene $\mathbf{2}_{cis}$ (10.0 mmol, 0.90 mL), styrylboronic acid **3** (10.0 mmol, 1.52 g), a base (D*i*PEA or Cs_2CO_3, 2.0 equiv., 20.0 mmol) and hexamethylbenzene (internal standard, 2.0 mmol, 325 mg). A dialysis bag (Aldrich, benzoylated cellulose membranes, MWCO = 1000 Da.) filled with 5 mL CH_2Cl_2 and dendritic catalyst **13** (2 mol% Pd, 0.167 mol% **13**, 16.7 µmol, 118 mg) that was closed by plastic clamps was added to this solution. In regular intervals, samples of the outer solution were taken and analyzed by GC. After the reaction has finished, the dialysis bag was directly placed in a fresh batch of substrates to start a new catalytic run. Again, in regular intervals, samples of the outer solution were taken and analyzed by GC. The runs were carried out in air at room temperature.

Protocol for one pot catalysis consisting of subsequent RCM and cross-coupling

In a schlenk were subsequently added a mixture of CH_2Cl_2 and MeOH (9:1, *v*/*v*, 6 mL), 2-(but-3-enyl)-3-vinyloxirane $\mathbf{1}_{rac}$ (0.6 mmol, 78 µL), hexamethylbenzene (internal standard, 0.12 mmol, 19.5 mg) and Hoveyda-Grubbs II catalyst **8** (5 mol%, 30 µmol). The reaction mixture was stirred at reflux temperature. In regular intervals, samples of the outer solution were taken and analyzed by GC analysis. As soon as this analysis pointed to the lack of further reaction progress, the second reaction step was initiated by addition of styrylboronic acid **3** (0.6 mmol, 81 mg), D*i*PEA (2 equiv., 1.2 mmol, 0.21 mL) and SCS-pincer palladium complex **12** (2 mol%, 12 µmol, 5.6 mg). Again, the reaction mixture was stirred at reflux temperatures and was followed by GC analysis.

References

(1) Fogg, D. E.; dos Santos, E. N. *Coord. Chem. Rev.* **2004**, *248*, 2365-2379.
(2) Wasilke, J. C.; Obrey, S. J.; Baker, R. T.; Bazan, G. C. *Chem. Rev.* **2005**, *105*, 1001-1020.

(3) Shindoh, N.; Takemoto, Y.; Takasu, K. *Chem. Eur. J.* **2009**, *15*, 12168-12179.
(4) Gagliardo, M.; Selander, N.; Mehendale, N. C.; van Koten, G.; Klein Gebbink, R. J. M.; Szabó, K. J. *Chem. Eur. J.* **2008**, *14*, 4800-4809.
(5) Pijnenburg, N. J. M.; Dijkstra, H. P.; van Koten, G.; Klein Gebbink, R. J. M. *Dalton Trans.* **2011**, *40*, 8896-8905, *or* ***Chapter 2*** *of this thesis*.
(6) Loones, K. T. J.; Maes, B. U. W.; Meyers, C.; Deruytter, J. *J. Org. Chem.* **2006**, *71*, 260-264.
(7) Jeong, N.; Sung, B. K.; Kim, J. S.; Park, S. B.; Seo, S. D.; Shin, J. Y.; In, K. Y.; Choi, Y. K. *Pure Appl. Chem.* **2002**, *74*, 85-91.
(8) Hafez, A. M.; Taggi, A. E.; Dudding, T.; Lectka, T. *J. Am. Chem. Soc.* **2001**, *123*, 10853-10859.
(9) Hafez, A. M.; Taggi, A. E.; Lectka, T. *Chem. Eur. J.* **2002**, *8*, 4114-4119.
(10) France, S.; Bernstein, D.; Weatherwax, A.; Lectka, T. *Org. Lett.* **2005**, *7*, 3009-3012.
(11) Germ, K.; Nöde, L.; Un, D.; Kaise, R.; Schmarre, N.; Bitt, E. *Chem. Commun.* **2006**, 2566-2568.
(12) Baumann, M.; Baxendale, I. R.; Ley, S. V.; Smith, C. D.; Tranmer, G. K. *Org. Lett.* **2006**, *8*, 5231-5234.
(13) Ley, S. V.; Baxendale, I. R.; Mansfield, A. C.; Smith, C. D. *Angew. Chem. Int. Ed.* **2009**, *48*, 4017-4021.
(14) Ley, S. V.; Baxendale, I. R.; Schou, S. C.; Sedelmeier, J. *Chem. Eur. J.* **2010**, *16*, 89-94.
(15) Pijnenburg, N. J. M.; Tomás González de Mendivil, E.; Mayland, K. E.; Kleijn, H.; Lutz, M.; Spek, A.; van Koten, G.; Klein Gebbink, R. J. M. *This thesis*, ***Chapter 6*****.**
(16) Fogg, D. E.; Monfette, S.; Crane, A. K.; Silva, J. A. D.; Facey, G. A.; dos Santos, E. N.; Araujo, M. H. *Inorg. Chim. Acta* **2010**, *363*, 481-486.
(17) Fogg, D. E.; Monfette, S. *Chem. Rev.* **2009**, *109*, 3783-3816.
(18) Breen, A. P.; Murphy, J. A. *J. Chem. Soc. Perkin Trans. 1* **1993**, 2979-2990.
(19) Jin, Y.; Lipscomb, J. D. *J. Biol. Inorg. Chem.* **2001**, *6*, 717-725.
(20) Lucena, N.; Casabo, J.; Escriche, L.; Sanchez-Castello, G.; Teixidor, F.; Kivekas, R.; Sillanpää, R. *Polyhedron* **1996**, *15*, 3009-3018.

Summary

Dendrimer-immobilized homogeneous catalysts have been used in many different organic reactions. These catalysts are able to combine the high activity, selectivity and tunability, and mild reaction conditions of homogeneous catalysis with the easy separation and recycling that is typical for heterogeneous catalysts. These macromolecular, soluble catalysts can be removed from the reaction mixtures via osmosis (dialysis), reverse osmosis (nano- or ultrafiltration), or precipitation, and can be reused for further catalytic applications.

The use of dendritic catalysts in tandem catalysis would lead to a further improvement in organic synthesis according to the principles of green chemistry. Shorter synthetic procedures lead to less reaction workup procedures in multi-step synthesis, less waste products, and as a result to lower production costs. Although hinted at for some time, no examples of dendritic tandem catalysis have been reported so far. In this thesis, the use of dendritic catalysts in tandem catalysis was investigated both in homogeneous solutions as well as in compartmentalized settings in order to arrive at tandem reaction setups with optimized catalyst performance and recyclability. The synthesis and catalytic performance of various dendritic Pd and Ru complexes is described for a number of tandem and single-step reactions and is benchmarked against the properties of their monomeric analogues.

In ***Chapter 1*** an overview is presented of dendritic palladium catalysts and their use in organic synthesis. The review focuses on palladacyclic compounds, i.e. compounds that contain complementary covalent Pd-C and dative Pd-hetero atom bonds in a cyclic structure, in which the Pd-center is strongly bound to its dendritic ligand. Such compounds suffer less from Pd-leaching and are, therefore, very well suited for use in recyclable catalytic systems. Many of the described palladacyclic dendrimers contain peripherally immobilized ECE-pincer Pd complexes.

Chapter 2 describes the first example of compartmentalized auto-tandem catalysis. Here, we report on the combination of the SCS-pincer Pd-catalyzed stannylation of cinnamyl chloride with hexamethylditin and the SCS-pincer Pd-catalyzed electrophilic addition of 4-

nitrobenzaldehyde to the in situ formed primary reaction product to form the secondary reaction product 1-(4-nitrophenyl)-2-phenylbut-3-en-1-ol in one pot (*figure 1*).

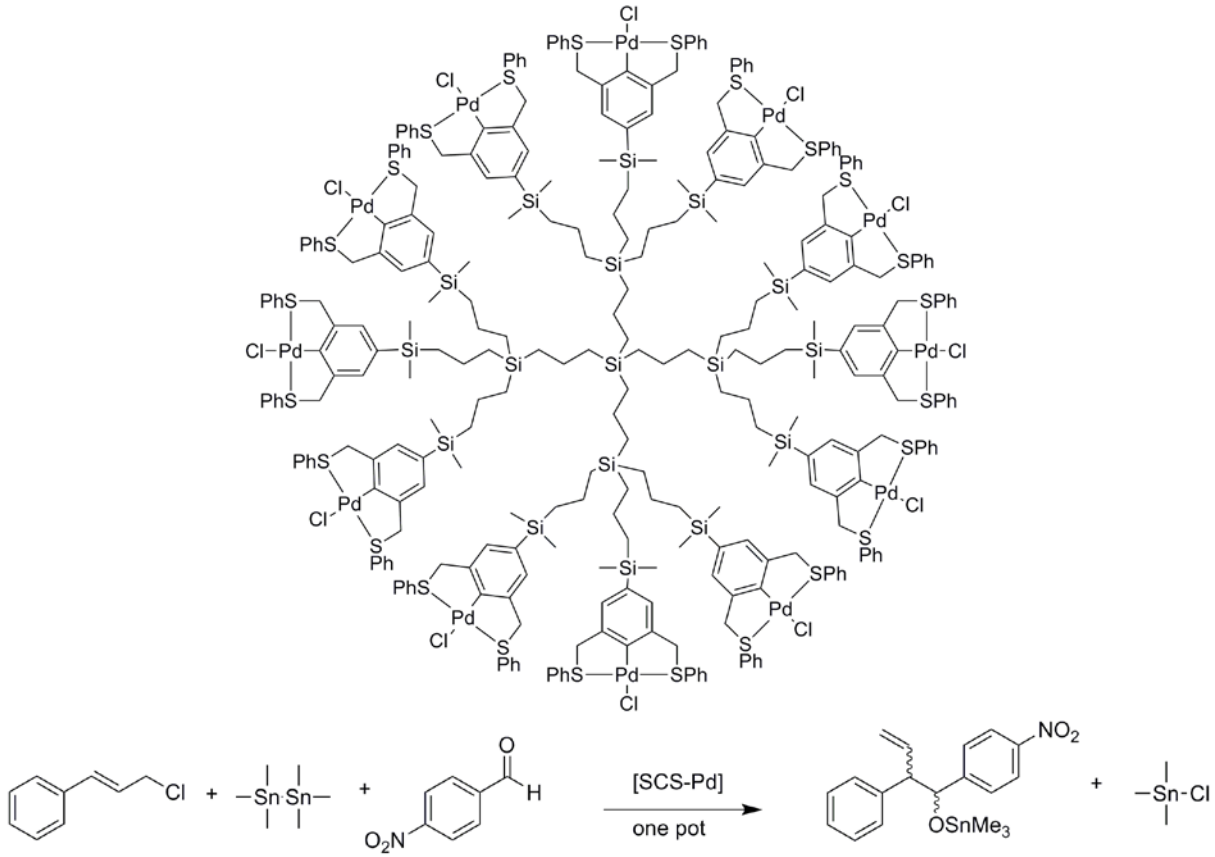

Figure 1: First generation dendritic SCS-pincer Pd complex used in the compartmentalized auto-tandem reaction comprised of the stannylation of cinnamyl chloride, followed by the electrophilic addition of 4-nitrobenzaldehyde.

Zeroth and first generation dendritic SCS-pincer complexes were synthesized in a short synthetic route and were fully characterized. The palladation of these dendrimers took place via direct C-H activation in the absence of reactive intermediates, which resulted in full palladium loadings (>97%). These dendritic SCS-pincer complexes showed a very similar reaction rate and a slightly higher *anti*/*syn* product ratio compared to monomeric SCS-pincer complexes in the tandem reaction (*anti*/*syn* product ratio = 5 for the monomeric complexes, 6 for the dendritic complexes). Overall, the tandem reaction was slow, as complete secondary tandem product formation was only obtained after 72 h. The largest (G_1) dendritic catalysts (MW = 7593 Da) was investigated in compartmentalized auto-tandem catalysis using a membrane dialysis bag with a molecular weight cut off (MWCO) of 1000 Da. The first run showed 64% secondary product formation after a week. After replacement of the

catalyst compartment into a solution with a new batch of substrates, the second catalytic run showed a very similar reaction profile. In the next two runs lower reaction rates and conversions were found. ICP-MS analyses showed significant Pd-leaching, which was caused by release of Pd from the pincer ligands rather than by leaching of palladadendrimers through the voids of the membrane.

To improve the applicability of this particular compartmentalized tandem catalysis, mechanistic studies on the SCS-pincer-catalyzed stannylation/addition reaction were performed in ***Chapter 3***. The catalytic auto-tandem reaction showed a remarkable reaction profile: a fast primary and secondary product formation in the first hours (part I), followed by a period of total reaction inactivity (part II), and finally a slow, but gradual completion of the secondary product formation after 5 days (part III). Through a combination of experiments aimed at unraveling the tandem mechanism, it was found that the role of the primary product cinnamyl trimethylstannane in this reaction is quite different from what was believed earlier. In the stannylation reaction of cinnamyl chloride with hexamethylditin, small amounts (<10%) of 1-phenyl-2-propenyl trimethylstannane **B**, the branched isomer of cinnamyl trimethylstannane **A**, were also found during the reaction. In the second reaction step, i.e. the SCS-pincer Pd-catalyzed electrophilic addition of 4-nitrobenzaldehyde to the primary reaction product, no immediate reaction was found when **A** was used in combination with the electrophile, whereas a fast reaction was observed when using **B**. It was therefore concluding that the branched stannane **B** is the primary reaction product that enters the second catalytic cycle (*figure 2*).

These observations led us to propose an alternative, three cycle tandem reaction mechanism. In the first cycle of this mechanism, the stannylation leads to a mixture of **A** and **B**. Stannane **B** (and not stannane **A**) is the starting point of the second catalytic cycle in which it reacts with the SCS-pincer Pd-Cl complex to form a Pd-η^1-allyl intermediate, which in turn reacts with 4-nitrobenzaldehyde to form the secondary reaction product. This second cycle follows a Pd(II)-only mechanism, which is fast with respect to the third cycle. This third catalytic cycle is based on the catalytic activity of slowly released palladium(0) species that are formed in the reaction setup. These particles are able to catalyze the electrophilic addition of cinnamyl trimethylstannane (**A**) with 4-nitrobenzaldehyde. A combination of the second and the third cycle allows for a full consumption of all of the primary reaction products.

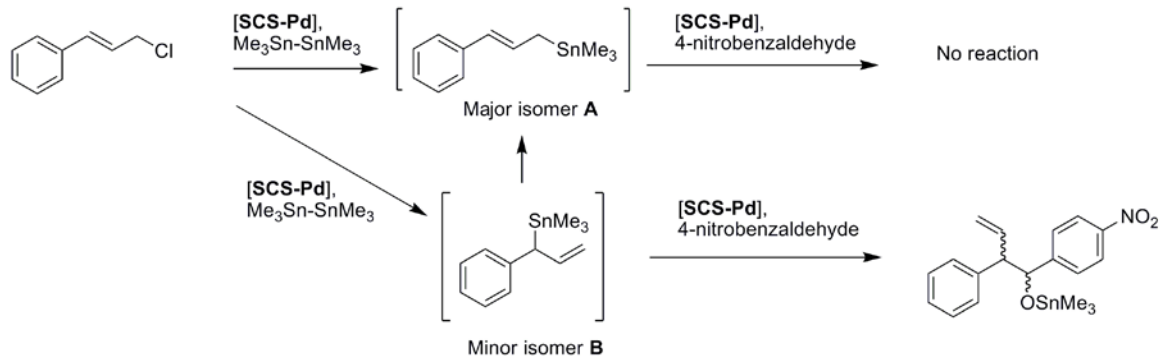

Figure 2: Alternative reaction pathway for the Pd-catalyzed tandem reaction between cinnamyl chloride, hexamethylditin, and 4-nitrobenzaldehyde to the secondary reaction product trimethyl(1-(4-nitrophenyl)-2-phenylbut-3-enyloxy)stannane.

This reaction mechanism is corroborated by DFT calculations and fully explains the remarkable reaction kinetics of the tandem reaction. With these new insights, the reaction conditions required for compartmentalized auto-tandem catalysis as described in ***Chapter 2*** could be improved significantly. By using three equivalents of cinnamyl chloride and hexamethylditin with respect to 4-nitrobenzaldehyde, the second catalytic cycle is continuously fed resulting in a spectacular decrease of the reaction time from 5 days to only 2 h. Furthermore, Pd(0) leaching could be prevented. Through these reaction conditions, compartmentalized auto-tandem catalysis was successfully performed for four runs, showing fast reaction rates, constant high product selectivities, and very minor palladium leaching.

In ***Chapter 4***, the role of the dendritic support in the catalytic performance of peripheral pincer Pd complexes was investigated and was benchmarked against monomeric catalysts. In this chapter, the catalytic activity and product selectivity of apolar carbosilane dendrimer-immobilized SCS-pincer Pd complexes and polar polyamidoamine (PAMAM) dendrimer-immobilized SCS-pincer Pd complexes were compared for two different reactions. Besides the auto-tandem stannylation/electrophilic addition (*figure 1*), the SCS-pincer Pd-catalyzed cross-coupling reaction between vinyl epoxide and styrylboronic acid was also investigated (*figure 3*).

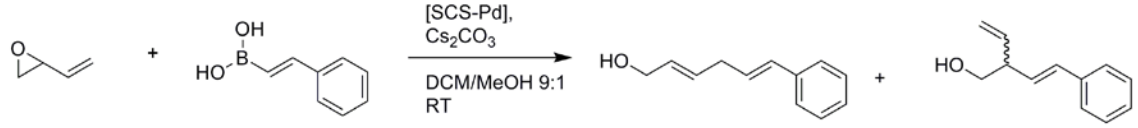

Figure 3: SCS-pincer Pd-catalyzed cross-coupling reaction between vinyl epoxide and styrylboronic acid.

Very similar reaction characteristics were observed for all tested catalysts in the tandem reaction, but interesting results caused by dendritic effects were obtained in the cross-coupling reaction. Here, the PAMAM dendrimer-immobilized complexes (*figure 4*) showed a similar reaction rate, but higher product selectivity than the monomeric parent catalyst. The carbosilane dendrimer-immobilized catalysts on the other hand, showed a lower reaction rate and similar product selectivity than the parent catalyst. These observations were explained by peripheral group backfolding for PAMAM dendrimers and dendrimer aggregation for carbosilane dendrimers.

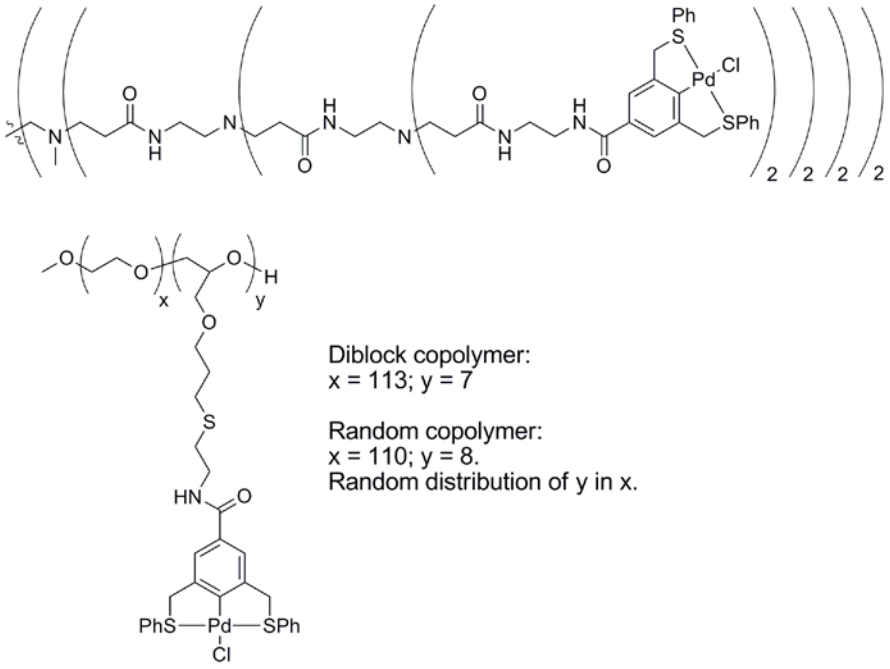

Figure 4: SCS-pincer Pd complexes immobilized on a PAMAM-dendrimer (top, ***Chapter 4****) and a PEG-polymer (bottom,* ***Chapter 5****).*

Chapter 5 investigates the structure-activity relationship for two types of PEG-copolymer-supported pincer Pd-catalysts in the cross-coupling reaction between vinyl epoxide and styrylboronic acid. These two copolymers are comprised of ethylene oxide and allyl glycidyl ether and show an identical chemical composition. The first copolymer has a random structure with a random distribution of the catalytic moieties, whereas the second copolymer is a diblock copolymer that contains a high local concentration of catalytic centers in the glycidyl ether block (*figure 4*). The overall activity of these two copolymers was found to be similar to each other and somewhat lower than the monomeric parent catalyst. The *l/b* product selectivity of the diblock copolymer (*l/b* = 14.9) showed to be almost twofold higher

than that of the random polymer (*l/b* = 8.1) and almost threefold higher than for the monomeric complex (*l/b* = 5.5). The difference in *l/b* product ratios is explained by the different steric demands of the S_N2 and S_N2' reaction paths leading to the branched and linear reaction products, respectively. Because of steric congestion of the catalytic centers, the S_N2 pathway is considered as less likely for the diblock copolymer.

In ***Chapter 6*** the scope of solution-phase and compartmentalized dendritic catalysis is extended to ruthenium-catalyzed olefin metathesis. Here, the synthesis of novel monomeric and dendritic Grubbs II-based and Hoveyda-Grubbs II-based catalysts is described (*figure 5*). These olefin metathesis catalysts were used in the ring-closing metathesis of diethyl diallylmalonate and compared to the most often used Grubbs and Hoveyda-Grubbs catalysts. The dendritic Grubbs II-type catalyst showed a better initial activity at room temperature when compared to its monomeric analogue, but was outperformed by the commercially available catalysts. At reflux temperature, the dendritic Grubbs II catalyst was somewhat slower than the monomeric catalyst. These two observations hint at a higher activity and a higher deactivation rate of the catalytic centers for the dendritic catalyst.

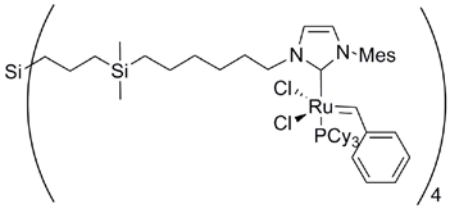

Figure 5: Dendritic Grubbs II-type complex used in the ring-closing metathesis of diethyl diallylmalonate.

Compartmentalized catalysis with this dendritic catalyst has been performed, but the high sensitivity of the catalyst towards moisture in combination with the presence of minute amounts of water in the dialysis tubing, hampered product formation. Also via catalyst precipitation, no catalyst separation and subsequent recycling could be accomplished.

Finally, in the ***Addendum*** an orthogonal tandem catalytic system was designed and investigated by using the dendritic Pd and Ru complexes that were described in ***Chapters 2 and 6***. Unfortunately, the low RCM-activity of the dendritic Ru complex for the substrate 2-(but-3-enyl)-3-vinyloxirane, the moisture sensitivity, and the base sensitivity of this catalyst hampered the first successful example of compartmentalized orthogonal tandem catalysis.

Samenvatting

Dendritische homogene katalysatoren zijn tot op heden voor een groot aantal verschillende organische reacties gebruikt. Deze katalysatoren combineren zowel de hoge activiteit en selectiviteit, als de modificeerbaarheid en de milde reactiecondities van homogene katalysatoren met de eenvoudige scheiding en de efficiënte wijze van hergebruik die kenmerkend zijn voor heterogene katalysatoren. Deze macromoleculaire, oplosbare katalysatoren kunnen van reactiemengsels worden gescheiden via osmose (dialyse), omgekeerde osmose (nano- of ultrafiltratie), of precipitatie en kunnen op deze manier hergebruikt worden voor verdere katalytische toepassingen.

Het gebruik van dendritische katalysatoren in tandemkatalyse leidt tot een verdere verbetering in de duurzaamheid van organisch chemische syntheses. Kortere syntheseprocedures leiden tot minder opwerkingsstappen, minder afvalproducten en daardoor lagere productiekosten. Hoewel het principe in enkele gevallen in de literatuur ter sprake is gebracht, zijn er tot dusver geen concrete voorbeelden van dendritische tandemkatalyse beschreven. In dit proefschrift wordt het gebruik van dendritische katalysatoren in tandemkatalyse onderzocht met als doel de katalytische eigenschappen en het hergebruik van deze katalysatoren in tandemreacties te optimaliseren. Deze katalysatoren zijn onderzocht in zowel homogene oplossingen, als in semi-permeabele compartimenten die geen macromoleculaire katalysatoren doorlaten, maar vrij doorlaatbaar zijn voor substraten, reactanten en reactieproducten met moleculaire gewichten beneden de 1000 Da. De synthese en katalytische eigenschappen van een aantal verschillende dendritische palladium- en rutheniumcomplexen worden beschreven voor een aantal (tandem)reacties en vervolgens vergeleken met de eigenschappen van hun monomere equivalenten.

In ***Hoofdstuk 1*** wordt een overzicht gegeven van dendritische palladiumkatalysatoren en hun gebruik in organische synthese. Het hoofdstuk spitst zich toe op palladacyclische verbindingen, d.w.z. verbindingen die zowel één covalente Pd-C- als non-covalente Pd-heteroatoom-bindingen bevatten in een cyclische structuur. In zulke verbindingen is de

palladiumkern stevig gebonden aan zijn dendritisch ligand, waardoor zij zeer geschikt zijn als onderdeel van herbruikbare katalytische systemen. Veel van de beschreven palladacyclische dendrimeren bevatten zogenaamde ECE-tang Pd-complexen die geïmmobiliseerd zijn aan de periferie van dendrimeren.

Hoofdstuk 2 beschrijft het eerste voorbeeld van gecompartimentaliseerde auto-tandemkatalyse. Hier wordt een combinatie van een SCS-tang Pd-gekatalyseerde stannylering van kaneelchloride met hexamethylditin en een SCS-tang Pd-gekatalyseerde electrofiele additie van 4-nitrobenzaldehyde met het in situ gevormde primaire reactieproduct beschreven. Deze éénpotsynthese leidt tot de vorming van het secundaire reactieproduct trimethyl(1-(4-nitrophenyl)-2-phenylbut-3-enyloxy)stannaan (*figuur 1*).

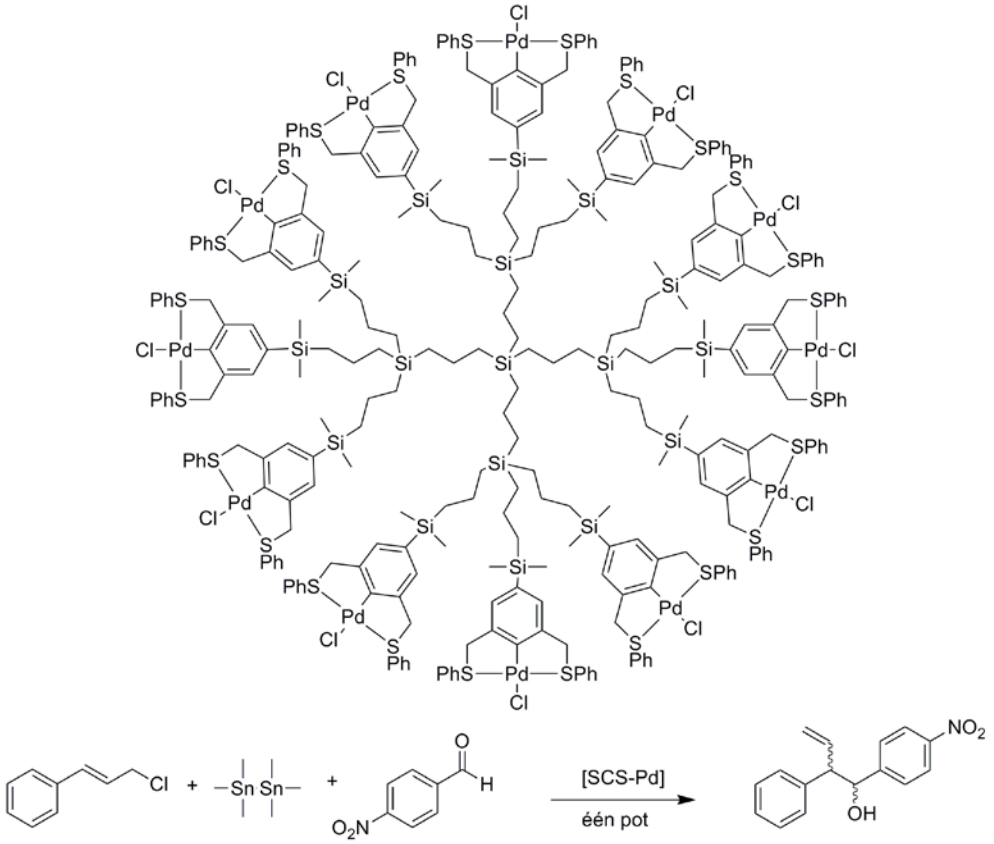

Figuur 1: Eerste generatie dendritische SCS-tang Pd-complex gebruikt in de gecompartimentaliseerde auto-tandemreactie bestaande uit de stannylering van kaneelchloride gevolgd door de electrofiele additie van 4-nitrobenzaldehyde.

Via een korte syntheseroute werden nulde en eerste generatie dendritische SCS-tang complexen gesynthetiseerd en volledig gekarakteriseerd. De palladering van deze dendrimeren vond plaats via een directe C-H activering waarbij geen instabiele intermediairen gevormd worden, hetgeen resulteerde in een volledige belading van het

dendrimeer met palladium (>97%). Deze dendritische SCS-tang complexen vertoonden een vergelijkbare reactiesnelheid en een wat hogere *anti*/*syn* productverhouding vergeleken met monomere SCS-tang complexen in de tandemreactie (*anti*/*syn* productverhouding = 5 voor de monomere complexen en 6 voor de dendritische complexen). De tandemreactie verliep echter langzaam: volledige vorming van het secundaire reactieproduct werd pas na 72 uur waargenomen. De grootste (G_1) dendritische katalysator (molecuulgewicht = 7593 Da) werd onderzocht in gecompartimentaliseerde auto-tandemkatalyse waarbij gebruik werd gemaakt van een membraandialysezakje met poriën ter grootte van 1000 Da. De eerste cyclus leidde tot de vorming van 64% secundair product na één week. Nadat het compartiment met daarin de katalysator overgebracht werd naar een nieuwe oplossing met reactiesubstraten vertoonde de tweede reactiecyclus een zeer vergelijkbaar reactieprofiel. In de twee volgende cycli werden lagere reactiesnelheden en omzettingen gevonden. ICP-MS analyses vertoonden aanzienlijk verlies van Pd, wat veroorzaakt werd door het vrijkomen van Pd uit het tangligand en niet door lekkage van de palladadendrimeren in het geheel door de poriën in het membraan.

Om de toepasbaarheid in deze specifieke gecompartimentaliseerde tandemkatalyse te verhogen, werd een serie mechanistische studies uitgevoerd aan de SCS-tang gekatalyseerde stannylering/additie-tandemreactie zoals is beschreven in ***Hoofdstuk 3***. De katalytische auto-tandemreactie vertoonde een opmerkelijk reactieprofiel: een snelle vorming van zowel het primaire als het secundaire reactieproduct in de eerste uren (deel I), gevolgd door een periode van totale inactiviteit (deel II) en tenslotte een langzame, maar geleidelijke voltooiing van de vorming van het secundaire reactieproduct na 5 dagen (deel III). Door een combinatie van experimenten die erop gericht waren om het tandemmechanisme te ontrafelen, bleek de rol van het primaire reactieproduct kaneeltrimethylstannaan anders was dan wat in eerste instantie aangenomen werd. In de stannylering van kaneelchloride met hexamethylditin werden tijdens de reactie kleine hoeveelheden (<10%) gevonden van het 1-phenyl-2-propenyltrimethylstannaan **B**; d.w.z. het vertakte isomeer van kaneeltrimethylstannaan **A**. In de tweede reactiestap, de SCS-tang Pd-gekatalyseerde electrofiele additie van 4-nitrobenzaldehyde met het primaire reactieproduct, werd geen directe reactie waargenomen wanneer alleen **A** werd gebruikt in combinatie met het electrofiel, terwijl een directe, snelle reactie plaatsvond wanneer **B** gebruikt werd als

substraat. Hiermee werd duidelijk dat het vertakte stannaan **B** het primaire reactieproduct is dat de tweede cyclus van de tandemreactie ingaat (*figuur 2*).

Aan de hand van deze observaties werd een alternatief reactiemechanisme voorgesteld dat bestaat uit drie katalytische cycli. In de eerste cyclus van dit mechanisme leidt de stannylering tot een mengsel van **A** en **B**. Stannaan **B** (en niet stannaan **A**) is het startpunt van de tweede katalytische cyclus waarin het reageert met het SCS-tang Pd-Cl complex om een Pd-η^1-allyl intermediair te vormen. Dit intermediair reageert met 4-nitrobenzaldehyde naar het secundaire reactieproduct. Deze tweede cyclus verloopt volledig via een Pd(II)-mechanisme en is veel sneller dan de derde cyclus. Deze derde cyclus is gebaseerd op de katalytische activiteit van palladium(0)-deeltjes die langzaam gevormd worden onder de reactiecondities. Deze deeltje zijn katalytisch actief in de electrofiele additie van kaneeltrimethylstannaan (**A**) met 4-nitrobenzaldehyde. Een combinatie van de tweede en derde cyclus leidt tot een volledige omzetting van alle primaire reactieproducten.

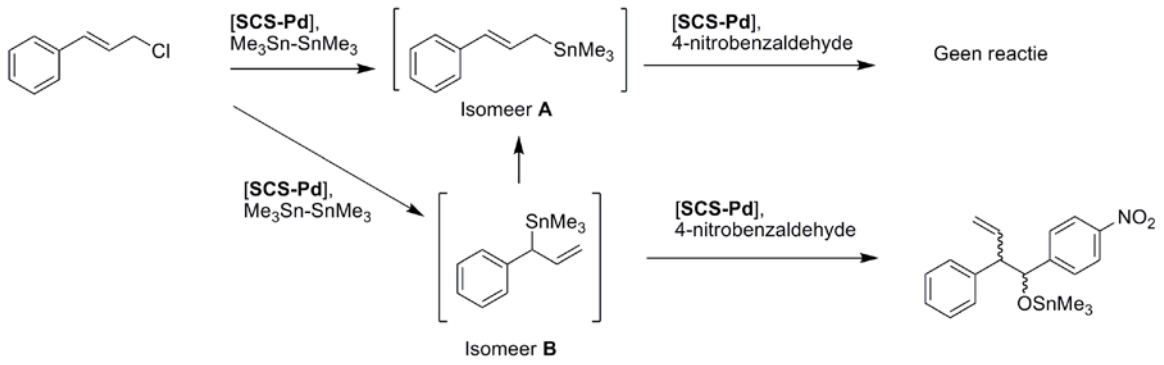

Figuur 2: Alternatief reactiepad voor de Pd-gekatalyseerde tandemreactie tussen kaneelchloride, hexamethylditin en 4-nitrobenzaldehyde tot het secundaire reactieproduct trimethyl(1-(4-nitrophenyl)-2-phenylbut-3-enyloxy)stannaan.

Dit reactiemechanisme wordt ondersteund door DFT-berekeningen en verklaart de opmerkelijke reactiekinetiek van de tandemreactie. Met deze nieuwe inzichten konden de reactiecondities voor gecompartimentaliseerde auto-tandemkatalyse zoals beschreven in ***Hoofdstuk 2*** aanzienlijk verbeterd worden. Door drie equivalenten kaneelchloride en hexamethylditin te gebruiken ten opzichte van 4-nitrobenzaldehyde, kan de tweede katalytische cyclus continu gevoed worden, wat resulteert in een spectaculaire afname van de reactietijd van 5 dagen naar slechts 2 uur. Verder kon op deze manier de vorming van Pd(0) deeltjes voorkomen worden. Met deze reactiecondities konden vier opeenvolgende

cycli van de auto-tandemreactie op gecompartimentaliseerde wijze uitgevoerd worden met korte reactietijden, een constante hoge productselectiviteit en met zeer gering palladiumverlies.

In ***Hoofdstuk 4*** is de rol van de dendritische drager op de katalytische eigenschappen van perifere tang Pd-complexen bestudeerd en vergeleken met monomere katalysatoren. In dit hoofdstuk zijn de katalytische activiteit en de productselectiviteit van apolaire carbosilaan dendrimeer-geïmmobiliseerde SCS-tang Pd-complexen vergeleken met die van polaire polyamidoamine (PAMAM) dendrimeer-geïmmobiliseerde SCS-tang Pd-complexen (*figuur 4, boven*) in twee verschillende reacties. Behalve de auto-tandem stannylering/electrofiele additie (*figuur 1*) werd ook de SCS-tang Pd-gekatalyseerde kruiskoppeling tussen vinylepoxide en styrylboorzuur onderzocht (*figuur 3*).

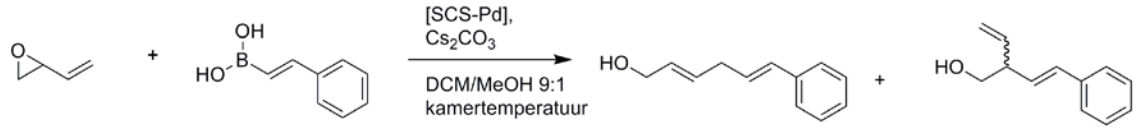

Figuur 3: SCS-tang Pd-gekatalyseerde kruiskoppeling tussen vinylepoxide en styrylboorzuur.

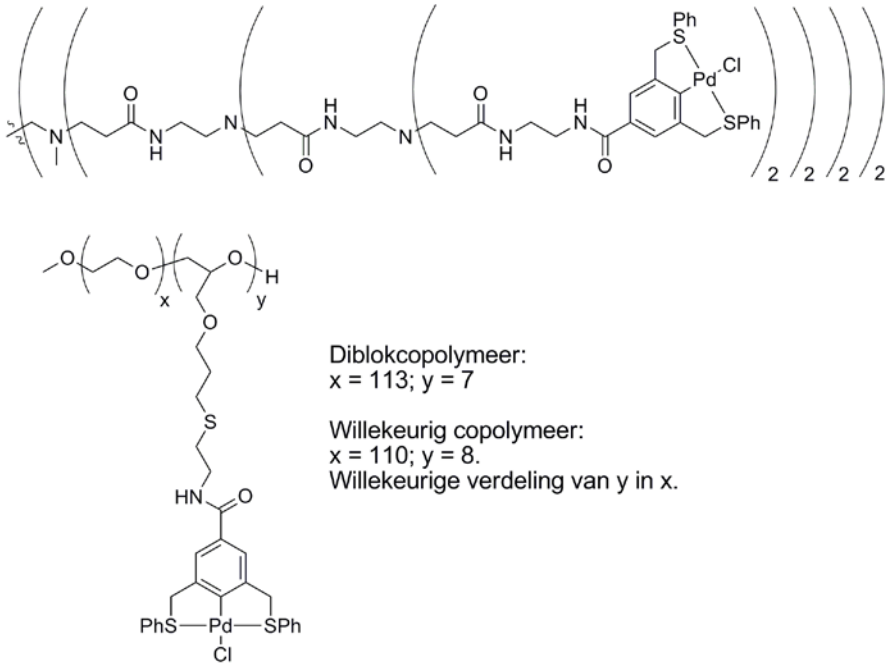

Figuur 4: SCS-tang Pd-complexen geïmmobiliseerd aan een PAMAM-dendrimeer (boven, Hoofdstuk 4) en aan een PEG-polymeer (onder, Hoofdstuk 5).

Voor alle onderzochte katalysatoren werden in de tandemreactie zeer vergelijkbare katalytische eigenschappen gevonden. Echter, voor de kruiskoppeling werden interessante verschillen gevonden. In deze reactie vertoonden de PAMAM-dendrimeer geïmmobiliseerde complexen een vergelijkbare reactiesnelheid, maar een hogere productselectiviteit dan de monomere katalysatoren. De carbosilaandendrimeer geïmmobiliseerde complexen vertoonden daarentegen een lagere reactiesnelheid en een vergelijkbare productselectiviteit dan de monomere katalysatoren. Deze waarnemingen zijn verklaard aan de hand van het naar binnen vouwen van de katalytische groepen ('backfolding') voor de PAMAM-dendrimeren en aan de hand van dendrimeeraggregatie voor de carbosilaandendrimeren.

In ***Hoofdstuk 5*** wordt de structuur-activiteitsrelatie tussen twee types PEG-copolymeer-ondersteunde tang Pd-complexen in de kruiskoppeling tussen vinylepoxide en styrylboorzuur onderzocht. Deze twee copolymeren zijn samengesteld uit ethyleenoxide en allylglycidylether en hebben een identieke chemische samenstelling. Het eerste copolymeer heeft een willekeurige structuur met een willekeurige plaatsing van de katalytische groepen, terwijl het tweede copolymeer een diblokcopolymeer is die een hoge lokale concentratie van katalytische centra omvat in het glycidyletherblok (*figuur 4*). De activiteit van deze copolymeren was vrijwel identiek aan elkaar en iets lager dan die voor de monomere katalysator. Echter, de productselectiviteit tussen het lineaire en het vertakte product (*l/b* verhouding) van het diblokcopolymeer (*l/b* = 14.9) was bijna tweemaal hoger dan de gevonden selectiviteit voor het willekeurige polymeer (*l/b* = 8.1) en bijna driemaal hoger dan voor het monomere complex (*l/b* = 5.5). Het verschil in de *l/b* verhouding wordt verklaard door de verschillende sterische eisen van de S_N2 en S_N2' reactiemechanismen die respectievelijk tot het vertakte en het lineaire reactieproduct leiden. Vanwege de hoge lokale katalysatorconcentratie wordt het S_N2 reactiepad als minder waarschijnlijk beschouwd voor het diblokcopolymeer.

In ***Hoofdstuk 6*** wordt een andersoortige dendritische katalyse in oplossing of in compartimenten beschreven aan de hand van ruthenium-gekatalyseerde olefinemetathese. In dit hoofdstuk wordt de synthese van nieuwe monomere en dendritische katalysatoren beschreven die gebaseerd zijn op Grubbs II en Hoveyda-Grubbs II complexen (*figuur 5*). Deze olefinemetathesekatalysatoren zijn gebruikt in de ringsluitingsmetathese van diethyldiallylmalonaat en vergeleken met veelgebruikte Grubbs- en Hoveyda-Grubbs-complexen. De dendritische Grubbs II-katalysator vertoonde een hogere initiële activiteit bij

kamertemperatuur vergeleken met zijn monomere equivalent, maar was langzamer dan de commercieel verkrijgbare katalysatoren. Wanneer hogere temperaturen gebruikt werden, was de dendritische katalysator iets langzamer dan zijn monomere equivalent. Deze waarnemingen duiden op een hogere activiteit en een hogere deactiveringssnelheid voor de katalytische centra in de dendritische katalysator.

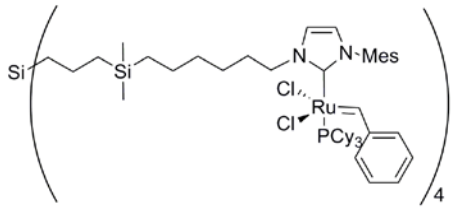

Figuur 5: Dendritisch Grubbs II-complex gebruikt voor de ringsluitingsmetathese van diethyldiallylmalonaat.

Pogingen tot het doen van gecompartimentaliseerde katalyse met deze dendritische katalysator hadden geen succes, aangezien productvorming werd gehinderd door de hoge vochtgevoeligheid van de katalysator in combinatie met de aanwezigheid van kleine hoeveelheden water afkomstig uit het gebruikte dialysezakje. Ook met behulp van precipitatie van de katalysator kon geen hergebruik van de katalysator worden bewerkstelligd.

Tenslotte is in het ***Addendum*** een katalytisch systeem voor orthogonale tandemkatalyse ontworpen en onderzocht. Hierbij werd gebruik gemaakt van de dendritische Pd- en Ru-complexen die beschreven staan in ***Hoofdstuk 2 en 6***. Helaas bleek de lage ringsluitingsmetatheseactiviteit van de dendritische Ru-complex voor het substraat 2-(but-3-enyl)-3-vinyloxiraan, de vochtgevoeligheid en de base-gevoeligheid van deze katalysator de realisatie van een eerste voorbeeld voor gecompartimentaliseerde orthogonale tandemkatalyse in de weg te staan.

Graphical abstract

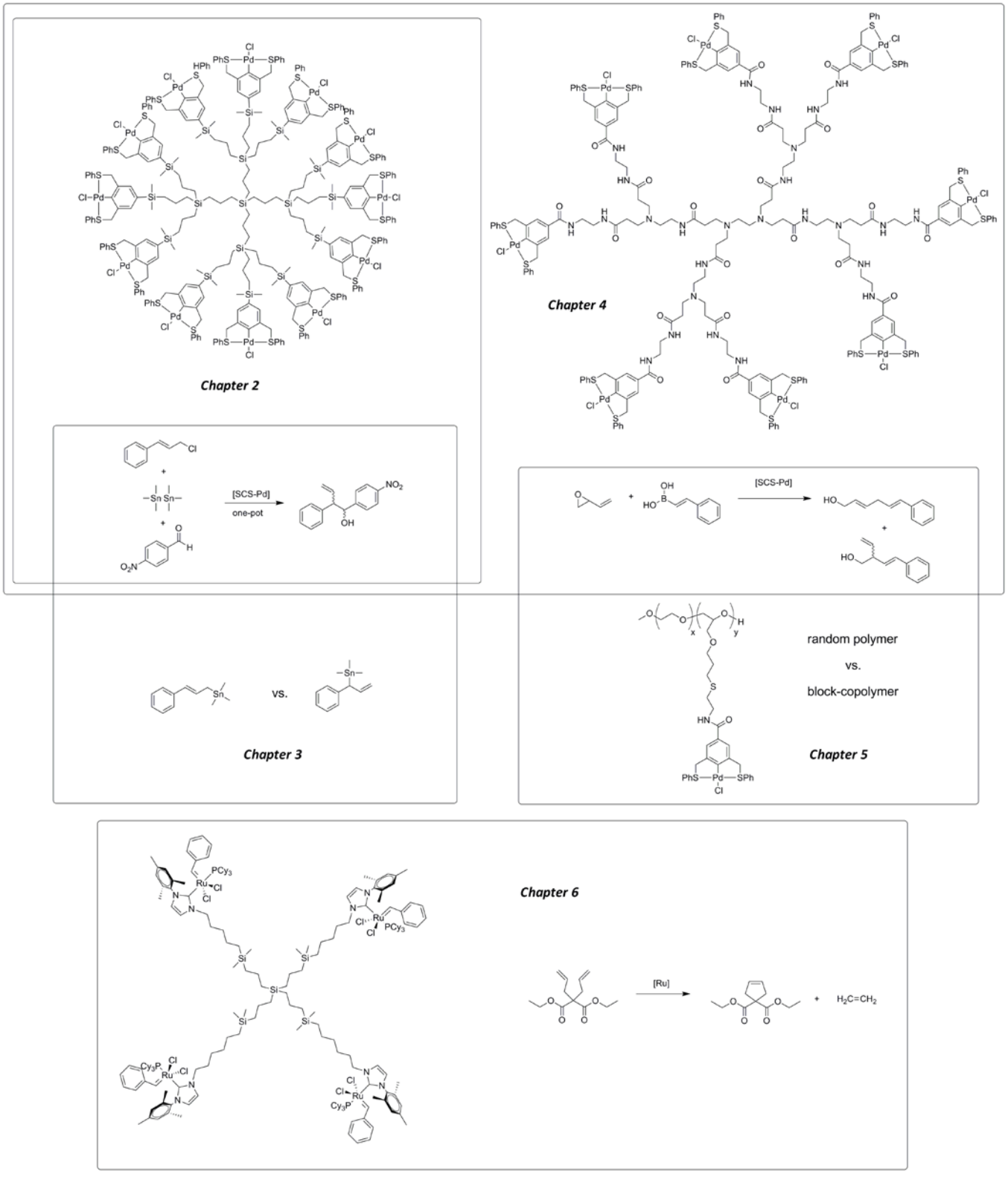

Acknowledgments

The research described in this thesis could not have been performed without the helping hands of many other people. I would like to thank the following people for their contribution to the realization of this thesis.

In the first place I would like to acknowledge my promoters professor Bert Klein Gebbink and professor Gerard van Koten. Dear Bert, thank you for all your support, guidance and input throughout the last five years. Your scientific knowledge and perfectionism have truly inspired me, and a part of my professional growth can be directly attributed to you. I am grateful for all your help and scientific discussions, but probably even more for the discussions about the more important matters in life than chemistry. Dear Gerard, especially in the first and the last parts of my research project we have dealt together. I am very truthful and proud that I am one of the last Ph.D. students that promote with a promoter with such a vast amount of knowledge and experience.

Johann Jastrzebski, Henk Kleijn and Milka Westbeek are acknowledged for being the three constant and driving forces in our research group. Johann, thanks for many organizational businesses that keeps the group going. Henk, thanks for all technical support, nice discussions, and of course the large amount of ESI-MS measurements you successfully recorded. You better should be proud of the ESI-spectrum of the dendritic ligand in Chapter 6. Milka, my gratitude for all the necessary paper work, especially close to my promotion date.

Professor Berth-Jan Deelman is accredited for being part of the reading committee and for giving me the opportunity to perform a post-doctoral project for Arkema Vlissingen directly after my PhD project. I have truly enjoyed this period and especially learned a lot about the industrial way of thinking in chemistry: an eye-opener.

Boris Obermeier and professor Holger Frey from the Johannes Gütenberg University in Mainz are acknowledged for the joint project I was part of. Although I have experienced the difficulties in working far from each other, I think we can be proud of this collaboration which can be read in Chapter 5. Boris, I will remember the good days we have had in Utrecht and Mainz.

Then I would like to acknowledge Maxime Siegler, Martin Lutz, and professor Anthony Spek for recording the four beautiful crystal structures that have appeared in my thesis.

During my stay at the group, I have been in the opportunity to work with many students varying from first year's students to BSc, HBO and Erasmus students. Except for some moments of frustration, supervising them has given me a lot of satisfaction. I would like to thank Tiemen van Mourik, Peter van den Boogerd, Robin Jastrzebski and Berend van der Wildt for picking my project proposals, and doing a good job by working hard in the lab during their Bachelor projects. Thomas Klimeck is acknowledged for writing a nice review on the field of tandem catalysis for me. Hassan el Harchaoui is thanked for being an excellent HBO student. You did a great job by pioneering the possibilities to connect dendrimers to Grubbs catalysts. Eder Tomas Gonzalez de Mendivil has worked in a later stage on this project for his Erasmus internship at our group. I would like to compliment you with the enormous amount of high quality work you have performed and with your fantastic working attitude. Furthermore, I think you are just a great guy to work with.

My last student is impossible to forget, as being my co-tandem driver in the last year of my PhD. Kimberley Mayland, I would like to thank you for all the work you did in the many projects we have worked on together. Although your never-ending flow of words made me mad more than once, I will mainly remember you for the great times we have had in this year.

In this period I have been also lucky to collaborate with some great colleague PhD students and post-doctoral fellows. I am grateful Harm Dijkstra, Jie Li, Bart Suijkerbuijk, Birgit Wieczorek, Guido Batema, Pieter Bruijnincx, Maaike Wander, Marcel Moelands, Elena Sperotto, Nesibe Demirörs-Cindir, Kees Kruithof, Erwin van der Geer, Silvia Gosiewska, Peter Hausoul, Sylvestre Bonnet, Aidan McDonald, Sipke Wadman, Marcella Gagliardo, and all other direct colleagues for the many scientific discussions and lots of fun we have had.

Yves Cabon is thanked for the DFT calculations in the chapter I am most proud of, and also for all corrections and advice you gave to me, whether I asked for it or not. Also during my post-doc period you always made time for discussions that gave me new knowledge and insights.

A special thank goes to Ties Korstanje for being co-author in the first chapter, everything you have arranged for my promotion ceremony, and for being a great friend in general. Also my fellow Brabander, Jacco Hoekstra is thanked in particular for the good times we have had at

the lab. You are the person that pulled my through the difficult writing period in Z810, and together we switched off the lights in the Kruyt building. My partner-in-crime, Morgane Virboul is also worth a special mention. We started our PhD's at the same time and we shared all our fantastic results, frustrations, and hopeless fails, which gave me a particular connection to you. I'd like to thank you for being my soul mate for almost five years.

Dennis Snelders, after being one of my best friends at our secondary school, you also played a huge role in my PhD from the early beginning until the very end. Thanks a lot for attending me for the vacancy in the group where I applied for, for being my paranymph, and for the many good moments in between. Wilco Pulskens, thanks for being my paranymph as well, and even more for all badminton, swimming and shoarma-related friendship.

My parents Sjaak and Els have been very important in all my undertakings in my life. I would like to thank them in the first place for giving me the chemistry genes you both possess, but more importantly I am very grateful for your love and the continuous support for literally everything I have done in my life so far. Thanks to my brothers Jesse and Rens as well, and in particular a special thank you for Jesse for putting his creativity in among others the cover of my thesis. I think you simply did a great job.

The last paragraph is reserved to thank the person I love most. Miranda, although your contribution to this thesis itself was minimal, I am in the lucky position that your contribution to everything else in my life is very large. Thanks for that, let's continue this in the same way!

Niels

Curriculum Vitae

Niels Pijnenburg was born on the 26th of January 1982 in Breda, the Netherlands. After graduating from high school (Mill Hill College in Goirle) in May 1999, he started studying Pharmacy at Utrecht University. After obtaining his propaedeutic diploma in May 2001, he obtained his MSc in the field of Medicinal Chemistry in June 2005. During this period, he performed internships in the groups of Bioorganic Chemistry (minor) and Medicinal Chemistry (major) at the same university. Furthermore, he did an internship via the Erasmus program at the group of Organic Chemistry in Helsinki.

In November 2005 he started his PhD project at the group of Organic Chemistry & Catalysis under supervision of prof. dr. Bert Klein Gebbink and prof. dr. Gerard van Koten. He worked in the field of homogeneous catalysis on immobilization of organometallic catalysts (mainly palladium and ruthenium) to dendrimers for performing tandem catalysis and for recycling purposes. Parts of the work described in this thesis were published in scientific journals (see List of Publications) and presented at several national (NCCC, Noordwijkerhout, 2006-2010) and international conferences (IDS, Toulouse 2007, Stockholm 2009).

From February until July 2010 he worked as an industrial postdoc for Arkema Vlissingen BV as research scientist for the synthesis of new ligands for Pd-catalyzed syntheses.

Currently, i.e. from July 2011, he is working as Associate Scientist in the R&D group Kitchen Care of Diversey Europe BV in Utrecht on optimizing formulations for among others mechanical warewash detergents.

List of publications

Preparation of S- and N-linked Glycosylated Amino Acid Building Blocks for Solid-phase Glycopeptide Library Synthesis.

C. Elizabeth. P. Maljaars, Koen M. Halkes, Wim L. De Oude, Seléne van der Poel, Niels J. M. Pijnenburg, Johannis P. Kamerling.

J. Carbohydrate Chem., **2005**, 24 (4-6), 353-367

Palladacycles on Dendrimers and Star-shaped Molecules for Applications in Catalysis

Niels J. M. Pijnenburg, Ties J. Korstanje, Gerard van Koten, Robertus J.M. Klein Gebbink. (*Chapter 1 in this thesis*)

Chapter 15 in *Palladacycles*; *Synthesis, Characterization & Applications*, Dupont, J., Pfeffer, M., *Wiley VCH*, Mannheim, **2008**, 365-398

SCS-pincer Palladium-catalyzed Auto-tandem Catalysis Using Dendritic Catalysts in Semi-permeable Compartments

Niels J. M. Pijnenburg, Harm P. Dijkstra, Gerard van Koten, Robertus J. M. Klein Gebbink. (*Chapter 2 in this thesis*)

Dalton Trans., **2011**, 40, 8896-8905

The Role of the Dendritic Support in the Catalytic Performance of Peripheral Pincer Pd-complexes

Niels J. M. Pijnenburg, Martin Lutz, Maxime A. Siegler, Anthony Spek, Gerard van Koten, Robertus J. M. Klein Gebbink. (*Chapter 4 in this thesis*)

New J. Chem., **2011**, accepted, DOI**:** 10.1039/C1NJ20366E